SANDIA REPORT
SAND2022-0780
Printed January, 2022

Sandia National Laboratories

Testing, Characterization, and Modeling of the Resonant Plate Test Environment

Tyler F. Schoenherr, David E. Soine, Bryan L. Witt

Prepared by
Sandia National Laboratories
Albuquerque, New Mexico 87185
Livermore, California 94550

Issued by Sandia National Laboratories, operated for the United States Department of Energy by National Technology & Engineering Solutions of Sandia, LLC.

Available to DOE and DOE contractors from

U.S. Department of Energy
Office of Scientific and Technical Information
P.O. Box 62
Oak Ridge, TN 37831

Telephone: (865) 576-8401
Facsimile: (865) 576-5728
E-Mail: reports@osti.gov
Online ordering: http://www.osti.gov/scitech

Available to the public from

U.S. Department of Commerce
National Technical Information Service
5301 Shawnee Road
Alexandria, VA 22312

Telephone: (800) 553-6847
Facsimile: (703) 605-6900
E-Mail: orders@ntis.gov
Online order: https://classic.ntis.gov/help/order-methods

ABSTRACT

The resonant plate shock test is a dynamic test of a mid-field pyroshock environment where a projectile is struck against a plate. The structure undergoing the simulated field shock is mounted to the plate. The plate resonates when struck and provides a two sided shock that is representative of the shock observed in the field. This test environment shock simulates a shock in a single coordinate direction for components looking to provide evidence that they will survive a similar or less shock when deployed in their operating environment. However, testing in one axis at a time provides many challenges. The true environment is a multi-axis environment. The test environment exhibits strong off-axis motion when only motion in one axis is desired. Multiple fixtures are needed for a single test series. It would be advantageous if a single test could be developed that tests the multi-axis environment simultaneously. In order to design such a test, a model must be developed and validated. The model can be iterated in design and configuration until the specified multi-axis environment is met. The test can then execute the model driven test design. This report discusses the resonant plate model needed to design future tests and the steps and methods used to obtain the model. This report also details aspects of the resonant plate test discovered during the process of model development that aids in our understanding of the test.

ACKNOWLEDGMENT

I first like to thank the co-authors on this report. Their contributions to this report make it complete and thorough. Between ensuring that we have the correct data or adjusting to complications on the fly, they used their respective expertise to deliver results.

Next, I would like to thank the technologists, Kevin Brenner and Tino Arias, that executed the resonant plate shock tests that gave us a treasure trove of information. Their patience with me and astute attention to details that are outside of their usual scope of work provided data with the quality needed to use with the model and learn about the resonant plate test setup not previously known.

Last, I would like to thank the peer review team that listened and provided thoughtful input to the work and ideas on how to make the data and results more transparent and impactful. These members are Ron Hopkins, Mikhail Mesh, Vit Babuska, Wil Holzmann, and Carl Sisemore.

CONTENTS

LIST OF FIGURES

LIST OF TABLES

1. INTRODUCTION

Testing components or subassemblies in the laboratory is a cheaper and faster alternative to testing an entire system in its field environments. In some instances, performing a field test of the environment is untenable. Of the multitude of environments that systems experience, the shock environment is a subset of those environments. One method the test laboratory tests shock environments is by using a resonant plate apparatus.

Sandia National Laboratories sometimes uses a resonant plate to create a two sided shock impulse that is a more representative shock environment than a one sided pulse. Photographs of a resonant plate test configuration are in Figure 1-1. This test setup requires that the plate be flexible so its resonance can amplify the motion of the unit under test bolted to the plate at a frequency range present in the field environment. This flexibility at resonance allows for uncontrollable, off-axis motion during the test. This is an issue as current environment specifications dictate that three orthogonal shock inputs are input separately to simulate one environment. Uncontrollable off-axis motion can add damage in an off axis direction that would inadvertently add over the three hits.

One solution to produce a more realistic environment is to develop a test that meets shock environments in all directions simultaneously. Performing a single shot eliminates the desire to suppress off axis motion when executing orthogonal type tests. Executing one test instead of three also reduces the time in the laboratory increasing the lab capacity. However, executing a single shot a test is difficult because there is little control over the test. The test fires a high speed projectile to impact the resonant plate. There is little control over the projectile besides the projectile speed, the programmer that the projectile hits, and the size of the projectile.

Due to the relatively little control that the test facility has in modifying the test, the success of the multi-axis test is contingent on the pre-test design using a finite element model. Characterization

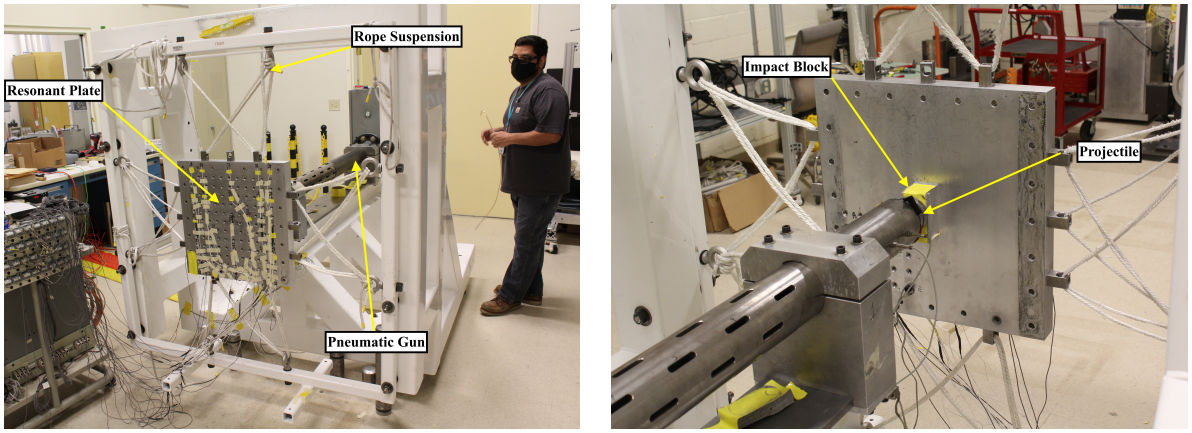

Figure 1-1. Photographs of the resonant plate test configuration without a test unit attached.

and designs of multi-axis shock have been previously explored [8] [9] [12]. These efforts place high focus on the response of the base of the unit under test and the unit under test itself. These efforts also explore moving both the unit under test and the impact location as possible means for designing a multi-axis test. Through these efforts, it is clear that the use of a finite element model is critical in designing a test for the given multi-axis environment. Guessing on the test setup parameters real time in the lab is untenable due to how long it takes to gather data on one option and the complexity of the resonant plate system.

Even with the use of a finite element model, information about the input force to the resonant plate must be known in order to produce a meaningful model response. Direct measurements are infeasible at such high levels and short durations due to hardware limitations of load sensors. In the absence of a direct measure of the input force, inverse methods must be used to calculate the force that causes the measured accelerations. This is a challenge as traditional inverse methods are susceptible to slight non-linearities in the structure. Another method to calculate the force is to use explicit models to determine these forces, however, modeling of the contact and programmer is difficult [5].

In order to determine the forces from the resonant plate tests, this body of work uses a spatial inverse method known as the Sum of Weighted Accelerations Technique - Time Eliminated Elastic Motions (SWAT-TEEM)[11]. This inverse method inverts spatial quantities (i.e. mode shapes) to calculate the causal force. Using mode shapes provides a buffer against most non-linearities as mode shapes are not as sensitive to system nonlinearities as natural frequency and damping.

Chapter 2 details basic modal analysis theory and the theory behind the force reconstruction technique SWAT-TEEM and its corresponding limitations. Chapter 3 provides descriptions and part numbers of the hardware used in the testing and the model. It lists the parameters and structure of the finite element model for posterity and repeatability of the results presented.

Chapter 4 details the two experimental modal analysis tests performed on the resonant plate test configuration. The modal results of the two modal tests are presented and compared to the model. The chapter discusses the calibration to the experimental modal data and documents the parameters of the final calibrated model.

Chapter 5 details the resonant plate shock data acquired on the resonant plate test configuration. The chapter details the process and strategy for processing the data. This includes the process of calculating the impact force imparted by the projectile for a series of runs. The process also includes details of using the acceleration data with the reconstructed force to execute an experimental modal analysis at shock level inputs. These modal parameters calculated at shock input levels are compared to the experimental modal results obtained at modal input levels to determine the linearity of the system.

Chapter 6 of this report demonstrates the use of the model with the calculated forces to validate the model with and without a concept fixture and in many different configurations. In addition to the model, the body of work investigates the ability to scale the input force from one run to another and the sensitivity of the input force's location with respect to the response of the resonant plate.

There are many conclusions from this body of work. This reports shows that high quality forces can be reconstructed from the testing environment on a bare resonant plate. It is also shown that those forces can be scaled in time and magnitude to represent all of the forces calculated that are dependent on programmer, projectile size, and projectile velocity.

The report shows that an experimental modal analysis test can be run using the reconstructed forces and the response measurements from a resonant test. The modal data taken at shock forcing levels show that there are some non-linearities in the frequency and damping that are mode dependent, but that a linear model calibrated to the modal data at high force levels can match the response of the structure.

Through all of this report, the goal is to create a model that can be used for future development of a multi-axis shock test. Validation runs show that the model of the test environment is sufficient for test design of a multi-axis shock test given shock environments.

2. THEORY AND BACKGROUND

This report uses modal analysis theory and the force reconstruction algorithm known as the Sum of Weighted Acceleration Technique - Time Eliminated Elastic Motion (SWAT-TEEM) in order to calibrate the model, process the shock data, and model the test environment. This chapter explains these topics in some detail to aid in digesting the analysis performed in this report, but the overview is not meant to be an exhaustive overview of the topics.

2.1. Modal Analysis

Modal analysis is a deep and rich topic of discussion for which whole books are written [1] [4] [7]. This section covers modal analysis at a high level so that the reader can understand its importance and how the system's modal parameters are extracted from the data acquired.

Modal analysis theory is first examined by producing the equations of motion of a generic structure. A structure's motion can be estimated by the 2nd order linear equations of motion

$$\mathbf{M}\ddot{\bar{x}} + \mathbf{C}\dot{\bar{x}} + \mathbf{K}\bar{x} = \bar{F}, \tag{2.1}$$

where $\mathbf{M}$ is the mass matrix, $\mathbf{C}$ is the damping matrix and $\mathbf{K}$ is the stiffness matrix of the system. The displacement of the structure can be described in the frequency domain and reorganized as

$$\frac{\ddot{\bar{x}}(j\omega)}{\bar{F}(j\omega)} = -\omega^2[-\omega^2\mathbf{M} + j\omega\mathbf{C} + \mathbf{K}]^{-1} \tag{2.2}$$

where j is the imaginary number. This form of the equations of motion is informative because it explicitly provides an input/output relationship between the displacement and the forcing function that caused the motion through a transfer function. This transfer function is specifically called a Frequency Response Function (FRF). Although the mass, damping, stiffness matrices of the finite element model can be calculated, these properties cannot be directly measured on a structure.

In order to be able to calculate and compare FRFs between the finite element model and the physical structure, an eigen analysis is performed on the structure. The eigen analysis in the finite element model calculates the eigenvalues and eigenvectors. The eigenvectors are calculated from the mass and stiffness matrices and are referred to in structural dynamics as the mode shapes. These shapes are related to the displacement of the structure through a linear combination shown as

$$x_i \approx \sum_{m=1}^{n} \phi_{im} q_m, \tag{2.3}$$

where ϕ_{im} is the m^{th} mode shape of the structure at degree of freedom i and q_m is the modal coordinate corresponding to the participation of that mode shape in the displacement of the structure. The substitution shown in Eqn 2.3 is linear, however, it has been shown to be valid for systems with slight nonlinearities stemming from frictional contacts [3]. The modal substitution decouples the equations of motion shown in Eqn 2.1 and 2.2. As a result, FRFs can be calculated for both the finite element model and experimental data. These FRFs in the modal domain are written as

$$\frac{\ddot{x}_i(j\omega)}{F_k(j\omega)} \approx \sum_{m=1}^{n_{\text{mode}}} \frac{-\omega^2 \phi_{im}\phi_{km}}{-\omega^2 + 2j\omega\omega_m\zeta_m + \omega_m^2}, \tag{2.4}$$

where ω_m is the m^{th} natural frequency of the structure and ζ_m is the modal damping corresponding to the m^{th} mode. This expression of the FRF matrix is computed element by element of the i^{th} response degree of freedom with respect to an input at the k^{th} degree of freedom. With the physical structure, a directly measured force and directly measured accelerations are obtained in order to calculate parts of the FRF matrix over the frequency range for which there is adequate excitation. The modal parameters of the structure are fit to the experimental FRFs using any number of methods.

In summary, modal analysis or eigen analysis is a method of transforming the data into a domain that allows for the comparison of finite element models and physical structures. Although the modal parameters are calculated from the finite element model, the experimental modal parameters need to be fit to the experimental FRFs.

2.2. Formulation of SWAT (Sum of Weighted Acceleration Technique)

The derivation of the SWAT-TEEM (Time Eliminated Elastic Motion) algorithm that is used to calculate the sum of the external forces begins with the 2nd order linear equations of motion,

$$\mathbf{M}\ddot{\bar{x}} + \mathbf{C}\dot{\bar{x}} + \mathbf{K}\bar{x} = \bar{F}, \tag{2.5}$$

where $\mathbf{M}$ is the mass matrix, $\mathbf{C}$ is the damping matrix and $\mathbf{K}$ is the stiffness matrix of the system. Modal substitution is used to estimate the physical response with modal degrees of freedom shown by

$$\phi\bar{q} \approx \bar{x}, \tag{2.6}$$

where ϕ is the matrix of mode shapes of the system and $\bar{q}$ is the vector of generalized modal coordinates. The modal approximation shown in Eq 2.6 is substituted into Eq 2.5 to get

$$\mathbf{M}\phi\ddot{\bar{q}} + \mathbf{C}\phi\dot{\bar{q}} + \mathbf{K}\phi\bar{q} = \bar{F}. \tag{2.7}$$

At this point, Eq 2.7 is premultiplied by the transpose of the rigid body, ϕ_r^T, modes to get

$$\phi_r^T\mathbf{M}\phi\ddot{\bar{q}} + \phi_r^T\mathbf{C}\phi\dot{\bar{q}} + \phi_r^T\mathbf{K}\phi\bar{q} = \phi_r^T\bar{F}. \tag{2.8}$$

Because there is no internal damping or internal stiffness forces for the rigid body degrees of freedom, Eq 2.8 simplifies to

$$\phi_r^T\mathbf{M}\phi\ddot{\bar{q}} = \phi_r^T\bar{F} \tag{2.9}$$

due to

$$\phi_r^T\mathbf{C} = 0 \;\&\; \phi_r^T\mathbf{K} = 0. \tag{2.10}$$

The physical degrees of freedom are substituted for the modal degrees of freedom using the relationship in Eq 2.6 into Eq 2.9 to get

$$\phi_r^T\mathbf{M}\ddot{\bar{x}} = \phi_r^T\bar{F}. \tag{2.11}$$

At this point a weighting matrix, w, is defined as

$$w^T = \phi_r^T\mathbf{M}. \tag{2.12}$$

and substituted into Eq 2.11 to obtain

$$w^T\ddot{\bar{x}} = \phi_r^T\bar{F}. \tag{2.13}$$

To solve for the weighting vector, an assumption of the input force is made. In the case where the structure is impacted by an external force and then in a free state, there are no external forces after impact and the accelerations of the system, $\ddot{\bar{x}}_{fd}$, are assumed to decay exponential and Eq 2.13 after the impact simplifies to

$$w^T\ddot{\bar{x}}_{fd} = 0. \tag{2.14}$$

To obtain a non-trivial solution, information about the rigid body modes needs to be included because they were not present in the free decayed response. The rigid body constraint is formed by post-multiplying Eq 2.12 by the rigid body shapes to get

$$w^T \phi_r = \phi_r^T \mathbf{M} \phi_r, \tag{2.15}$$

which can be simplified to

$$w^T \phi_r = M_r. \tag{2.16}$$

Equation 2.16 is added to Eq 2.14 to get

$$w^T \left[\phi_r \, \ddot{\bar{x}}_{fd} \right] = \left[M_r \, 0 \right]. \tag{2.17}$$

Equation 2.17 is solved for w^T and substituted back into Eq 2.13 to solve for the sum of external forces acting on the center of gravity written as

$$\left[M_r \, 0 \right] \left[\phi_r \, \ddot{\bar{x}}_{fd} \right]^+ \ddot{\bar{x}} = \phi_r^T \bar{F}. \tag{2.18}$$

Equation 2.18 is solved for the six weighting vectors in a constrained least squares problem with the rigid body term being the constraint. The pseudo-inverse of the rigid body shapes and the responses of the free decayed response are multiplied by both sides to solve for the weighting vector. These weight vectors are then substituted back into Equation 2.13 to solve the for the external forces. Because the pseudo-inverse includes the time domain response of the system which is a linear combination of the mode shapes, the mode shapes of the system do not need to be separately calculated.

3. FINITE ELEMENT MODEL

This section describes the final models of the different structures used in this report and descriptions of their parts and how they are modeled. These models are developed through the calibration process described in Chapter 4. There are two main structures used in this report, the resonant plate and the concept test fixture. A summary of the meshed parts of the model and their details can be found in Table 3-1. There is no mesh convergence study in this report and there is no effort to limit the size of the model. Future efforts will examine such advances of the model.

3.1. Resonant Plate

The resonant plate by itself is not descriptive enough as there are resonant plates of many different sizes and designs. The resonant plate of interest for this report is the 1000 Hz resonant plate with drawing number 60217SLLHRF-01. The resonant plate system weighs approximately 122 lbs. A photograph of the resonant plate assembly can be found in Figure 3-1 and a drawing of the plate can be found in Figure 3-2.

This resonant plate is composed of several parts. These parts are referred throughout this report as the resonant plate, damping bars, damping bar pads, impact block, rope anchors, and balancing rods. The finite element models of the parts used in this report can be found in Figures 3-3 through 3-8 respectively.

Table 3-1. Details of the 1000 Hz Resonant Plate Finite Element Model

Component	Element Type	Element Count
Resonant Plate	Hex8	176k
Damping Bars	Hex8	53k
Damping Bar Pads	Hex8	4.8k
Impact Block	Hex8	2.9k
Rope Anchors	Hex8	3.3k
Balance Rods	Hex8	3.6k
Concept Fixture	Hex8	102k
Total		349k

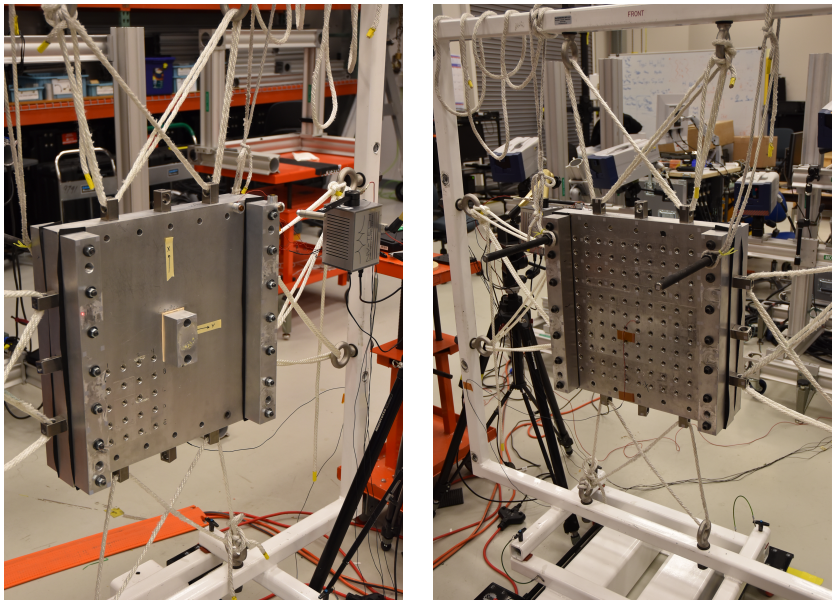

Figure 3-1. Photographs of the 1000 Hz resonant plate used in this report

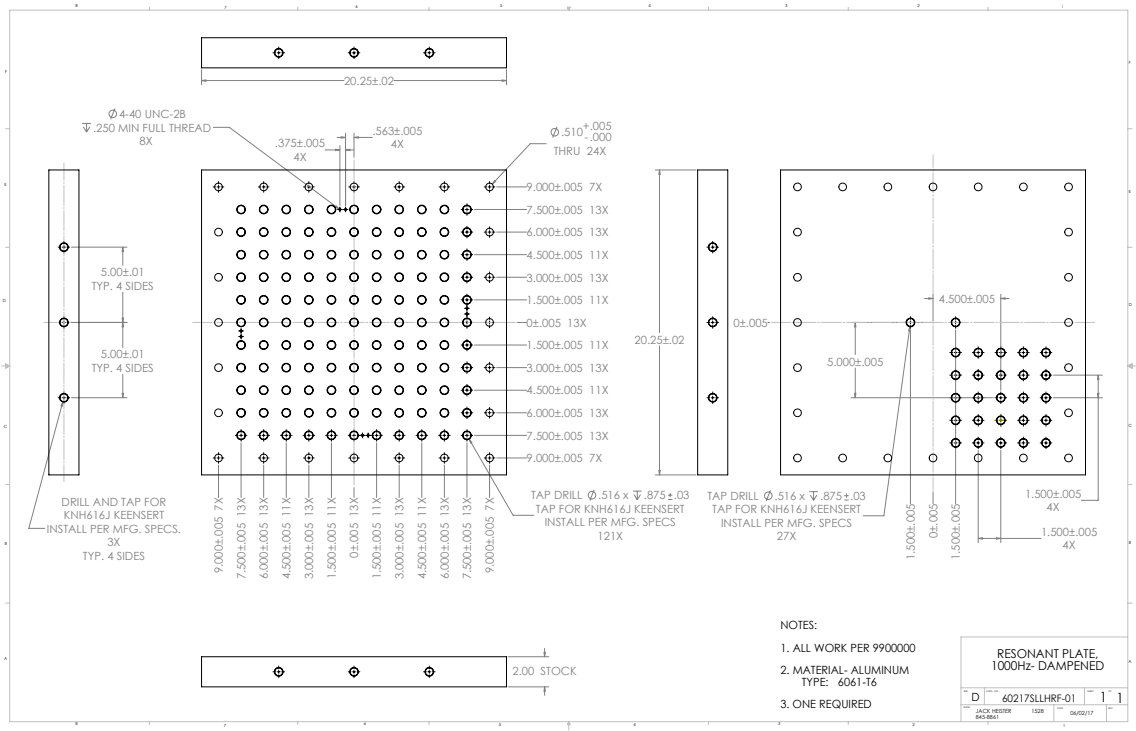

Figure 3-2. Drawing of the 1000 Hz resonant plate used in this report

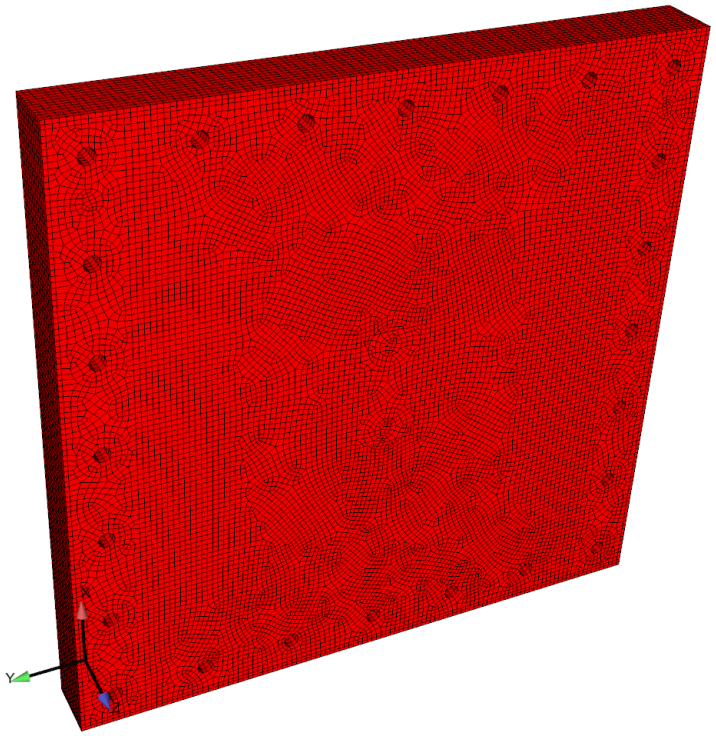

Figure 3-3. Mesh of the 1000 Hz Resonant Plate component

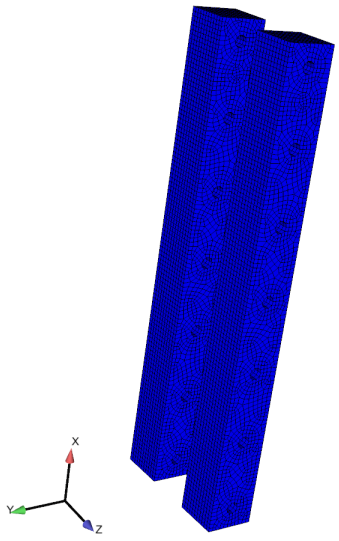

Figure 3-4. Mesh of the Damping Bars

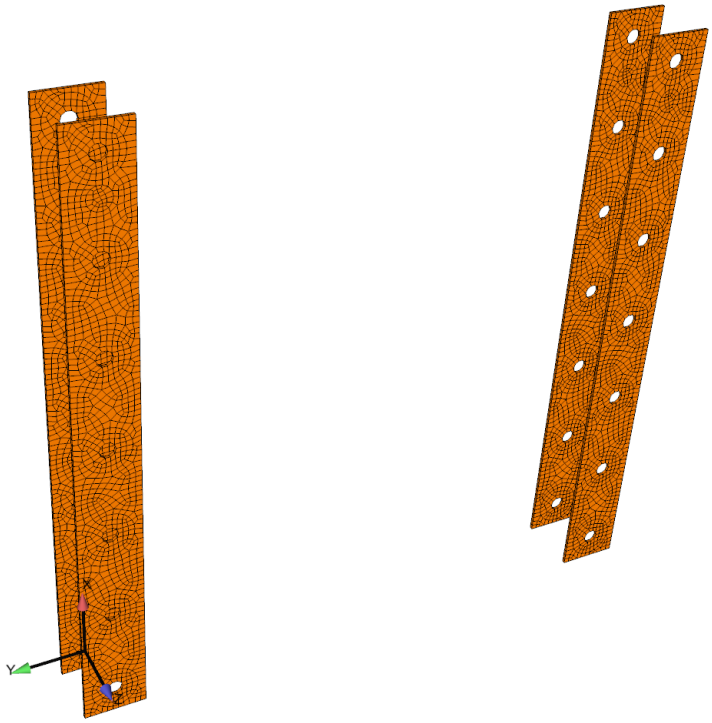

Figure 3-5. Mesh of the Damping Bar pads

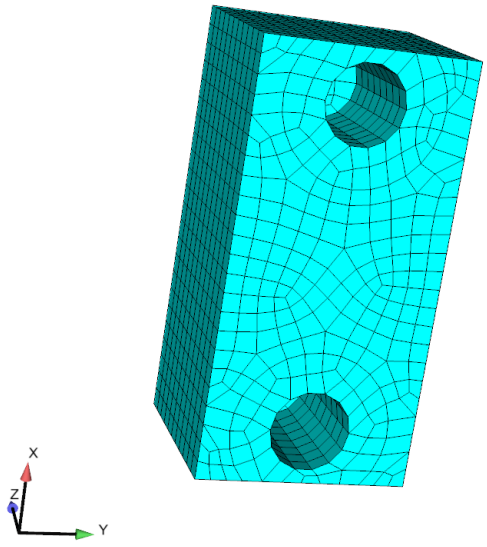

Figure 3-6. Mesh of the Impact Block

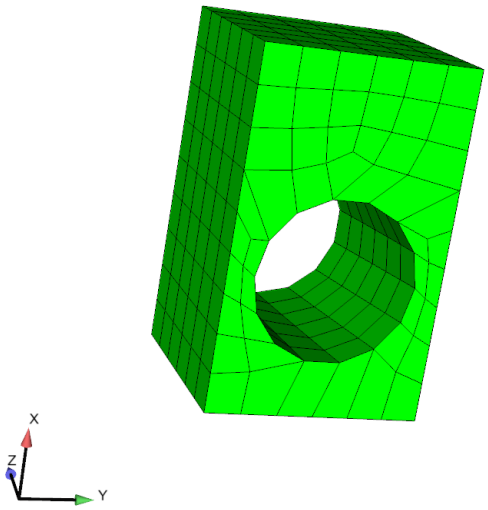

Figure 3-7. Mesh of the Rope Anchor

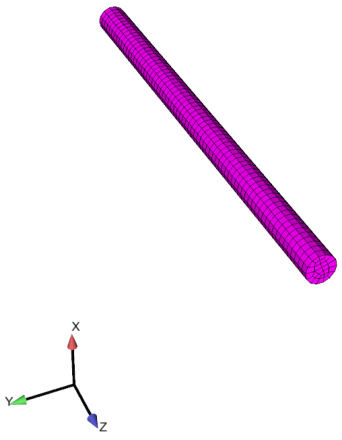

Figure 3-8. Mesh of the Balance Rod

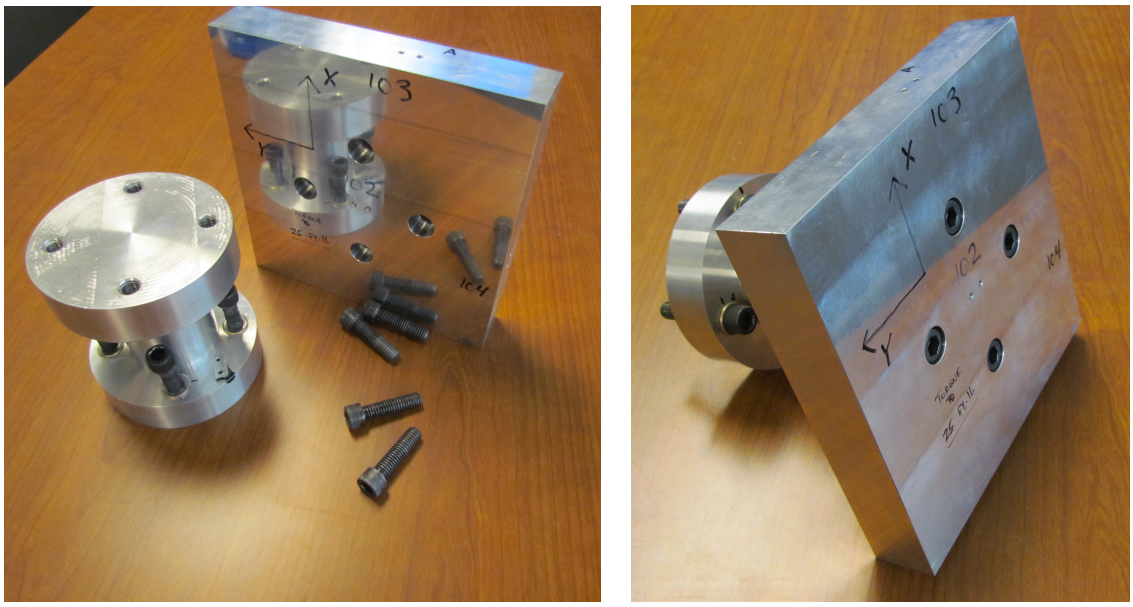

Figure 3-9. Photograph of the concept test fixture disassembled (left) and assembled (right)

3.2. Concept Test Fixture

The concept test fixture is designed in order to amplify off-axis motion through rotations and resonances. This fixture serves as a proof of concept that a test configuration could be designed for a multi-axis environment. The drawing number for this test fixture is 72320SLLHRF3A-01 and it weighs approximately 9.7 lbs. It has a dumbbell type configuration with a circular base, a cylinder support, and a square top. Conceptually, the component under test would be bolted to the top of the concept fixture and the top plate of the concept fixture would be the input to the component. Photographs of the fixture can be seen in Figure 3-9 and the mesh in Figure 3-10. Drawings of the concept fixture parts can be seen in Figures 3-11 and 3-12.

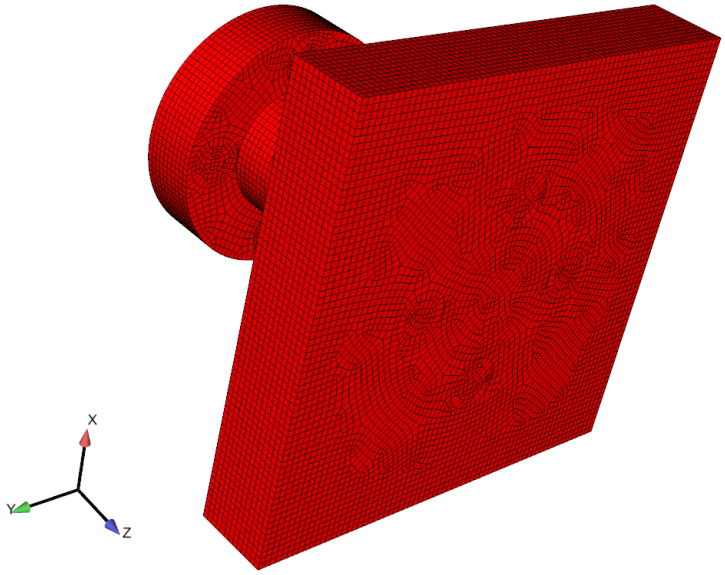

Figure 3-10. Mesh of the Concept Fixture

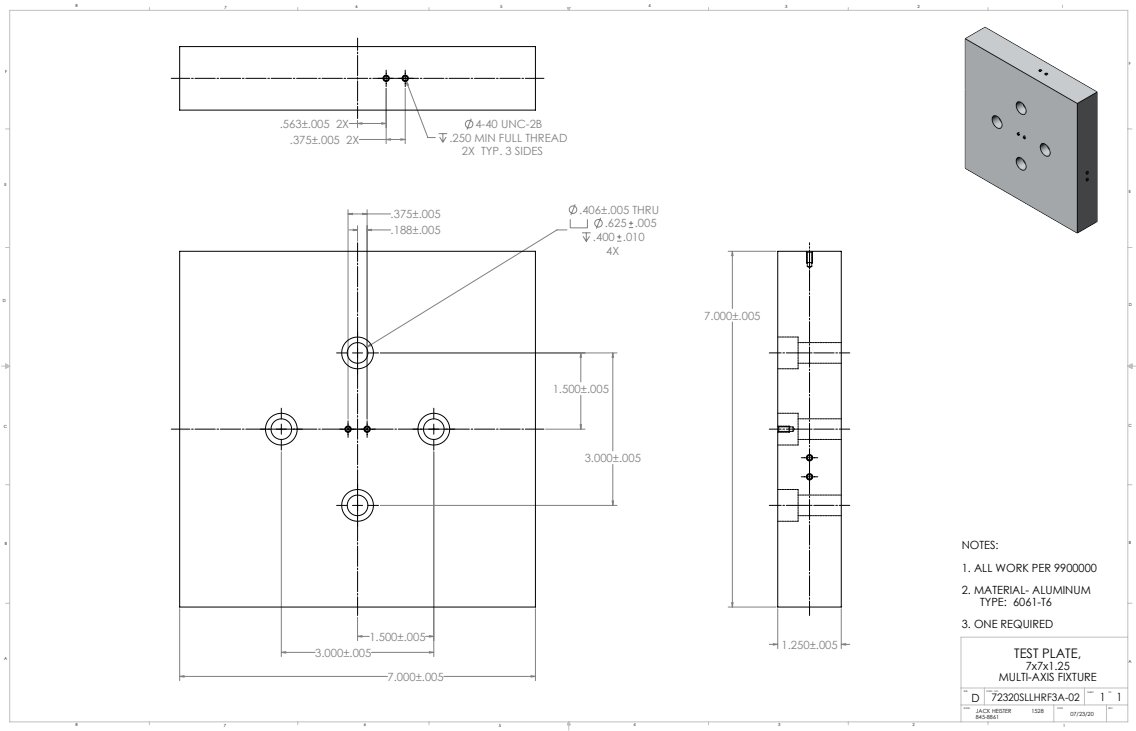

Figure 3-11. Drawing of the top plate of the concept fixture used in this report

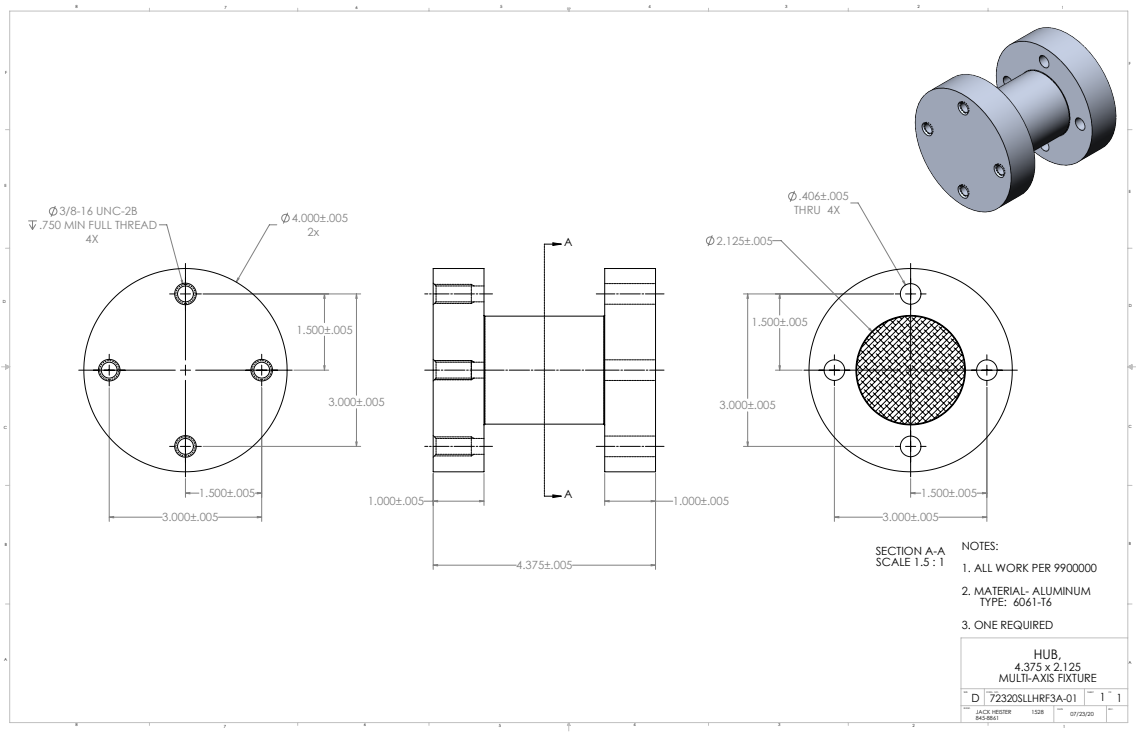

Figure 3-12. Drawing of the support cylinder of the concept fixture used in this report

4. MODAL ANALYSIS TESTING OF THE RESONANT PLATE

This chapter contains the details of executing an experimental modal test at low forcing levels of the resonant plate in two different configurations. The two configurations are the resonant plate in the test environment setup with and without the damping bars. The chapter discusses the results of the modal test along with conclusions drawn from the test data. This chapter also includes the comparison and calibration of the FEM to the experimental modal test data.

4.1. Modal Test of the Bare Plate

A photo of the modal test setup of the 1000 Hz resonant plate is in Figure 4-1. The test used a 3D laser doppler vibrometer system to measure the responses and an automatic hammer to excite the structure. The response locations measured on the front side of the plate are shown in Figure 4-2. Not shown are the response measurements on the impact block.

The modal parameters of the structure were fit to the data using the SMAC [6] algorithm. The first four modes fit to the data are shown in Figures 4-3 to 4-6. The first three modes of the system appear to match analytical plate modes. However, the fourth mode shows just one of the rope anchors having an isolated mode. It appears that that there is something wrong with the center rope anchor located on the -X normal face of plate as shown in 4-6.

The rope anchor that exhibited questionable results skewed the modal fitter. In order to avoid that error, the modes were refit and the anchor degrees of freedom were excluded. The refit modal parameters were used in the final comparison to the FEM. The shapes that were fit from the data that excluded the rope anchor degrees of freedom can be seen in Appendix A.

I addition to extracting modal parameters, hits on the impact block were performed at multiple forcing levels to determine linearity of the system. Frequency response functions (FRFs) between the impact force on the impact block and a drive point accelerometer on the other side of the resonant plate were calculated for each of the hits and plotted in Figure 4-7. The plot of the FRFs shows that there are virtually no shifts in damping or natural frequency for the load levels imparted by the different hammer hits. These results show that the bare plate behaves like a linear system. The reason the plate behaves linearly is because there are only a couple of sources of frictional surfaces for the bare resonant plate without damping bars.

4.2. FEM Calibration of Bare Plate Model to Modal Data

The initial model of the bare plate is shown in Figure 4-8. Through the calibration of the model, many model parameters and model forms were implemented on the model and compared to the

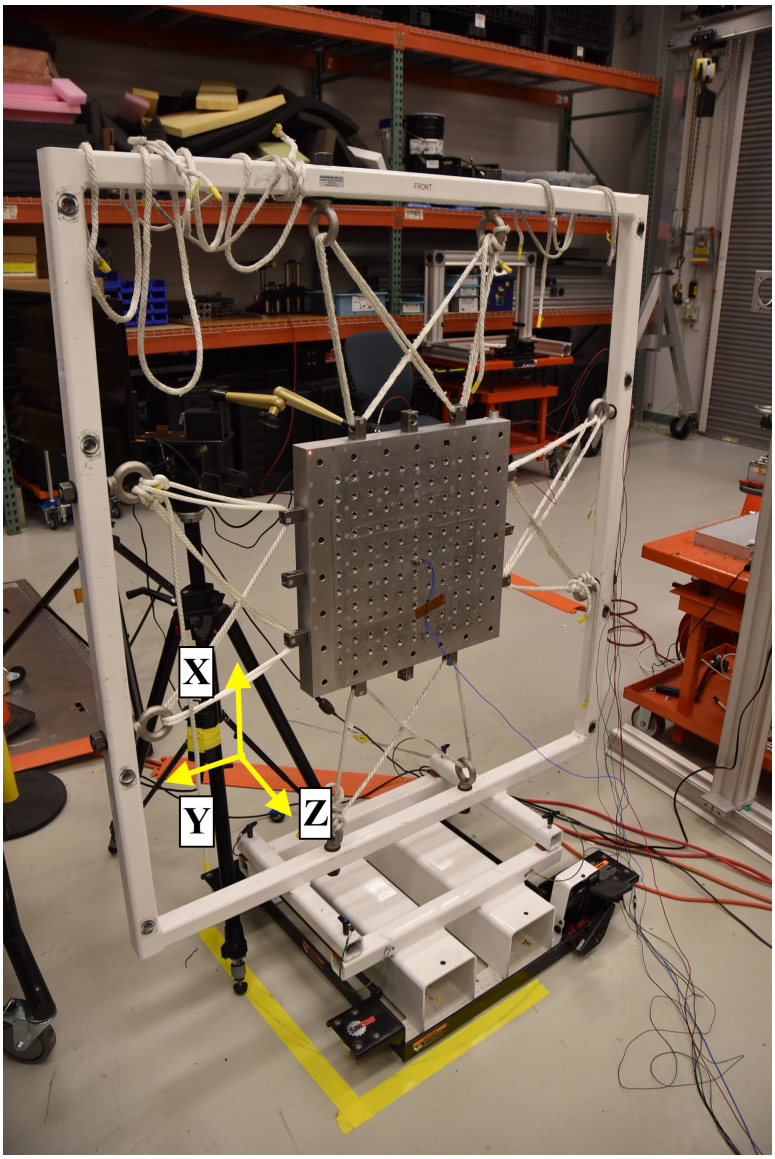

Figure 4-1. Overview of the modal test setup of the bare plate configuration

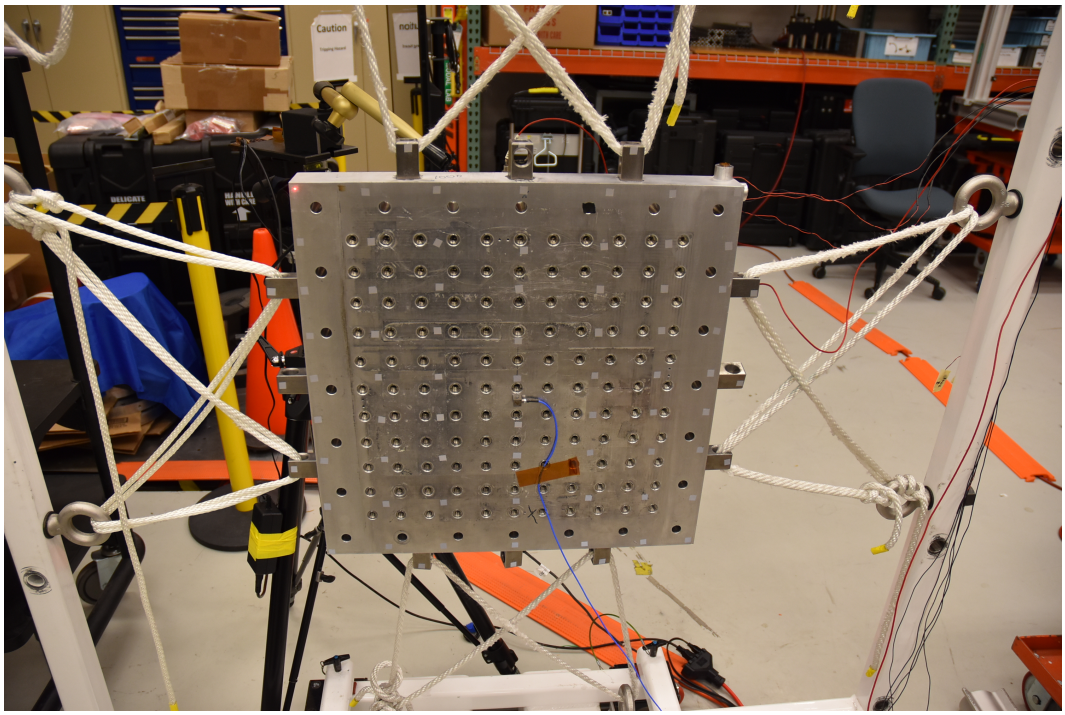

Figure 4-2. Locations of the response measurements as indicated by the grey stickers

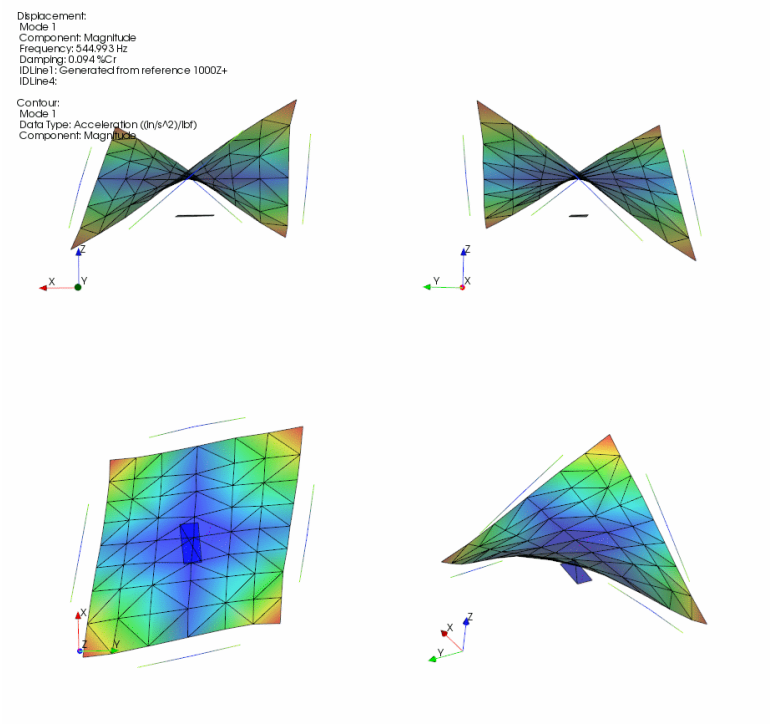

Figure 4-3. 1st Elastic mode shape of the bare resonant plate fit at 545 Hz and 0.094% Damping

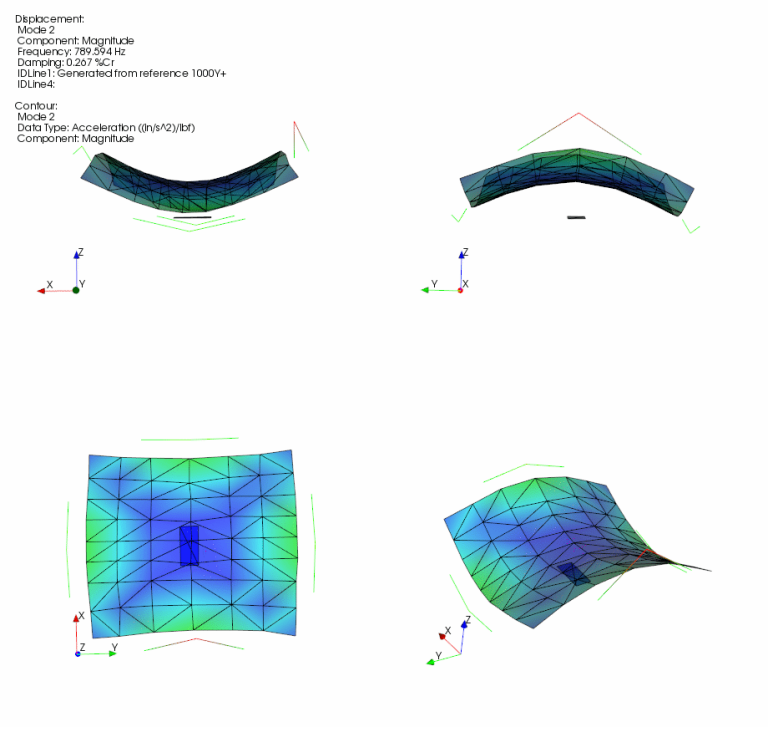

Figure 4-4. 2nd Elastic mode shape of the bare resonant plate fit at 790 Hz and 0.267% Damping

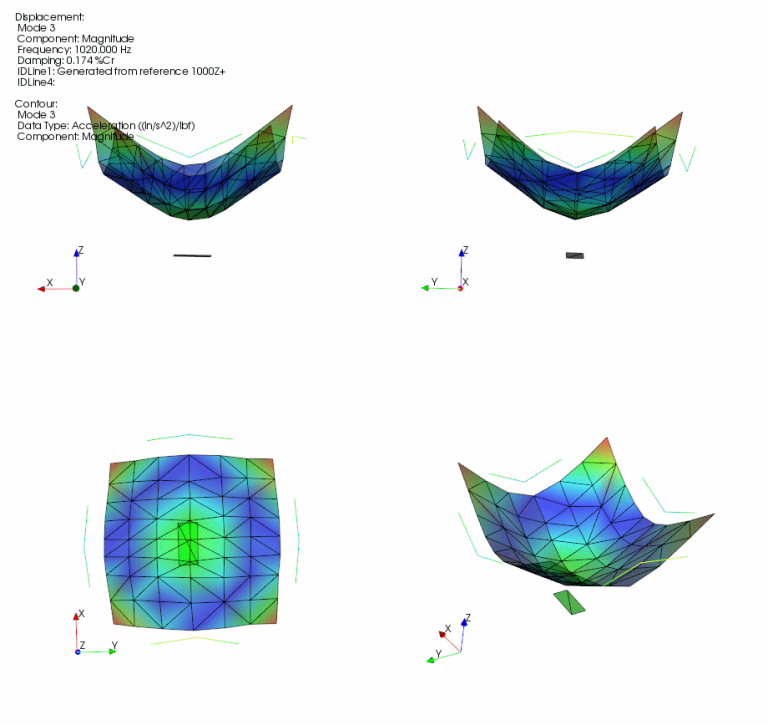

Figure 4-5. 3rd Elastic mode shape of the bare resonant plate fit at 1020 Hz and 0.174% Damping

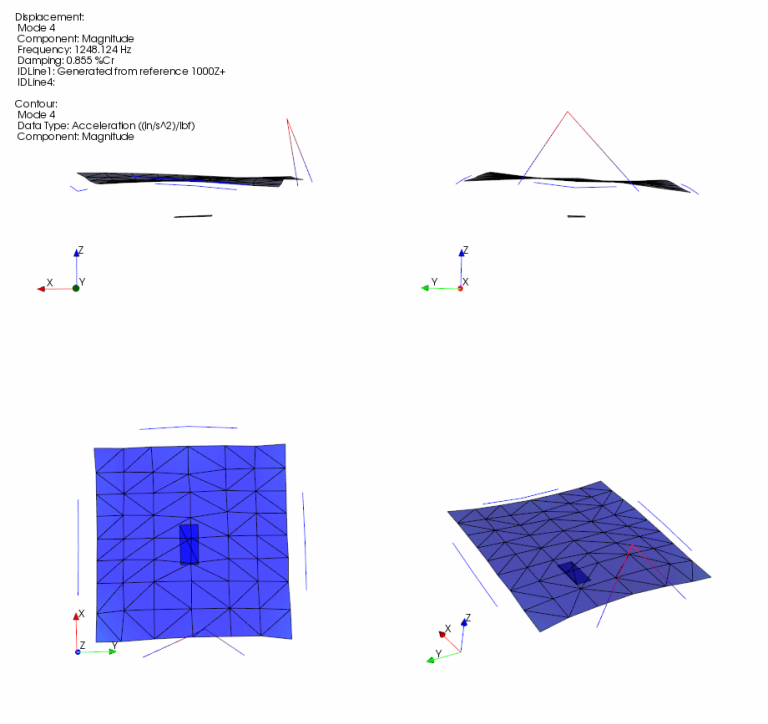

Figure 4-6. 4th Elastic mode shape of the bare resonant plate fit at 1248 Hz and 0.855% Damping

Figure 4-7. Nonlinear analysis of the bare resonant plate

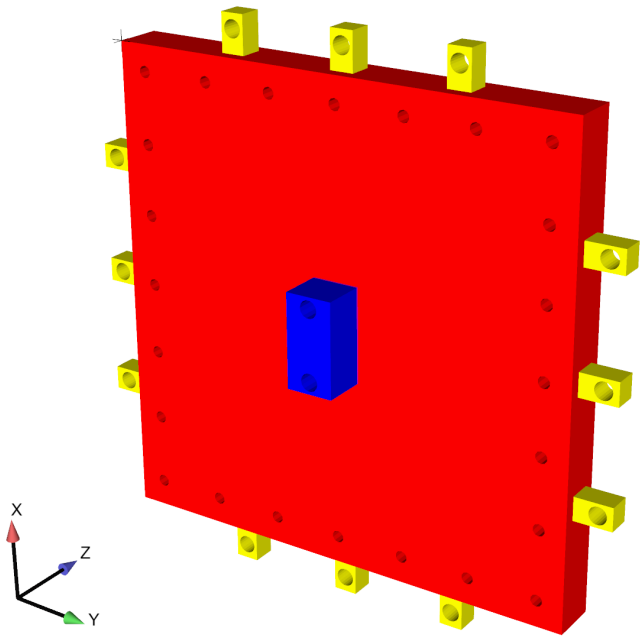

Figure 4-8. Initial model form of the bare plate configuration

experimental modal test parameters. The following model parameters were considered for calibration, but had minimal effect on the dynamics of the structure:

- Paper between the impact block and the resonant plate.
- Modulus of the plate
- Density of the rope anchors

The data show that one of the rope anchors behaves as if it is loose. This is because the rope anchor in question has a local mode that is much lower than the other rope anchor modes and there is no evidence that the measurement is compromised. Instead of trying to model this loose anchor phenomenon, the rope anchor is removed from the FEM.

Another factor in the dynamics is the contact area of the impact block to the resonant plate. Initially, the entire surface between the impact block and resonant plate were fixed to each other. Through calibration, the fixed contact area was modified to only include a circular area around the boltholes of a radius of 0.75".

The final parameter added was the top rope system that connects the resonant plate to the supporting frame as shown in Figure 4-1. The side and bottom rope systems were not included as they did not have tension on them during testing. The ropes were modeled as truss elements, only

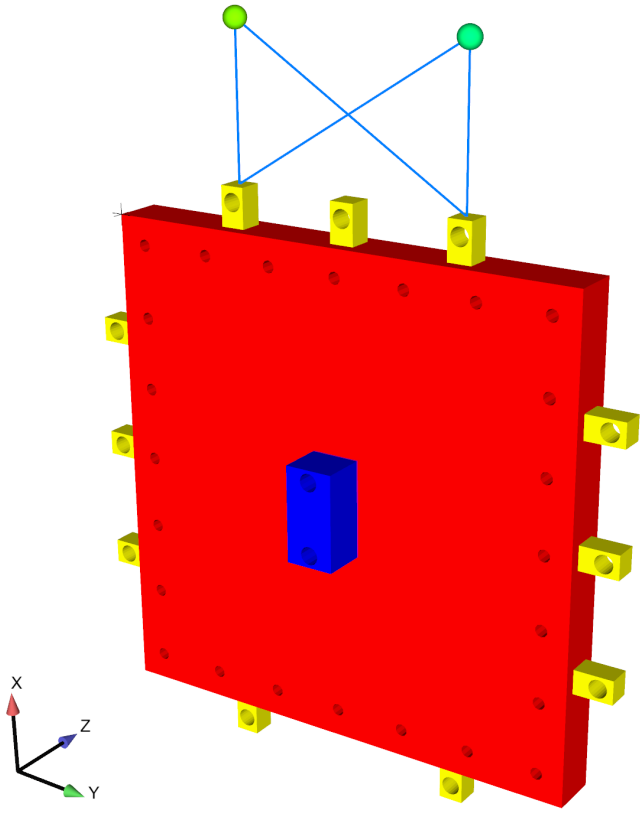

Figure 4-9. Final model form of the bare plate configuration

having axial stiffness. The ropes connected the top anchors to fixed points as shown in the final bare plate model configuration shown in Figure 4-9.

Natural frequencies and the modal assurance criteria (MAC) were computed and compared between the model and test data during the calibration effort. The comparison between the initial model and the test data is in Figure 4-10. The comparison shows very good agreement between test and model of the first three modes and not again until higher frequency modes. After the model changes detailed above were made, the comparison between the final model and the test data were redone and is in Figure 4-11. One of the goals of this report is to understand the effect of the boundary conditions of the resonant plate. Therefore, the ropes were removed from the final model and the comparison between the model without ropes and the test data can be seen in Figure 4-12. The removal of the ropes from the model causes the model to no longer correlate well to modes 6, 7, and 8 of the test data.

The conclusion of the calibration effort to the resonant plate without damping bars is that the model needs to include the rope anchors, proper joint modeling of the impact block, and ropes to represent the dynamics of the hardware. Even with the inclusion of these parameters, there is error in the model. A possible source of error is the effects of the side and bottom rope systems that are not included in the model. Another possible error is the complete elimination of the bottom rope anchor. Although removing the loose rope anchor improves the comparison between

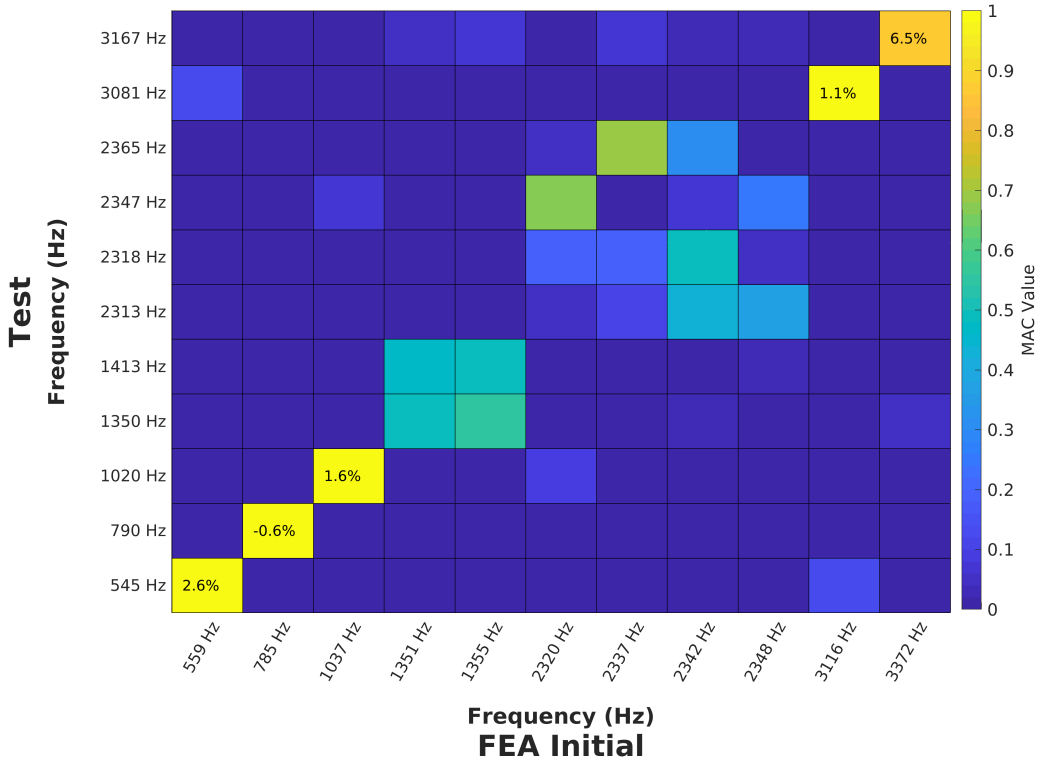

Figure 4-10. Test data compared to the initial finite element model

the model and test data, there probably are still mass effects of the rope anchor that the simplification does not consider.

4.3. Modal Test of the Plate with Damping Bars

The damping bars were installed on the 1000 Hz resonant plate in its laboratory test configuration and an experimental modal test was conducted. A photo of the test setup is in Figure 4-13. The 3D laser doppler vibrometer system was used to measure the responses and an automatic hammer was used to excite the structure. The response locations measured on the front side of the plate are shown as grey stickers in Figure 4-14. Not shown is the response measurements on the impact block.

Although the damping bar response was measured, it is not the goal of this finite element model to accurately model the motion of the damping bars. The goal of this model is to characterize the response of the resonant plate and the effects the damping bars have on the resonant plate.

The modal parameters are fit to the data using the SMAC [6] algorithm. A subset of the modes fit to the data are shown in Appendix B. The calibration of the model excludes the modes that are local to the balance rods or the damping bars.

Hammer hits on the impact block were imparted at multiple levels to determine linearity of the resonant plate with damping bars. Frequency response functions between this impact location and

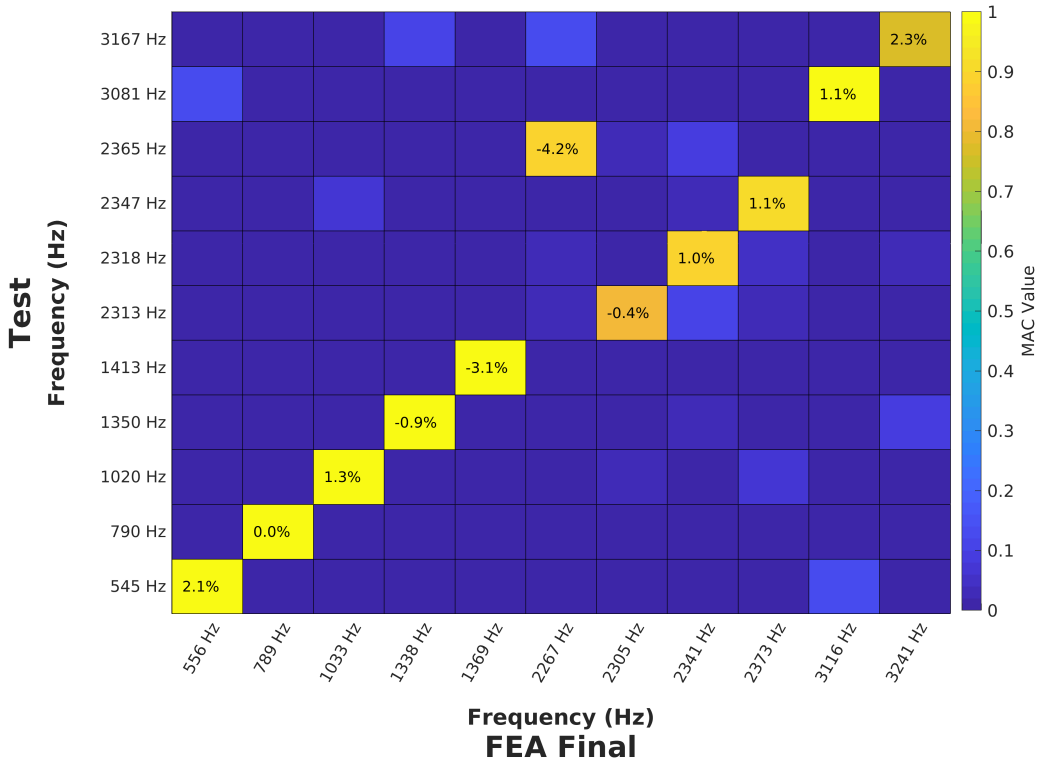

Figure 4-11. Test data compared to the final finite element model

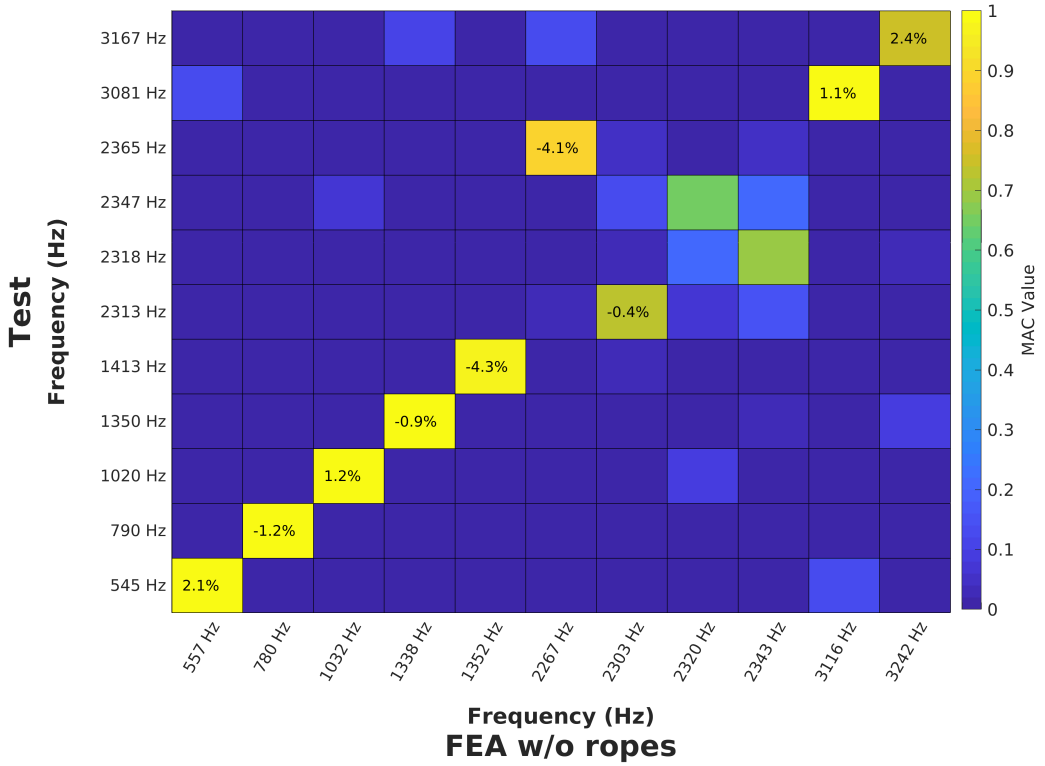

Figure 4-12. Test data compared to the final finite element model without modeled ropes

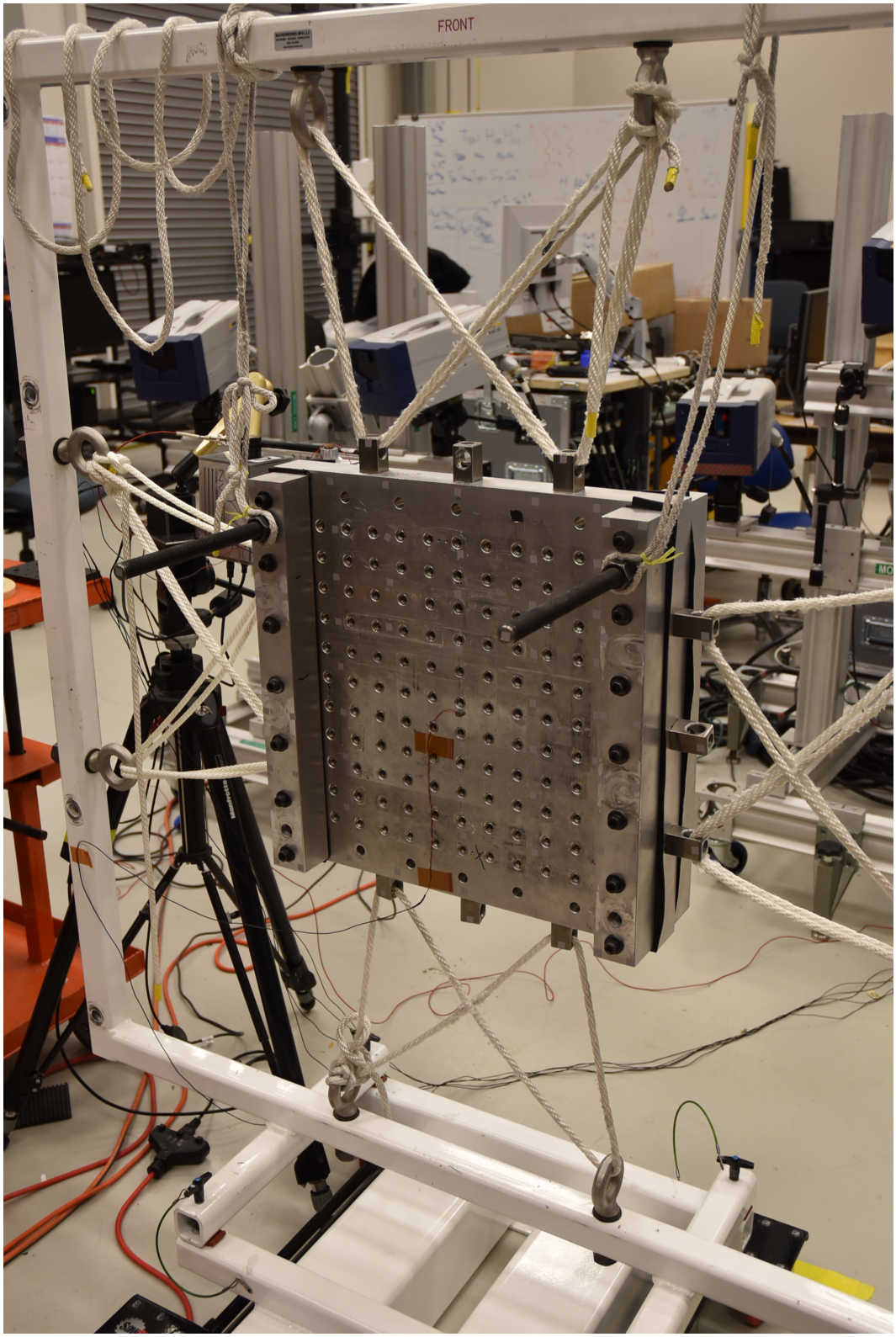

Figure 4-13. Overview of the modal test setup for the resonant plate with damping bar configuration

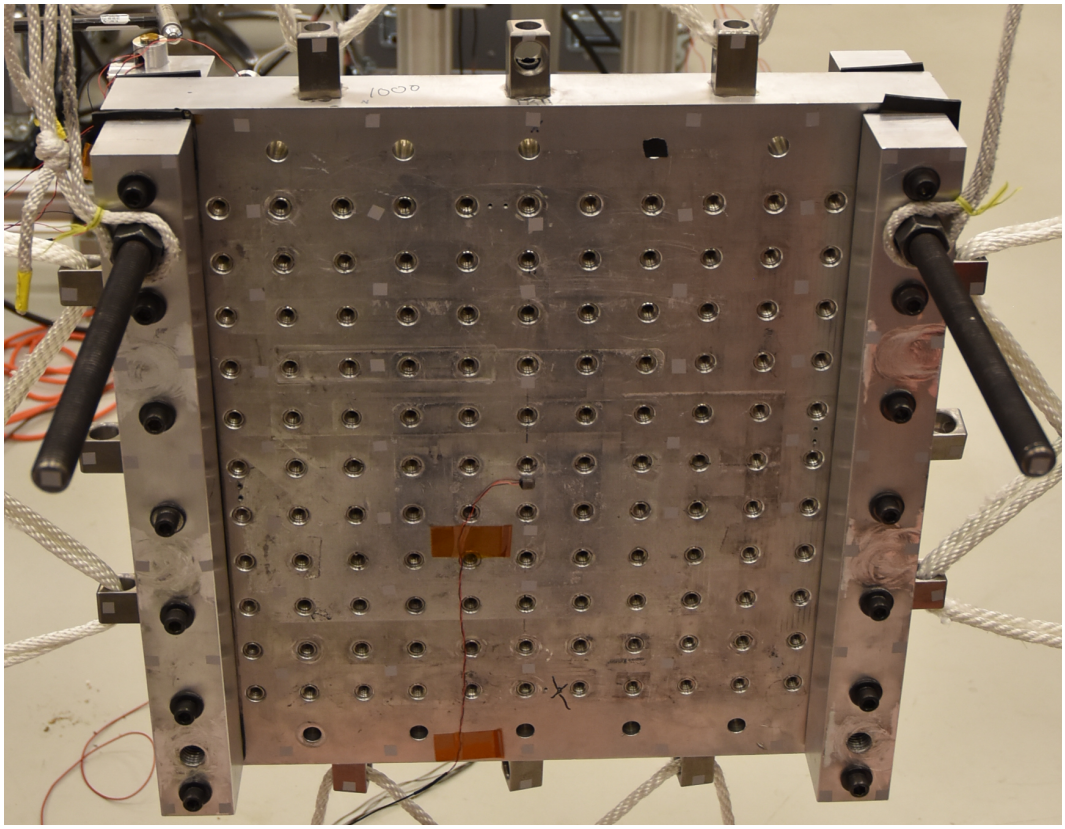

Figure 4-14. Locations of the response measurements as indicated by the grey stickers

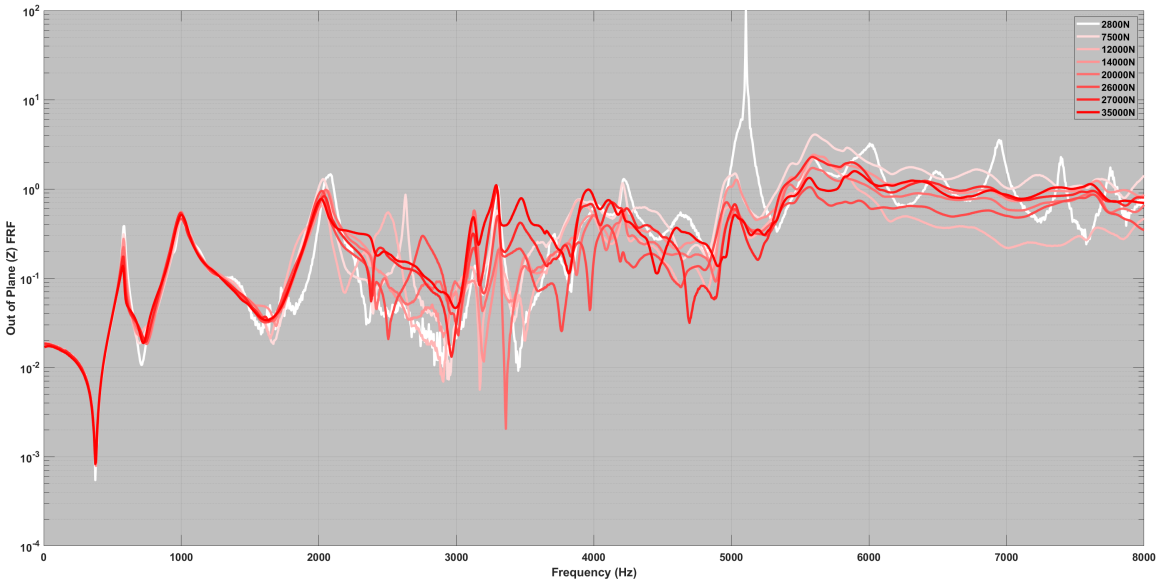

Figure 4-15. Nonlinear analysis of the resonant plate with damping bars

a drive point accelerometer on the other side of the resonant plate were calculated for each of the hits and plotted in Figure 4-15. This non-linearity test shows several modes change frequency and damping values with respect to different input force levels. These shifts in natural frequency and damping should change even more during an actual resonant plate test.

4.4. FEM Calibration of Resonant Plate with Damping Bars to Modal Data

The initial model for the resonant plate with damping bars is the final version of the bare plate configuration with the damping bars added and is shown in Figure 4-16.

The construction of the connection between the damping bars and resonant plate was the focus of the calibration and there were many parameters considered. A difficulty of modeling the test configuration was how to include the rubber material pressed in between the aluminum damping bars and the aluminum resonant plate. The model of the damping bars's connection to each other and the resonant plate is in Figure 4-17. The parameters considered for this calibration were as follows:

- Connection area between the rubber and the resonant plate
- Modulus of the rubber
- Bolt radius
- Bolt modulus

Two different configurations are considered for connecting the rubber to the resonant plate and damping bars. The first connection configuration is to imprint and merge the entire surface of the rubber to the resonant plate. The second method is to imprint and merge just a circular area

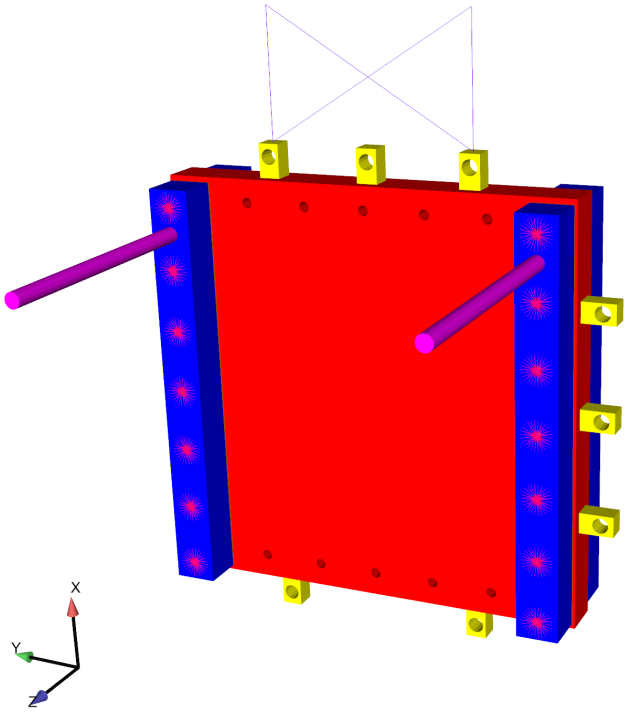

Figure 4-16. Initial model form of the resonant plate with damping bars configuration

around each of the boltholes that connects the two damping bars. An illustration of this circular area is in Figure 4-17.

The damping bars are held in place by a series of 3/8 inch bolts that are equally spaced along the length of the damping bar as shown in Figure 4-13. These bolts have a grip length of approximately 6 inches and are deemed significant to the motion of the damping bars and their coupling to the resonant plate. Each of the bolts is modeled with beam elements that span the grip length of the outer edge of one damping bar to the other. Rigid elements tie the ends of the beam elements to an annular area around the bolthole. An illustration of this configuration is in Figure 4-17.

Several configurations of the model are iterated upon in order to minimize the difference between the FEM's modal parameters and the experimental modal data. The parameters of these iterations are in Table 4-1. Optimization algorithms were not used to better match the model to the data because there is expected to be a lot of unit to unit variability for the dynamics of the resonant plates with ropes and damping bars.

The initial comparison between the test data and the FEM is shown as a MAC plot in Figure 4-18. In this MAC plot and every subsequent MAC plot in this section, several FEM modes are not included due to multiple local modes of the balancing rods and damping bar bolts. These modes are removed to increase the clarity of the comparison between the important modes and their matches to the test data.

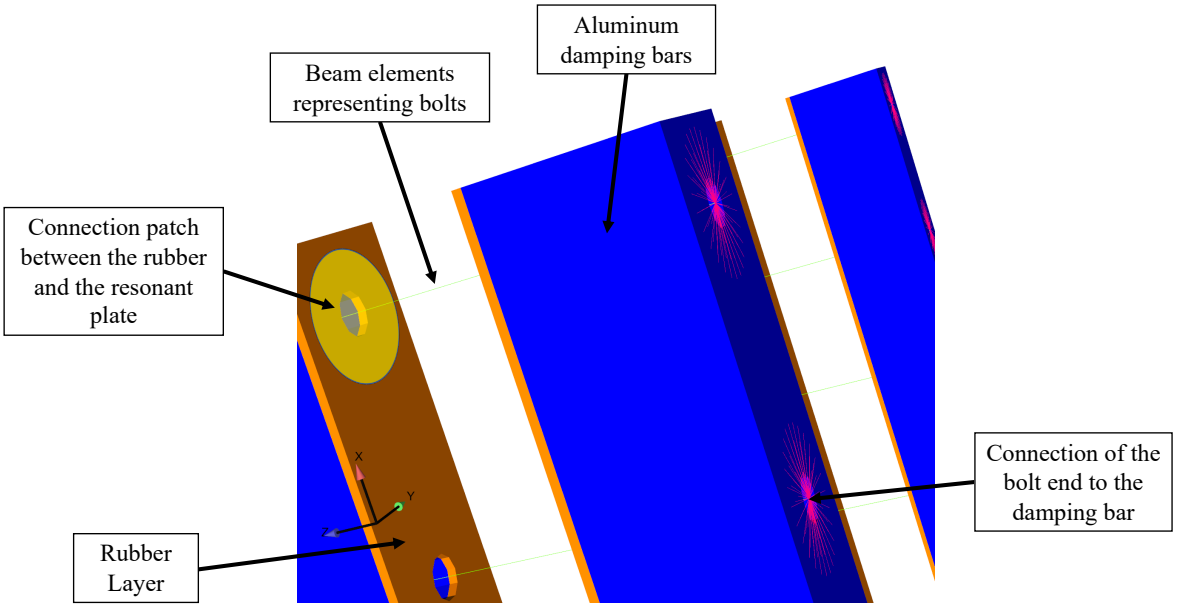

Figure 4-17. Model form of the damping bar, bolt, and resonant plate joints

Table 4-1. Runs, parameters, and results used to calibrate the resonant plate with damping bar FEM. Config RevC is full connection between resonant plate and rubber. Config RevB is the annular connection between resonant plate and rubber.

								Test Mode Number									Test Mode Number								
Model Parameters								2	3	9	11	15	16	17	18	21	2	3	9	11	15	16	17	18	21
Run #	Config	rubber E	Rope E	Bottom tab	bolt radius (in)	Bolt E	Rod E	MAC									Percent Frequency Difference								
run002	revB	1450		include	0.25	28e6	28e6	0.809									-12.7								
run003	revC	1450		include	0.25	28e6	28e6	0.968	0.630		0.811	0.771					-5.1	-33.2		-7.4	-21.2				
run004	revC	3000		include	0.25	28e6	28e6	0.993	0.836	0.720	0.635	0.839			0.635		-2.0	-16.7	-0.8	-5.7	-13.2			-7.9	
run005	revC	3000		remove	0.25	28e6	28e6	0.993	0.833	0.748	0.642	0.832			0.636		-2.0	-16.7	-0.3	-5.7	-12.1			-7.9	
run006	revC	3000		remove	0.35	28e6	28e6	0.991	0.844	0.740	0.946	0.852	0.741		0.961		-4.7	-17.8	-0.9	-6.6	-13.9	-13.8		-0.8	
run007	revC	3000		remove	0.25	35e6	28e6	0.993	0.835	0.746	0.774	0.849			0.953		-1.9	-16.5	-0.1	-5.3	-12.0			-0.2	
run008	revC	6000		remove	0.25	35e6	28e6	0.997	0.961		0.938	0.874	0.804	0.804	0.957		0.0	-5.0		-1.6	-6.6	-6.8	-6.2	0.9	
run009	revC	6000		remove	0.25	35e6	28e7	0.995	0.960			0.864	0.774	0.699	0.939		3.9	2.6			-6.9	6.1	-5.3	1.5	
run010	revB	12000		remove	0.25	28e6	28e6	0.994	0.874	0.689	0.934		0.782	0.734			-1.5	-14.5	1.8	-3.0		-8.5	-8.2		
run011	revB	120000		remove	0.25	28e6	28e6	0.997	0.974	0.829	0.830						2.7	4.2	21.8	23.1					
run012	revB	120000		remove	0.25	35e6	28e6	0.997	0.974	0.829	0.862						2.7	4.2	21.9	23.2					
run013	revC	12000	5.80E+06	remove	0.25	28e6	28e6	0.998	0.985	0.890	0.897	0.844	0.660	0.684	0.943		1.6	0.8	5.9	3.9	-1.8	-0.1	-0.1	2.7	2.8
run014	revC	12000	2.80E+06	remove	0.25	28e6	28e6																		
run015	revC	9000	2.80E+06	remove	0.1875	28e6	28e6	0.998	0.982	0.744	0.952	0.863	0.773	0.695	0.955		2.5	-0.2	3.8	2.5	-3.0	-3.0	-2.0	2.2	
run016	revC	12000	2.80E+06	remove	0.1875	28e6	28e6	0.998	0.985	0.885	0.886	0.832	0.686	0.673	0.955		3.1	1.7	6.5	5.1	-0.9	-0.1	0.3	3.1	

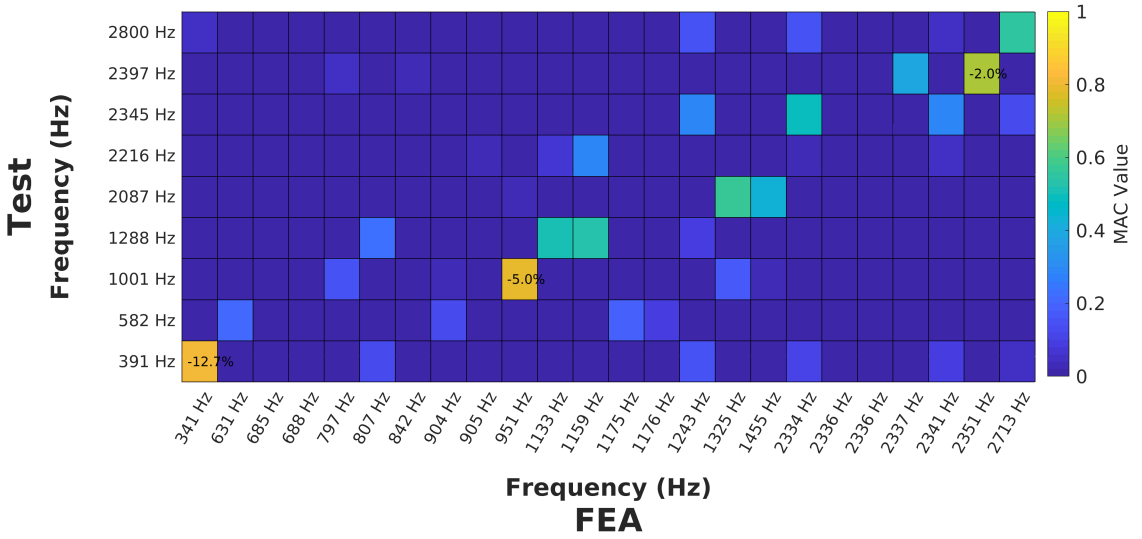

Figure 4-18. Initial comparison between the resonant plate with damping bar FEM and test data

Also not included in these comparisons are all of the modes fit from the test. The test measured local modes of the balancing rods and damping bars. The goal of this model is not to model the response of the damping bars, but the resonant plate. Therefore, these local modes are manually removed from the calibration of the model.

After the calibration process shown in Table 4-1, the final parameters for the model are selected to match those from run015. The comparison between the FEM and modal data for this final configuration is in Figure 4-19. Only the FEM modes that pertain to the test data are shown in order to help with clarity.

Although the final comparison in Figure 4-19 is much improved over the initial comparison, some of the modes had MAC values that are less than desired. After visual examination of these modes, the main decrease of the MAC value is due to the degrees of freedom on the damping bars. As stated previously, these degrees of freedom are not the priority. To mitigate the degrees of freedom of the damping bars on the effect on the MAC calculation, they are removed from the MAC calculation and only the resonant plate degrees of freedom are compared. The resultant comparison can be seen in Figure 4-20. Visualizations of the FEM modes can be seen in the Figures in Appendix C. Removal of the damping bar degrees of freedom from the MAC calculation shows that the model does a good job of calculating the motion of the resonant plate degrees of freedom.

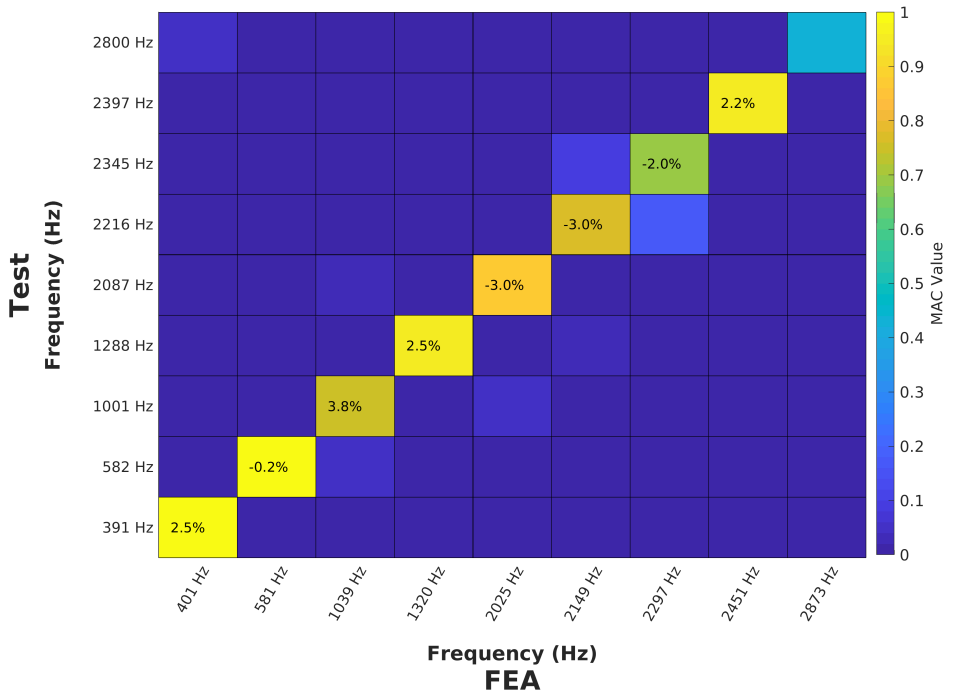

Figure 4-19. Final comparison between the resonant plate with damping bar FEM and test data

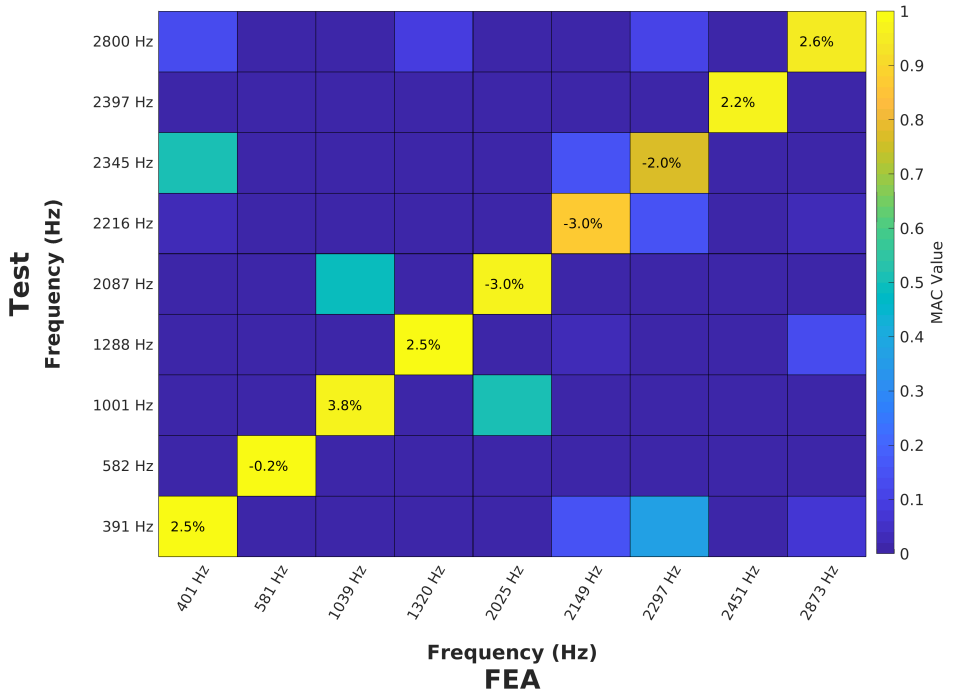

Figure 4-20. Final comparison between the resonant plate with damping bar FEM and test data without including the damping bars in the MAC calculation

5. DATA PROCESSING OF RESONANT PLATE

This chapter describes the data processing and results of the resonant plate impact tests on the resonant plate with and without damping bars. This chapter also details the many shock test runs that were acquired to be the basis of evidence to answer many questions of the resonant plate environment and provide further calibration and validation data for the finite element model. The objectives of these test runs are as follows:

- What is the hit to hit variability for a nominally identical hit?
- What are the mode shapes of the plate at shock levels and how do they compare to the low level experimental modal results?
- Can the projectile impact force be calculated during the environment and what is that force in the time and frequency domain?
- Does the rope suspension system have an effect on the plate dynamics and can it be quantified?
- What are the modal frequencies and damping for modes measured during test?

The procedure of processing the data in this report is uncommon to typical resonant plate signal processing as the objectives of the test are different than comparing the shock response spectrum to a specification. The procedure is visualized in a flow chart in Figure 5-1 with the data quality checks at the appropriate steps. Each of these steps are detailed in the following sections.

The shock data was acquired over three separate test times in two separate resonant plate test cells. Each of the three tests have different test sequence numbers with a corresponding run log. These run logs are in Appendix D. There were many different configurations of the test setup with respect to the configuration of the plate, inclusion of a test fixture, and location of the test fixture and impact. The data in this chapter focuses on the data acquired on the resonant plate with damping bars and no attached fixture from test sequence SHK5142. Photos of the test setup can be seen in Figure 5-2. The chapter on validating the model to the test environment uses the data from the other test sequences.

5.1. Data Acquisition and Quality Checks

The resonant plate was instrumented with 24 uniaxial Endevco 7270 accelerometers. Each of these accelerometers measured the acceleration in the out of plane direction of the plate, the Z-axis. The node numbers and general locations of these accelerometers are in Figure 5-3

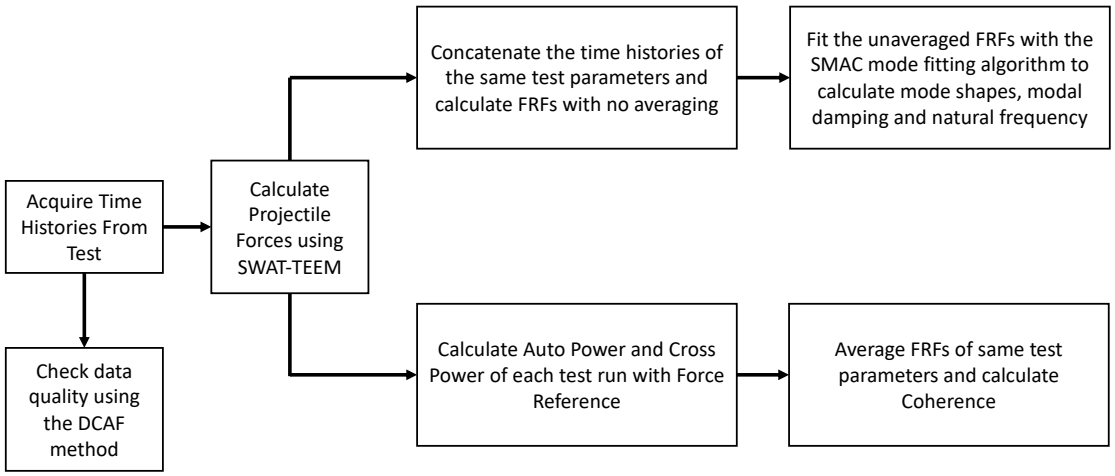

Figure 5-1. Procedure and flow of how data was processed for the resonant plate test with bare plate with and without damping bars.

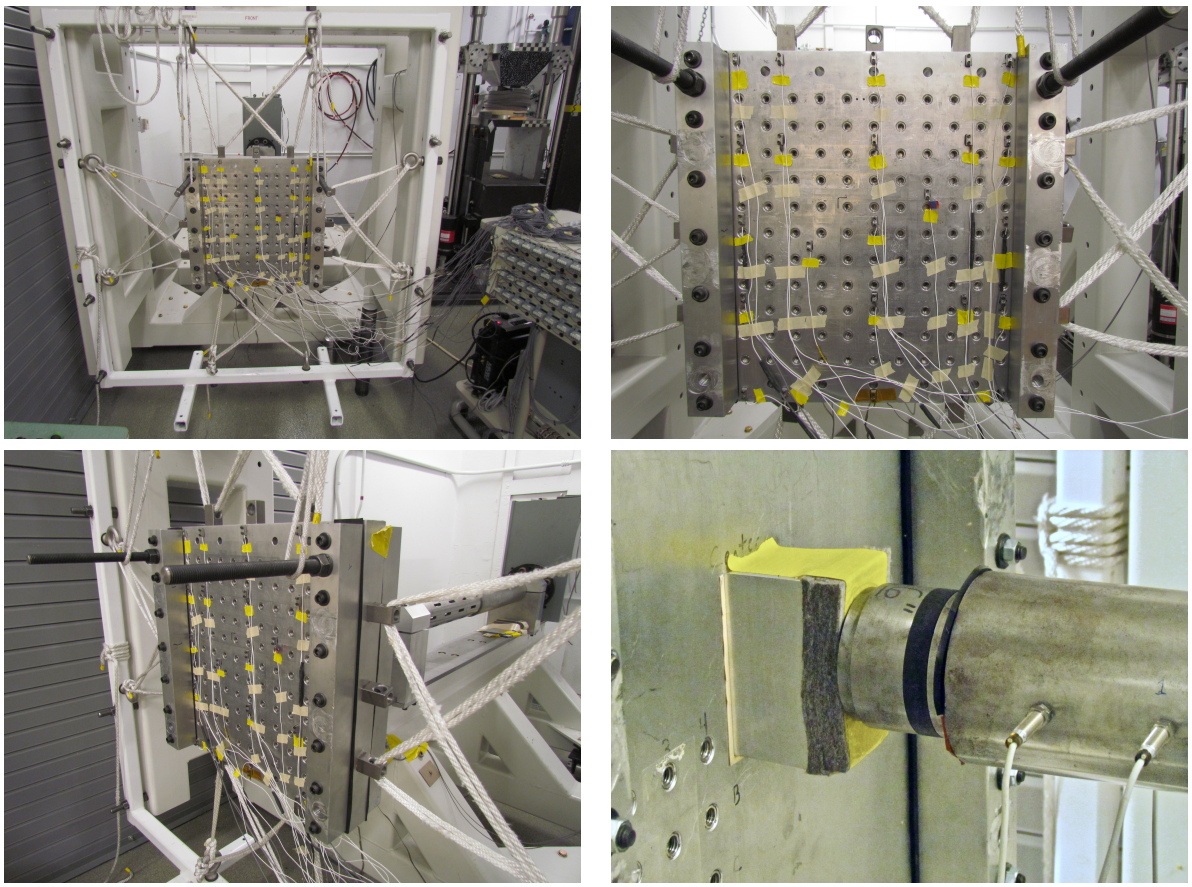

Figure 5-2. Photos of the bare resonant plate with damping bars setup.

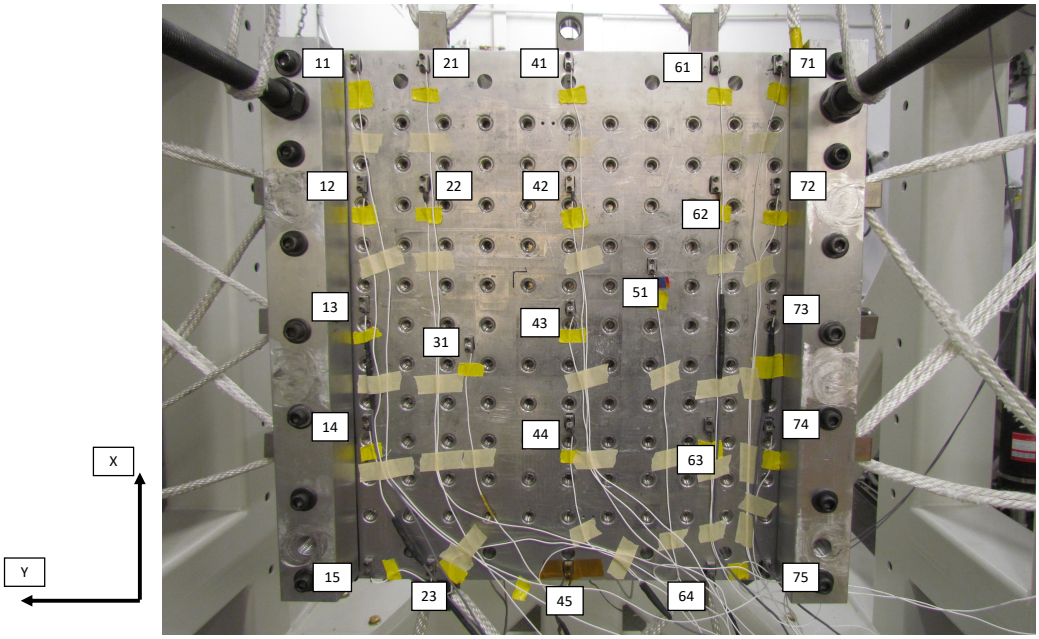

Figure 5-3. Instrumentation location and node numbers for the accelerometers on the resonant plate.

There were many tests executed of the bare plate with damping bars in the SHK5142 test sequence. The general form of the runs was to repeat a shot with identical parameters at least 4 times. This allowed for different "sets" of data and is referenced as sets throughout this report. Sixteen sets of data were taken and are documented in Table 5-1. Some test runs are omitted from the analysis for many reasons including accelerometers falling off during test, clipping, and unacceptable noise in the data.

Runs 14 through 91 from the SHK5142 test series are valid runs. Runs 1 through 13 are omitted from the analysis. It was discovered that the bottom rope anchor that caused issues during the experimental modal tests had a loose Keensert. The rope anchor in question was physically removed from the test configuration after run 13. Runs 18-20 are omitted due to over-ranging of the accelerometers and accelerometers being knocked off during the test. Run 40 is not included as it had an accelerometer fall off during the test.

Some of the test runs underwent a process known as DCAF [2] to check the data quality. This technique uses mode shapes either from a FEM or experimental modal analysis to fit the data using the SEREP expansion technique [10]. The DCAF technique computes the expansion using all of the data except one degree of freedom. The excluded degree of freedom is then compared to the measured data. If there is a huge discrepancy between the expanded data and the measured data, then there is reason to believe that the test data has inconsistencies. This process is repeated for all of the degrees of freedom measured in the test.

The DCAF method was utilized for a subset of test runs. The FEM mode shapes were used as the basis vectors for expansion with the understanding that the FEM was calibrated and should provide reasonable expansion results. The analysis showed that none of the accelerometers

Table 5-1. Table of the run sets and associated test parameters from the SHK5142 test series

Run Set Name	Test Runs	Pressure (psi)	Felt Thk (in)	Projectile Length (in)	Average Projectile Speed (ft/s)
Set 14	[14:17]	10	1/8" Grey	6"	21.5
Set 21	[21:27]	14	1/8" Grey	6"	28.1
Set 28	[28:31]	10	1/8" Grey	6"	21.3
Set 32	[32:35]	10	1/2" Grey	6"	21.4
Set 36	[36:39]	20	1/2" Grey	6"	35.7
Set 41	[41:47]	20	1" Grey	6"	36.0
Set 48	[48:51]	40	1" Grey	6"	53.5
Set 54	[54:57]	50	1" Grey	6"	59.8
Set 58	[58:61]	20	1" Grey	12"	23.9
Set 62	[62:65]	40	1" Grey	12"	37.1
Set 66	[66:68]	60	1" Grey	12"	46.1
Set 69	[69:72]	15	1/2" Grey	12"	19.5
Set 73	[73:76]	25	1/2" Grey	12"	27.8
Set 78	[78:81]	35	1/2" Grey	12"	34.1
Set 82	[82:85]	15	1/8" Grey	12"	19.1
Set 86	[86:91]	25	1/8" Grey	12"	27.5

provided bad data through this. It is noted that this quality check does not mean that all bad data has been removed.

5.2. Force Reconstruction with SWAT-TEEM

The impact force of the projectile on the impact block was reconstructed for all of the test runs in Table 5-1 using the SWAT-TEEM algorithm detailed in Chapter 2. The accelerations were low-pass filtered in order to compute the pseudo inverse. The filter is necessary because the response measurement needs to uniquely identify the shapes in the response measurements and there isn't enough instrumentation to uniquely identify the high frequency shapes. The acceleration data of each run analyzed was filtered at 6kHz. This means that the subsequent calculated force is bandwidth limited to 6kHz. The time domain of each run was examined to determine the appropriate ring-down time history segment as the time steps immediately after the impact are critical in the reconstruction.

Every acceleration measurement is examined in each of the reconstructions to determine if the measurement benefited the reconstruction. It was found that for all test runs analyzed, the acceleration at node 43 either reduced the fidelity or provided no benefit. This reduction in fidelity can be seen in Figure 5-4. The reduction in fidelity is recognized by a change in the pulse by eliminating the degree of freedom that is unchanged by eliminating other degrees of freedom. Another means of observing a reduction in quality of the SWAT-TEEM algorithm is a ring down

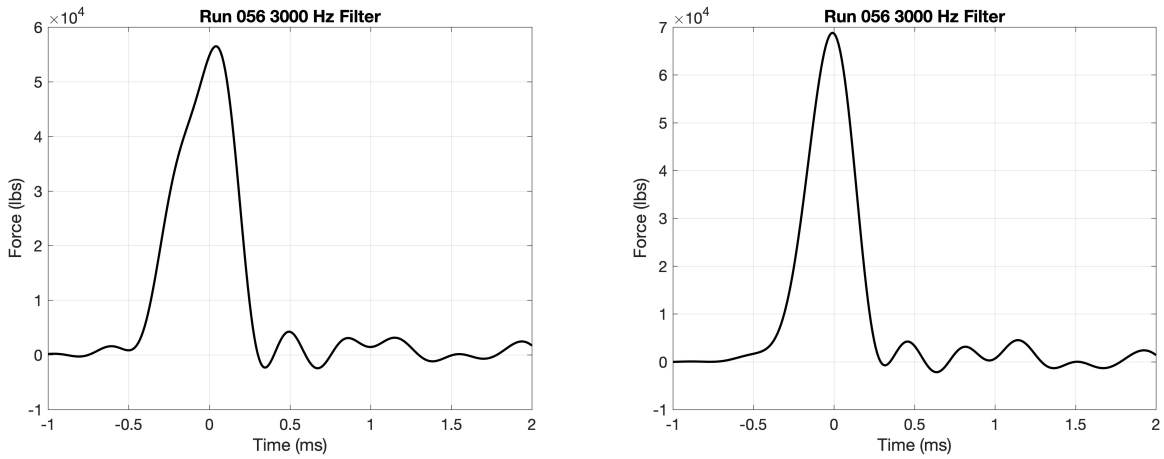

Figure 5-4. The reconstructed force from run 56 prior to the removal of poor responses (left) and after the removal of poor responses (right) from the reconstruction calculation.

in force after the main force pulse. This ring down in force is an artifact of the accelerations not being filtered from the inverse as it is known that the force is zero after impact.

Knowledge of the shape of the input force is a tool in determining the fidelity of the force reconstruction. Another computation to test the integrity of the force reconstruction uses the conservation of momentum shown as

$$mv_0 + \int_{t_1}^{t_2} F(t)dt = mv_f \tag{5.1}$$

where m is the mass of the resonant plate system, v is the velocity of the resonant plate at the initial and final moments, and $F(t)$ is the imparted force calculated by SWAT-TEEM.

Because the initial velocity of the plate is zero for each of the runs, the final velocity of the plate could be calculated by dividing the impulse of the force by the mass of the plate. This was done for runs 32 and 78 when low-pass filtered at 6kHz. These two runs are chosen because run 32 has a projectile with minimal energy while run 78 has a high energy projectile when compared to the whole set of data.

The velocity of the plate is calculated by integrating the accelerations. Although there is a spread of velocities of these integrated accelerometers due to rigid rotations, the velocity calculated through Eqn 5.1 is compared to the general integrated velocities. This integration of the measured accelerations is shown in Figures 5-5 and 5-6. The velocity of the plate calculated through the conservation of momentum is approximately the average of the integrated accelerations for both test runs.

The conservation of momentum process is considered for the projectile instead of the plate. Using the projectile is advantageous as its initial velocity is directly measured and has small uncertainties. However, the projectile bounces back after striking the resonant plate and that speed of the projectile is unknown. Therefore, any calculation using the projectile and assumes the projectile speed is zero after impact would be an underestimate on the change in momentum.

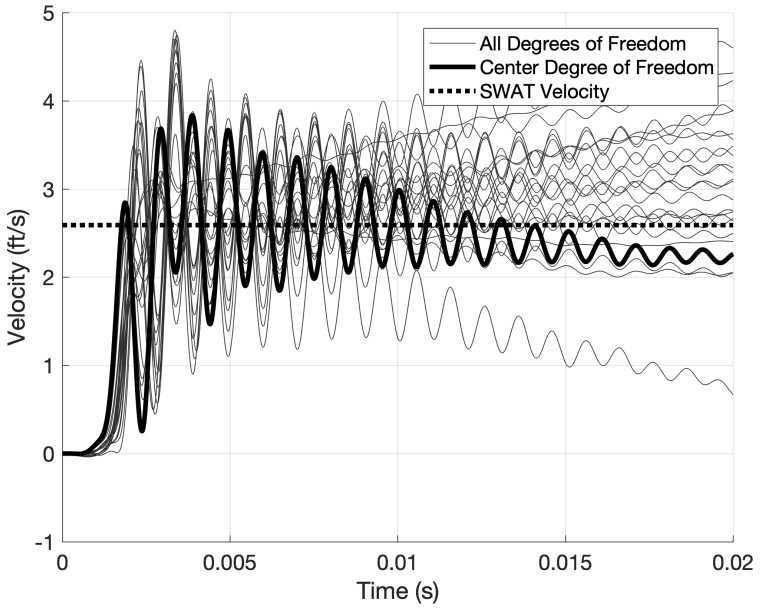

Figure 5-5. Integrated velocities from acceleration responses in run 32 with the response at the center of the plate highlighted. The velocity calculated from the impulse equation using the reconstructed force is 2.59 ft/s.

This form of the conservation of momentum is not used because the velocity of the projectile after impact is not known.

The forces calculated by SWAT-TEEM in this report are transformed into the frequency domain for examination. Examination in the frequency domain allows for direct comparison between the different test parameters and to determine at which bandwidth exists the majority of the energy. This concatenation of forces in the frequency domain can be seen in Figure 5-7.

Conclusions from examining the forces calculated are that the forces are relatively consistent when using the same test parameters: gun pressure, projectile size, felt thickness. Increasing the felt thickness does not significantly change the energy imparted by the projectile. When the felt thickness increases, the length of the pulse increases which reduces the high frequency force and increases the force at low frequencies.

Increasing the gun pressure and consequentially the projectile speed increases the energy of the impact and also reduces the pulse width of the impact. This provides a whole bandwidth increase in load. However, that increase in force is not uniform over the bandwidth.

The last test parameter is the projectile size or weight. An increase in projectile weight with the other parameters constant provides a proportional increase in energy to the resonant plate. Another effect of increasing the weight of the projectile is a change in the pulse width of the force. This increases the forces for lower frequencies and reduces the force at higher frequencies.

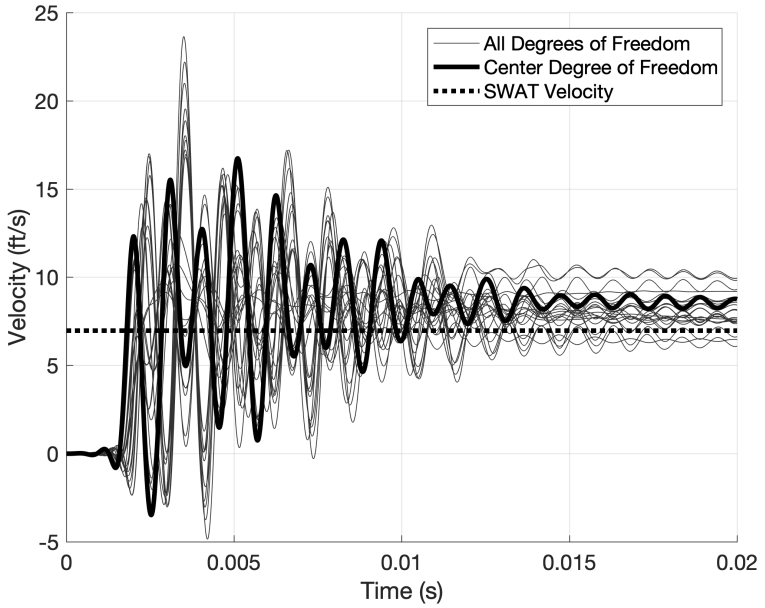

Figure 5-6. Integrated velocities from acceleration responses in run 78 with the response at the center of the plate highlighted. The velocity calculated from the impulse equation using the reconstructed force was 6.97 ft/s.

5.3. Frequency Response Function Creation and Fitting Modal Parameters to Data

From the forces calculated from each test run, Frequency Response Functions (FRFs) were calculated for each run by dividing each of the accelerations by the calculated force in the frequency domain. By using the reconstructed force, there is an understanding that the errors inherent to the force reconstruction calculation cause errors in the FRF calculation. With this knowledge, the FRFs have higher fidelity at lower frequencies due to the high frequency breakdown of the reconstructed forces at high frequencies.

One of the objectives of this work is to determine how linear the system is at shock type levels. The primary indicator used in this analysis is the Coherence function shown as

$$\gamma^2 = \frac{|\hat{G}_{XF}|^2}{\hat{G}_{XX}\hat{G}_{FF}} \tag{5.2}$$

where G_{XF} is the cross power spectra between the response and forcing function, G_{XX} is the auto power of the response, G_{FF} is the auto power of the forcing function, the hat symbol denotes the average over several runs, and γ^2 is the coherence.

The coherence is calculated for many response degrees of freedom over many sets of data averaged together. Since coherence is a function of the force, any error in the calculated force could be exhibited as a poor coherence. A subset of the calculated coherence functions are

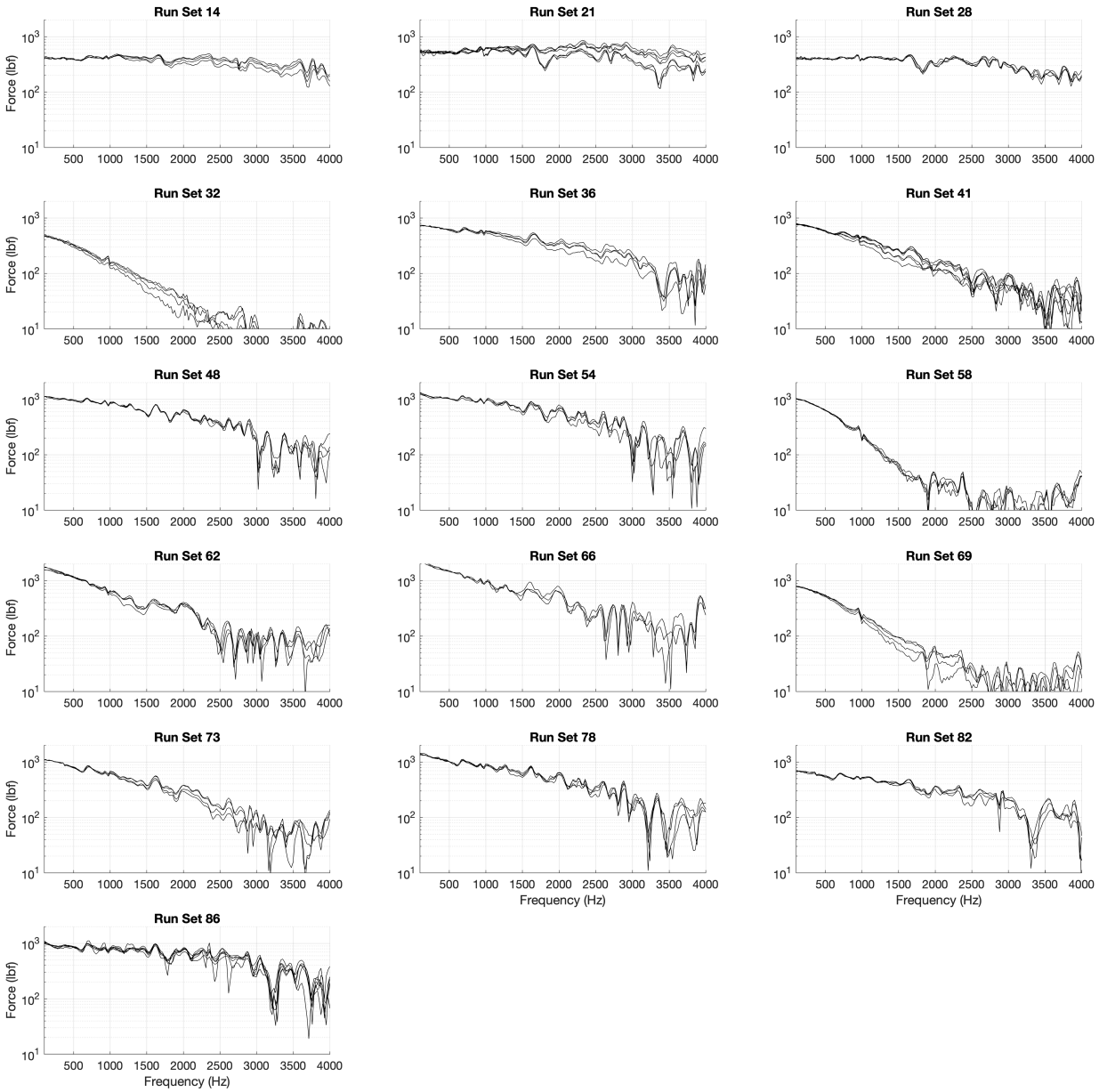

Figure 5-7. Forces of all the shots on the bare resonant plate with damping bars in the frequency domain.

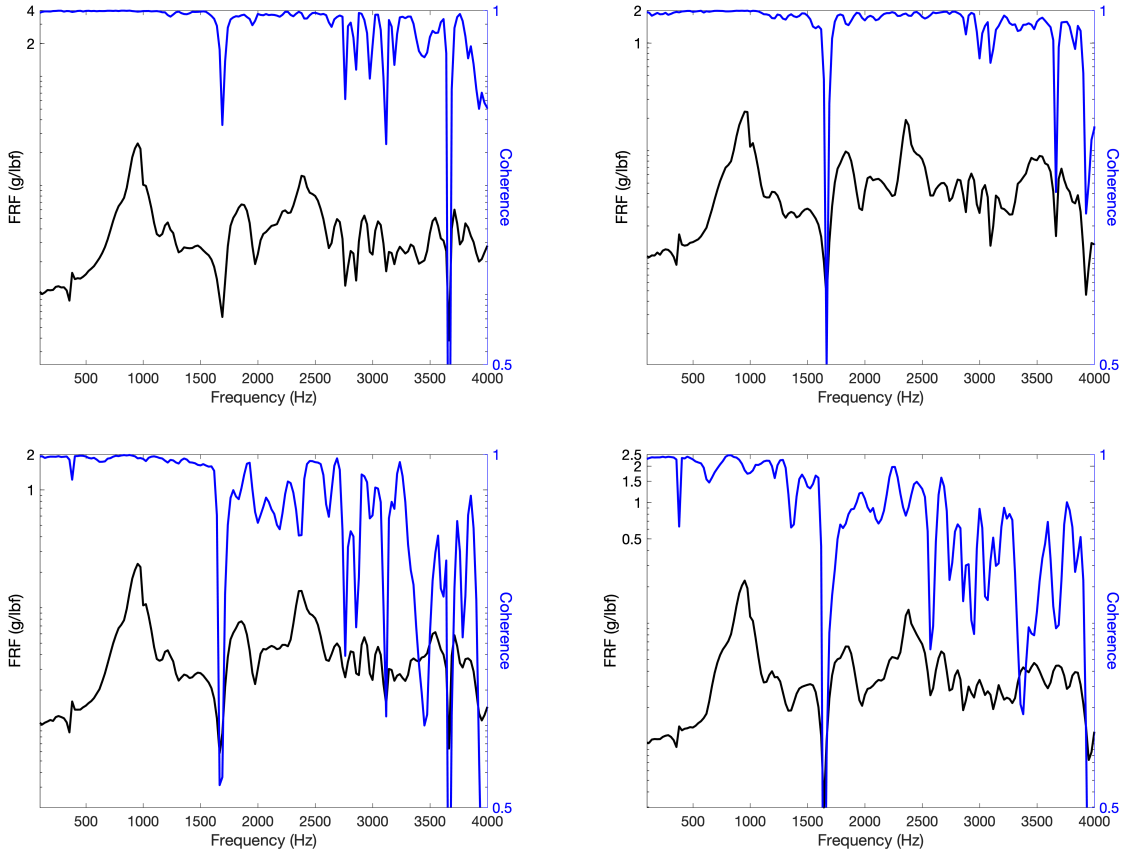

Figure 5-8. FRFs and coherence of node 11 for set 14 (upper left), set 28 (upper right), set 14 + set 28 (lower left), and set 14 + set 21 (lower right).

included here to indicate linearity for shock tests. Coherence of node 11 is plotted for different groupings of shock tests. The FRFs and coherence of these runs can be seen in Figure 5-8.

The top two coherence plots in Figure 5-8 are of the two individual sets of data from set 14 and 28. Each plot averaged four test runs and the coherence between the four runs with identical parameters is very high, greater than 0.97, except at frequencies of anti-resonances. The top two plots show that the repeatability of shots with identical test parameters is very good and can produce a linearized estimation of the FRF at the tested forcing level.

One objective of this research is to determine if the ropes have an effect of the dynamics of the resonant plate. Sets 14 and 28 are tested to the same test parameters besides their boundary conditions. Set 28 had the side and bottom ropes effectively removed from the test setup while set 14 had those ropes with tension typical to resonant plate tests.

The lower left plot of Figure 5-8 shows the coherence of all the test runs of sets 14 and 28. The coherence for the runs with side ropes and without side ropes included are high for frequencies below 1500 Hz, however, the coherence drops at frequencies above that which indicate a change in FRFs between the two sets. This change in FRFs can be cause either by a change in the system or non-linearities in the system. Since the test levels are shown to be very repeatable and sets 14

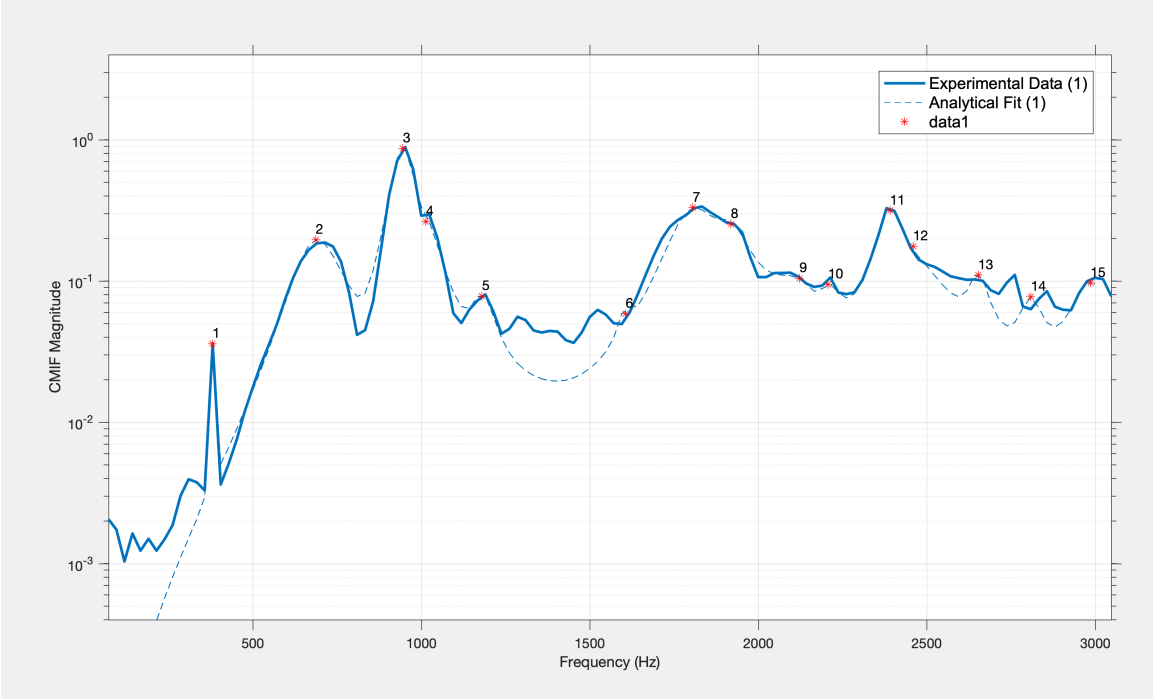

Figure 5-9. Resynthesized CMIF from fit modal parameters to the CMIF from data for set 14.

and 28 had the same test parameters, it is determined that the side ropes cause a change in the resonant plate dynamics above 1500Hz. This conclusion corroborated the result seen in the modal calibration in Chapter 4. This comparison does not investigate the removal of the top ropes that participate in most of the support of the resonant plate.

The difference between sets 14 and 21 is the speed of the projectile due to the increased pressure in set 21. The coherence of the combination of the runs from these two sets can be seen in the lower right plot of Figure 5-8. This plot shows that there is an overall reduction in coherence that indicates non-linearities present in the data due to the change in forcing function. However, the main modes of the plate below 1500 Hz still all have coherence above 0.9. This result shows that the system is fairly linear for the first plate modes.

The FRFs averaged from a set are combined and modal parameters are fit to the FRFs using the SMAC [6] algorithm. There are a couple of challenges when fitting the modal parameters. The first is that some of the modes have high damping and the second is the large frequency spacing in the frequency domain due to the short duration of the test environment. Even though there are difficulties, the modal fits are calculated and the resynthesized Complex Modal Indicator Functions (CMIFs) for sets 14 and 28 show good comparison to the measured CMIF as shown in Figures 5-9 and 5-10 respectively. The quality of the modal parameter fits are indicated by how well the reconstructed CMIF matches the test data CMIF.

One of the benefits of fitting the modal parameters of the resonant plate at shock force levels is to get an estimation of damping. There is no good method of predicting damping for such a complicated structure. Fitting the data using a modal fitter such as SMAC also provides better estimates of the natural frequency than peak picking in the frequency domain. The modal

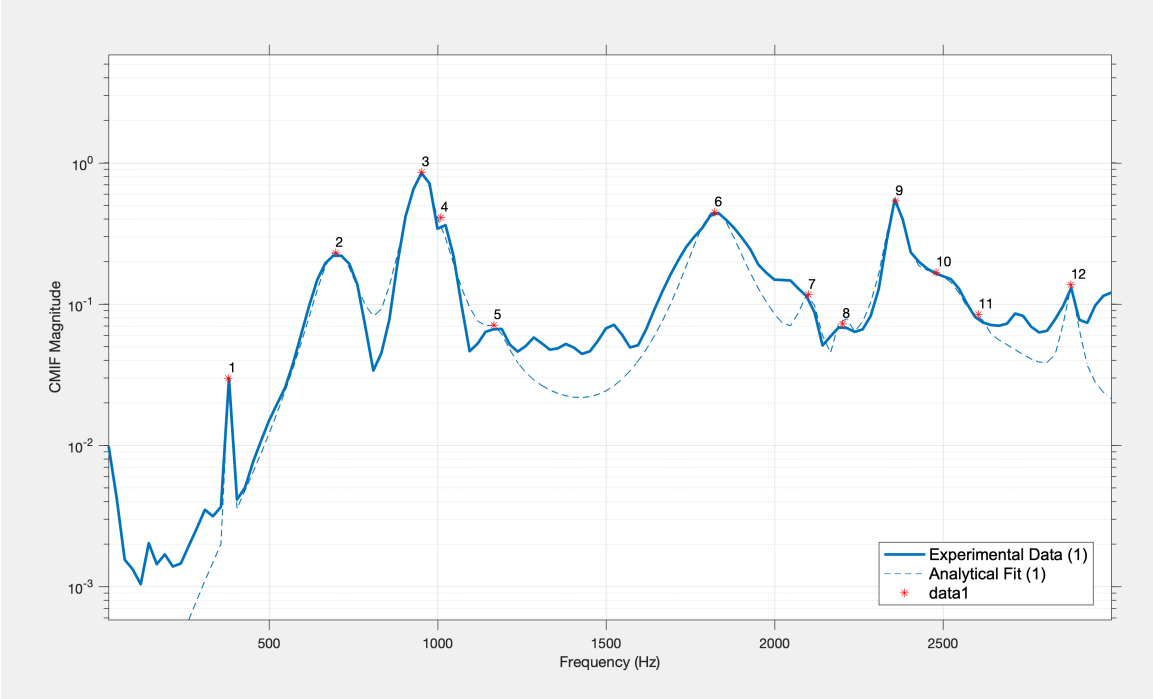

Figure 5-10. Resynthesized CMIF from fit modal parameters to the CMIF from data for set 28.

parameters for corresponding modes for sets 14, 28, and 86 are compared to the experimental modal analysis in Table 5-2.

Table 5-2 provides a comprehensive comparison of the dynamics of the resonant plate at low and high levels, providing an insight on the nonlinearities of the structure. There are two observations regarding the nonlinearities of the system. The first is that the damping increases as the input force increases, although not equally mode per mode. This is a typical nonlinear phenomena. The second observation is that all the modes decrease in natural frequency when the input force increases, except for mode two. Mode two is different as its damping drastically increases and its natural frequency also increases as input force increases.

Not all of the shapes fit from the data are clear with respect to a unique shape and not all of the shapes are fit from the data. The fitting of the data could be done for each data set, but only sets 14, 28, and 86 are shown here. Three Modal Assurance Criteria (MAC) plots are computed to compare the shapes and frequencies between different modal sets of data. In these MACs, only shapes that are well defined in the test are used.

The MAC and natural frequency comparison between sets 14 and 28 can be found in Figure 5-11. This comparison shows only small differences between the shapes and frequencies. As previously stated, not all of the modes are fit from the data due to the short time histories, but from the set of modes shown here, there appears to be only small differences between the configuration with and without side ropes.

Another useful comparison is between a low level impact and a high level impact. The purpose of the comparison is to determine if there is a shift in modal parameters due to the non-linearities of

Table 5-2. Comparison of modal damping levels from experimental modal tests and resonant plate shock tests. Shapes of the modes correspond to the FEM shapes in Appendix C. NF = Mode Not Found

Mode Parameter	Exp Modal Test	Set 14	Set 28	Set 86
Mode 1 Frequency	391 Hz	380 Hz	379 Hz	383 Hz
Mode 1 Damping	0.35%	1.2%	0.41%	0.40% Hz
Mode 2 Frequency	582 Hz	686 Hz	697 Hz	656 Hz
Mode 2 Damping	1.4%	12%	9.6%	6.9%
Mode 3 Frequency	1001 Hz	945 Hz	953 Hz	952 Hz
Mode 3 Damping	2.6%	4.2%	5.1%	3.9%
Mode 4 Frequency	1288 Hz	1180 Hz	1167 Hz	NF
Mode 4 Damping	2.5%	3.6%	4.5%	NF
Mode 5 Frequency	2087 Hz	1805 Hz	1822 Hz	NF
Mode 5 Damping	1.0%	4.8%	4.0%	NF
Mode 8 Frequency	2397 Hz	NF	2359 Hz	NF
Mode 8 Damping	0.93%	NF	1.2%	NF

the system. The two sets chosen for comparison are sets 14 and 86. The comparison computed between sets 14 and 86 is in Figure 5-12. This comparison shows a slight shift in the frequency when going to higher input levels. Some shapes appear to change when going from low to high levels. A deep dive investigation to the change in shapes is not included in this report.

The FEM is calibrated to the experimental modal data as discussed in Chapter 4. The calibrated model is compared to the modal parameters fit to set 28. The comparison between the modal parameters fit from set 28 and calculated from the finite element model can be found in Figure 5-13. The comparison shows that the modes of the finite element model still have good agreement when compared to the shock level modal parameters. The comparison shows that most of the natural frequencies of the hardware decreased except for the second natural frequency.

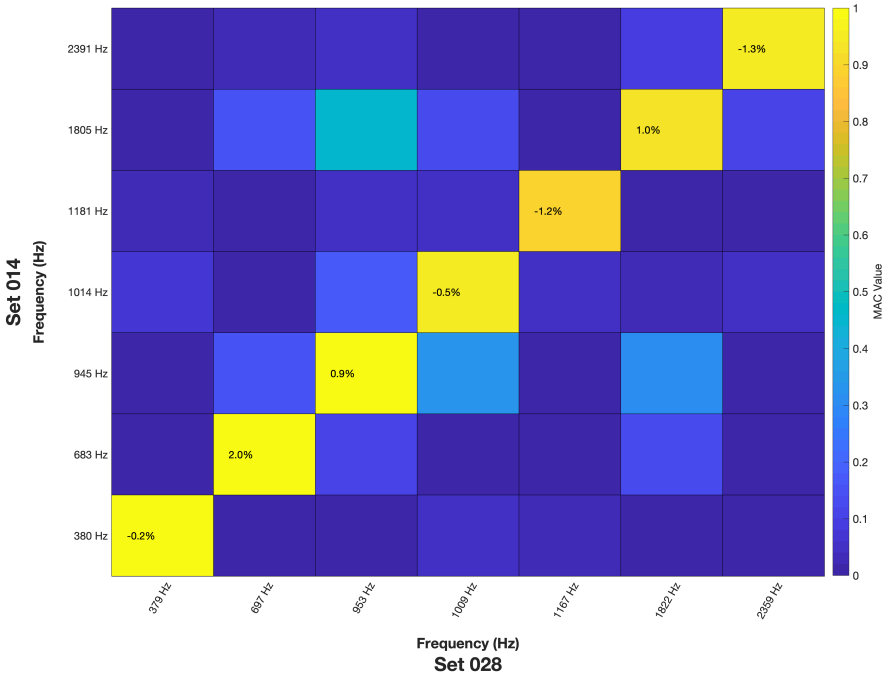

Figure 5-11. MAC and frequency comparison between sets 14 and 28.

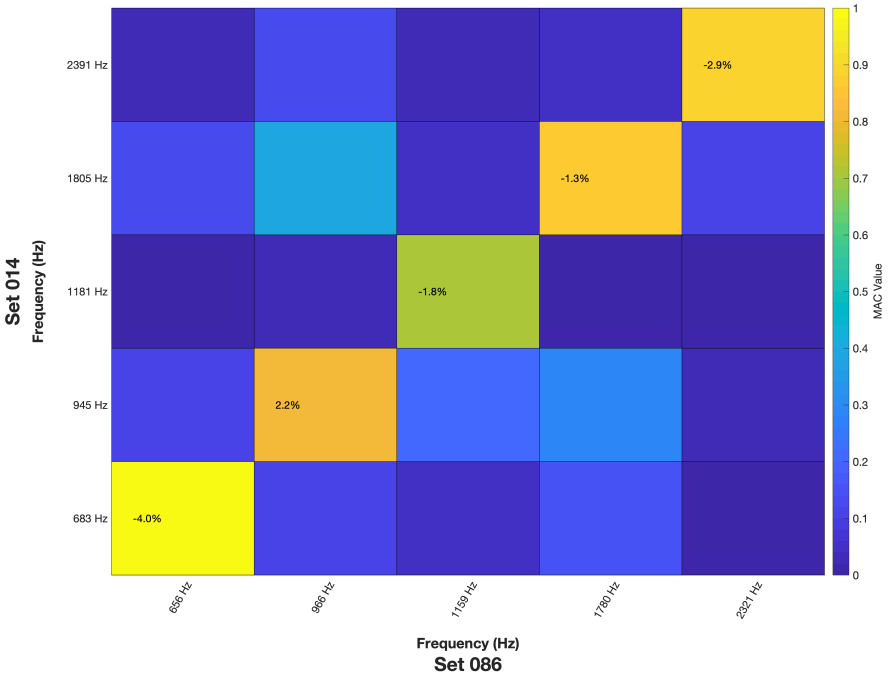

Figure 5-12. MAC and frequency comparison between sets 14 and 86.

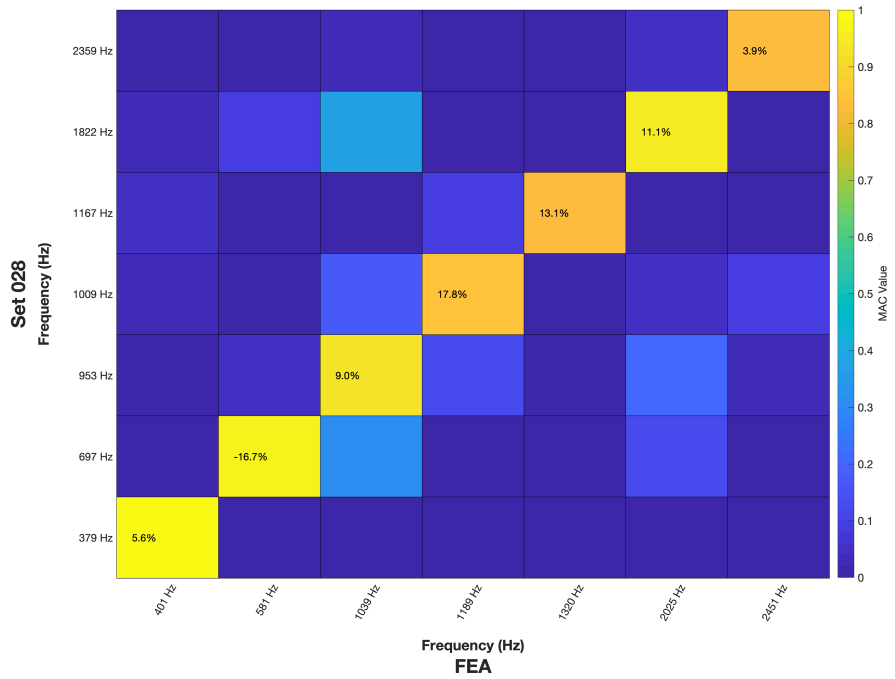

Figure 5-13. MAC and frequency comparison between set 28 and the finite element model calibrated to modal data.

6. VALIDATION OF THE MODEL TO THE MULTI-AXIS TEST BED

This chapter is broken into two separate sections for clarity between using the data to validate our understanding of the physics of the resonant plate test and validation of the finite element model developed to simulate the environment.

The first section is the validation of the model to resonant plate tests when there is nothing mounted to the resonant plate. In this section the force reconstruction method is examined to see if it can be used and extrapolated to test conditions not included in this test series. All of the data presented in this section is from the SHK5142 test series.

The last section in this chapter validates the model when a multi axis concept fixture is attached. The validation runs include comparing the FEM and data with different locations for the fixture and input block. This chapter also includes examining methods of connecting the fixture to the plate and boundary conditions to determine their effect on the test environment. The data presented from this section are from the SHK5153 and SHK5182 test series.

6.1. Calibration of the 1000Hz Resonant Plate Model to Shock Levels

It is expected that the resonant plate has non-linear dynamics with respect to the input force. Therefore, the modal parameters from set 28 are used to update the finite element model dynamics to represent the resonant plate at shock forcing levels. In order to update the model to best match the shock level modal parameters, the modulus of the rubber is decreased from 9000 psi to 2000 psi. A note on this change of the reduction of the modulus is that it reduced the natural frequency of all of the FEM modes, but it raised the natural frequency of the second plate mode which also happened in the data. This shows that even though there are non linear phenomena happening in the rubber interface, linear material models are adequate for modeling the system at a given input force level. The modification of the rubber is the only parameter changed to better match shock levels. The MAC and frequency comparison between the FEM with updated rubber modulus and set 28 modal data is in Figure 6-1.

6.2. Validation of the 1000 Hz Resonant Plate Model

This section examines and validates the resonant plate model with damping bars to test data. The model that is calibrated to shock levels in the previous section is the singular model used for all of the validation results.

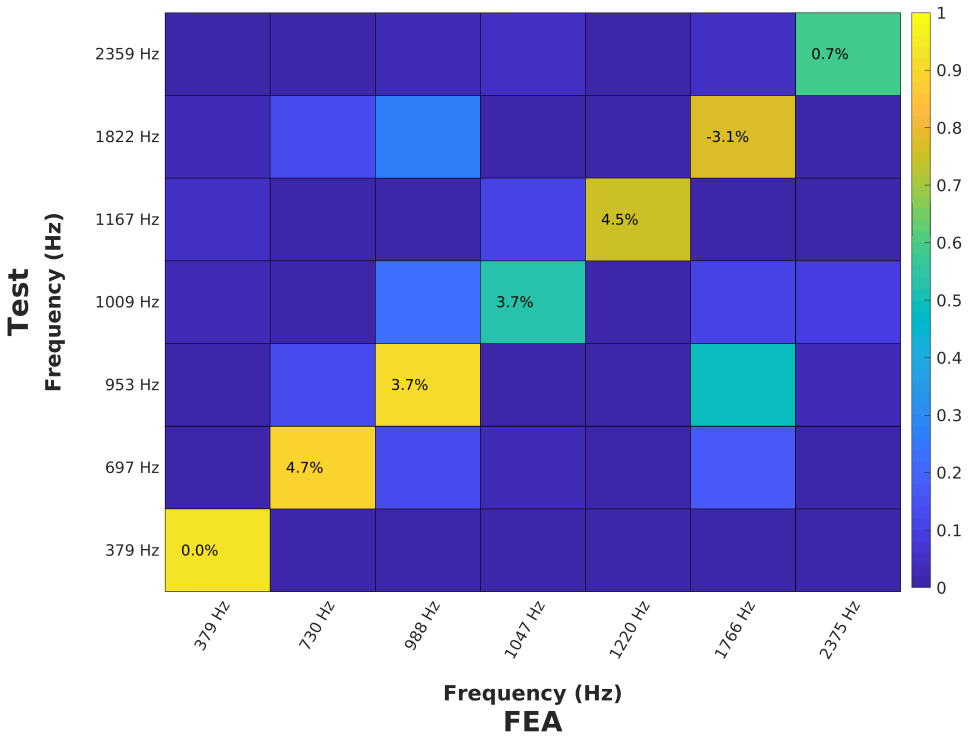

Figure 6-1. MAC and frequency comparison between set 28 modal parameters and FEM calibrated to shock level modal data.

Table 6-1. List of validation runs for the resonant plate and their purposes

Test Run Data	Forcing Function	Purpose of the Validation Run
Run 34	Run 34	To determine if the response can be replicated from a forcing function acquired from that run.
Run 35	Run 34	To determine if the response can be replicated from a forcing function acquired from a run with similar parameters.
Run 38	Scaled Run 34	To determine if the response can be replicated from a scaled forcing function acquired from a run with similar parameters but higher projectile velocity.
Run 86	Scaled Run 34	To determine if the response can be replicated from a scaled forcing function acquired from a run with all test parameters varied.

In order to determine if the model is validated, a variety of environments and configurations are needed. A series of validation analyses were run, each testing different assumptions and if those assumptions are validated. These series of validation runs are listed in Table 6-1.

The first validation run compares the model to run 34. The model uses the reconstructed force from run 34 as an input to the model. The force calculated is uniformly distributed as a traction force in the Z direction at the side set shown in Figure 6-2. A modal transient solution type is used to compute the response of the resonant plate system.

The initial sideset chosen for the location of the load does not excite the second bending mode at 2300 Hz shown in the magnitude of the response in the frequency domain shown in Figure 6-3. Changing the location of the load to the sideset shown in Figure 6-4 provides a much better comparison as it excites the second bending mode appropriately. The improved response for the force applied at the sideset shown in Figure 6-4 can be found in Figure 6-5.

The reason for the increased participation of the second bending mode of the plate is based on the reciprocity of the structural dynamics of they system. If the response degree of freedom is zero for a given mode, then that degree of freedom does not respond when the mode is excited. Conversely, if the input force is located at a degree of freedom that is zero for a mode, the mode is not excited and the entire shape does not exist in the response. By shifting the centroid of the traction force up by 0.75", the mode is excited and the response at the node 11 degree of freedom is observed.

From the evidence presented in Figures 6-2 through 6-5, it is concluded that the response of the system is sensitive to the location and orientation of the forcing function. Further examination of the test setup reveals plastic deformation in the impact block shown in Figure 6-6. This permanent deformation along with the offset in the projectile modifies the angle of impact and a 10 degree offset is added to the forcing function at the area specified in Figure 6-2. This offset from normal along with the sideset shown in Figure 6-2 is used for all of the validation runs that follow.

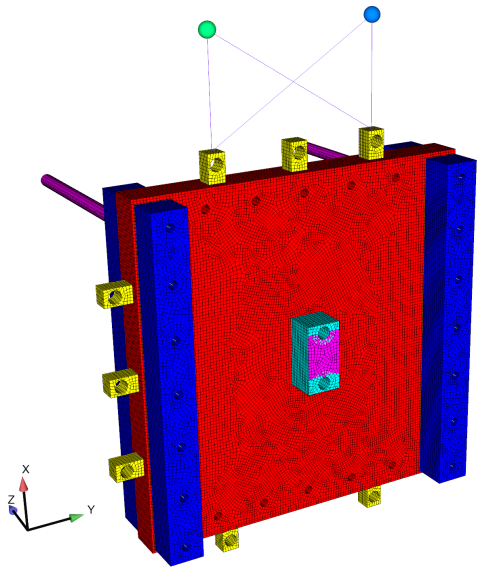

Figure 6-2. Location of the imparted load on the model as designated by the magenta colored sideset on the impact block. Area chosen based on visual inspection of the test.

Even though a single model is used throughout the validation process, the physical location of the projectile with respect to the impact block varied for each hit as the ropes could tighten and sag over time and change that location. This change in location where the projectile hits the impact block is an uncertainty in the modeling of the test environment.

The validation results are examined several different ways. For each of the runs, the measured data is compared at 4 different locations to capture the spatial accuracy of the model. The nodes chosen for consistent comparison are nodes 11, 43, 62, and 63 shown in Figure 5-3. These nodes are selected because they span different parts of the resonant plate that should respond differently from each other or are potential locations for test fixtures. The time and frequency domain of each of the responses are compared along with the Shock Response Spectra (SRS). The time and frequency domain of the forcing function are included in the comparison for reference.

The time histories from run 38 for the four nodes used in validation are plotted to show the different responses due to the initial impact force and how they differed from each other. The time response for nodes 11, 43, 62, and 63 can be found in Figure 6-7. From the time history, it is difficult to determine the magnitude or the duration of the input force as the initial pulse in acceleration differs between the different degrees of freedom measured.

The forcing function calculated from run 34 is used as an input and compared to the response of the aforementioned nodes from run 34. This is expected to be the best case scenario for the model as there would only be small errors on the input to the model. The real, imaginary and magnitude of the responses were compared in the frequency domain. The SRS and the time domain of the responses are compared. All of these comparisons for the nodes of interest can be found in Figures 6-8 to 6-11.

Examination of the validation results between the model and test show that there is excellent

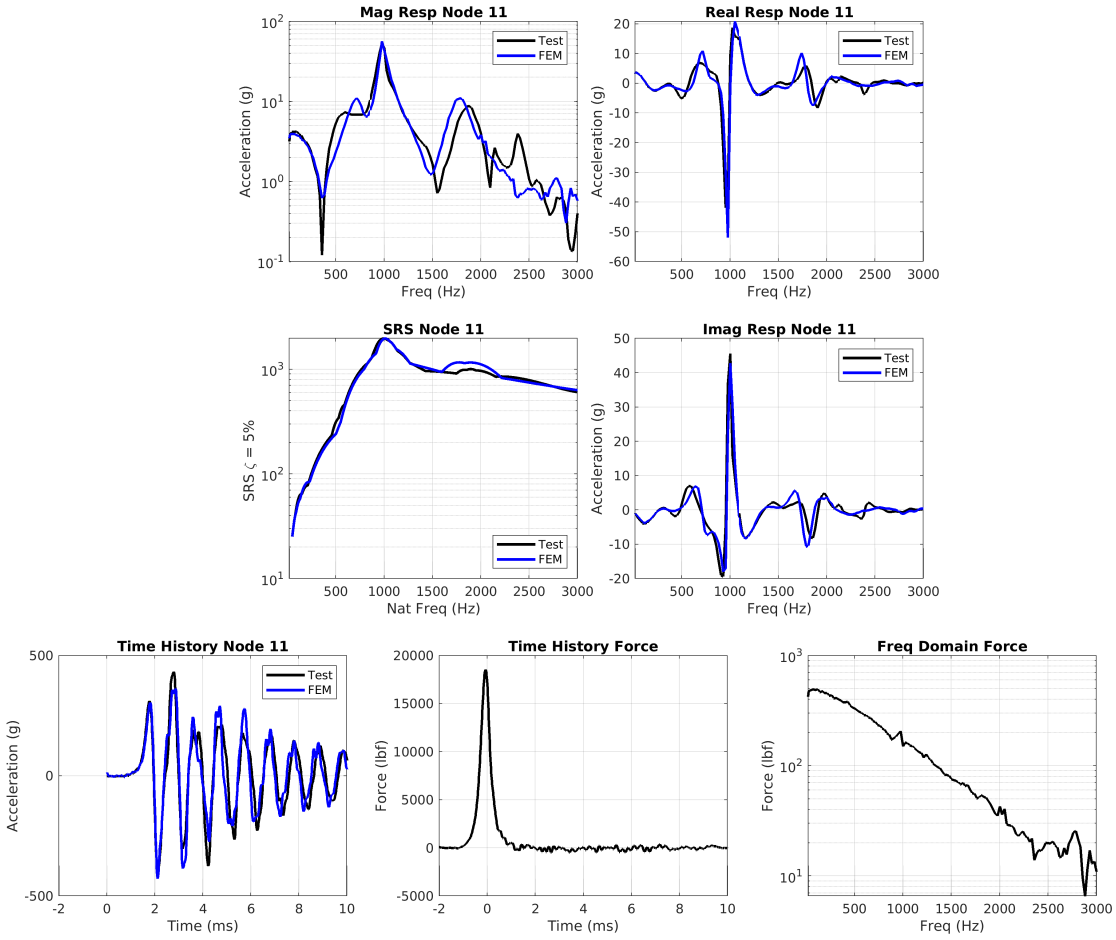

Figure 6-3. Node 11 validation comparisons for the force imparted at the location designated by visual inspection

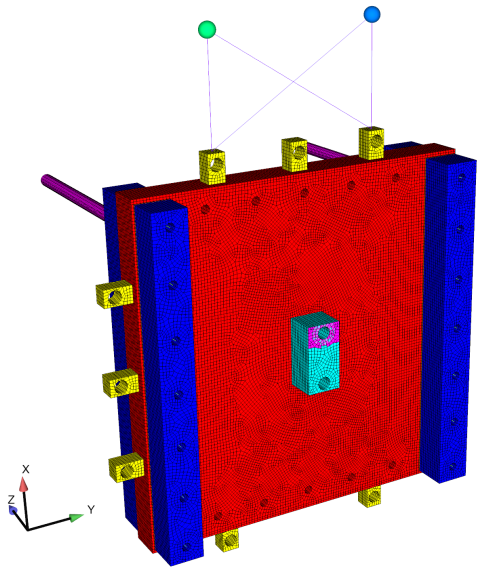

Figure 6-4. Location of the imparted load on the model as designated by the magenta colored sideset on the impact block. Area chosen based on improved match to the test.

agreement of the response of the four nodes of interest under 2000 Hz. Above 2000 Hz, there are some discrepancies between the model and the test data. This could be due to either a mode shape not being accurately represented in the model or the location of the forcing function not being accurate as demonstrated on the 2300 Hz mode in Figures 6-3 and 6-5.

All of the comparison data presented in Figures 6-8 through 6-11 provide a lot of information, however, the intent of this model is to be able to predict the response motion of a location of the plate with respect to an SRS test specification. In order to determine how well that objective is met, the dB error between the model and test SRSs are calculated. The results of the four nodes of interest can be found in Figure 6-12. This figure is important because one of the goals of the report is to show that the model can be used to design a resonant plate test. In order to design the test, the model must be accurate within the tolerances of a typical resonant plate test. The dB error in Figure 6-12 shows that there is little error over the bandwidth calculated. This error is especially important at the 1000 Hz knee frequency, where the error is almost zero for each of the four degrees of freedom tested.

The next validation test takes the forcing function from run 34 and applies it to the model. The model response is compared to run 35 measurements. Run 35 has the same projectile, gun pressure, and programmer as run 34, so this validation run examines the usability of the force from one run to a nominally identical run. The response comparisons between the four nodes of interest are shown in Figures 6-13 through 6-16.

The results of using the force from run 34 to predict the response from run 35 shows comparable validation results when compared to response of run 34. This is expected as there is very little difference calculated between the force and response between runs 34 and 35 as shown in Chapter 5. This again shows that there is very little shot to shot variability for the resonant plate system when impacted with identical shot parameters.

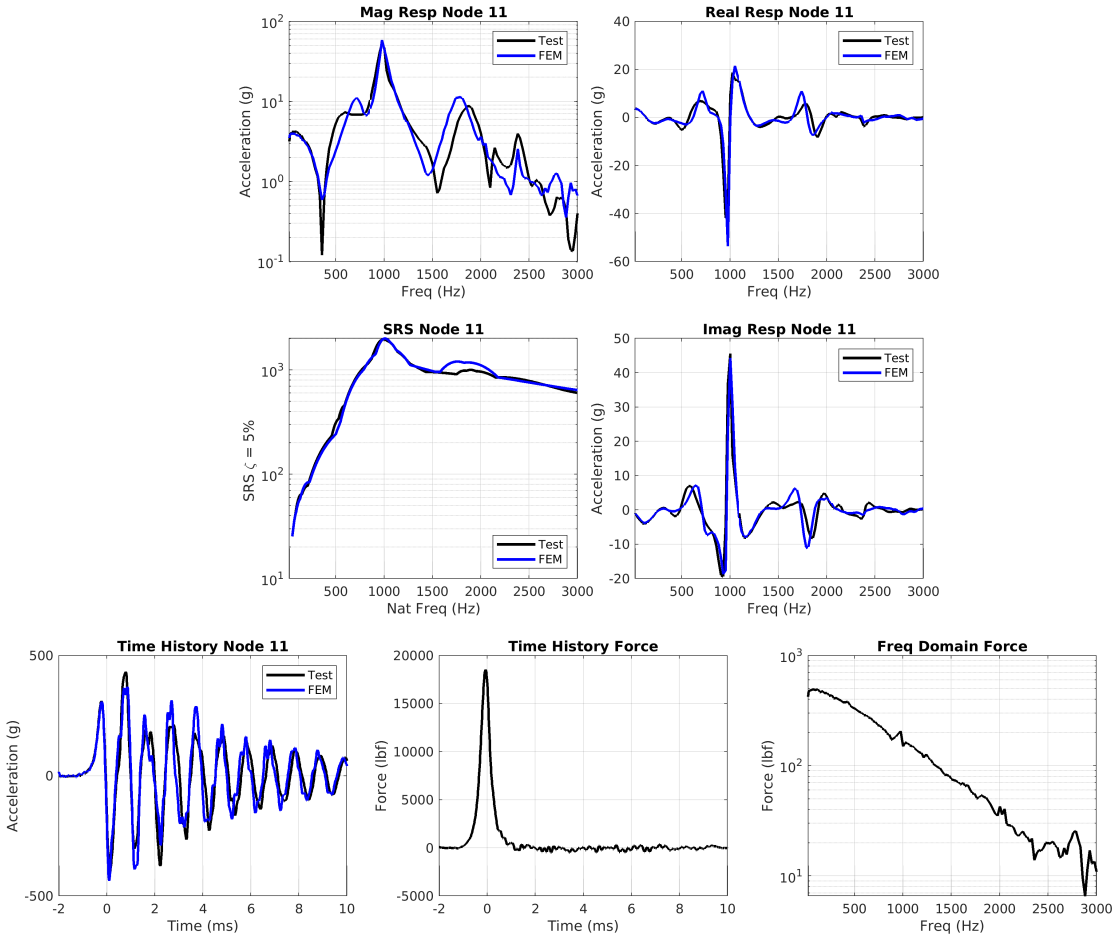

Figure 6-5. Node 11 validation comparisons for the force imparted at the location that provided better results

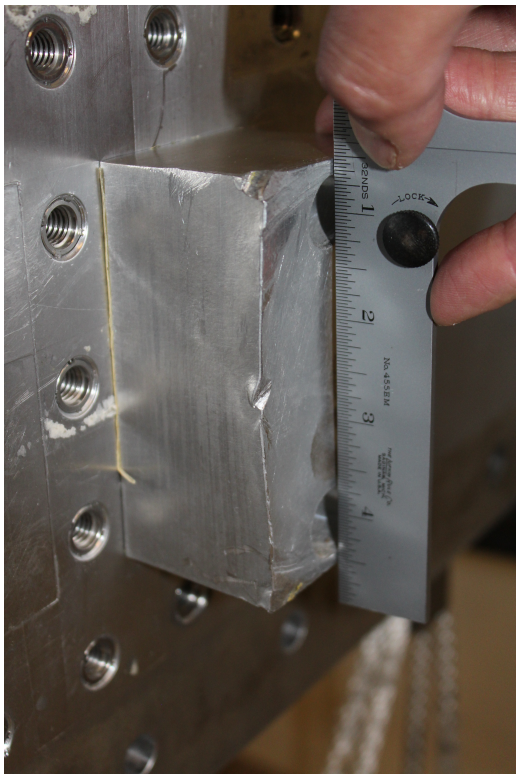

Figure 6-6. Photo of the impact block and the its plastic deformation

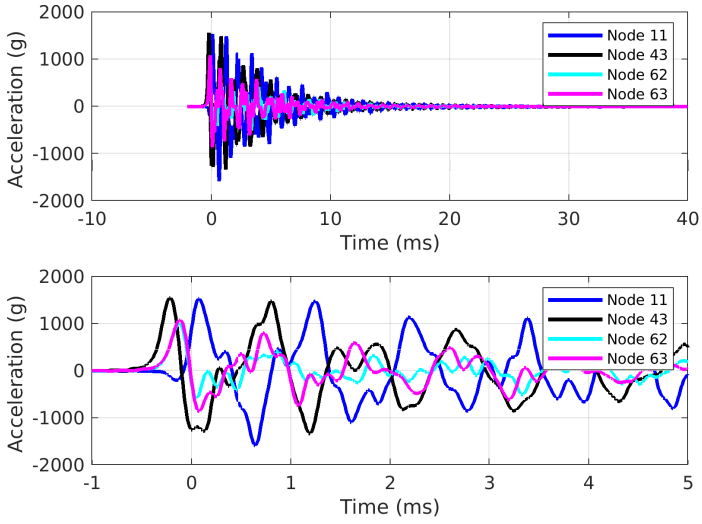

Figure 6-7. Time history of nodes of interest from test run 38

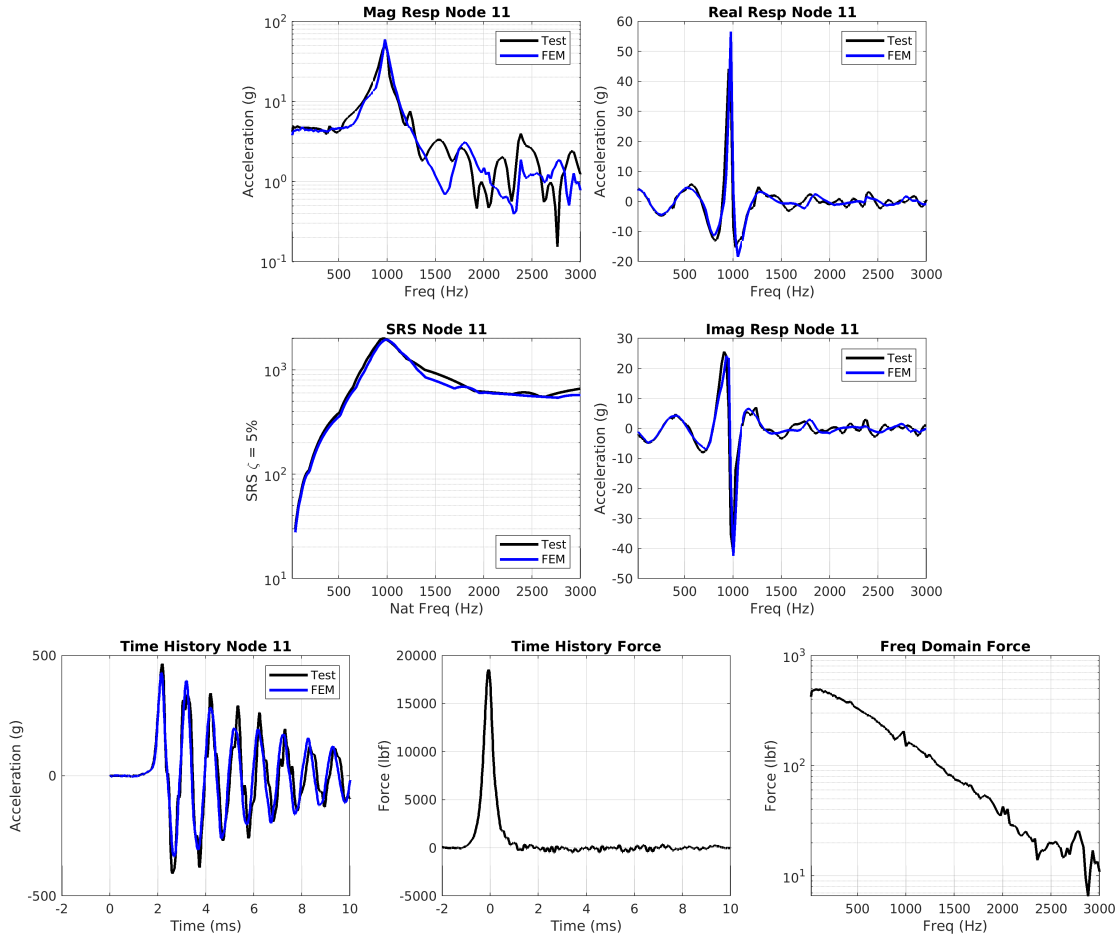

Figure 6-8. Node 11 validation comparisons for the run 34 force imparted on the model compared to the test response from run 34

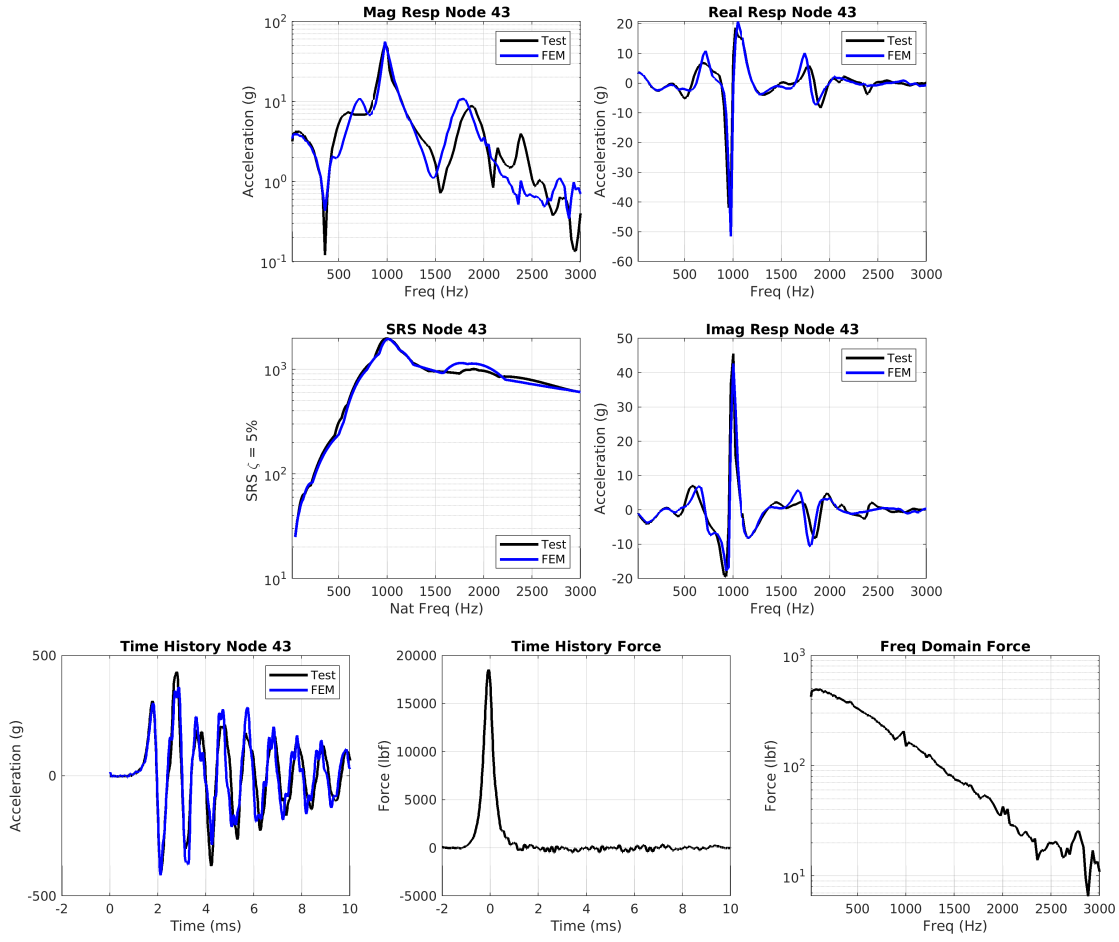

Figure 6-9. Node 43 validation comparisons for the run 34 force imparted on the model compared to the test response from run 34

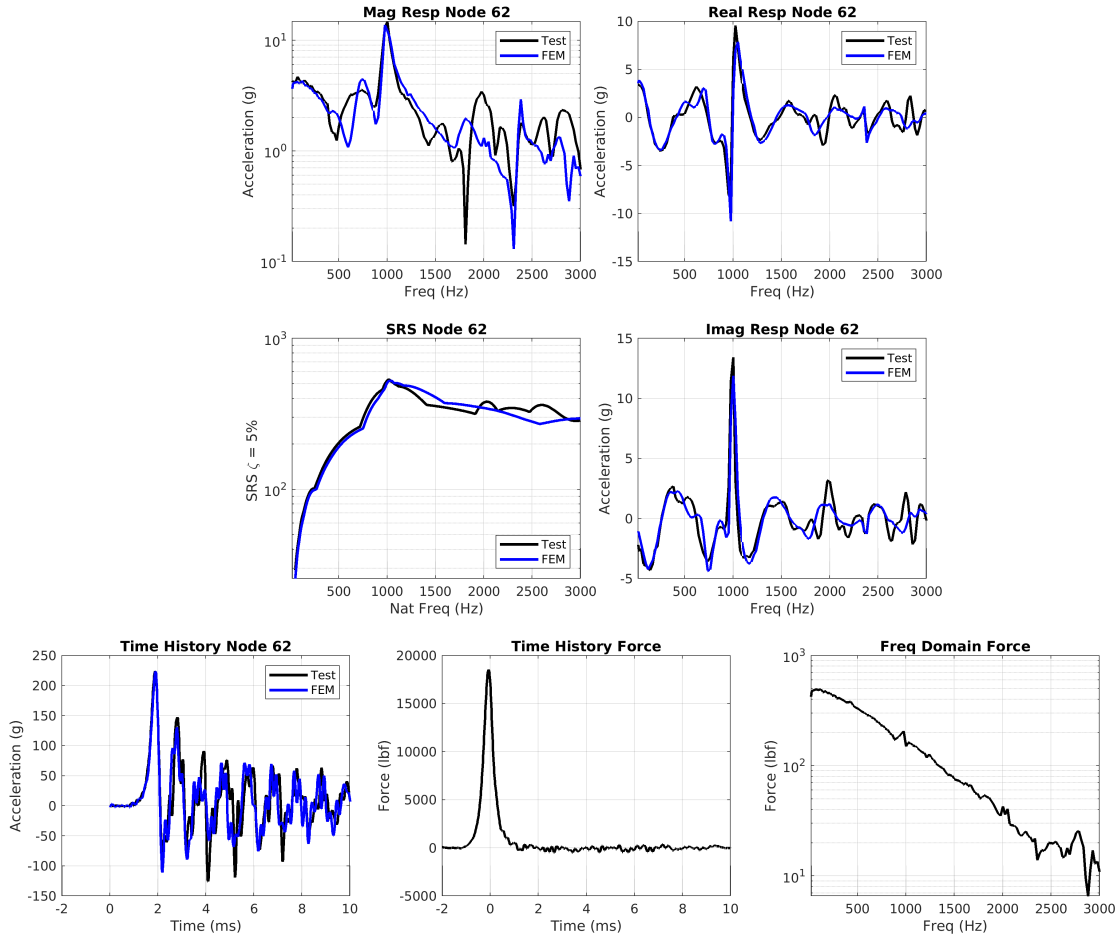

Figure 6-10. Node 62 validation comparisons for the run 34 force imparted on the model compared to the test response from run 34

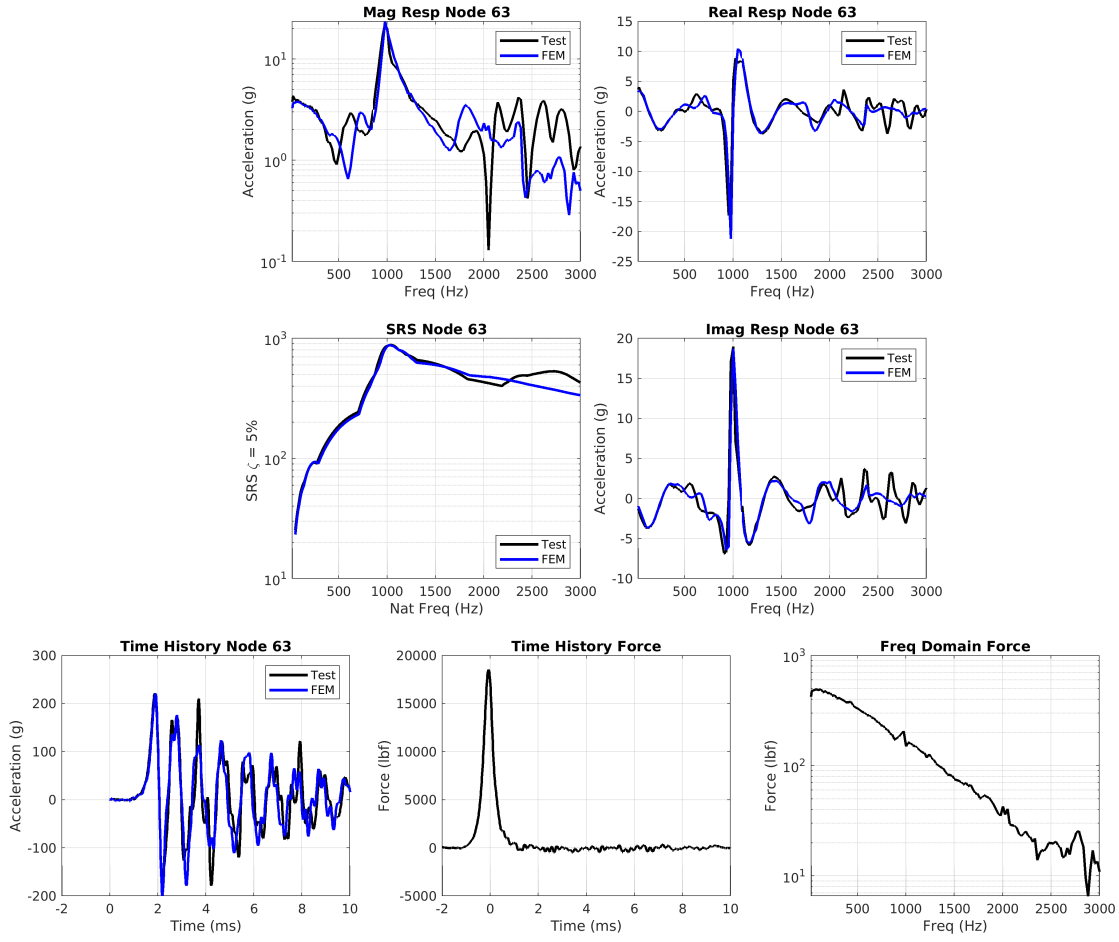

Figure 6-11. Node 63 validation comparisons for the run 34 force imparted on the model compared to the test response from run 34

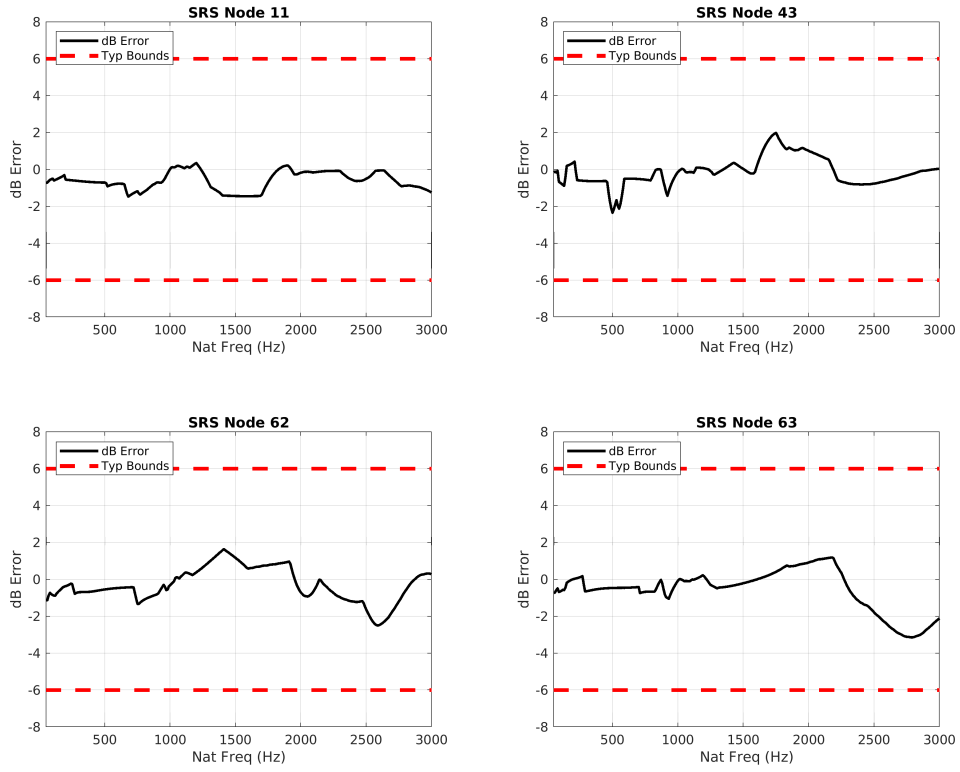

Figure 6-12. Relative SRS error of the FEM with respect to the data from Run 34.

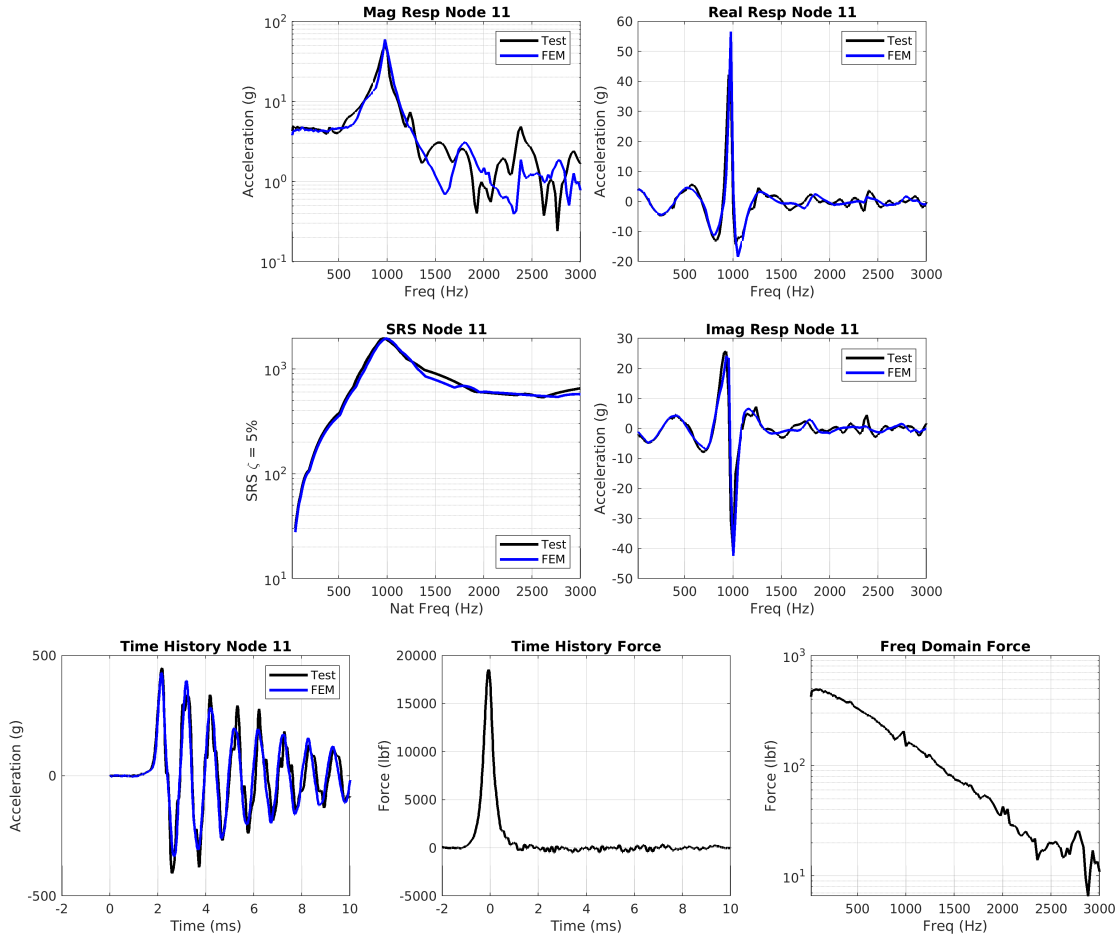

Figure 6-13. Node 11 validation comparisons for the run 34 force imparted on the model compared to the test response from run 35

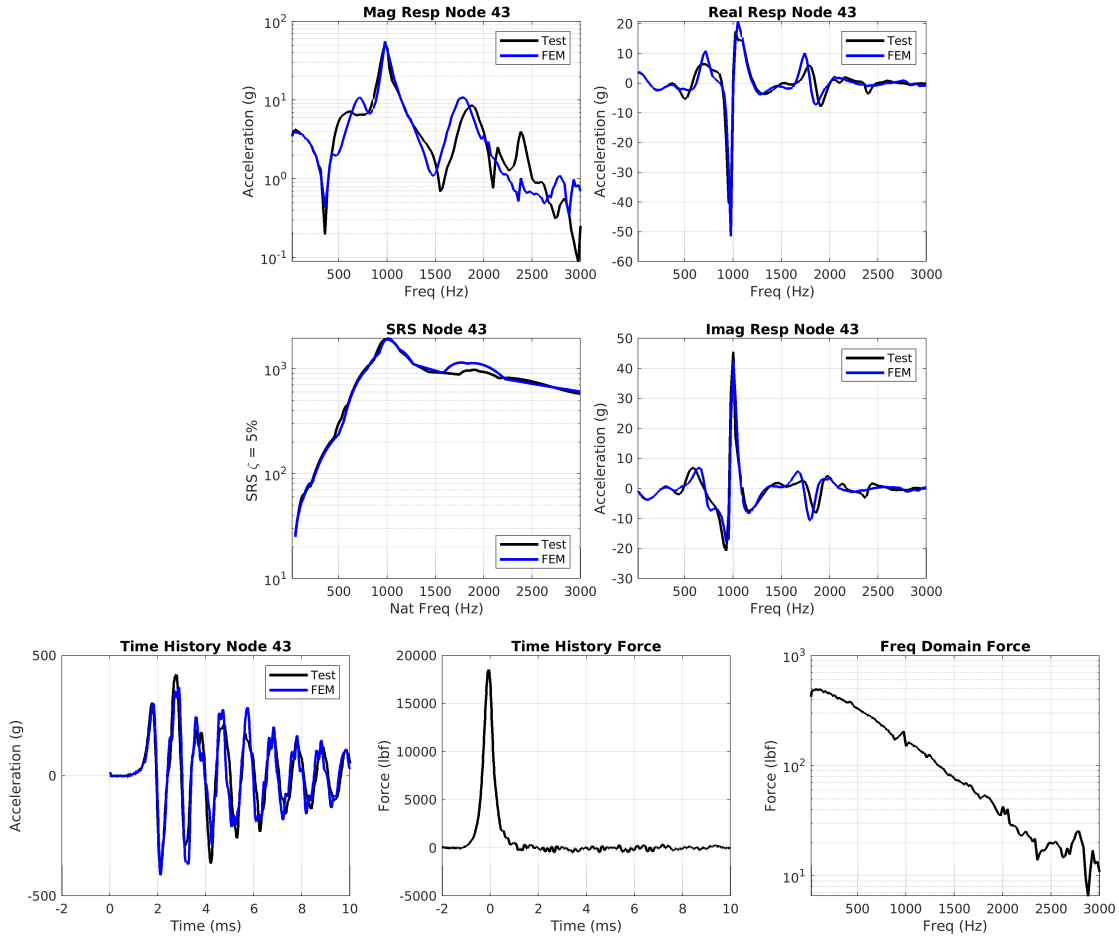

Figure 6-14. Node 43 validation comparisons for the run 34 force imparted on the model compared to the test response from run 35

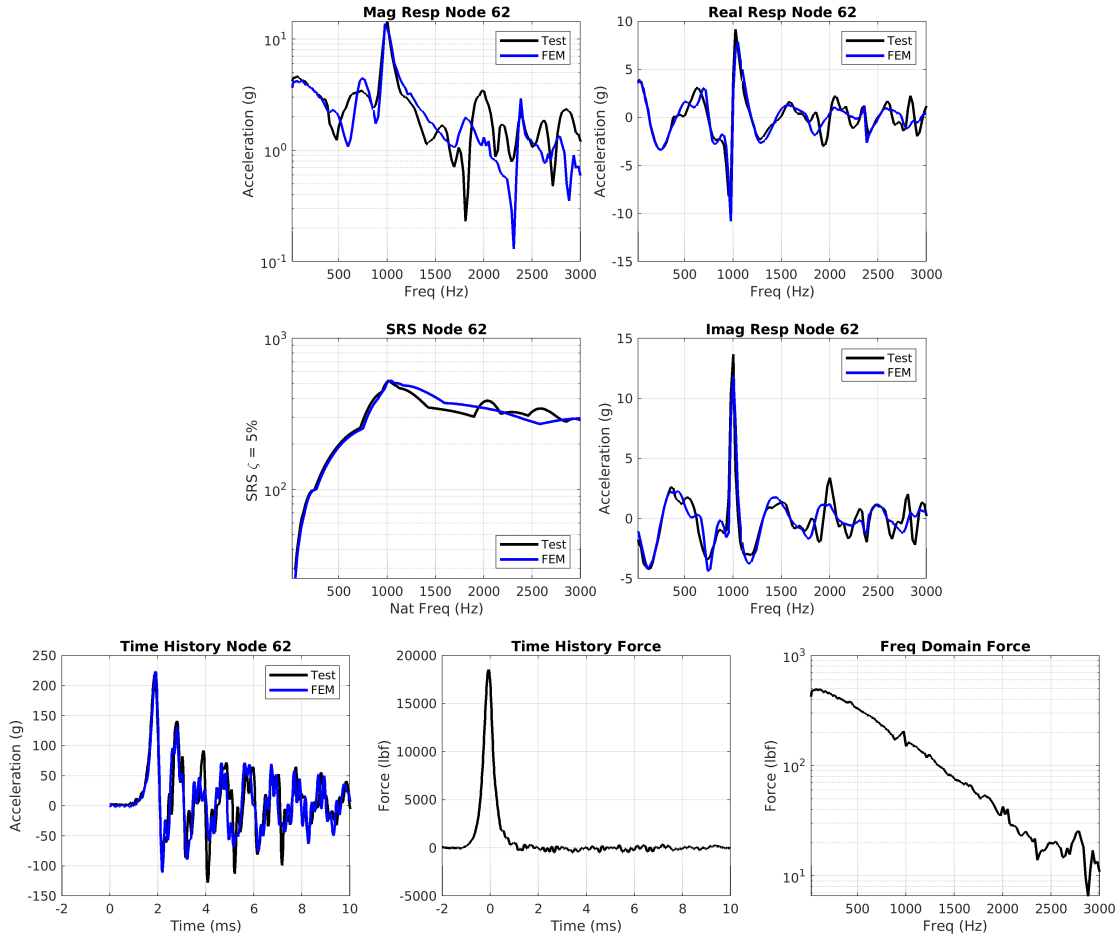

Figure 6-15. Node 62 validation comparisons for the run 34 force imparted on the model compared to the test response from run 35

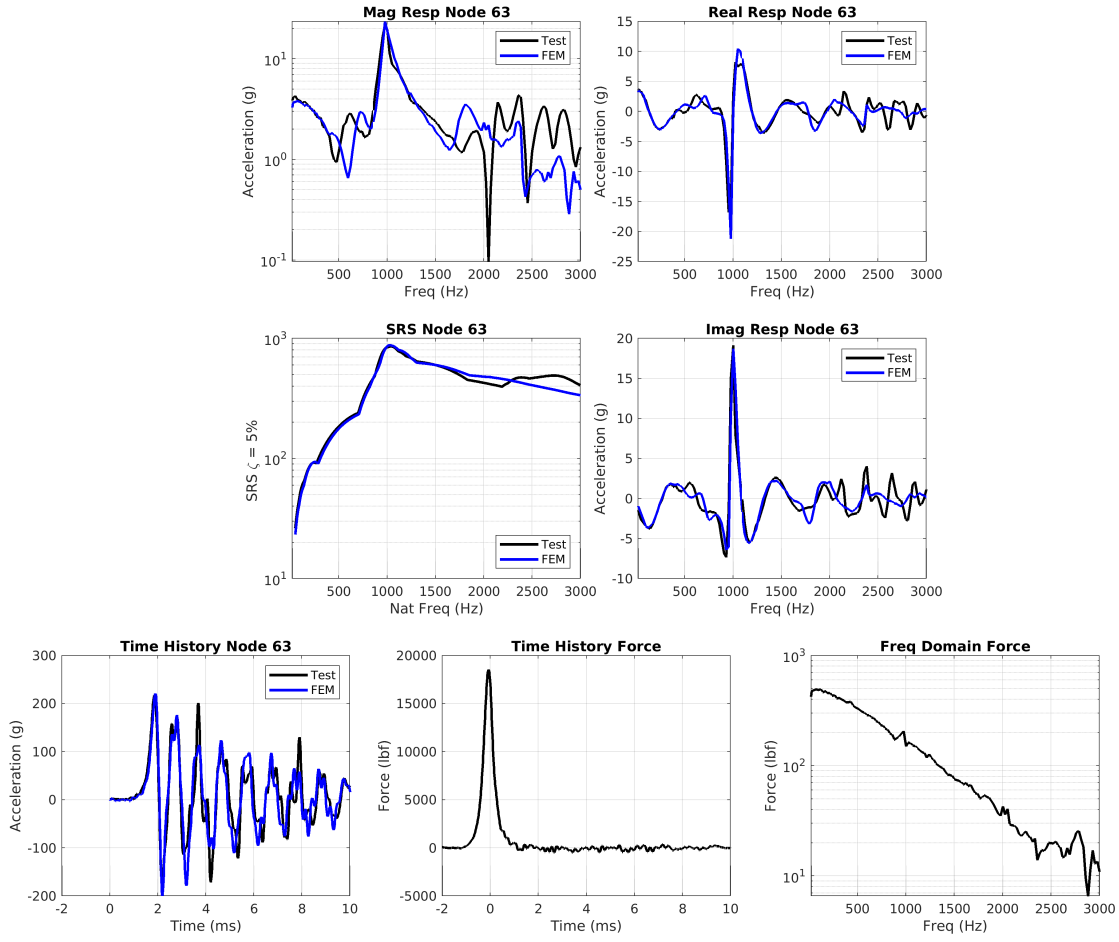

Figure 6-16. Node 63 validation comparisons for the run 34 force imparted on the model compared to the test response from run 35

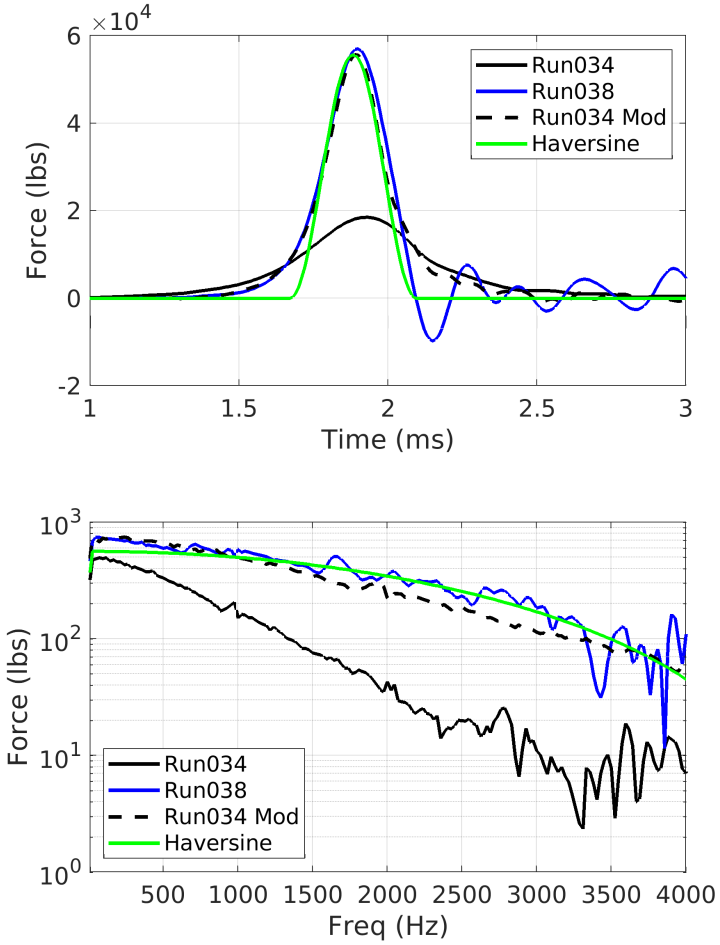

Figure 6-17. Comparison of synthesized forces and calculated forces from data

The next validation test is to use the force from run 34 and apply it to produce the response from run 38. This task is significantly more difficult as the gun pressure for run 38 is double that of run 34. The increase of gun pressure increases the forcing function across all frequencies with the increase not being uniform over the bandwidth.

There are two options for calculating a forcing function to use in the FEM. The first is to use the forcing function calculated from run 38. However, it is not expected that the laboratory be confined to executing tests with the parameters from this report. The second option is to modify the force from run 34 to match the force from run 38. The force is modified by shortening the pulse width and modifying the magnitude until the modified force best matches the reconstructed force from run 38. The calculated forces from run 34, run 38, modified run 34, and a representative haversine are compared in Figure 6-17. A haversine is included in the comparison to determine the effects of using a haversine instead of a modified reconstructed force from the environment.

Figure 6-17 shows that scaling the force from run 34 produces almost an identical representation

of the force from run 38. The only difference in the time domain between the two forces is the forcing function after the peak. The forcing function after the peak force for run 38 has error in it due to the force reconstruction process not being able to eliminate the elastic motion from the responses. Due to the known high frequency error, the modified force from run 34 may be a better calculation of the actual force for run 38 than the force calculated directly from run 38.

In addition to comparing the SWAT-TEEM forces, a haversine signal is generated that matches the lobes and the peak force. The time domain comparison shows that there is significant error at the beginning and end of the haversine. This difference in the time domain modifies the frequency domain signature of the haversine input. The difference between the modified run 34 and haversine is 16% at 500 Hz. The difference between the modified run 34 and haversine is 46% at 2700 Hz.

The modified force from run 34 shown in Figure 6-17 is imparted on the model to compare to the response from run 38. The response of nodes 11, 43, 62 and 63 are compared and are in Figure 6-18. Only the magnitude of the frequency domain signal and the SRS are compared because the timing of the impulse is not guaranteed to be identical run to run. Having an offset in the timing of the signals would produce a phase error that does not affect the result of the test.

Due to the harder hit of the modified force when compared to run 34, the 1000 Hz natural frequency shifted down due to the nonlinear nature of the mode. The relative error is calculated between the FEM and test data SRSs and is in Figure 6-19. The overall comparison of the four locations shows errors within tolerances between the FEM and the test data in spite of the nonlinearities of the system between a 'soft' and 'hard' hit.

The validation of the FEM to the test data from run 38 shows that one can transform the force with the same projectile and programmer but higher gun pressure. To determine if this observation can be made with different programmers and projectiles, the force from run 34 is modified to match the following test runs: run 27, run 62, run 78, and run 86. This range covers different programmers, different projectiles, and different gun pressures. These replications show that by modifying the pulse width and magnitude of the force calculated from run 34 while keeping the form of the impulse, the forces from all of the other impulses of different programmer, velocity and projectile sizes can be derived.

The reproduction of the different forces derived from the run 34 force are in Figures 6-20 through 6-23. Each of these cases show that the force modified from run 34 does a great job of reproducing the force of the other runs even though the other runs have different programmers, projectiles, and gun pressures. This conclusion is important as it would be very expensive and time consuming to characterize all of the different forces possible that the lab can execute to be an input to the model. With the data given, the model can prescribe a forcing function based off data and then the lab can use the information in Table 5-1 and Figure 5-7 as a starting point to hit that force signature and iterate until the desired response is realized.

The final validation run uses the modified forcing function of run 34 to replicate the response from run 86. Validating to run 86 is significant because it has a different programmer thickness, projectile, and pressure than run 34. The result of this comparison is shown in Figure 6-24.

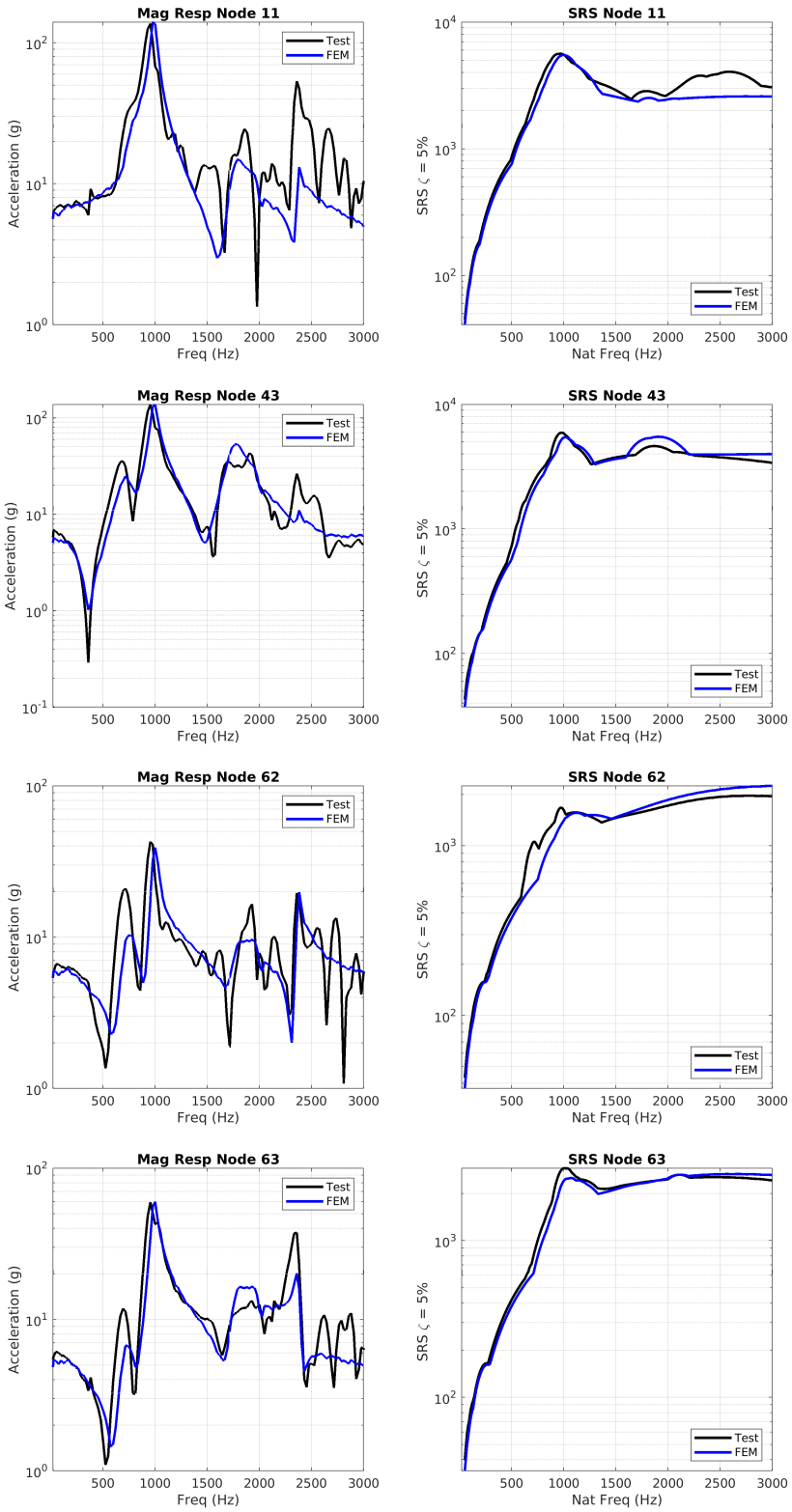

Figure 6-18. Validation comparisons for the modified run 34 force imparted on the model compared to the test response from run 38

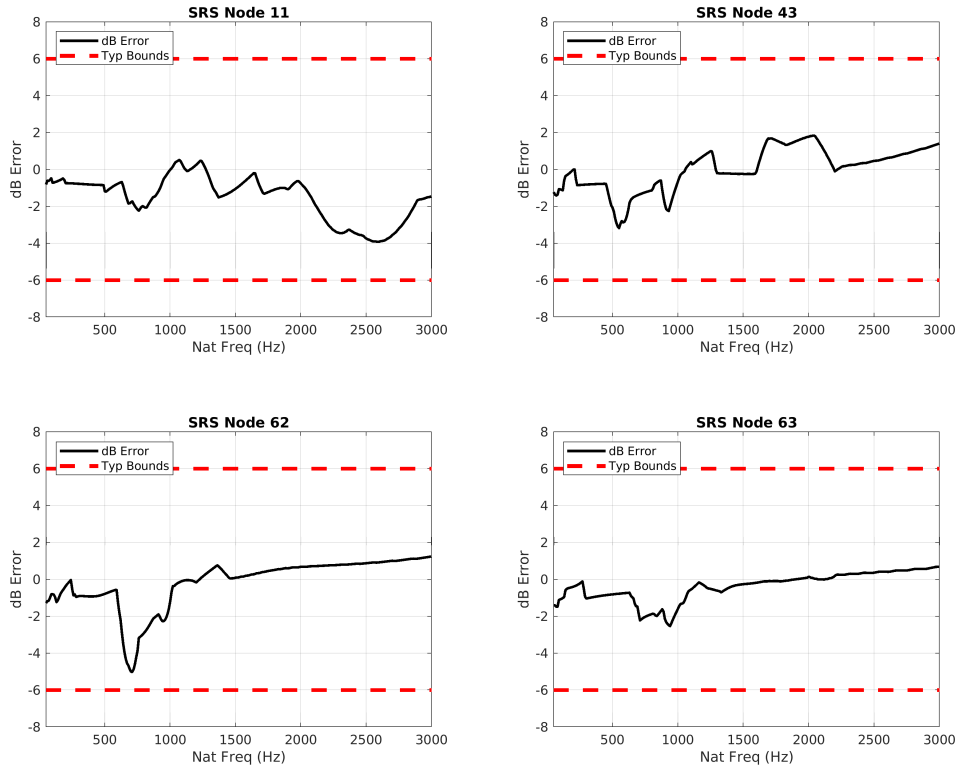

Figure 6-19. Relative SRS error of the FEM with respect to the data from Run 38.

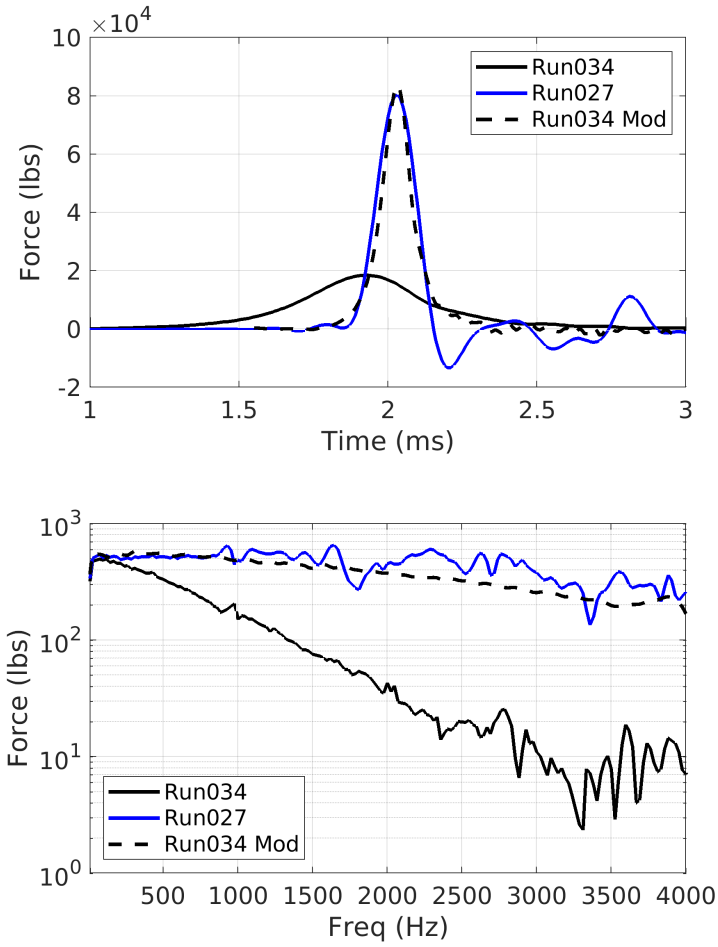

Figure 6-20. Comparison of the modified run 34 force to the force measured during run 27

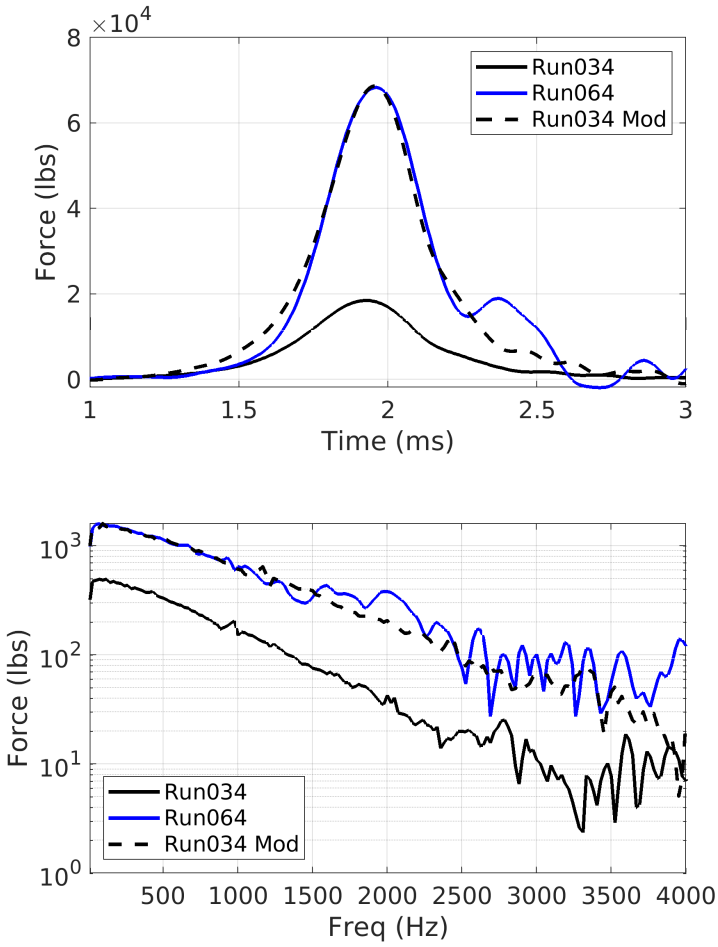

Figure 6-21. Comparison of the modified run 34 force to the force measured during run 64

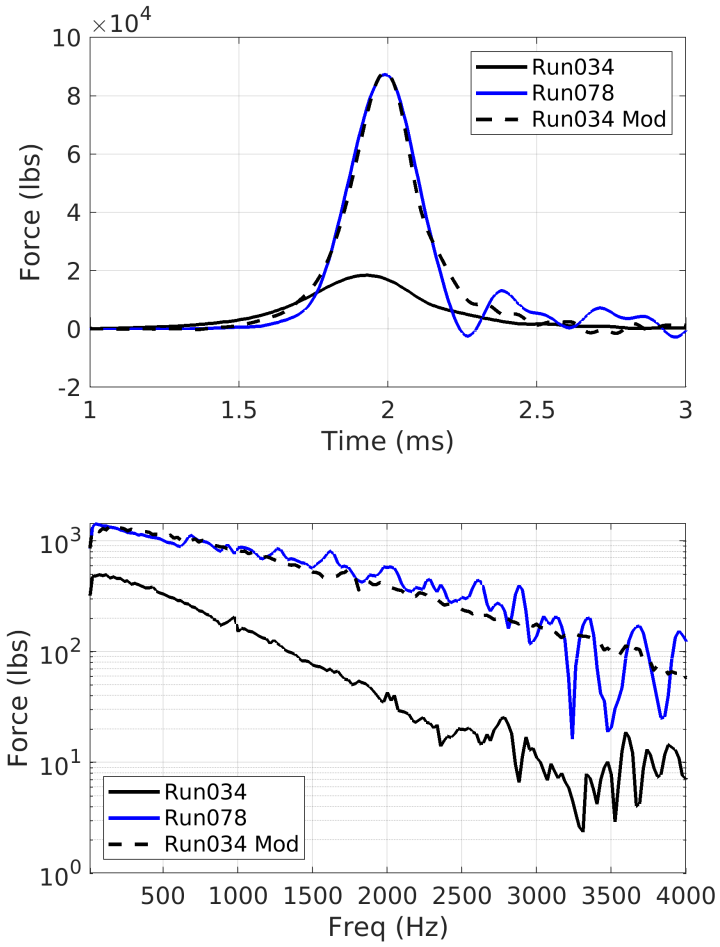

Figure 6-22. Comparison of the modified run 34 force to the force measured during run 78

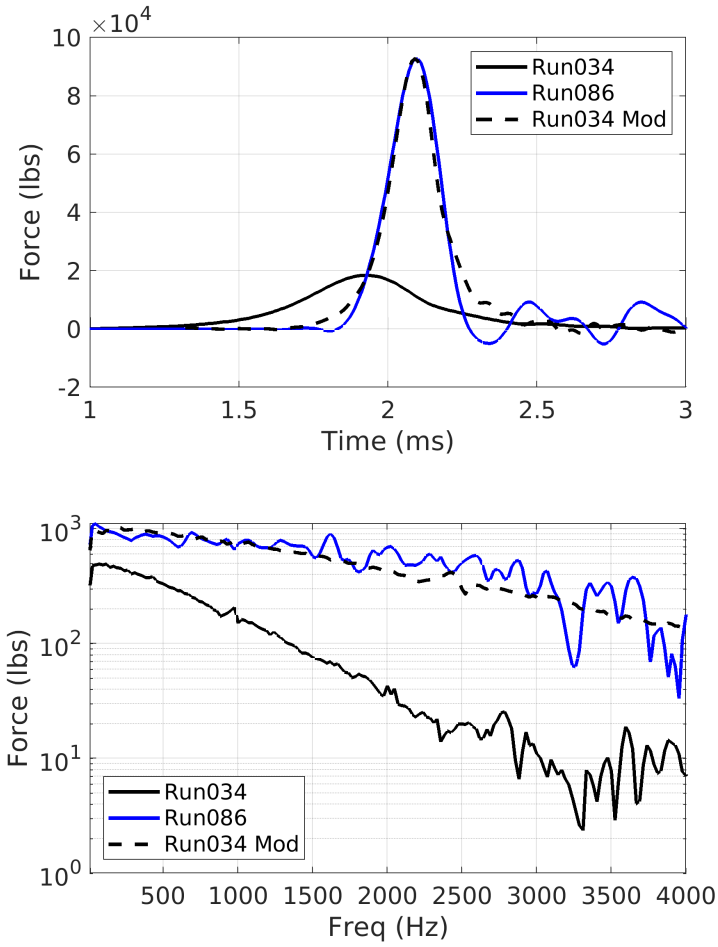

Figure 6-23. Comparison of the modified run 34 force to the force measured during run 86

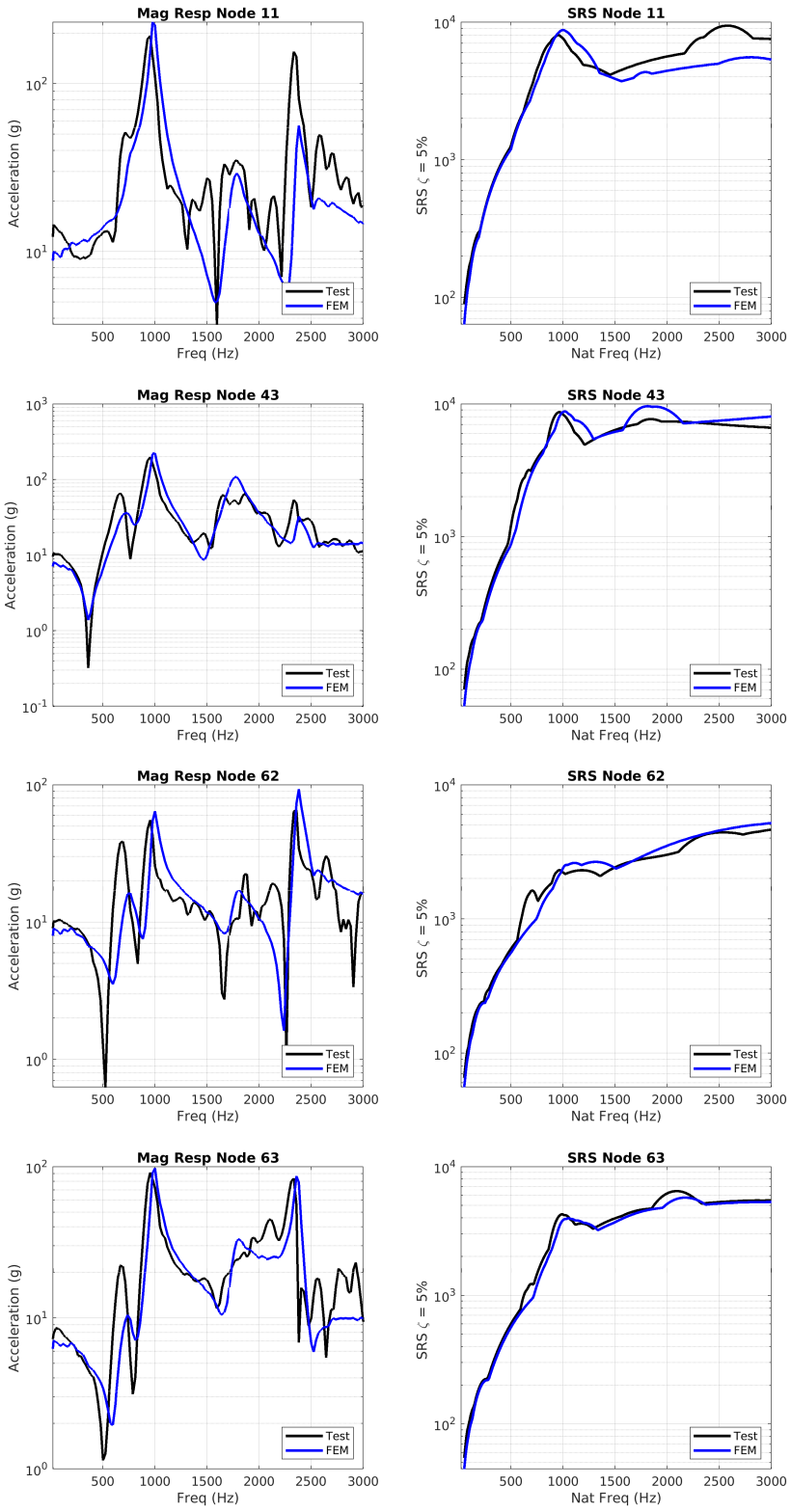

Figure 6-24. Validation comparisons for the modified run 34 force imparted on the model compared to the test response from run 86 at different node locations

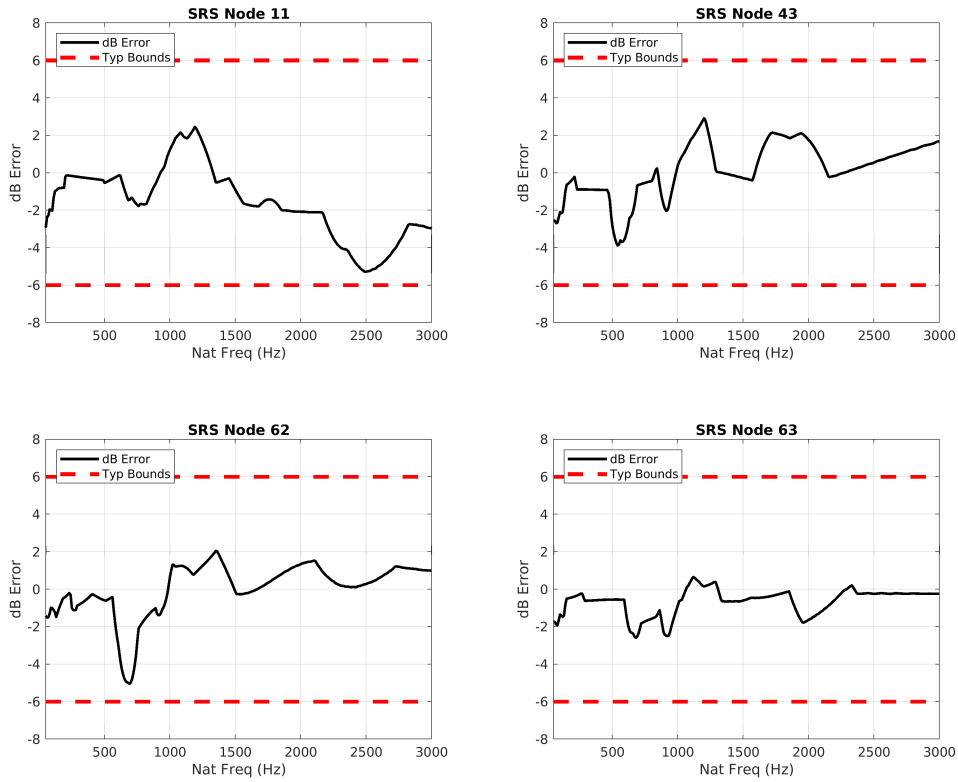

Figure 6-25. SRS relative error between the FEM and the data from run 86

The purpose of the model is to predict the input levels to the unit under test that is bolted to the resonant plate. In order to call the model validated, the purpose of the model has to be quantitatively examined. The input levels to the unit under test are related to the response of the surface of the resonant plate which has been compared to this point. Current specifications are written as SRSs. Therefore, the SRSs between the test data and the model are compared. In order to have some confidence that the test can achieve the model's prediction and execute a test within tolerances, the tolerances are included as the bounds of the comparison. This validation comparison is found in Figure 6-25. Figure 6-25 shows the relative error between the test data SRSs and the FEM SRSs for the four different degrees of freedom examined throughout this section. The result shows that the relative error for all of the degrees of freedom fall within the test tolerances of executing a test. Therefore, the model is able to predict how the surface of the resonant plate will respond at different shock levels before the test is set up with acceptable errors.

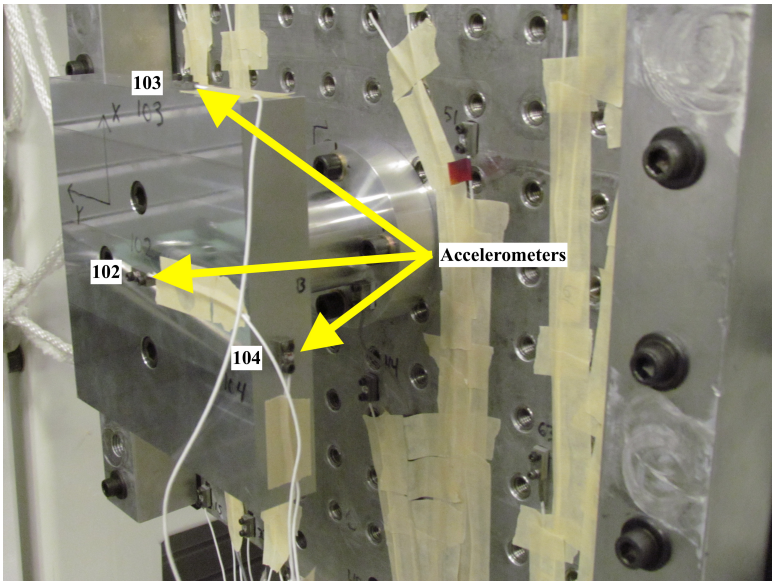

Figure 6-26. Photograph of the concept fixture mounted to the resonant plate and the validation measurement locations

6.3. Validation of the 1000Hz Resonant Plate with the Multi Axis Concept Fixture

This section validates the 1000 Hz resonant plate model with the multi-axis concept fixture attached shown in Figure 6-26. The fixture is designed to amplify off axis response through the resonances of the fixture and the rotations of the resonant plate. Although the resonances of the concept fixture are not tuned to deliver a specific environment, the concept fixture could be redesigned with the unit under test to deliver a range of resonant frequencies. A triaxial accelerometer, not shown in Figure 6-26 is attached to the base of the fixture and is designated as node 101. Three uniaxial accelerometers all measuring the three different cartesian directions are attached to the top plate. The uniaxial accelerometers are the instruments predominately used for model validation.

The configuration of the concept fixture attached to the resonant plate is not calibrated to test data. If better results are needed than the validation results presented in this section, a calibration test could be executed prior to test design to enhance the quality of the model with a given test fixture.

In addition to the inclusion of the test fixture, the location of the test fixture and the impact block are varied in order to observe more or less off axis motion of the fixture with respect to the impact direction and to determine if the model will predict the response of the different configurations. Because there is no calibration data for any of these configurations that combine the test fixture and the resonant plate, there is additional uncertainty in the model form of the fixture.

To help in the modeling of the fixture, the tests were executed with and without spacers between the test fixture and the resonant plate. The purpose of these spacers is to localize the contact area between the two structures and simplify the model of the joint. Photographs of these spacers can

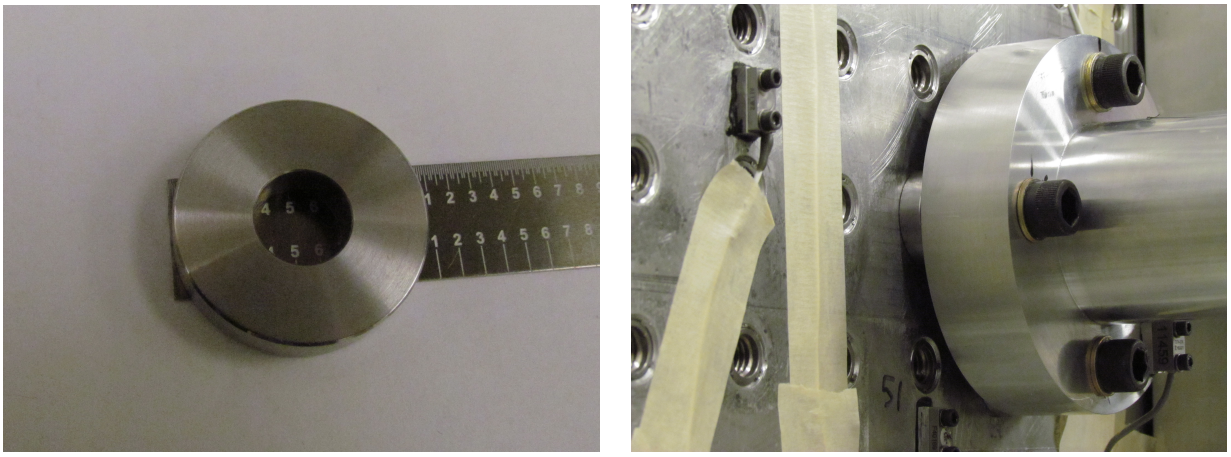

Figure 6-27. Photograph of the spacers used between the concept fixture and the resonant plate

Table 6-2. List of validation runs for the concept fixture attached to the resonant plate configuration

Test Series	Test Run Data	Spacers Included	Boundary Condition	Location of the Fixture (in)	Location of the Impact (in)
SHK5182	Run 62	Yes	Ropes	(0,0)	(0,0)
SHK5182	Run 56	Yes	Ropes	(4.5,0)	(0,0)
SHK5182	Run 115	Yes	Bungees	(4.5,0)	(0,0)
SHK5182	Run 46	Yes	Ropes	(4.5,-4.5)	(0,0)
SHK5153	Run 53	No	Ropes	(4.5,-4.5)	(0,0)
SHK5153	Run 61	No	Ropes	(4.5,-4.5)	(-4.5,-5.0)

be found in Figure 6-27. Validation of the model with the concept fixture will focus on the three accelerometers mounted on the top section of the fixture plate shown in Figure 6-26. Test node 102 measures in the Z direction, node 103 measures in the X direction, and node 104 measures in the Y direction.

Example pictures of moving the impact block and test fixture can be found in Figure 6-28. Moving the fixture relative to the test equipment is a relatively simple process as the resonant plate is designed to attach many different sizes of hardware to the plate. However, the location of the impact block is limited to the center and one quadrant of the resonant plate. In addition, since the location of the air gun is fixed relative to the frame that supports the resonant plate, the rope suspension has to be heavily modified to aim the air gun to hit off center of the resonant plate.

In order to validate the model and learn more about the test configuration, different configurations of fixture and impact block are considered. The different configurations of the concept fixture and impact block that are considered for validation can be found in Table 6-2. These test runs were executed in two separate series on two separate weeks. These test series are also different than the test series of the data taken and presented in Section 6.1.

The validation runs use the forcing function derived from the run 34 forcing function calculated and modified to match test run 78. Test run 78 is used because it has the same projectile,

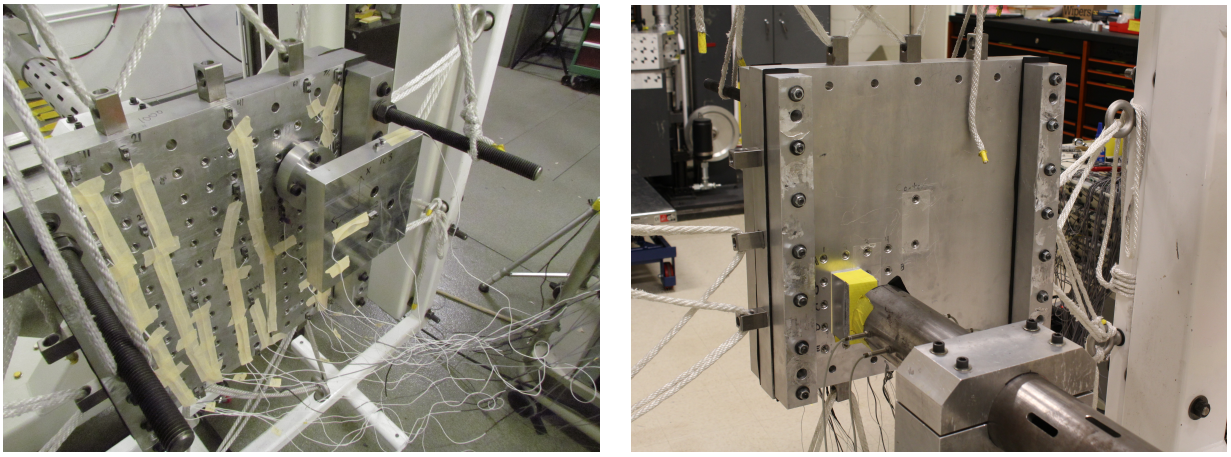

Figure 6-28. Photograph of the concept test fixture at location (4.5in, -4.5in) (left) and the impact block at an off center location (right)

programmer, and gun pressure as the runs in Table 6-2. The location of the forcing function with respect to the impact block in the FEM is kept constant throughout all of the runs and matches the location selected in the validation done without the fixture in section 6.1.

6.3.1. Validation of run 62: spacers, ropes, centered fixture, centered impact

The first model validation run is compared to Run 62 from the SHK5182 test series. The comparison between the finite element model and the test data are in Figure 6-29.

The comparison of the test and model response for the configuration shown in Figure 6-29 does not fare well. The Z direction is adequate, but the X direction looks low for the knee frequency at 500 Hz. The Y direction appears to miss the modes between 600 and 1000 Hz.

The relative error of the prediction in relation to the measured SRS is shown in Figure 6-30. The relative error shows what can be qualitatively observed. The response prediction in the Z direction is adequate, but the off-axis motion predictions are unacceptable.

The majority of these errors are due to a misrepresentation of the location of the input force. It is previously shown that the location of the forcing function in the model has an effect on the response predicted. This effect is further exaggerated by the off axis motion being dependent on the rotational modes of the plate and the fixture being placed on the node lines of the plate modes.

As we know from classical modal analysis, a force located at a place of high modal response allows the forcing function to excite that mode. Through examination of the 500 Hz mode of the system in Figure 6-31, the mode shape has a high gradient along the impact block and any error in the location of the force will result in a high error in the amplitude of the 500 Hz mode.

These theories explaining the errors in Figure 6-29 are demonstrated by comparing the test data to the same model but with a 0.75" offset in the location of the input force. This is the same as moving the force around from the whole surface of the impact block to the subset of element

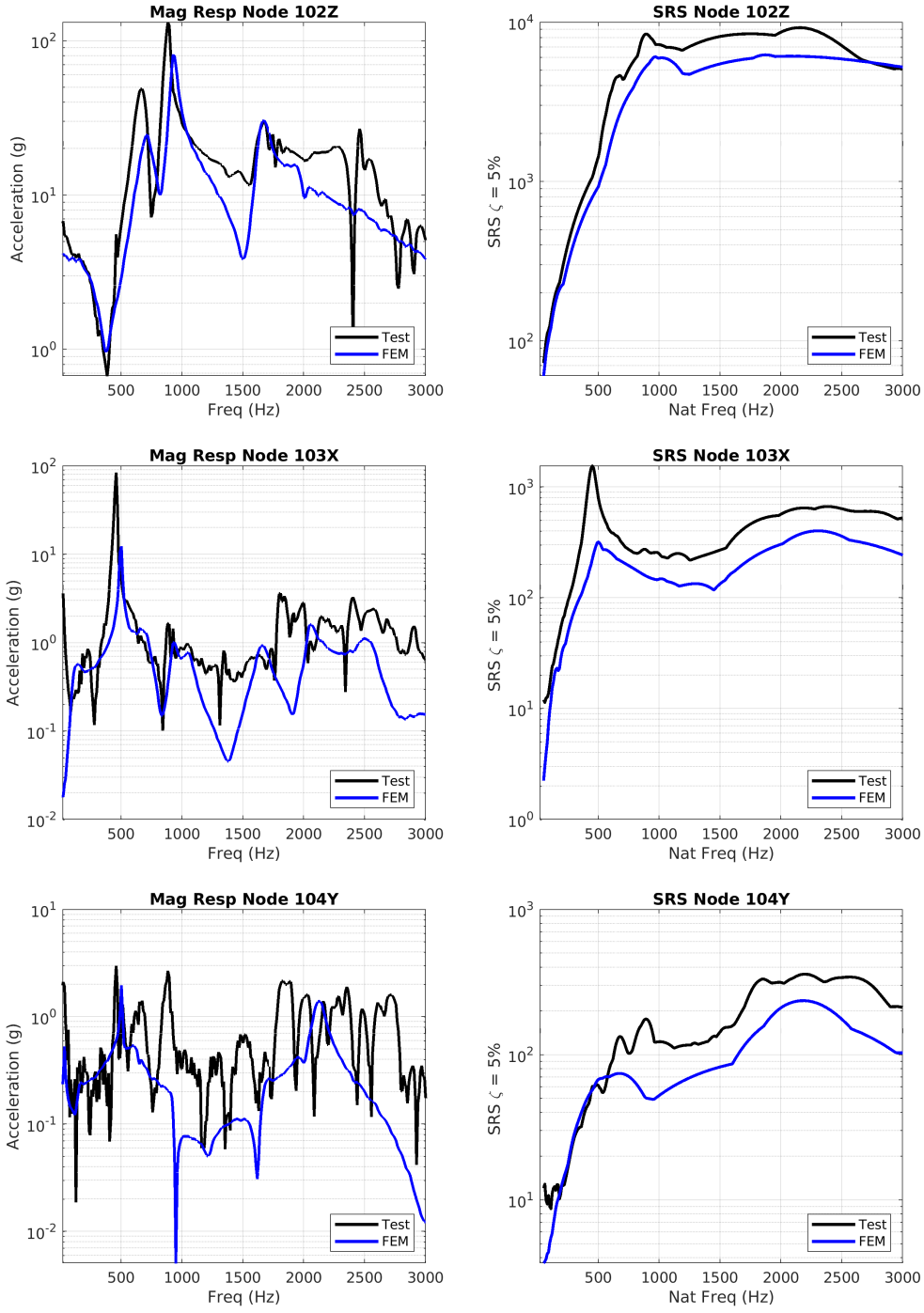

Figure 6-29. Comparison of the response between the FEM and Run62 in test series SHK5182

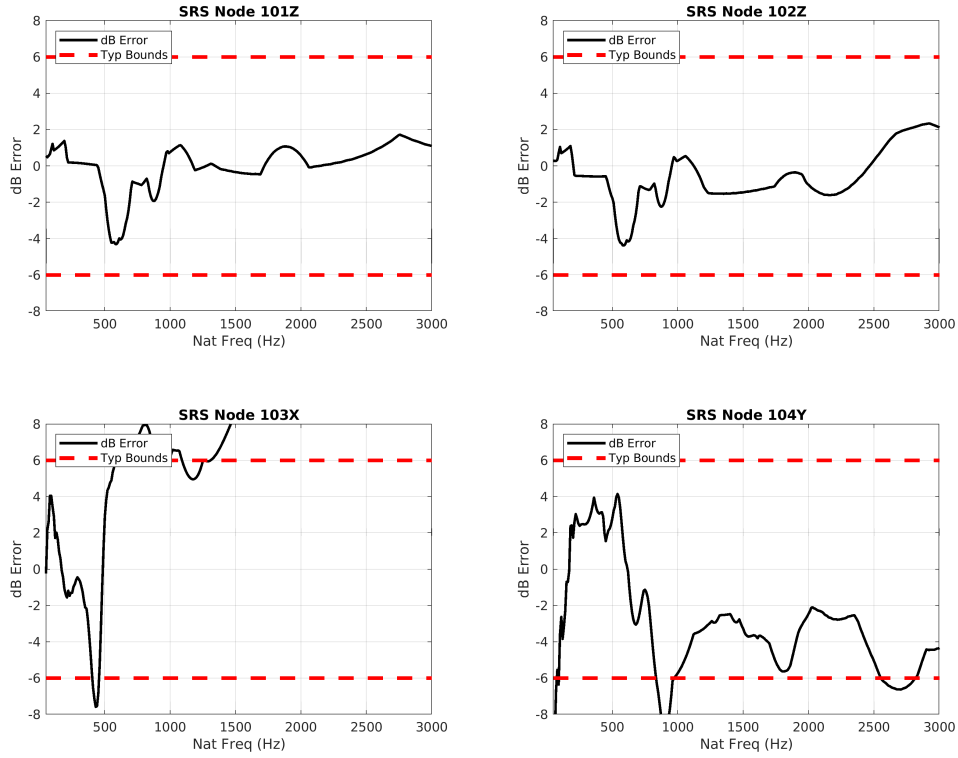

Figure 6-30. SRS validation comparison between the FEM and the data from SHK5182 run 62

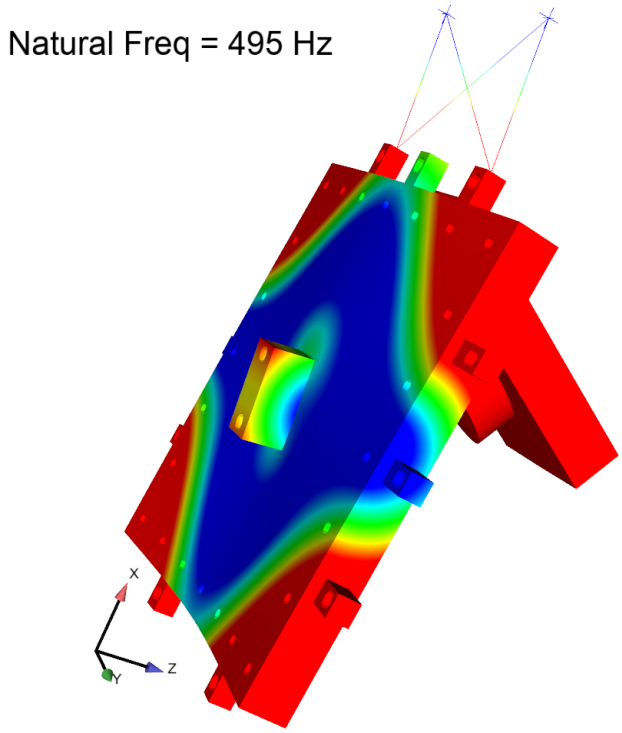

Figure 6-31. Fixture mode in the X direction that is sensitive to the X location of the impact. Colormap is relative displacement with blue having zero magnitude and red having high magnitude.

faces shown in Figure 6-2. The model is rerun and compared to the test data with the new input force location. The comparison between the two response sets can be seen in Figure 6-32.

The comparison of the response in Figure 6-32 where the impact force is shifted by approximately 0.75" inch shows large differences when compared to the original input location. The biggest difference is in the X direction responses as the SRS is amplified by approximately a factor of 2. This difference in the models can be seen directly in Figure 6-33. This difference proves that the response of the resonant plate system in this configuration is sensitive to the location of the force location.

6.3.2. Validation of run 56: spacers, ropes, fixture offset (X), centered impact

The next validation comparison is of the data taken from run 56 in the SHK5182 test series. This test has the impact block located at the center of the plate and the test fixture off-center in the X direction. The response comparison is shown in Figure 6-34 with the relative error of the SRS in Figure 6-35.

The comparisons in Figures 6-34 and 6-35 show the model doing an adequate job predicting the response in the Z and X direction, but provides a poor result in the Y direction. This result is similar to the result shown for run 62 in Figures 6-29 and 6-32. There are two reasons for the poor results in the Y direction. The first is from the previously mentioned error of the input force being

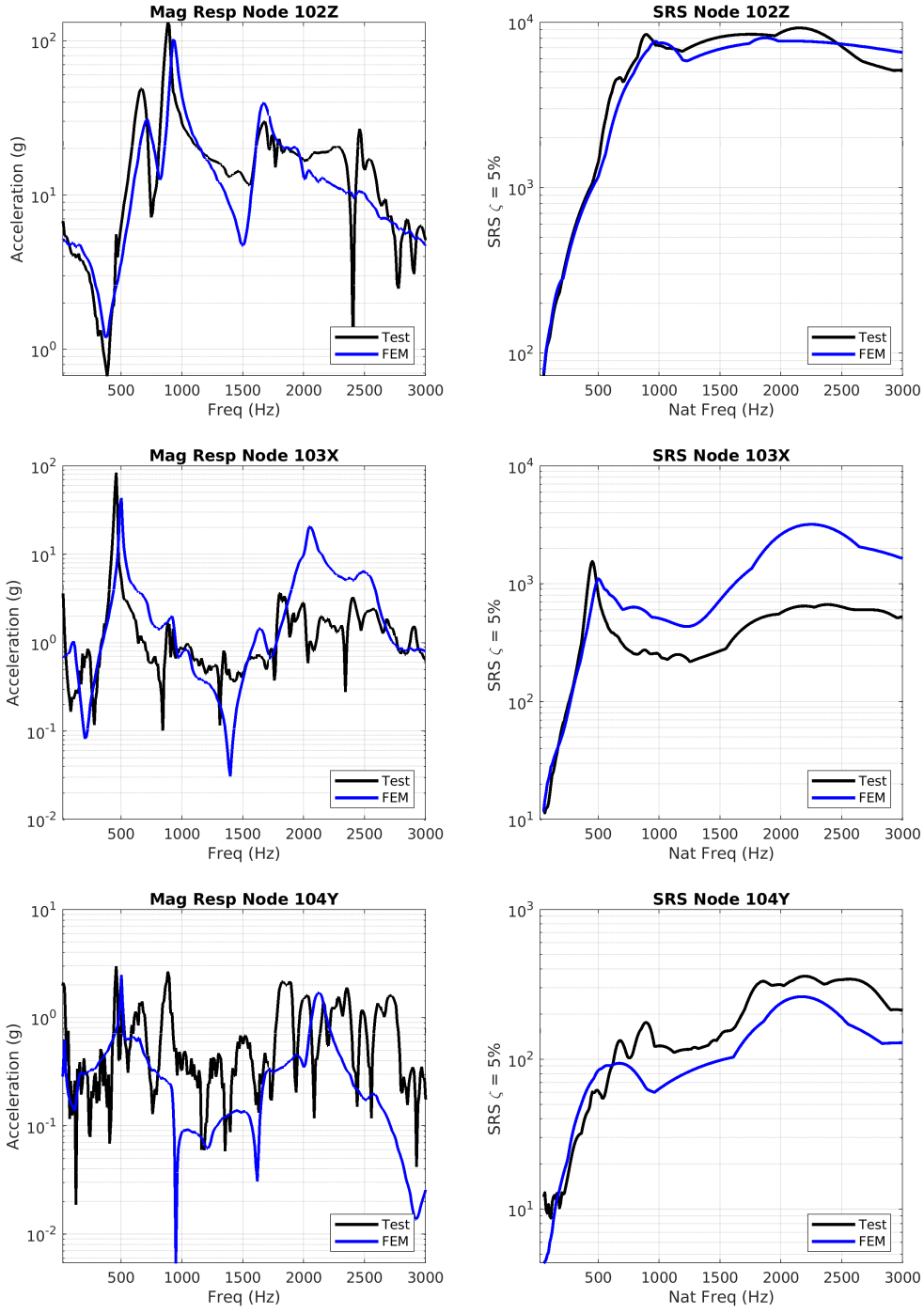

Figure 6-32. Comparison of the response between the FEM and Run62 in test series SHK5182

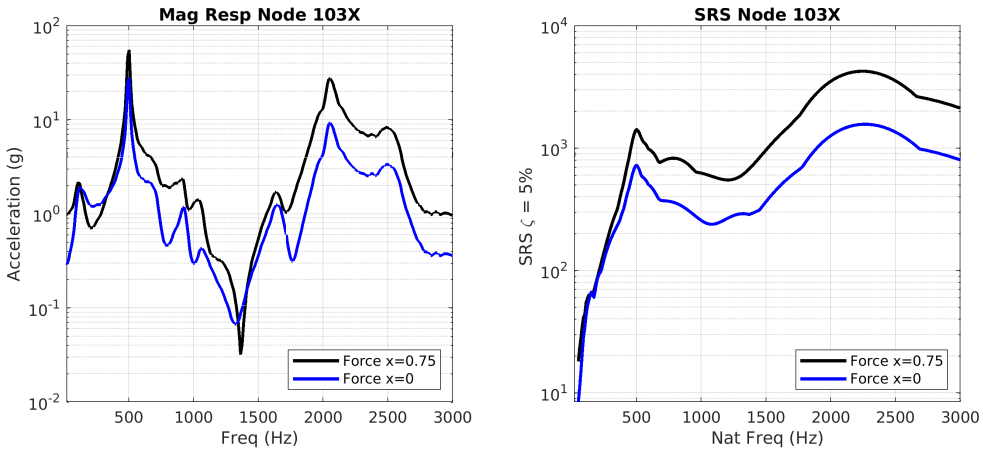

Figure 6-33. Comparison of the response between the FEM with the force centered on the impact block and with a 0.75" offset

at a different location than is modeled. The second is the low level of response in the Y direction to begin with. The response in the Y direction is a factor of 10 less than the X direction and about a factor of 30 lower than the Z direction. Due to the low level, the absolute error in the Y direction can lead to a larger relative error when compared to the other directions.

It is also noted that the prediction of the X direction response is considerably better with the fixture offset in the X direction than when the fixture is centered. This is due to the fact that the gradient across the impact block for the mode shape makes it highly susceptible to errors in modeling the amplitude of the mode shape. Moving the fixture off center reduces any mode shape gradients across the impact block and, therefore, reduces the sensitivity in the location error of the input force.

6.3.3. Validation of run 115: spacers, bungees, fixture offset (X), centered impact

A goal for this research is to explore the effect of the boundary conditions of the plate during a resonant plate test. It is shown in Chapter 4 that the ropes have an effect on the mode shapes of the plate during modal level tests. In order to determine if the ropes have an effect on the system for shock tests, the ropes were replaced with bungees to execute run 115. The data from run 115 is compared run 56 which has the same test configuration besides the suspension. A photo of the bungee boundary condition setup can be seen in Figure 6-36. The data taken with bungees for the plate boundary conditions can be seen in Figure 6-37.

Using data to determine the effect of the boundary condition is difficult as there are many factors that go into comparing the model to the test data. Comparing the two predictions of the FEM to data shown in Figures 6-37 and 6-34 show that the model prediction with bungees is slightly better when comparing the top plate of the test fixture. The SRS comparisons for Z and X are closer and the Y direction has high relative errors due to reasons previously explained.

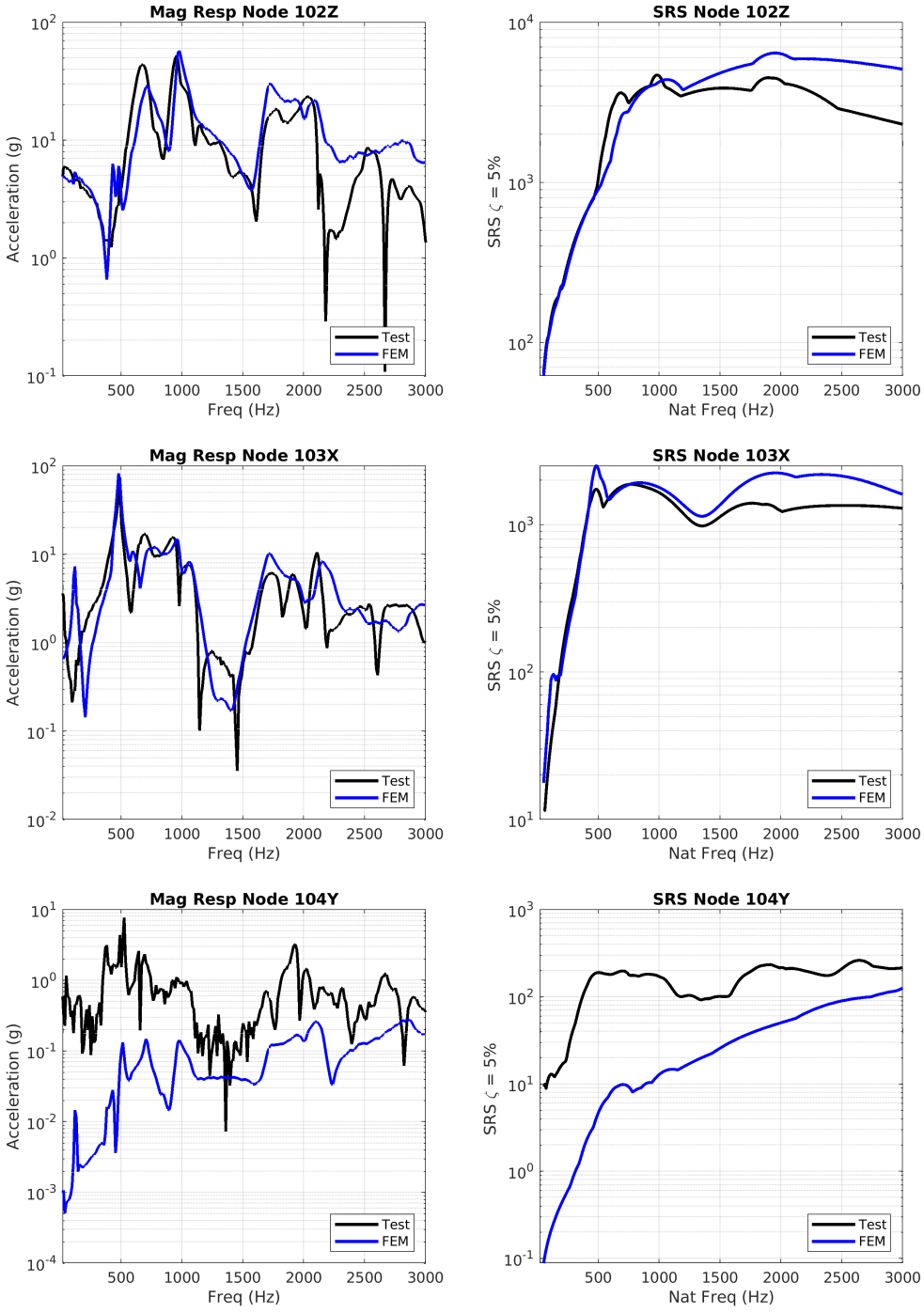

Figure 6-34. Comparison of the response between the FEM and Run56 in test series SHK5182

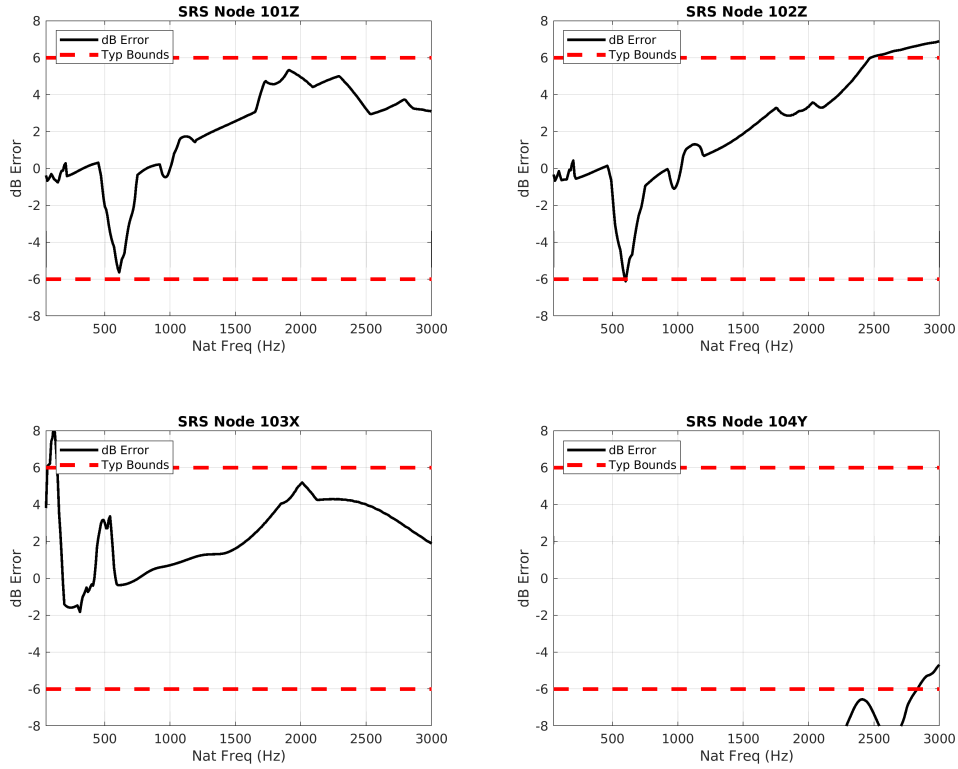

Figure 6-35. SRS validation comparison between the FEM and the data from SHK5182 run 56

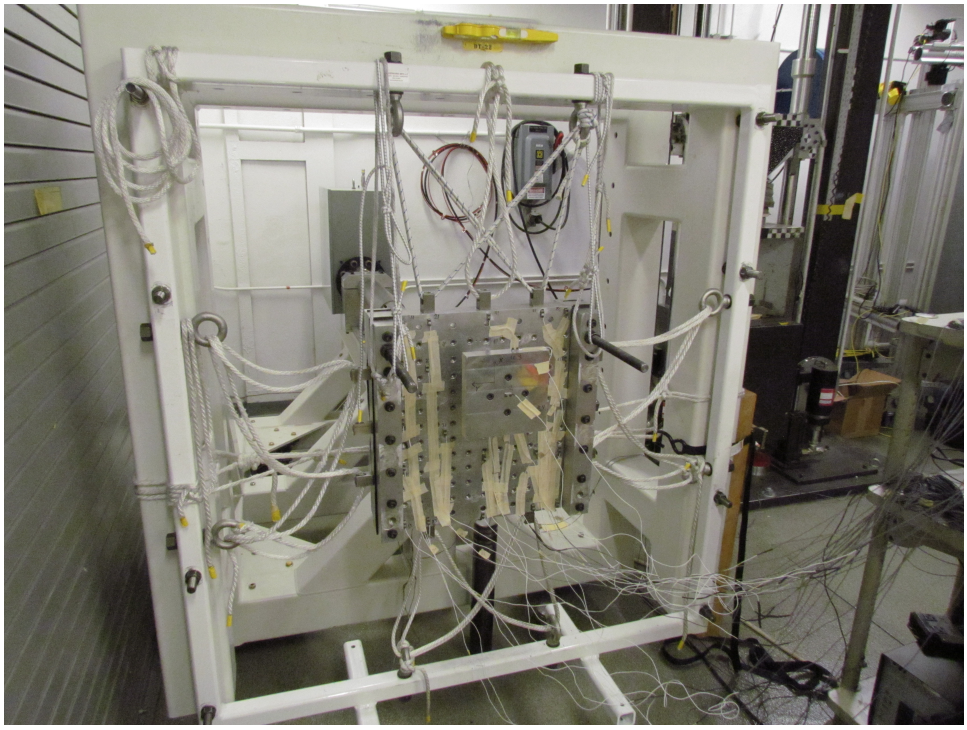

Figure 6-36. Photo of the resonant plate supported solely by bungee cords

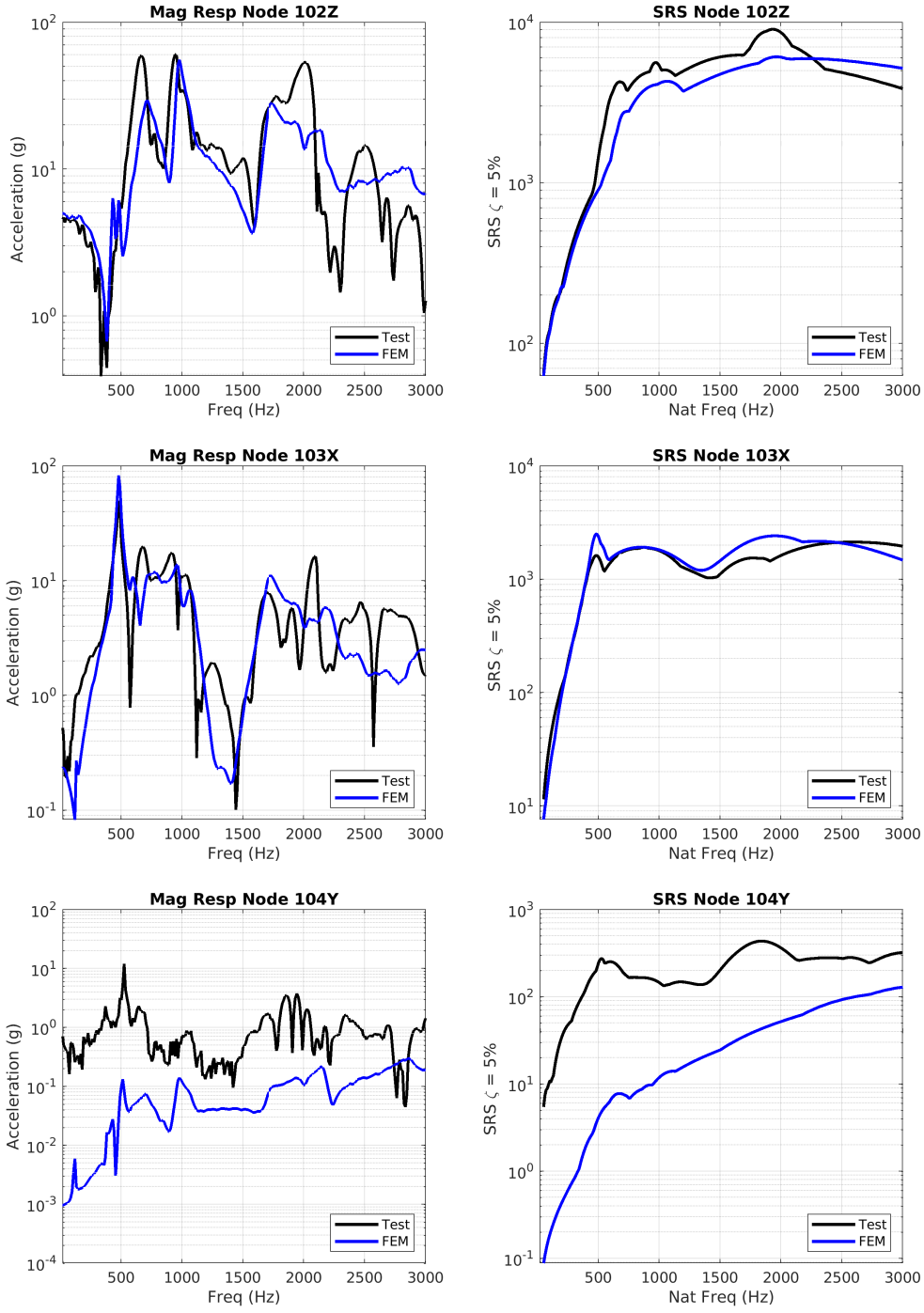

Figure 6-37. Comparison of the response between the FEM and Run115 in test series SHK5182

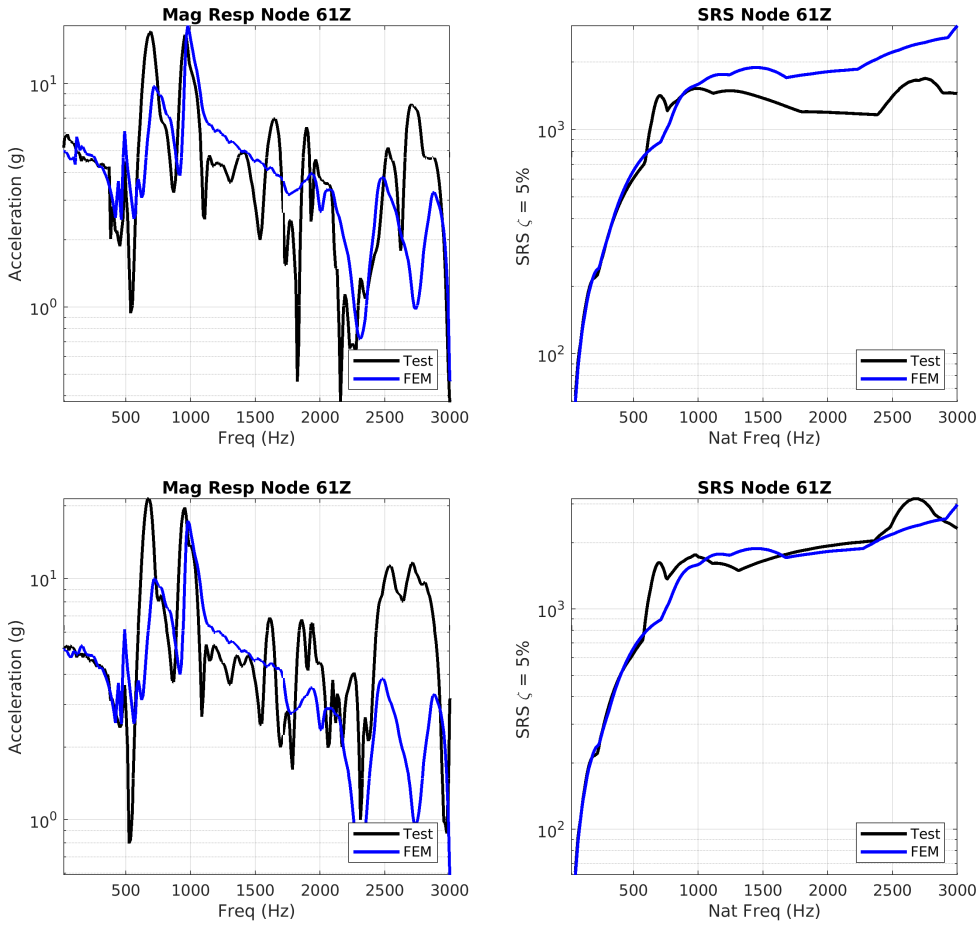

Figure 6-38. Comparison of the response of node 61 between the FEM and test data with ropes (top) and bungees (bottom) as boundary conditions

In addition to comparing the prediction of the top plate of the fixture, a node on the resonant plate is compared for the data taken with and without ropes. Examination of the response of node 61, a node located adjacent to one of the top rope anchors, shows that the plate supported by bungees does a better job matching the FEM than the plate with ropes as shown in Figure 6-38. It is assumed that the reason for this increase in model fidelity is the elimination of the modeling of the ropes as the bungees do not need to be modeled.

One last comparison of the bungee and rope boundary conditions is to compare the test data without any model comparison. The degrees of freedom from test runs 56 and 115 are compared and the response with bungees is higher at resonances. This is demonstrated by looking at the response at the center of the plate in Figure 6-39. Examination of this measured response from the two different test runs shows that the response of the center of the plate is higher with the bungees than with the ropes in the frequency range examined.

Another aspect of comparing the two sets of test data is the response at high frequencies. Typically for pyroshock tests, the limitation for the accelerometers is due to exciting the accelerometer's internal resonance and going over the acceleration limit of the accelerometer.

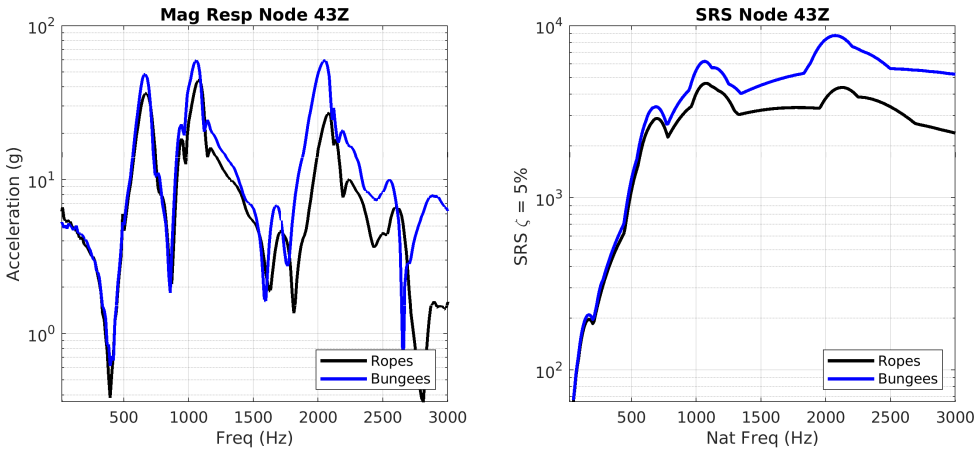

Figure 6-39. Comparison of the test data at the center of the plate between run 056 and run 115 in test series SHK5182

Exciting this resonance is unavoidable for pyroshock tests. The internal resonance for Endevco 7270-20k type accelerometers is between 300 and 500 kHz.

In order to observe a difference in the plate response caused by the boundary condition. The frequency domain of the response with the bungees and the ropes is examined by taking a ratio of the two for any given frequency. This ratio is in Figure 6-40. Figure 6-40 reiterates the result from Figure 6-39 where the bungee boundary condition produces higher response in the examined frequency range, 10-3000 Hz. However, the ropes produce a higher response beginning around 200 kHz. This is critical because the bungees reduce the amount of energy put into the accelerometer resonance and allow for the same accelerometer to have a higher mechanical shock limit.

6.3.4. Validation of run 46: spacers, ropes, fixture offset (X&Y), centered impact

Run 46 from the SHK5182 test series has the spacer between the fixture and the resonant plate just like all of the previous fixture comparisons. The impact block is located at the center of the plate and the concept fixture is offset in both the X and Y directions. The comparison of responses between the FEM and the test data for this run is in Figure 6-41.

The relative error comparing the SRSs of the FEM to the SRSs from run 46 is in Figure 6-42. This simulation does better than the previous simulations as all of the degrees of freedom fall within the tolerances except for a short portion in the X direction. It appears that the location of the test fixture and impact block is at a less sensitive location with respect to the mode shapes of the resonant plate.

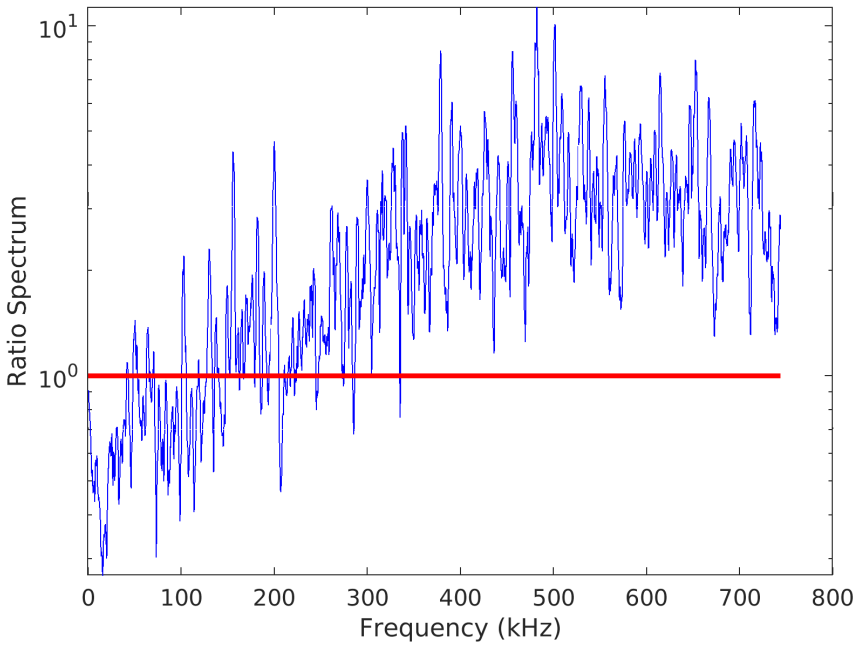

Figure 6-40. Ratio of the frequency response at the center of the plate from run 56 over run 115 from test series SHK5182

6.3.5. Validation of run 53: no spacers, ropes, fixture offset (X&Y), centered impact

Validation test run 53 has the same configuration as run 46, but with the spacers removed from the test and simulation. The purpose of the spacers is to localize contact to provide a more linear system that is easier to model. The responses of this test are shown in Figure 6-43.

In addition to the visual comparison of the responses in Figure 6-43, the relative error of the SRSs is shown in Figure 6-44. When comparing the errors in Figures 6-42 and 6-44, the model of the system with the spacers has better results when compared to the model without spacers. In addition to the comparison of the responses, the damping in the model without spacers was increased after examination of the data. The damping was increased for the fixture modes from 2 to 4 percent. This increase in damping is not surprising as the connection area without spacers is large and more micro-slip is expected.

6.3.6. Validation of run 61: no spacers, ropes, fixture offset (X&Y), offset impact

Validation run 61 is the only run that has an off center impact location. To execute the test, the test operator has to heavily manipulate the rope system to move the impact block in front of the gas gun. As a result of that manipulation, there was about a one inch offset in the Y direction between the projectile and the impact block which is not accounted for in the model as shown in

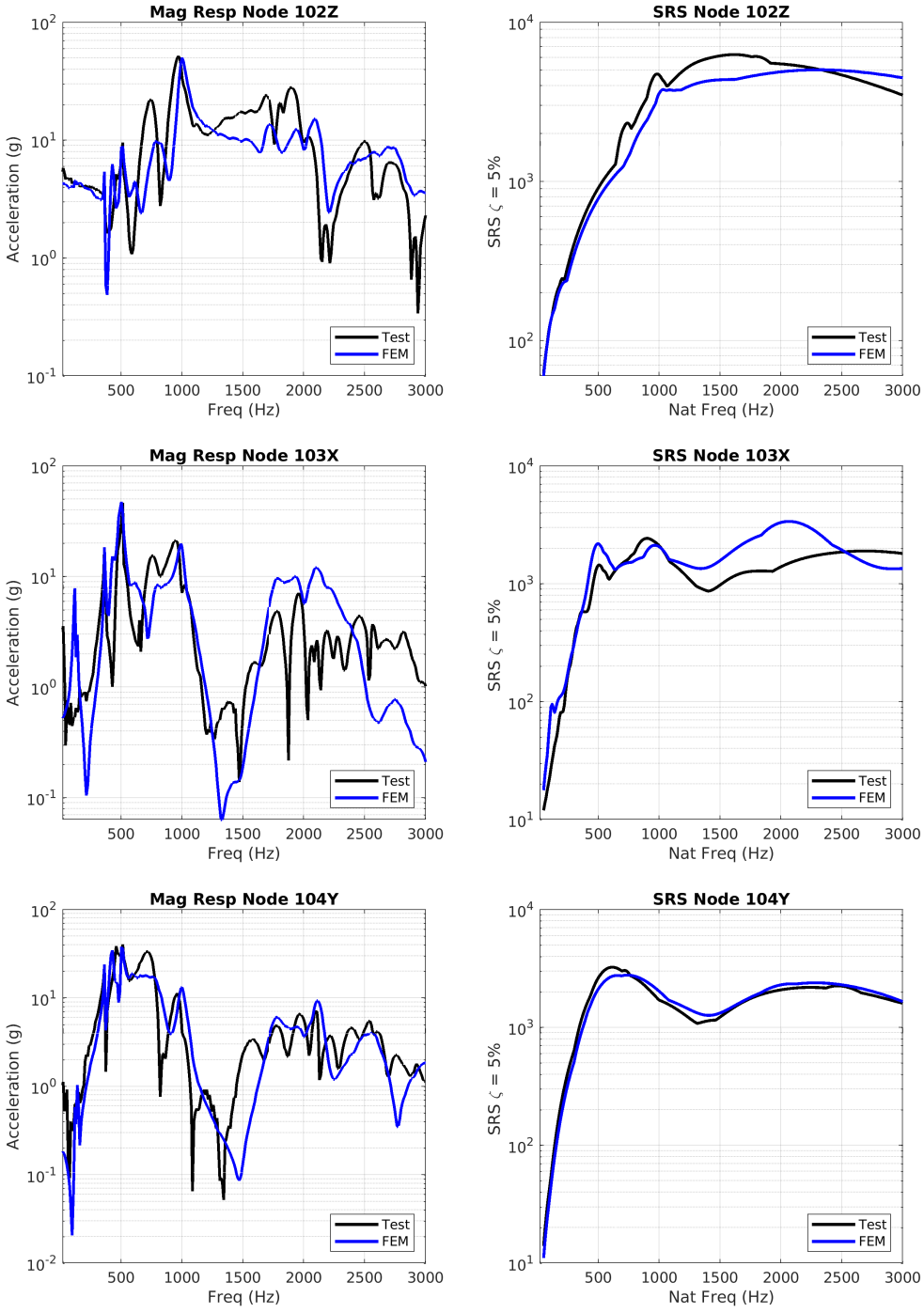

Figure 6-41. Comparison of the response between the FEM and run 46 in test series SHK5182

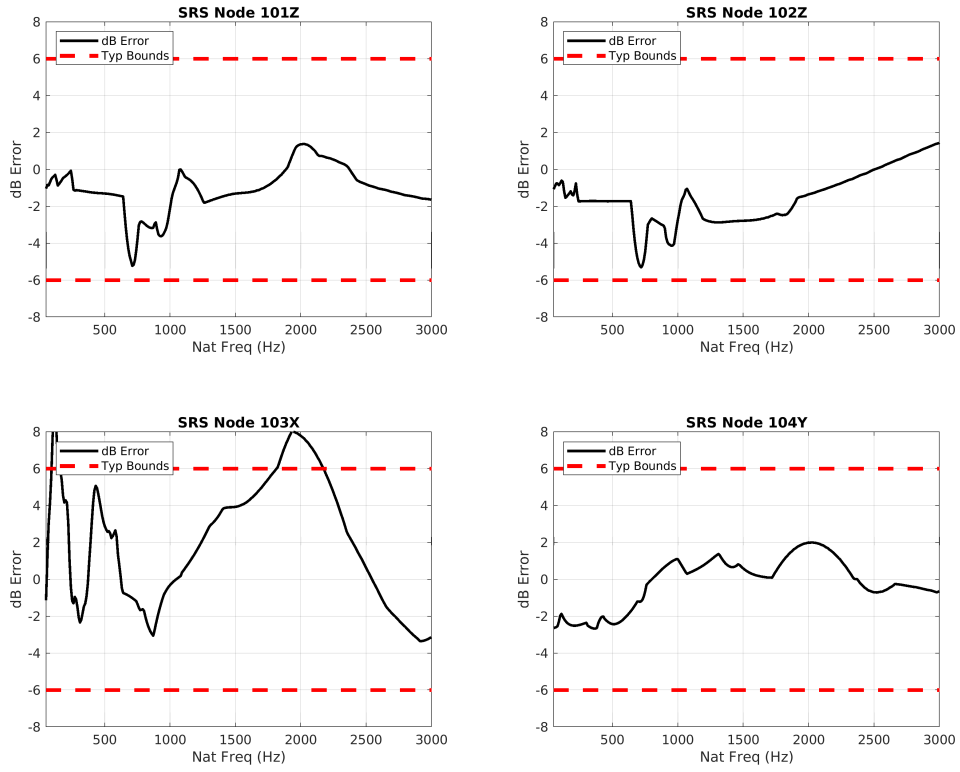

Figure 6-42. SRS validation comparison between the FEM and the data from SHK5182 run 46

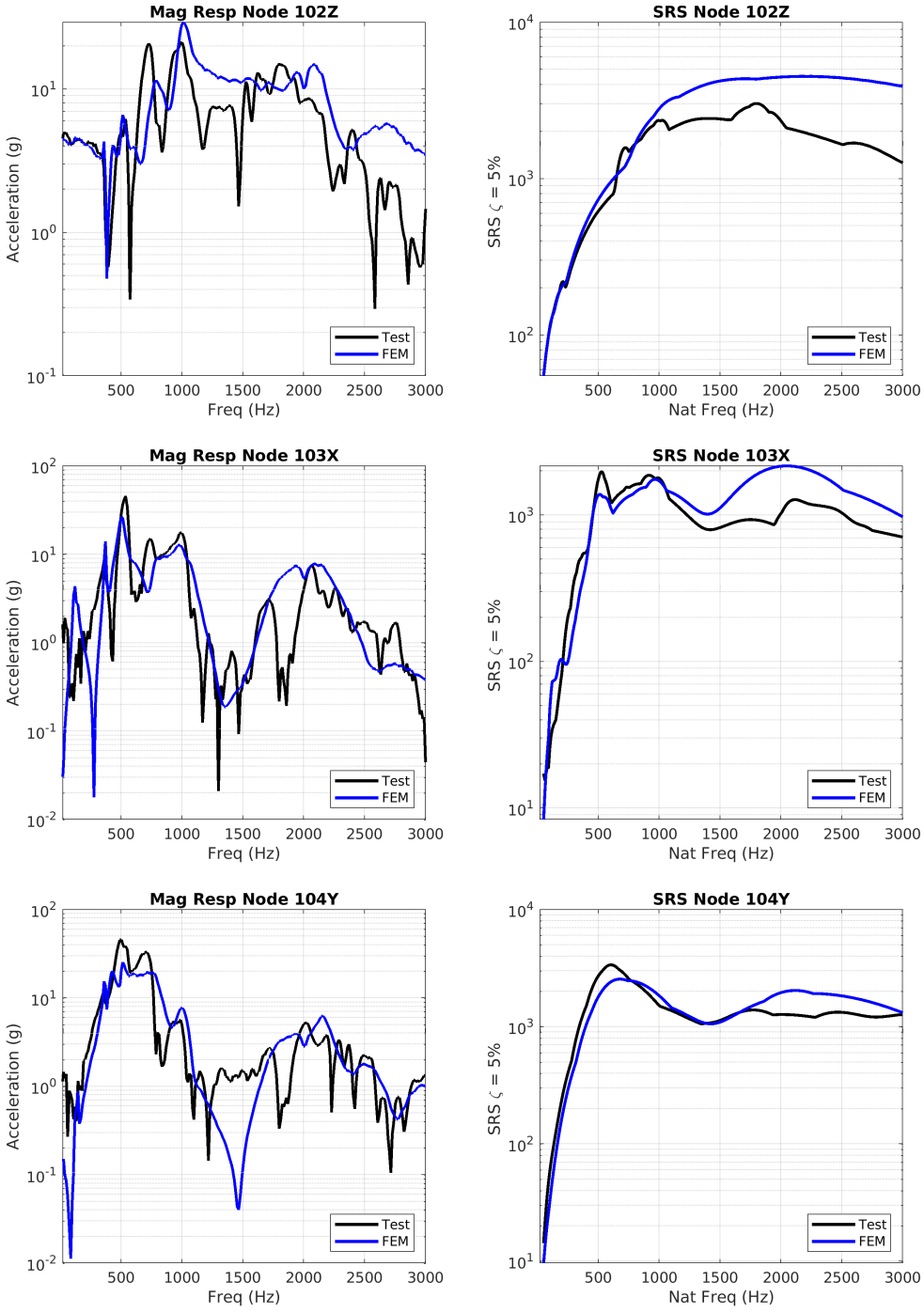

Figure 6-43. Comparison of the response between the FEM and Run 53 in test series SHK5153

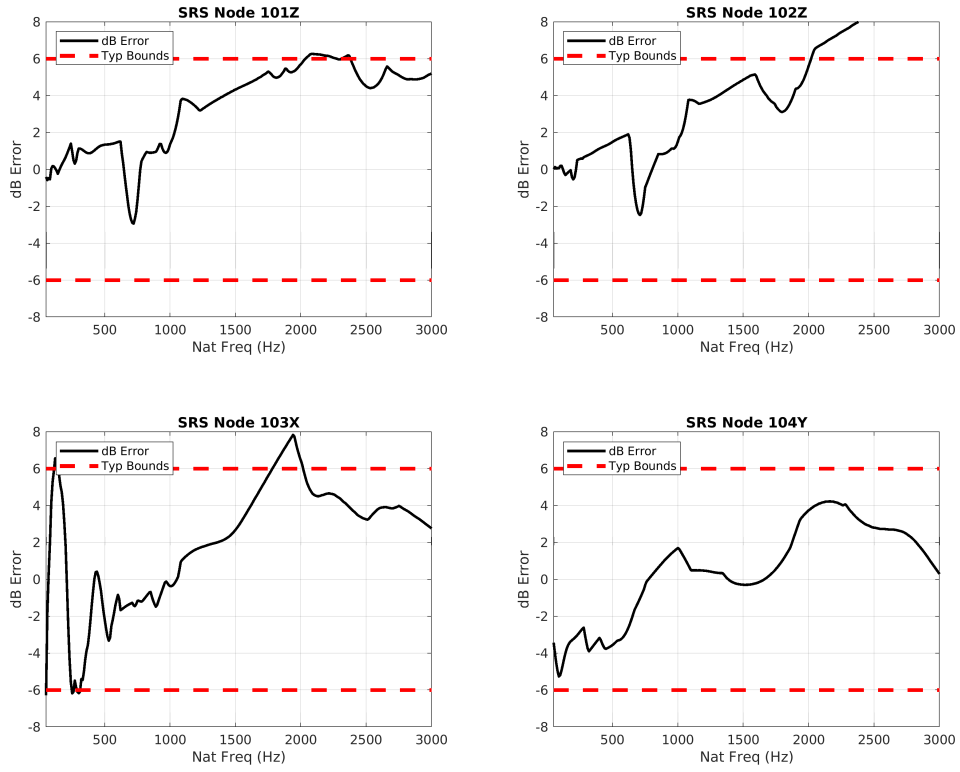

Figure 6-44. SRS validation comparison between the FEM and the data from SHK5153 run 53

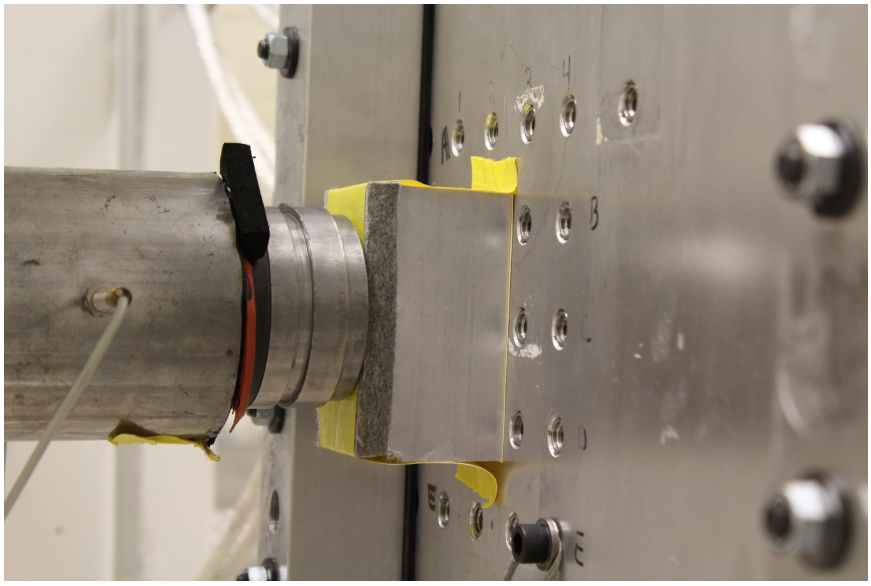

Figure 6-45. Location of the projectile hitting the impact block for SHK5153 run 61

Figure 6-45. The side ropes are also fully engaged in this configuration when compared to the other configurations where the side ropes are mostly loose.

The comparison between the data from run 61 in test series SHK5153 and the FEM is in Figure 6-46, and the relative error in the SRSs is in Figure 6-47. These results show that the general prediction in the X, Y, and Z directions are within tolerances at frequencies below 2 kHz. The result for this configuration is acceptable given the error in where the impact force is located in the model, the lack of spacers, and the engagement of side ropes which are not modeled.

There are two other conclusions drawn from this final validation comparison. The first is with respect the relative amplitudes of the SRSs for run 61. They are generally within a factor of 2 for all directions and all frequencies from each other. This demonstrates some of the flexibility that the test facility has in executing multi-axis shock tests. The second conclusion is how the knee frequency of the Z direction SRS changed from 1000 Hz to 2000 Hz when compared to prior test runs. This is due to the impact location poorly exciting either of the two bending modes at 700 and 1000 Hz. The model did predict the change in knee frequency, but with an over-prediction in amplitude.

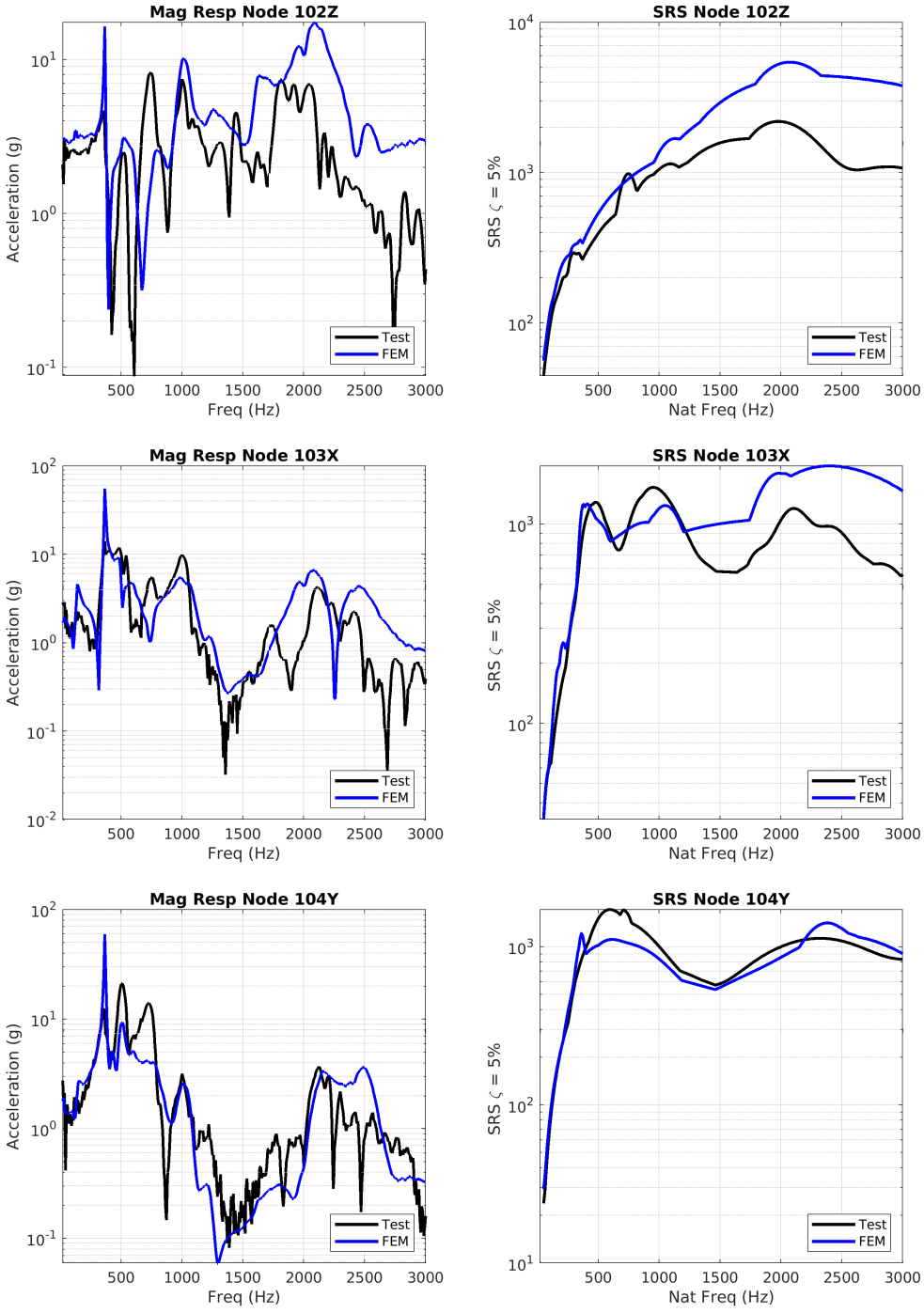

Figure 6-46. Comparison of the response between the FEM and run 61 in test series SHK5153

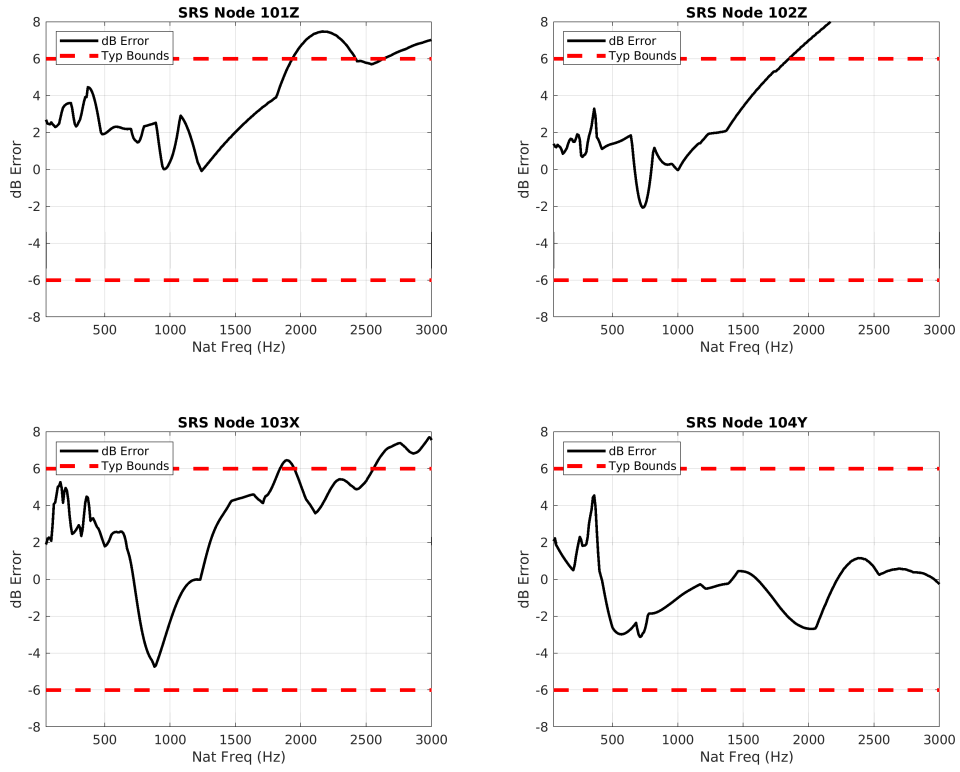

Figure 6-47. SRS validation comparison between the FEM and the data from SHK5153 run 61

7. CONCLUSIONS

The primary goal of this body of work is to build, develop, and validate a finite element model of the resonant plate test environment. The scope of the model is be able to design the test environment (resonant plate, impact location, test fixture design, test fixture location) in order to execute a multi-axis shock test and a unit under test to a specified environment.

The report begins by building a model with linearized 1st principles in mind. The joints are modeled with linearizing the contact area with respect to bolt theory. The model is calibrated to test data at low force levels and updated to represent the hardware when excited at shock type forces. The outcome is a model of the resonant plate with damping bars that is validated to shock tests. In addition to the finite element model, the process of calculating the forces from the projectile are calculated so that the the entire environment is modeled. This whole model is validated to resonant plate with damping bar data and to data with a concept fixture attached.

Traditional experimental modal tests are executed on the bare plate configuration and the plate with damping bar configuration. This test data is used to calibrate the model to low level excitation. Through these tests, it is discovered that a rope anchor is loose and that the ropes suspension system needs to be modeled in order to match higher frequency mode shapes. It is also found that the rubber between the damping bars and the resonant plate need to be imprinted and merged over the whole surface for agreement with data. This is contrary to typical metal to metal contact where only a small surface area around the bolted connection is connected to represent the joint. Using a linear elastic model of the rubber with a modulus that is calibrated about a force input provides a linearized calibrated model. The rubber causes non-linearities in damping and natural frequency but not equally per mode.

A series of resonant plate shock tests are executed on the resonant plate with damping bars installed. From these tests, the forces from the projectile hitting the resonant plate are reconstructed using a technique called SWAT-TEEM. Also, a force at one test configuration can be used to approximate a force calculated from a different configuration. With the calculated forces and the calibrated model, the model of the resonant plate with damping bars is validated by examining the response at multiple locations giving confidence in the validation of the whole model.

Another outcome from the shock tests on the plate with damping bars is the method of computing scaled modal data by using the projectile as the input force. Having modal parameters at the high forcing levels of the environment provides calibration data for the linearized model at shock levels and corresponding damping values. This provides a better linearized model around the forcing levels expected in a shock test versus the force levels from an experimental modal analysis test.

The test series of resonant plate shock tests with the multi-axis concept test fixture provides a lot of information about the fidelity of the model and insight on the execution of the multi-axis shock

test. With respect to the concept fixture design, it provides off-axis motion that can be manipulated through the placement of the impact block and the placement of the fixture. It is shown that the response levels can go from a factor of 30 difference to a factor of two difference from each other depending on the configuration.

The validation tests show that including bosses or washers in the design of the test fixture helps the modeling of the contact between the resonant plate and the test fixture. This allows for a higher fidelity model without calibration data which is critical for the design of the multi-axis tests. It is recommended that this boss or washer element be designed into the multi-axis shock tests.

It is shown in two separate examples that small variations in the location of the impact force influences the response. In addition, the sensitivity of the location of the force with respect to the response is dependent on the location of the test fixture and the impact block in relation to the modes that are excited. When designing multi-axis tests, the impact block and fixture should be placed on parts of the resonant plate that are not sensitive to slight errors in the location of the force.

The boundary conditions for the resonant plate are tested by comparing tests where the plate is suspended with the typical ropes and tests with the plate suspended by bungee cords. There are minor improvements when comparing the test data to the model when the bungees are utilized. However, there is a significant difference in the response of the accelerometers at high (>200 kHz) frequencies. When comparing the test data from two otherwise identical tests, the test with the bungees had a lower acceleration when comparing the raw data, but higher acceleration when examining data under 10 kHz. This is important because it is the resonance of the accelerometer that limits the capacity of the accelerometer. Using the bungees for the boundary condition of the resonant plate would allow for higher inputs at frequency ranges of interest.

It is shown that the model with the addition to the concept fixture is validated when compared to test data because it is able to model the response within the tolerances of a resonant plate shock test. There are model errors due to small errors in the test setup and these errors can be minimized through a careful design of the test configuration. The model is validated against multiple configurations of moving the impact block and test fixture on the surface of the resonant plate. It is recommended that this model of the test configuration be used when developing multi-axis tests for a given environment.

BIBLIOGRAPHY

[1] Peter Avitabile. *Modal testing: a practitioner's guide*. John Wiley & Sons, 2017.

[2] Yuanchang Chen, Peter Avitabile, and Jacob Dodson. Data consistency assessment function (dcaf). *Mechanical Systems and Signal Processing*, 141:106688, 2020.

[3] Melih Eriten, Mehmet Kurt, Guanyang Luo, D Michael McFarland, Lawrence A Bergman, and Alexander F Vakakis. Nonlinear system identification of frictional effects in a beam with a bolted joint connection. *Mechanical Systems and Signal Processing*, 39(1-2):245–264, 2013.

[4] David J Ewins. *Modal testing: theory, practice and application*. John Wiley & Sons, 2009.

[5] Brian A Ferri and Ronald N Hopkins. *A Method for Determining Impact Force for Single and Tri Axis Resonant Plate Shock Simulations*, pages 65–71. Springer, 2020.

[6] Daniel P. Hensley and Randy L. Mayes. Extending smac to multiple references, proceedings of the 24^{th} International Modal Analysis Conference. pages 220–230, January 2006.

[7] Ward Heylen, Stefan Lammens, Paul Sas, et al. *Modal analysis theory and testing*, volume 200. Katholieke Universiteit Leuven Leuven, Belgium, 1997.

[8] Ronald Neil Hopkins and Carl Lee Sisemore. Design of a resonant plate shock test for simultaneous multi-axis excitation. Report SAND2019-0777C, Sandia National Lab.(SNL-NM), Albuquerque, NM (United States), 2019.

[9] Erica M Jacobson. *Using Frequency Based Substructuring to Optimize Multi-Axis Resonant Plate Shock Tests*. Thesis, 2019.

[10] John C O'Callahan. System equivalent reduction expansion process. In *Proc. of the 7th Inter. Modal Analysis Conf., 1989*.

[11] Tyler F Schoenherr. *Calculating the impact force of supersonic hail stones using SWAT-TEEM*, pages 67–79. Springer, 2015.

[12] Carl Sisemore, Vit Babuska, and Robert-X Flores. Multi-axis resonant plate shock testing evaluation and test specification development. Report SAND2020-10224, Sandia National Lab.(SNL-NM), Albuquerque, NM (United States), 2020.

APPENDIX A. Experimental Mode Shapes of the Resonant Plate without Damping Bars

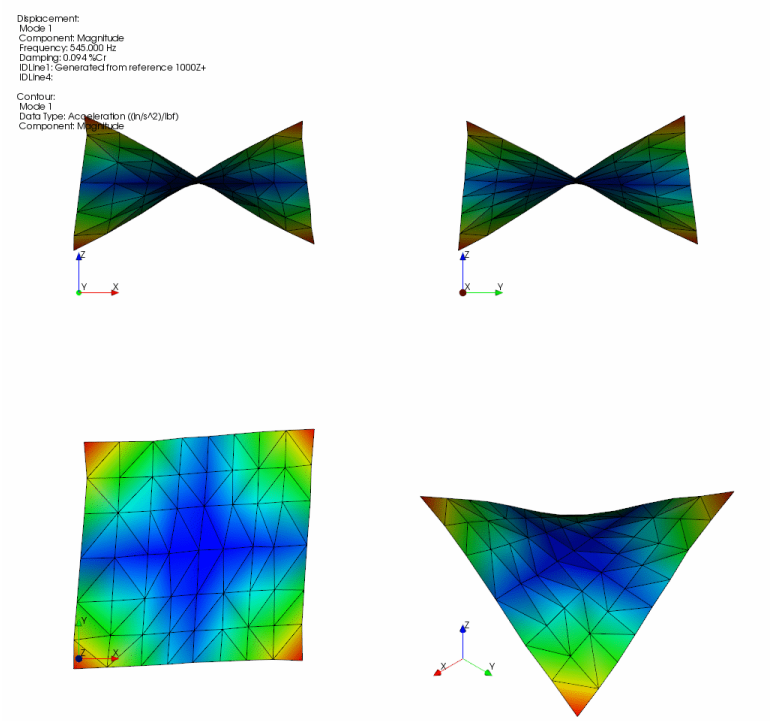

Figure A-1. 1st elastic mode shape of the resonant plate without damping bars fit at 545.0 Hz and 0.094% Damping

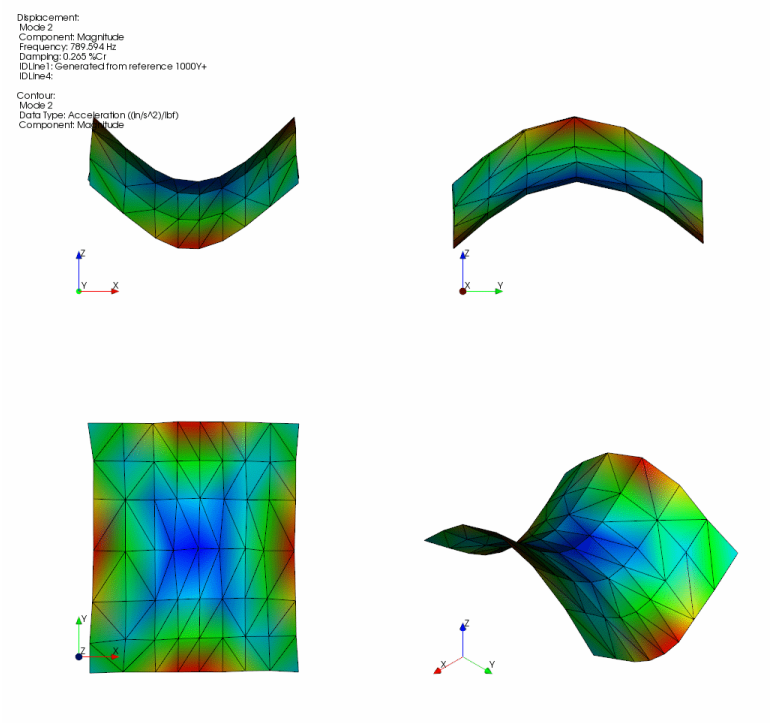

Figure A-2. 2nd elastic mode shape of the resonant plate without damping bars fit at 789.6 Hz and 0.27% Damping

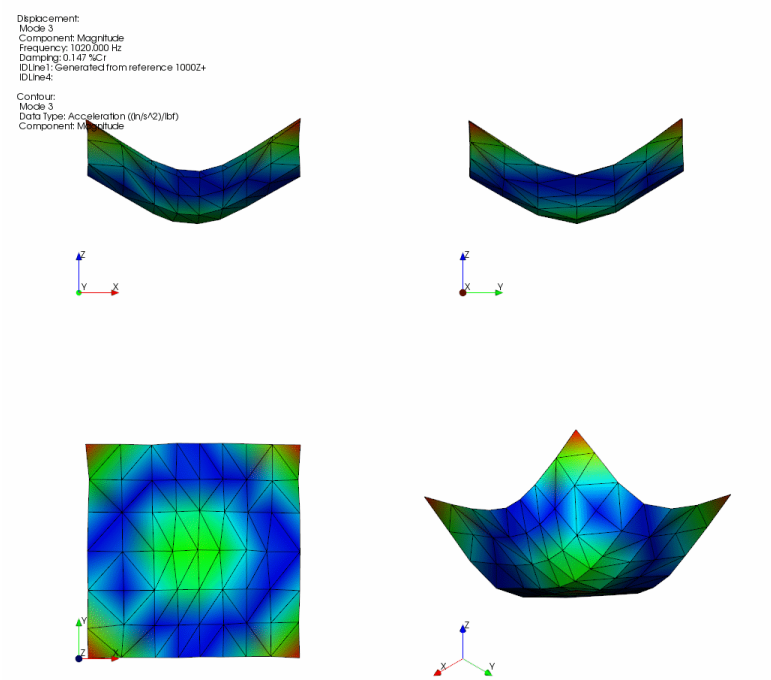

Figure A-3. 3rd elastic mode shape of the resonant plate without damping bars fit at 1020 Hz and 0.147% Damping

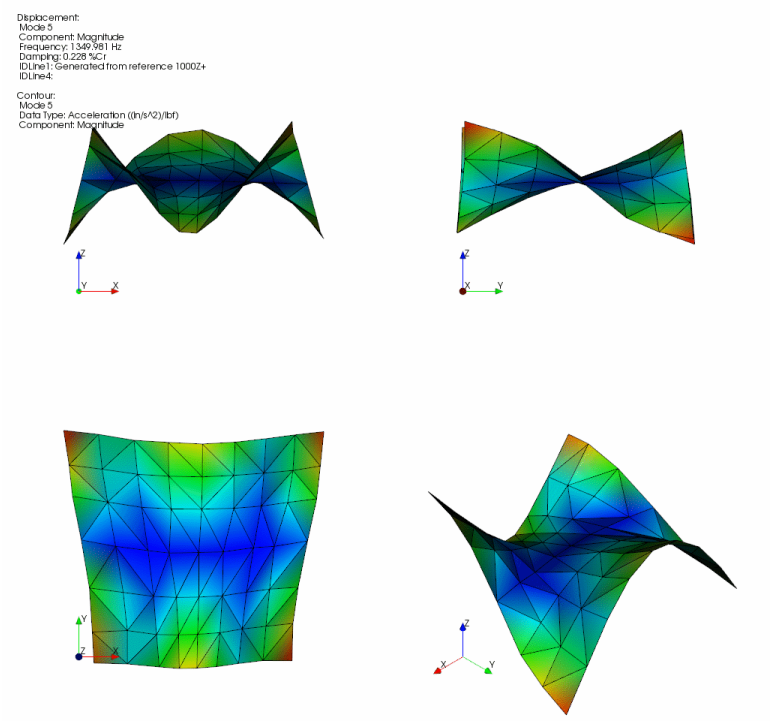

Figure A-4. 4th elastic mode shape of the resonant plate without damping bars fit at 1350 Hz and 0.23% Damping

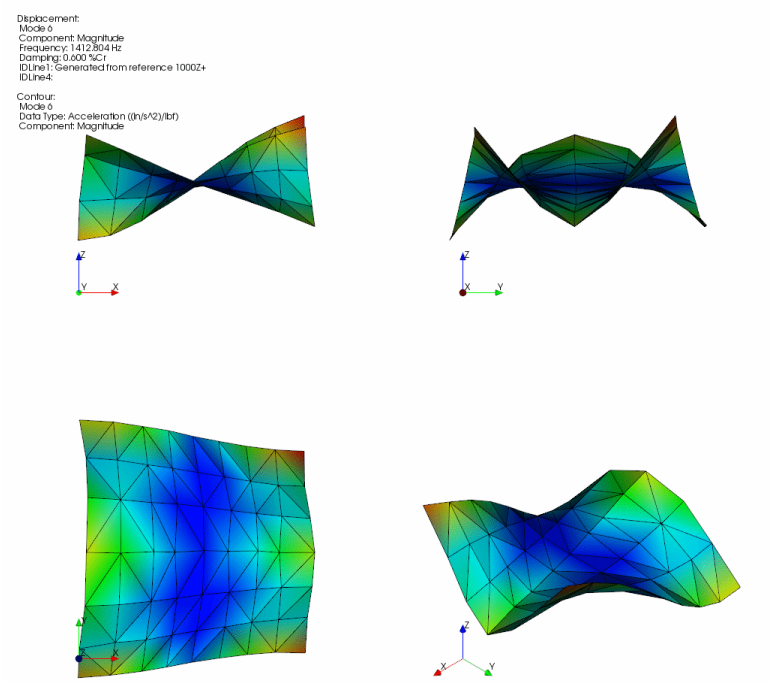

Figure A-5. 5th elastic mode shape of the resonant plate without damping bars fit at 1413 Hz and 0.60% Damping

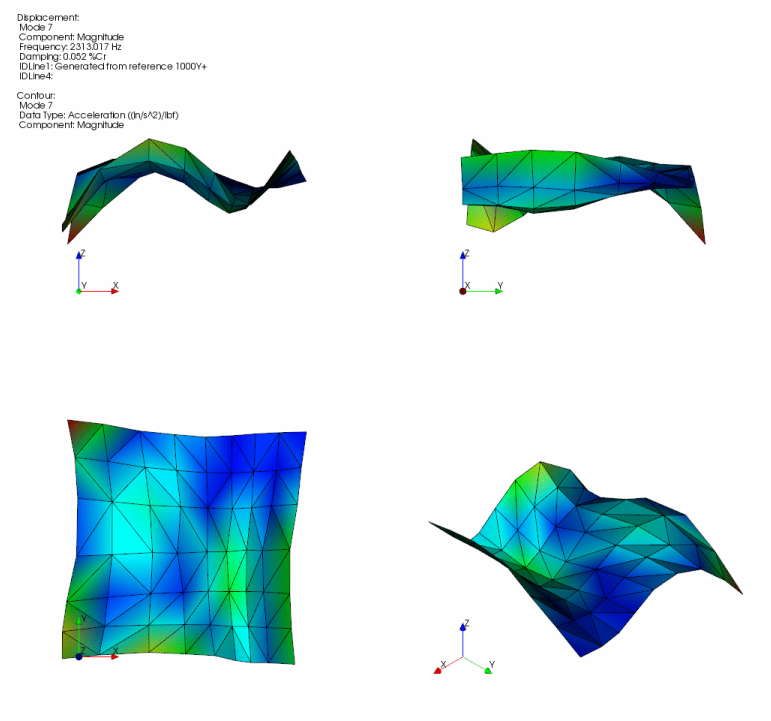

Figure A-6. 6th elastic mode shape of the resonant plate without damping bars fit at 2313 Hz and 0.052% Damping

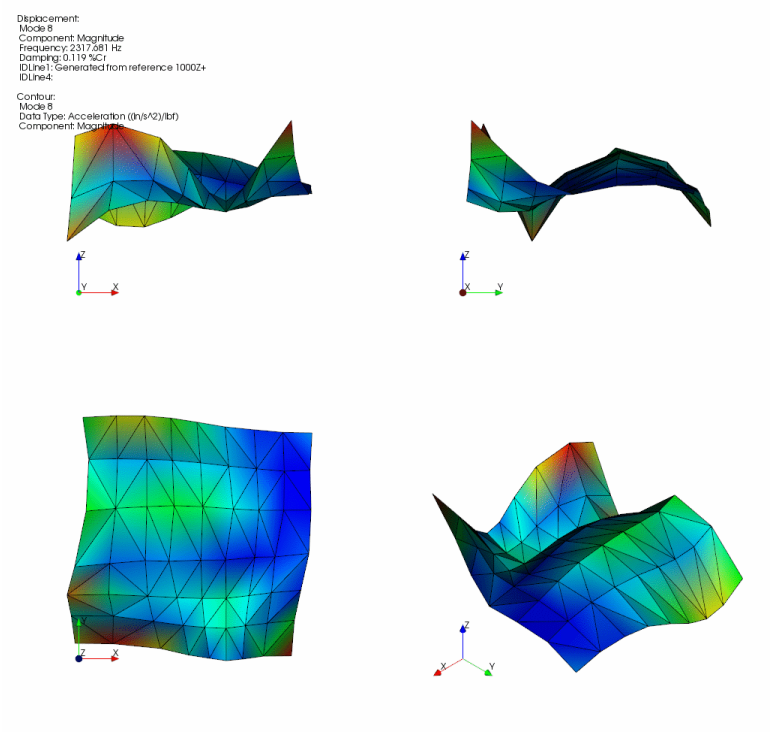

Figure A-7. 7th elastic mode shape of the resonant plate without damping bars fit at 2318 Hz and 0.12% Damping

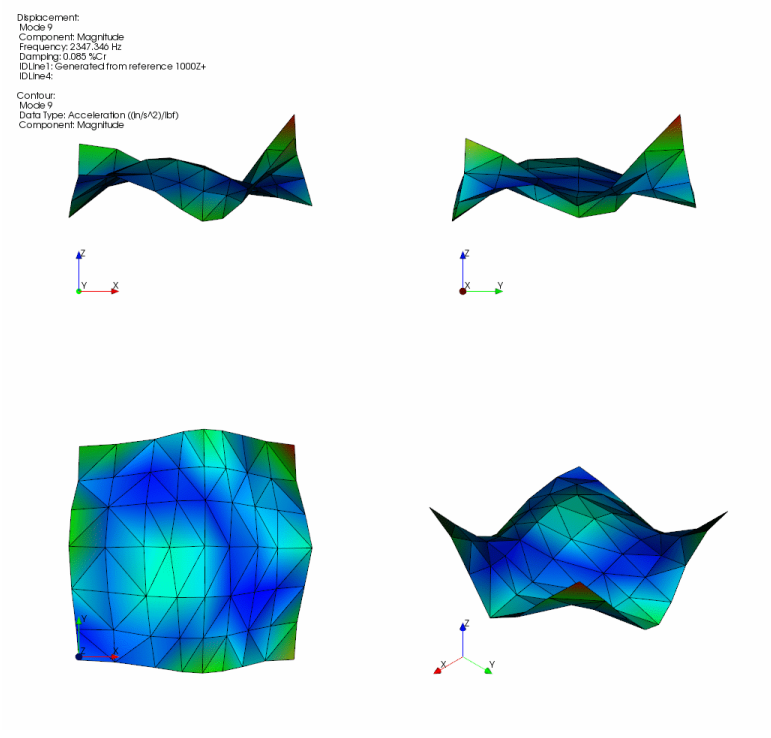

Figure A-8. 8th elastic mode shape of the resonant plate without damping bars fit at 2347 Hz and 0.085% Damping

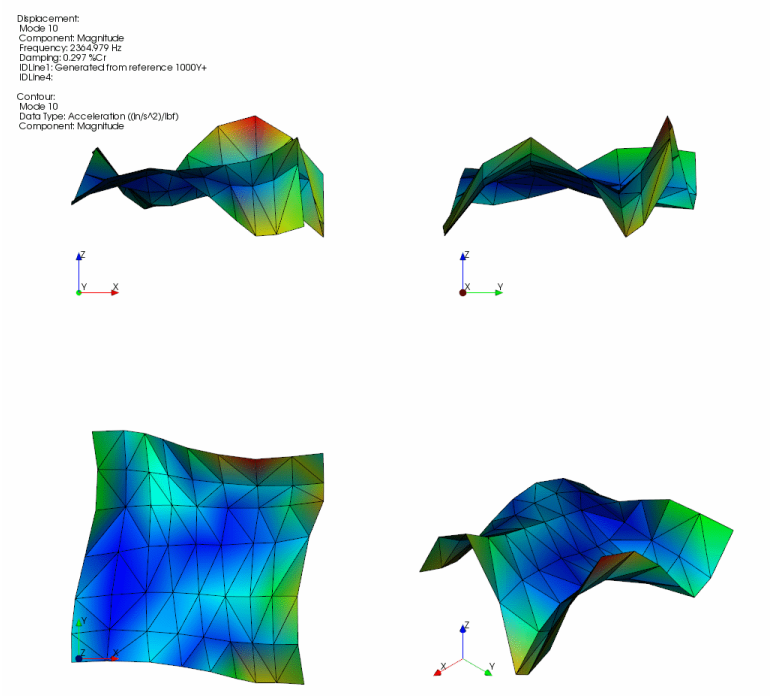

Figure A-9. 9th elastic mode shape of the resonant plate without damping bars fit at 2365 Hz and 0.30% Damping

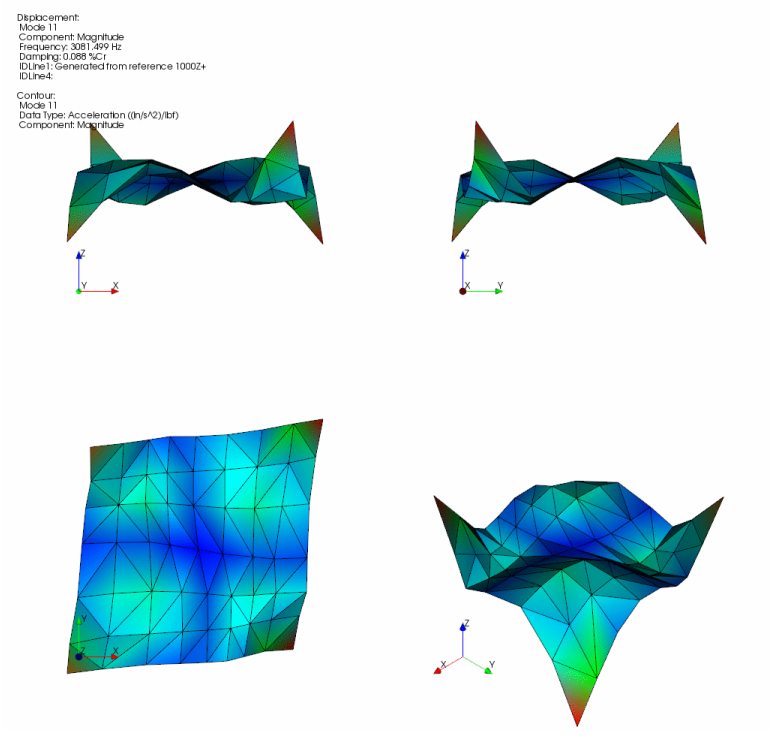

Figure A-10. 10th elastic mode shape of the resonant plate without damping bars fit at 3081 Hz and 0.088% Damping

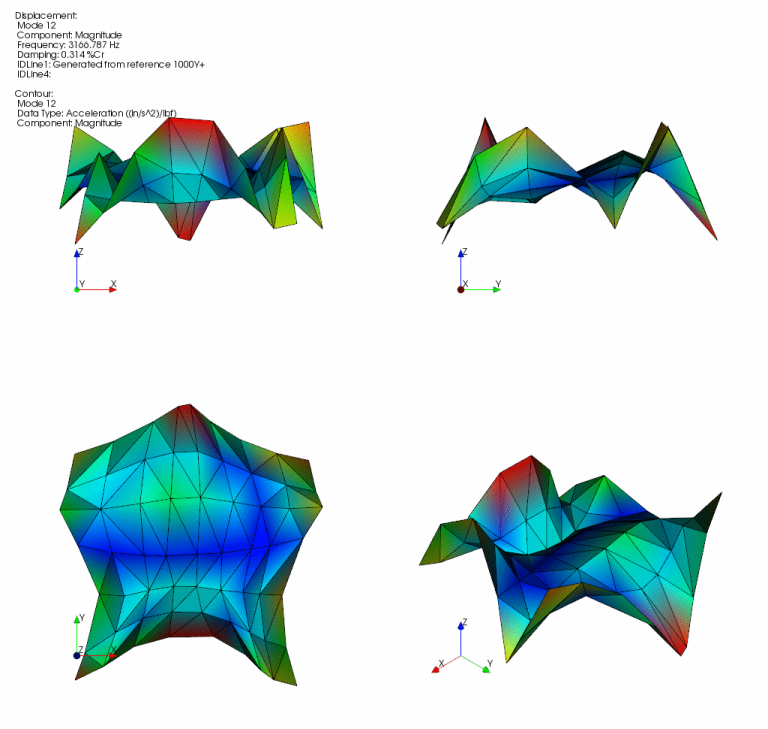

Figure A-11. 11th elastic mode shape of the resonant plate without damping bars fit at 3167 Hz and 0.31% Damping

APPENDIX B. Experimental Mode Shapes of the Resonant Plate with Damping Bars

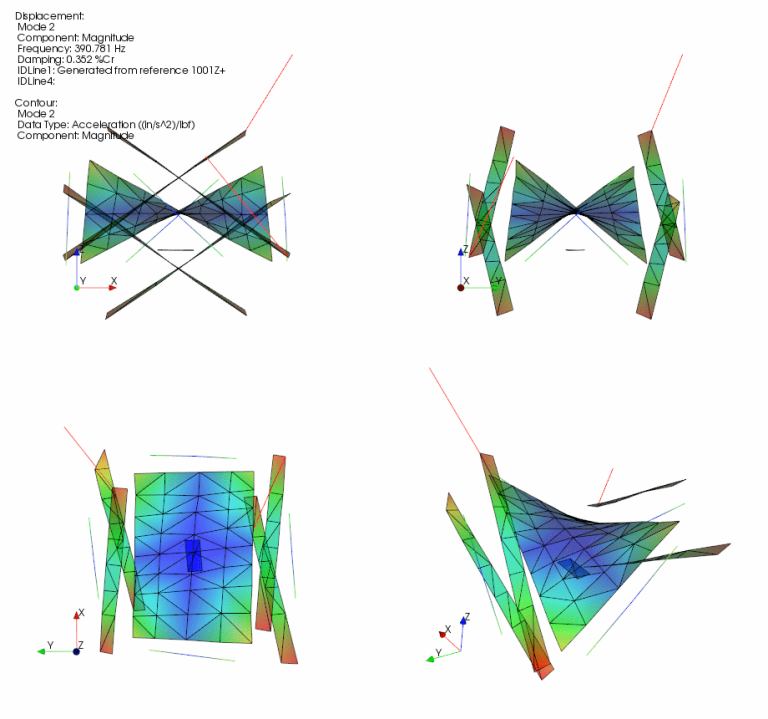

Figure B-1. 1st elastic mode shape of the resonant plate with damping bars fit at 391 Hz and 0.35% Damping

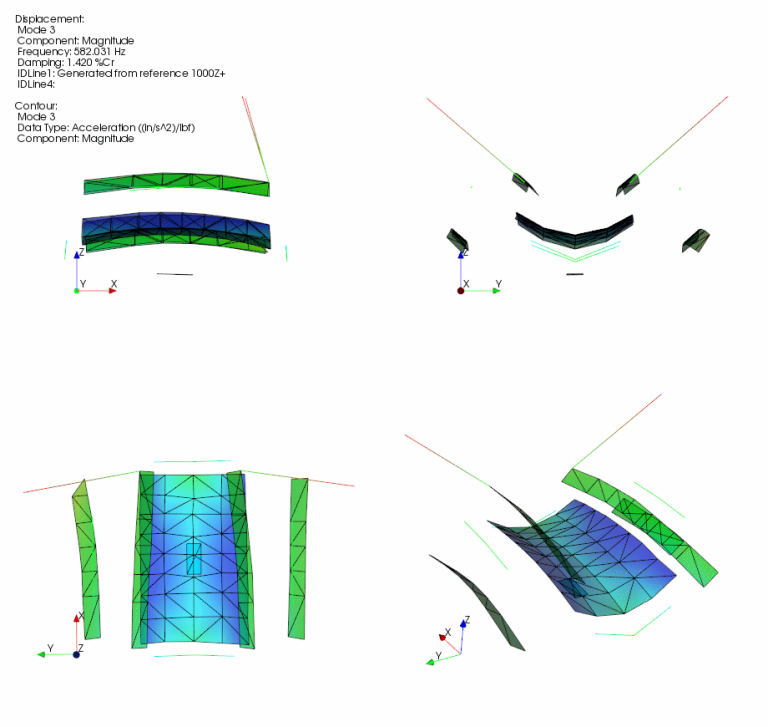

Figure B-2. 2nd elastic mode shape of the resonant plate with damping bars fit at 582 Hz and 1.4% Damping

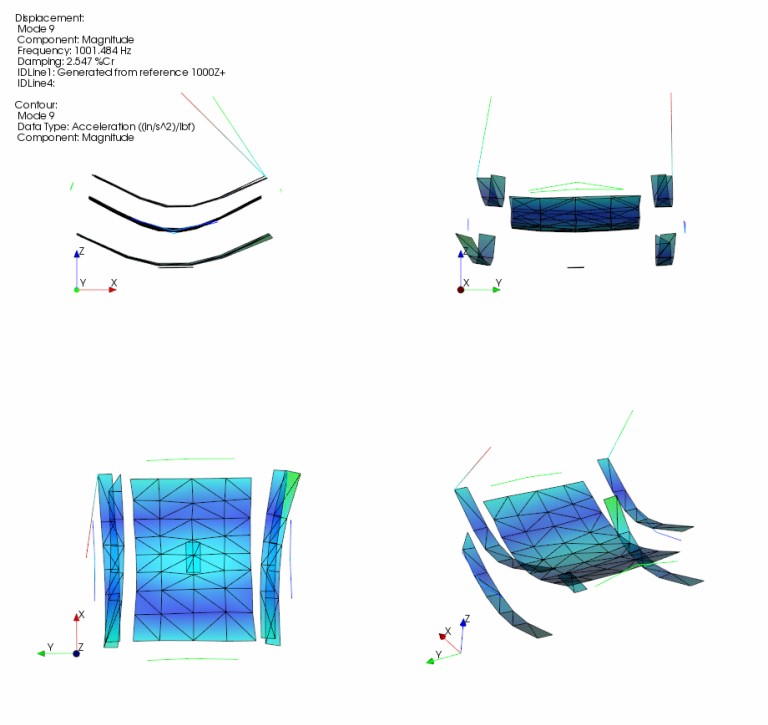

Figure B-3. 3rd elastic mode shape of the resonant plate with damping bars fit at 1001 Hz and 0.094% Damping

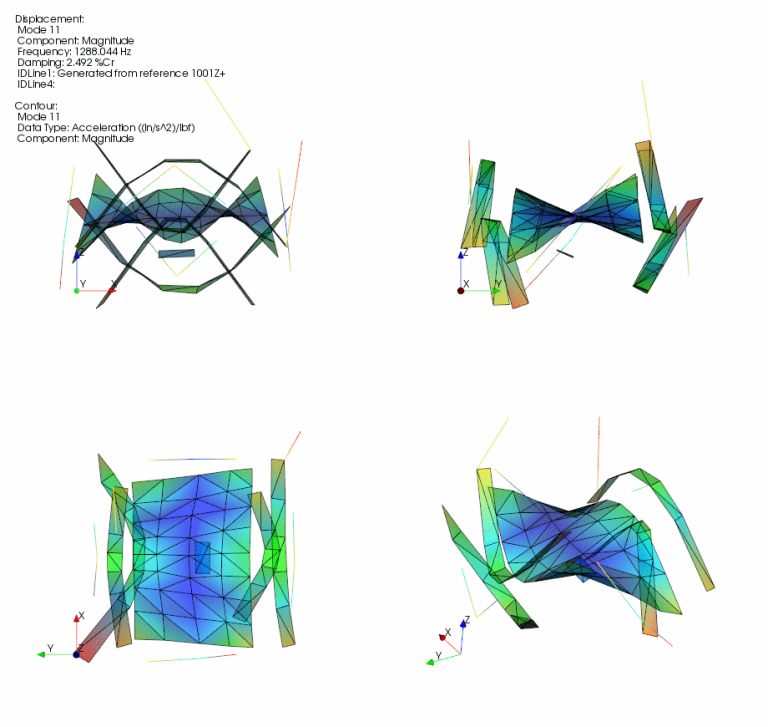

Figure B-4. 4th elastic mode shape of the resonant plate with damping bars fit at 1288 Hz and 2.5% Damping

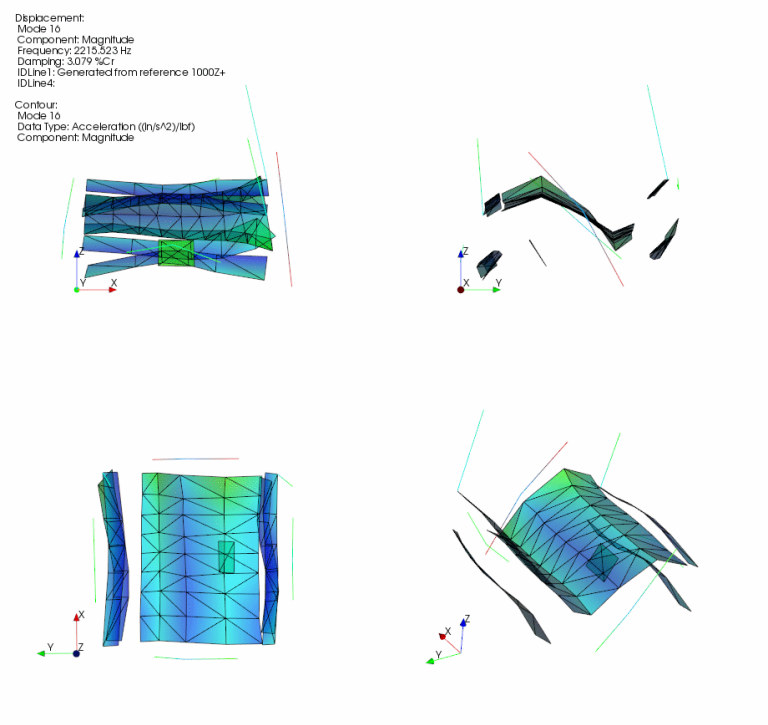

Figure B-5. 5th elastic mode shape of the resonant plate with damping bars fit at 2215 Hz and 3.1% Damping

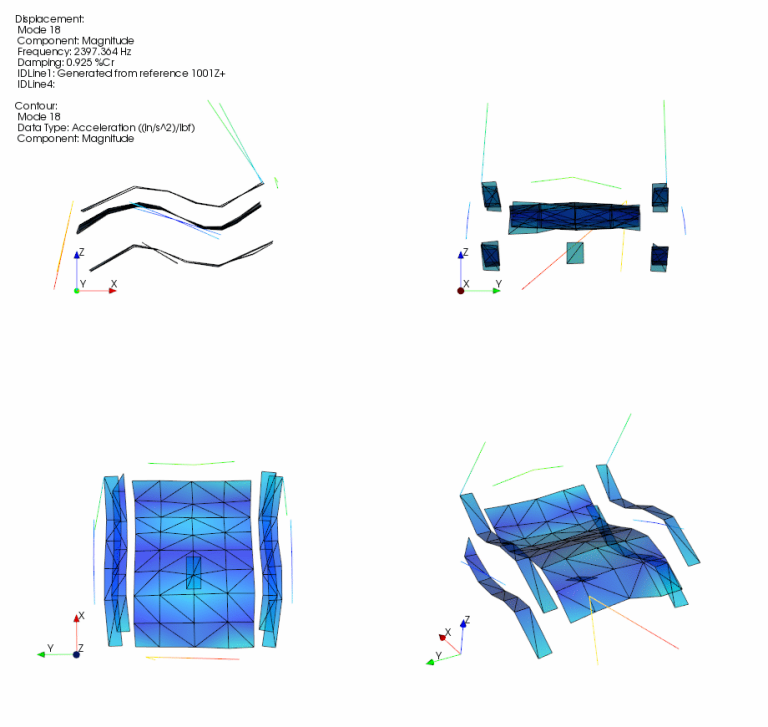

Figure B-6. 6th elastic mode shape of the resonant plate with damping bars fit at 2397 Hz and 0.93% Damping

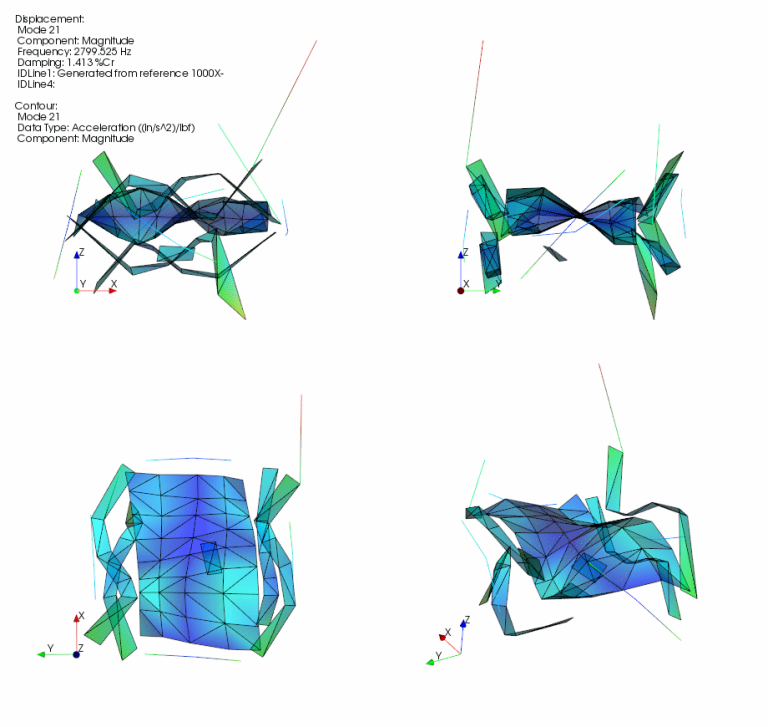

Figure B-7. 7th elastic mode shape of the resonant plate with damping bars fit at 2800 Hz and 1.4% Damping

APPENDIX C. Resonant Plate with Damping Bars Mode Shapes

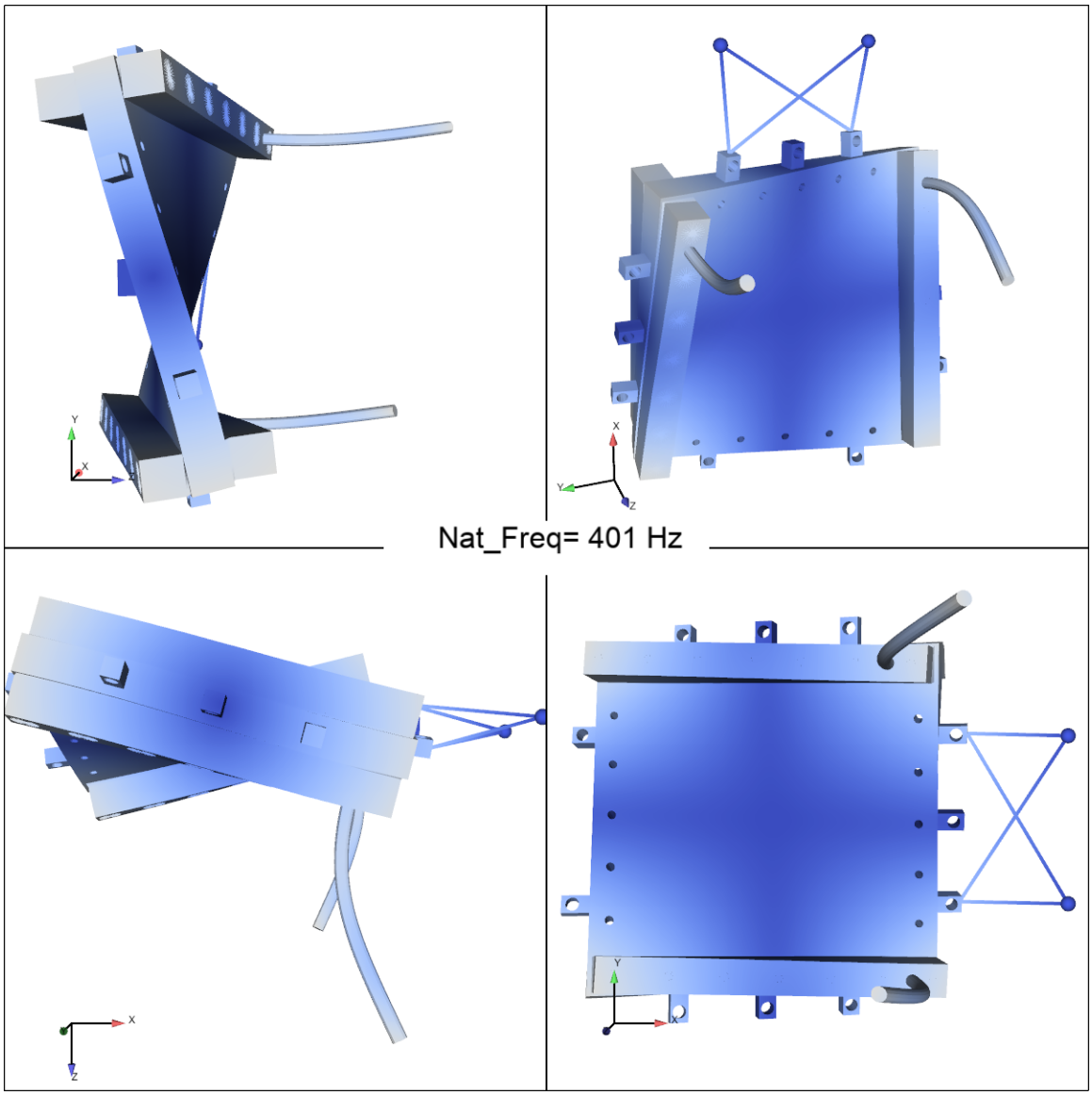

Figure C-1. 1st elastic mode shape compared to the experimental modal data with damping bars

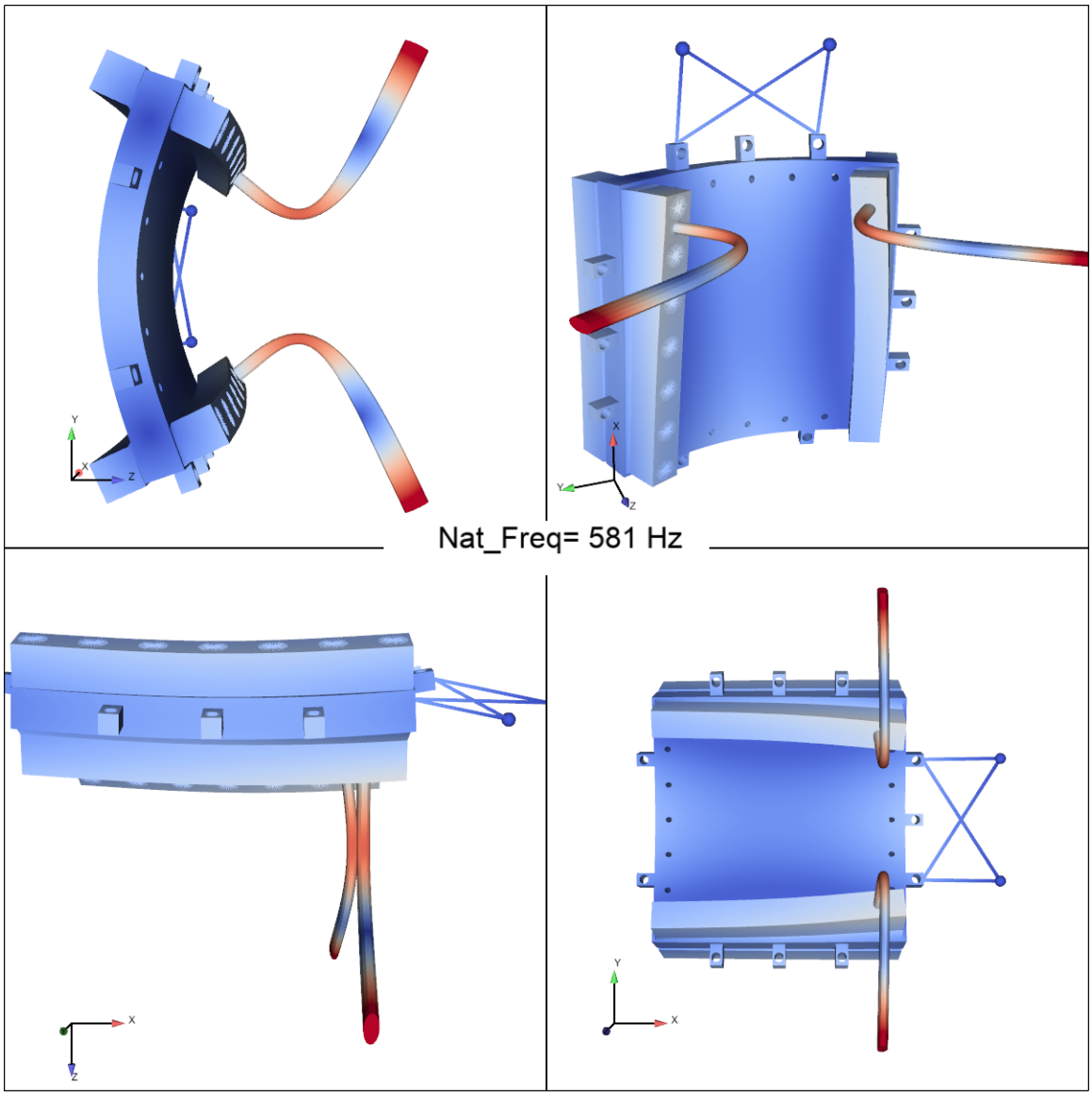

Figure C-2. 2nd elastic mode shape compared to the experimental modal data with damping bars

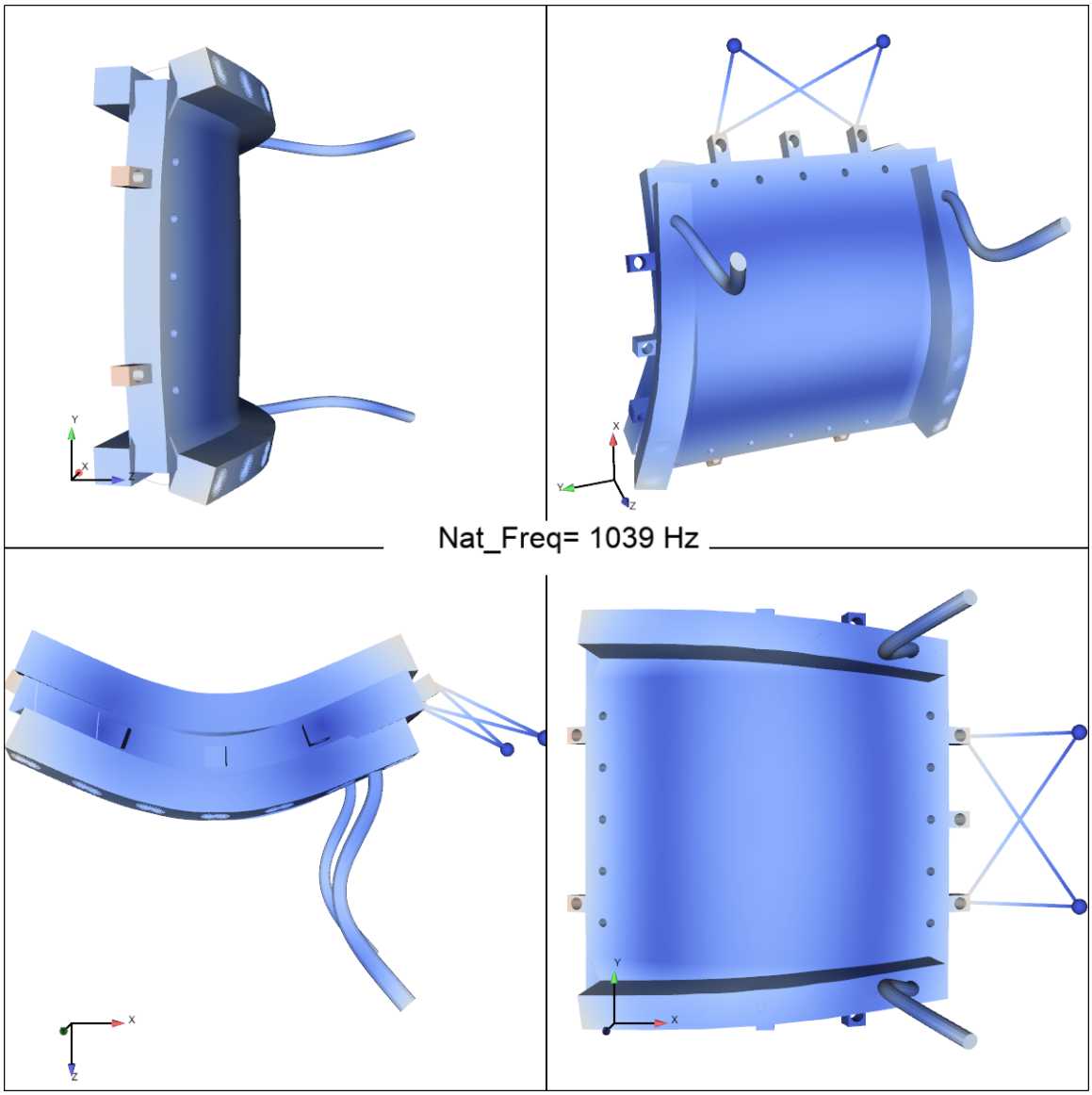

Figure C-3. 3rd elastic mode shape compared to the experimental modal data with damping bars

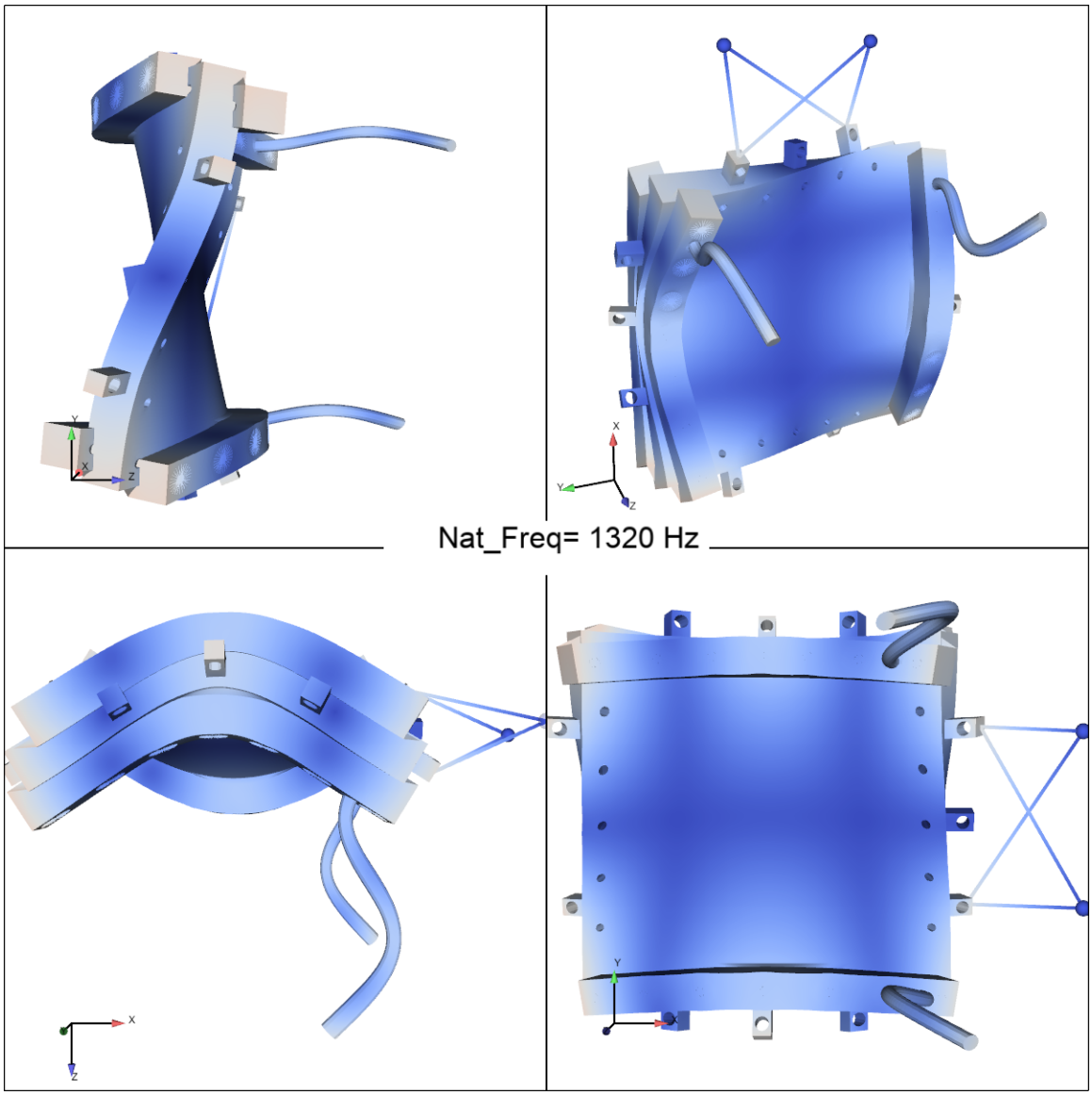

Figure C-4. 4th elastic mode shape compared to the experimental modal data with damping bars

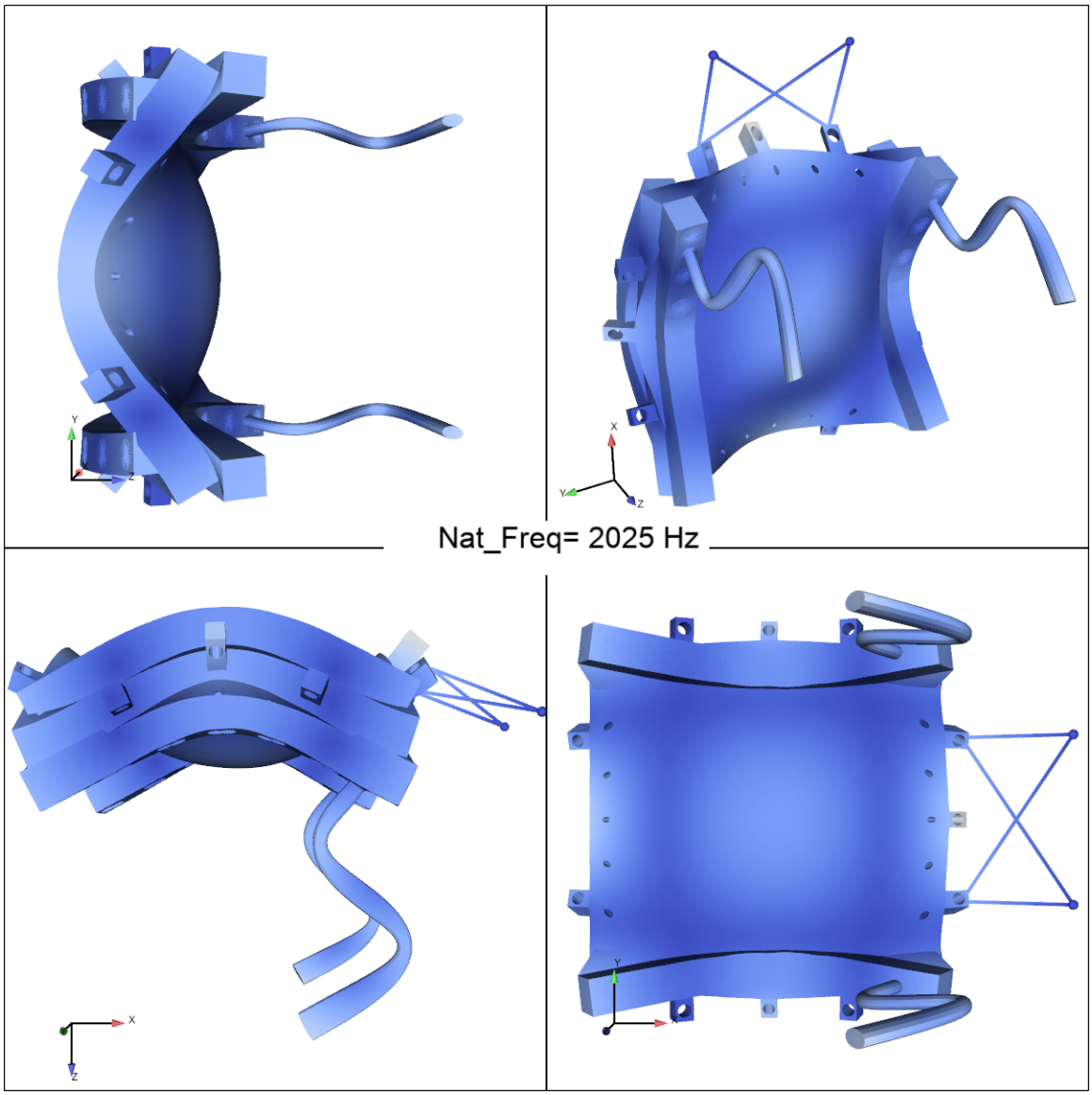

Figure C-5. 5th elastic mode shape compared to the experimental modal data with damping bars

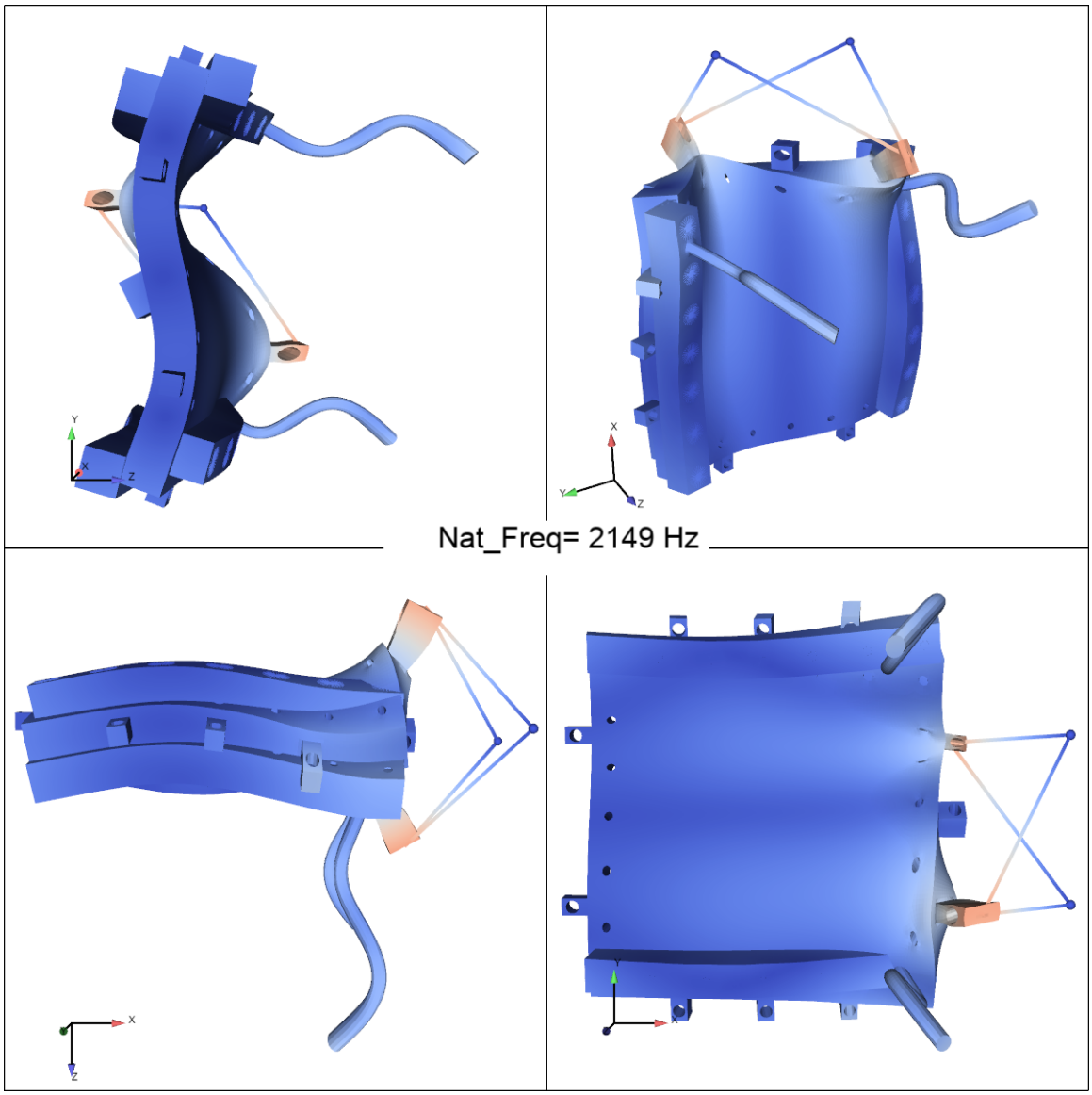

Figure C-6. 6th elastic mode shape compared to the experimental modal data with damping bars

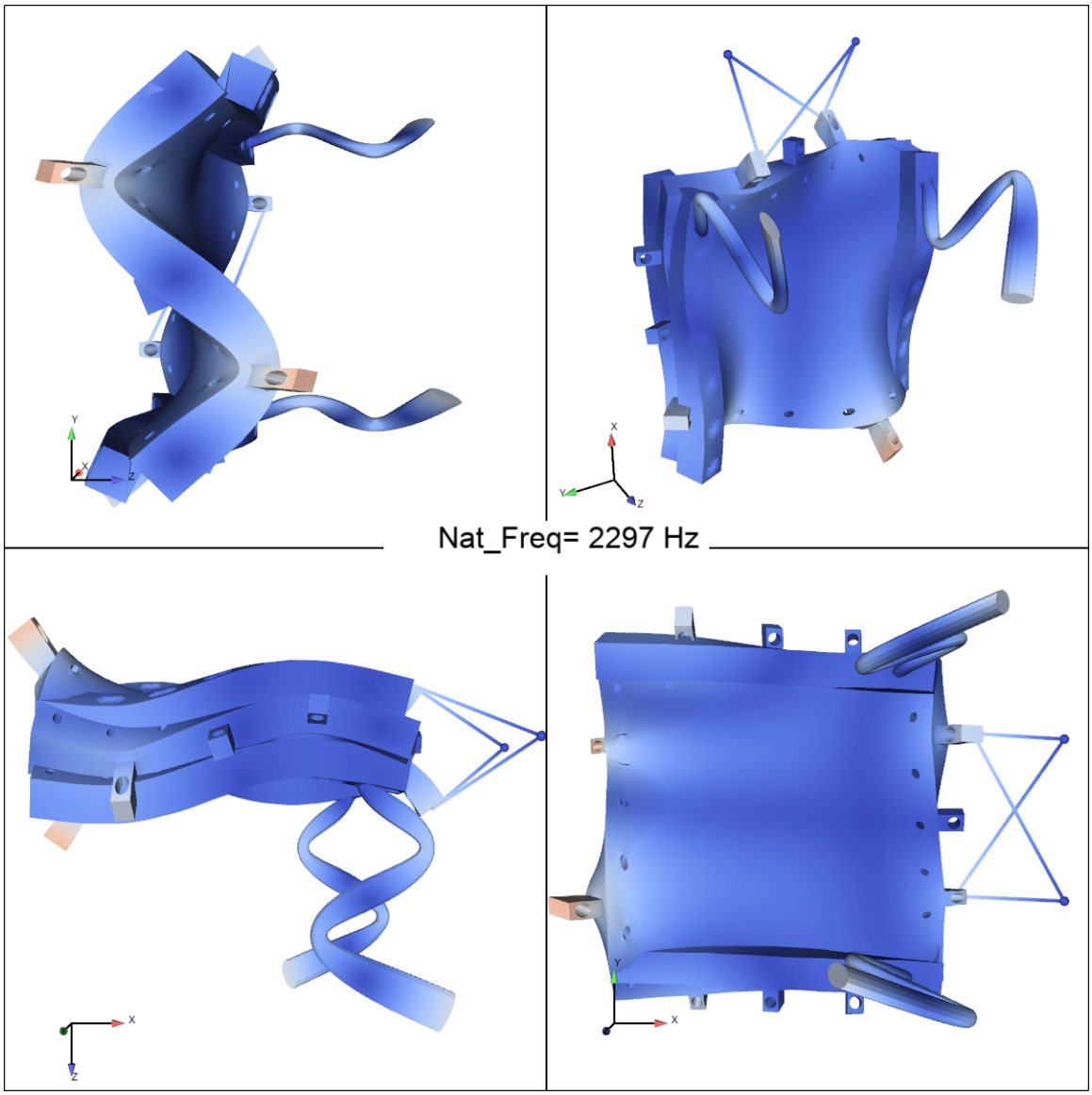

Figure C-7. 7th elastic mode shape compared to the experimental modal data with damping bars

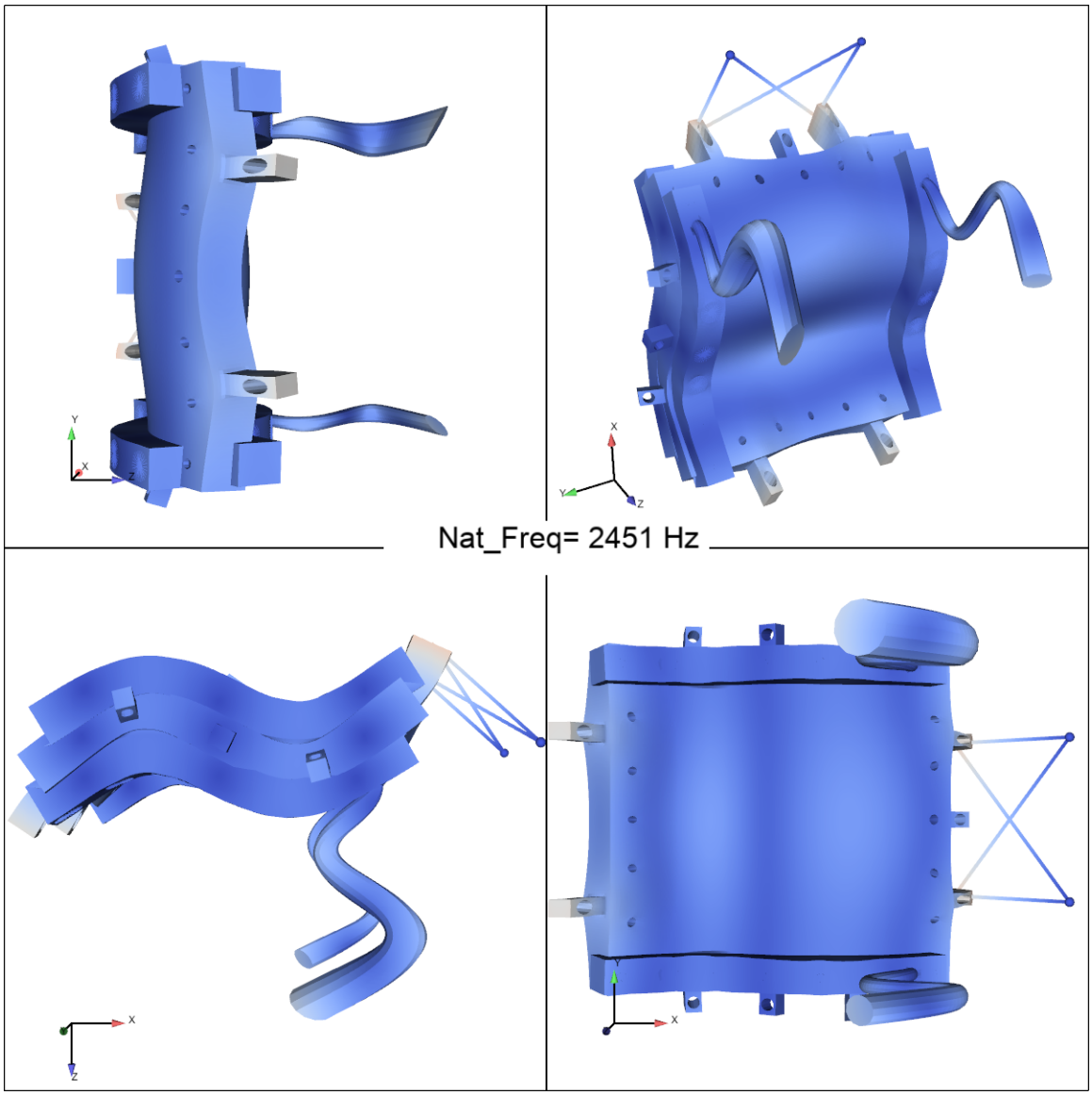

Figure C-8. 8th elastic mode shape compared to the experimental modal data with damping bars

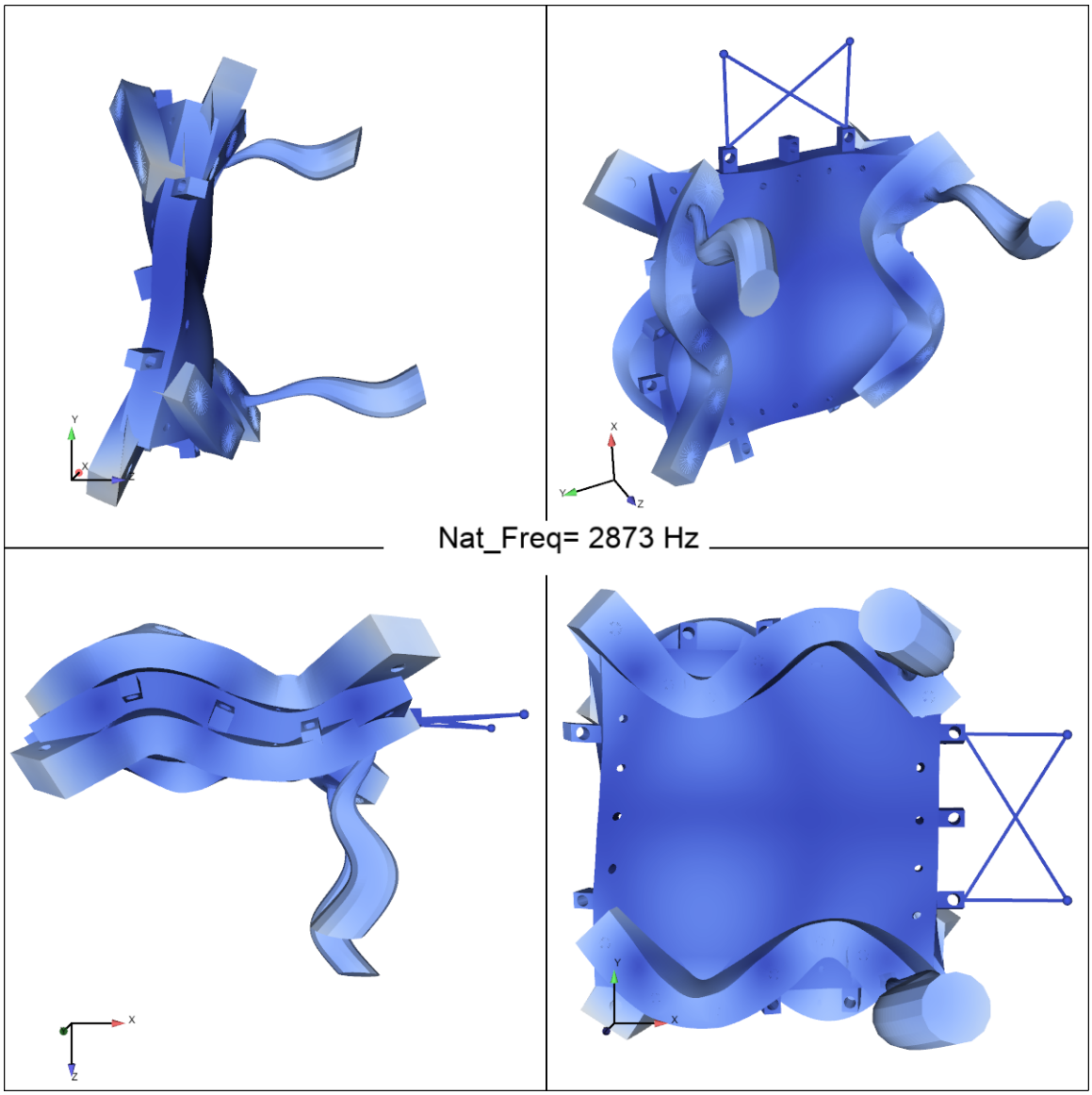

Figure C-9. 9th elastic mode shape compared to the experimental modal data with damping bars

APPENDIX D. Run Logs from Resonant Plate Test Cells

MECHANICAL SHOCK TEST RESULT RECORD SHEET

Test Item: SHK 5142 Multi Axis			**Date:** 2/23/21	**Project/Task:** 188979\56.09.02
Air Gun Number: DT22	**Calibration Shots:** Click or tap here to enter text.	**Test Shots:** Click or tap here to enter text.	**Quantity Tested:** Click or tap here to enter text.	**Quantity Tested at One Time:** Click or tap here to enter text.

Test No.	Test Axis	Test Item and Serial No.	Accel or Strain Gage Location	Air Gun Pressure (psi)	Barrel Vent Configuration	Comments (Projectile Dimensions, Material, Weight, Hopkinson Bar Configuration etc.)
1	X	Bare Plate	Plate	10	All Back All Open	1000Hz Plate, 4 Bolted Bars, Black Rubber between Bars, 6" Steel Projectile, 1/8" Gray **#45 Popped and re-glued**
2	X	Bare Plate	Plate	20	All Back All Open	1000Hz Plate, 4 Bolted Bars, Black Rubber between Bars, 6" Steel Projectile, 1" Gray **#75 Popped off and re-glued.** **Replaced #45 with accel F51080**
3	X	Bare Plate	Plate	10	All Back All Open	1000Hz Plate, 4 Bolted Bars, Black Rubber between Bars, 6" Steel Projectile, 1/8" Gray
4	X	Bare Plate	Plate	10	All Back All Open	1000Hz Plate, 4 Bolted Bars, Black Rubber between Bars, 6" Steel Projectile, 1/8" Gray 21.5fps
5	X	Bare Plate	Plate	10	All Back All Open	1000Hz Plate, 4 Bolted Bars, Black Rubber between Bars, 6" Steel Projectile, 1/8" Gray 21.8fps **#11 Popped off and re-glued.** **Replaced #45 with AP7D5.**
6	X	Bare Plate	Plate	15	All Back All Open	1000Hz Plate, 4 Bolted Bars, Black Rubber between Bars, 6" Steel Projectile, 1/8" Gray 29.8fps **#41, #63, #15 Popped off and re-glued.**
Wednesday 2/24/21						
7	X	Bare Plate	Plate	15	All Back All Open	1000Hz Plate, 4 Bolted Bars, Black Rubber between Bars, 6" Steel Projectile, 1/8" Gray 29.4fps **#21 and #64 Popped off. Won't re-glue them until after 3 consecutive shots to help eliminate all accels that will pop off.**
8	X	Bare Plate	Plate	15	All Back All Open	1000Hz Plate, 4 Bolted Bars, Black Rubber between Bars, 6" Steel Projectile, 1/8" Gray 29.1fps **#61 and #44 Popped off.**

9	X	Bare Plate	Plate	15	All Back All Open	1000Hz Plate, 4 Bolted Bars, Black Rubber between Bars, 6" Steel Projectile, 1/8" Gray 29.3fps **#31 Popped off.**
Reglued accels that popped off over last 3 shots. Replaced #62 due to higher noise level.						
10	X	Bare Plate	Plate	10	All Back All Open	1000Hz Plate, 4 Bolted Bars, Black Rubber between Bars, 6" Steel Projectile, 1/8" Gray 21.0fps **#72 Popped off and re-glued.**
11	X	Bare Plate	Plate	10	All Back All Open	1000Hz Plate, 4 Bolted Bars, Black Rubber between Bars, 6" Steel Projectile, 1/8" Gray 21.6fps
12	X	Bare Plate	Plate	10	All Back All Open	1000Hz Plate, 4 Bolted Bars, Black Rubber between Bars, 6" Steel Projectile, 1/8" Gray 21.4fps
13	X	Bare Plate	Plate	10	All Back All Open	1000Hz Plate, 4 Bolted Bars, Black Rubber between Bars, 6" Steel Projectile, 1/8" Gray 21.1fps
Added a .75" Bolt to bottom center rope anchor Keensert to eliminate rattling of Keensert.						
14	X	Bare Plate Channel Tbl 1 Config 1	Plate	10	All Back All Open	1000Hz Plate, 4 Bolted Bars, Black Rubber between Bars, 6" Steel Projectile, 1/8" Gray 21.6fps
15	X	Bare Plate Channel Tbl 1 Config 1	Plate	10	All Back All Open	1000Hz Plate, 4 Bolted Bars, Black Rubber between Bars, 6" Steel Projectile, 1/8" Gray 21.5fps
16	X	Bare Plate Channel Tbl 1 Config 1	Plate	10	All Back All Open	1000Hz Plate, 4 Bolted Bars, Black Rubber between Bars, 6" Steel Projectile, 1/8" Gray 21.3fps
17	X	Bare Plate Channel Tbl 1 Config 1	Plate	10	All Back All Open	1000Hz Plate, 4 Bolted Bars, Black Rubber between Bars, 6" Steel Projectile, 1/8" Gray 21.4fps
18	X	Bare Plate Channel Tbl 1 Config 1	Plate	15	All Back All Open	1000Hz Plate, 4 Bolted Bars, Black Rubber between Bars, 6" Steel Projectile, 1/8" Gray 29.6fps
Increased accel ranges from 20k to 40k.						
19	X	Bare Plate Channel Tbl 1 Config 1	Plate	15	All Back All Open	1000Hz Plate, 4 Bolted Bars, Black Rubber between Bars, 6" Steel Projectile, 1/8" Gray 29.5fps
20	X	Bare Plate Channel Tbl 1 Config 1	Plate	15	All Back All Open	1000Hz Plate, 4 Bolted Bars, Black Rubber between Bars, 6" Steel Projectile, 1/8" Gray 29.5fps
Replaced Felt						

21	X	Bare Plate Channel Tbl 1 Config 1	Plate	14	All Back All Open	1000Hz Plate, 4 Bolted Bars, Black Rubber between Bars, 6” Steel Projectile, 1/8” Gray 28.0fps
22	X	Bare Plate Channel Tbl 1 Config 1	Plate	14	All Back All Open	1000Hz Plate, 4 Bolted Bars, Black Rubber between Bars, 6” Steel Projectile, 1/8” Gray 27.8fps
23	X	Bare Plate Channel Tbl 1 Config 1	Plate	14	All Back All Open	1000Hz Plate, 4 Bolted Bars, Black Rubber between Bars, 6” Steel Projectile, 1/8” Gray 28.2fps
24	X	Bare Plate Channel Tbl 1 Config 1	Plate	14	All Back All Open	1000Hz Plate, 4 Bolted Bars, Black Rubber between Bars, 6” Steel Projectile, 1/8” Gray 28.3fps
25	X	Bare Plate Channel Tbl 1 Config 1	Plate	14	All Back All Open	1000Hz Plate, 4 Bolted Bars, Black Rubber between Bars, 6” Steel Projectile, 1/8” Gray 28.0fps
Replaced Felt						
26	X	Bare Plate Channel Tbl 1 Config 1	Plate	14	All Back All Open	1000Hz Plate, 4 Bolted Bars, Black Rubber between Bars, 6” Steel Projectile, 1/8” Gray 28.1fps
27	X	Bare Plate Channel Tbl 1 Config 1	Plate	14	All Back All Open	1000Hz Plate, 4 Bolted Bars, Black Rubber between Bars, 6” Steel Projectile, 1/8” Gray 27.8fps
Made the bottom, left and right ropes holding the plate very loose.						
28	X	Bare Plate Channel Tbl 1 Config 1	Plate	10	All Back All Open	1000Hz Plate, 4 Bolted Bars, Black Rubber between Bars, 6” Steel Projectile, 1/8” Gray 21.1fps
29	X	Bare Plate Channel Tbl 1 Config 1	Plate	10	All Back All Open	1000Hz Plate, 4 Bolted Bars, Black Rubber between Bars, 6” Steel Projectile, 1/8” Gray 21.5fps
30	X	Bare Plate Channel Tbl 1 Config 1	Plate	10	All Back All Open	1000Hz Plate, 4 Bolted Bars, Black Rubber between Bars, 6” Steel Projectile, 1/8” Gray 21.2fps
31	X	Bare Plate Channel Tbl 1 Config 1	Plate	10	All Back All Open	1000Hz Plate, 4 Bolted Bars, Black Rubber between Bars, 6” Steel Projectile, 1/8” Gray 21.3fps
32	X	Bare Plate Channel Tbl 1 Config 1	Plate	10	All Back All Open	1000Hz Plate, 4 Bolted Bars, Black Rubber between Bars, 6” Steel Projectile, 1/2” Gray 21.3fps
33	X	Bare Plate Channel Tbl 1 Config 1	Plate	10	All Back All Open	1000Hz Plate, 4 Bolted Bars, Black Rubber between Bars, 6” Steel Projectile, 1/2” Gray 21.4fps

34	X	Bare Plate Channel Tbl 1 Config 1	Plate	10	All Back All Open	1000Hz Plate, 4 Bolted Bars, Black Rubber between Bars, 6" Steel Projectile, 1/2" Gray 21.7fps
35	X	Bare Plate Channel Tbl 1 Config 1	Plate	10	All Back All Open	1000Hz Plate, 4 Bolted Bars, Black Rubber between Bars, 6" Steel Projectile, 1/2" Gray 21.2fps
36	X	Bare Plate Channel Tbl 1 Config 1	Plate	20	All Back All Open	1000Hz Plate, 4 Bolted Bars, Black Rubber between Bars, 6" Steel Projectile, 1/2" Gray 35.7fps
37	X	Bare Plate Channel Tbl 1 Config 1	Plate	20	All Back All Open	1000Hz Plate, 4 Bolted Bars, Black Rubber between Bars, 6" Steel Projectile, 1/2" Gray 35.8fps
38	X	Bare Plate Channel Tbl 1 Config 1	Plate	20	All Back All Open	1000Hz Plate, 4 Bolted Bars, Black Rubber between Bars, 6" Steel Projectile, 1/2" Gray 35.5fps
39	X	Bare Plate Channel Tbl 1 Config 1	Plate	20	All Back All Open	1000Hz Plate, 4 Bolted Bars, Black Rubber between Bars, 6" Steel Projectile, 1/2" Gray 35.7fps
40	X	Bare Plate Channel Tbl 1 Config 1	Plate	40	All Back All Open	1000Hz Plate, 4 Bolted Bars, Black Rubber between Bars, 6" Steel Projectile, 1/2" Gray 53.7fps **#13 Popped off and re-glued.**
41	X	Bare Plate Channel Tbl 1 Config 1	Plate	20	All Back All Open	1000Hz Plate, 4 Bolted Bars, Black Rubber between Bars, 6" Steel Projectile, 1" Gray 36.0fps
42	X	Bare Plate Channel Tbl 1 Config 1	Plate	20	All Back All Open	1000Hz Plate, 4 Bolted Bars, Black Rubber between Bars, 6" Steel Projectile, 1" Gray 35.6fps
43	X	Bare Plate Channel Tbl 1 Config 1	Plate	20	All Back All Open	1000Hz Plate, 4 Bolted Bars, Black Rubber between Bars, 6" Steel Projectile, 1" Gray 36.1fps
44	X	Bare Plate Channel Tbl 1 Config 1	Plate	20	All Back All Open	1000Hz Plate, 4 Bolted Bars, Black Rubber between Bars, 6" Steel Projectile, 1" Gray 36.0fps
45	X	Bare Plate Channel Tbl 1 Config 1	Plate	20	All Back All Open	1000Hz Plate, 4 Bolted Bars, Black Rubber between Bars, 6" Steel Projectile, 1" Gray 36.2fps
46	X	Bare Plate Channel Tbl 1 Config 1	Plate	20	All Back All Open	1000Hz Plate, 4 Bolted Bars, Black Rubber between Bars, 6" Steel Projectile, 1" Gray 36.3fps
47	X	Bare Plate Channel Tbl 1 Config 1	Plate	20	All Back All Open	1000Hz Plate, 4 Bolted Bars, Black Rubber between Bars, 6" Steel Projectile, 1" Gray 36.2fps

48	X	Bare Plate Channel Tbl 1 Config 1	Plate	40	All Back All Open	1000Hz Plate, 4 Bolted Bars, Black Rubber between Bars, 6” Steel Projectile, 1” Gray 53.5fps
49	X	Bare Plate Channel Tbl 1 Config 1	Plate	40	All Back All Open	1000Hz Plate, 4 Bolted Bars, Black Rubber between Bars, 6” Steel Projectile, 1” Gray 53.6fps
50	X	Bare Plate Channel Tbl 1 Config 1	Plate	40	All Back All Open	1000Hz Plate, 4 Bolted Bars, Black Rubber between Bars, 6” Steel Projectile, 1” Gray 53.7fps
51	X	Bare Plate Channel Tbl 1 Config 1	Plate	40	All Back All Open	1000Hz Plate, 4 Bolted Bars, Black Rubber between Bars, 6” Steel Projectile, 1” Gray 53.2fps
52	X	Bare Plate Channel Tbl 1 Config 1	Plate	60	All Back All Open	1000Hz Plate, 4 Bolted Bars, Black Rubber between Bars, 6” Steel Projectile, 1” Gray 65.2fps
53	X	Bare Plate Channel Tbl 1 Config 1	Plate	55	All Back All Open	1000Hz Plate, 4 Bolted Bars, Black Rubber between Bars, 6” Steel Projectile, 1” Gray 62.6fps
54	X	Bare Plate Channel Tbl 1 Config 1	Plate	50	All Back All Open	1000Hz Plate, 4 Bolted Bars, Black Rubber between Bars, 6” Steel Projectile, 1” Gray 59.8fps
55	X	Bare Plate Channel Tbl 1 Config 1	Plate	50	All Back All Open	1000Hz Plate, 4 Bolted Bars, Black Rubber between Bars, 6” Steel Projectile, 1” Gray 59.7fps
Replaced Felt						
56	X	Bare Plate Channel Tbl 1 Config 1	Plate	50	All Back All Open	1000Hz Plate, 4 Bolted Bars, Black Rubber between Bars, 6” Steel Projectile, 1” Gray 59.8fps
57	X	Bare Plate Channel Tbl 1 Config 1	Plate	50	All Back All Open	1000Hz Plate, 4 Bolted Bars, Black Rubber between Bars, 6” Steel Projectile, 1” Gray 59.7fps
58	X	Bare Plate Channel Tbl 1 Config 1	Plate	20	All Back All Open	1000Hz Plate, 4 Bolted Bars, Black Rubber between Bars, 12” Steel Projectile, 1” Gray 23.7fps
59	X	Bare Plate Channel Tbl 1 Config 1	Plate	20	All Back All Open	1000Hz Plate, 4 Bolted Bars, Black Rubber between Bars, 12” Steel Projectile, 1” Gray 23.9fps
60	X	Bare Plate Channel Tbl 1 Config 1	Plate	20	All Back All Open	1000Hz Plate, 4 Bolted Bars, Black Rubber between Bars, 12” Steel Projectile, 1” Gray 23.9fps
61	X	Bare Plate Channel Tbl 1 Config 1	Plate	20	All Back All Open	1000Hz Plate, 4 Bolted Bars, Black Rubber between Bars, 12” Steel Projectile, 1” Gray 24.0fps

62	X	Bare Plate Channel Tbl 1 Config 1	Plate	40	All Back All Open	1000Hz Plate, 4 Bolted Bars, Black Rubber between Bars, 12” Steel Projectile, 1” Gray 37.1fps
63	X	Bare Plate Channel Tbl 1 Config 1	Plate	40	All Back All Open	1000Hz Plate, 4 Bolted Bars, Black Rubber between Bars, 12” Steel Projectile, 1” Gray 37.2fps
64	X	Bare Plate Channel Tbl 1 Config 1	Plate	40	All Back All Open	1000Hz Plate, 4 Bolted Bars, Black Rubber between Bars, 12” Steel Projectile, 1” Gray 37.0fps
65	X	Bare Plate Channel Tbl 1 Config 1	Plate	40	All Back All Open	1000Hz Plate, 4 Bolted Bars, Black Rubber between Bars, 12” Steel Projectile, 1” Gray 36.9fps
66	X	Bare Plate Channel Tbl 1 Config 1	Plate	60	All Back All Open	1000Hz Plate, 4 Bolted Bars, Black Rubber between Bars, 12” Steel Projectile, 1” Gray 46.1fps
67	X	Bare Plate Channel Tbl 1 Config 1	Plate	60	All Back All Open	1000Hz Plate, 4 Bolted Bars, Black Rubber between Bars, 12” Steel Projectile, 1” Gray 46.2fps
68	X	Bare Plate Channel Tbl 1 Config 1	Plate	60	All Back All Open	1000Hz Plate, 4 Bolted Bars, Black Rubber between Bars, 12” Steel Projectile, 1” Gray 46.0fps
69	X	Bare Plate Channel Tbl 1 Config 1	Plate	15	All Back All Open	1000Hz Plate, 4 Bolted Bars, Black Rubber between Bars, 12” Steel Projectile, 1/2” Gray 19.3fps
70	X	Bare Plate Channel Tbl 1 Config 1	Plate	15	All Back All Open	1000Hz Plate, 4 Bolted Bars, Black Rubber between Bars, 12” Steel Projectile, 1/2” Gray 19.4fps
71	X	Bare Plate Channel Tbl 1 Config 1	Plate	15	All Back All Open	1000Hz Plate, 4 Bolted Bars, Black Rubber between Bars, 12” Steel Projectile, 1/2” Gray 19.6fps
72	X	Bare Plate Channel Tbl 1 Config 1	Plate	15	All Back All Open	1000Hz Plate, 4 Bolted Bars, Black Rubber between Bars, 12” Steel Projectile, 1/2” Gray 19.5fps
73	X	Bare Plate Channel Tbl 1 Config 1	Plate	25	All Back All Open	1000Hz Plate, 4 Bolted Bars, Black Rubber between Bars, 12” Steel Projectile, 1/2” Gray 27.8fps
74	X	Bare Plate Channel Tbl 1 Config 1	Plate	25	All Back All Open	1000Hz Plate, 4 Bolted Bars, Black Rubber between Bars, 12” Steel Projectile, 1/2” Gray 27.7fps
75	X	Bare Plate Channel Tbl 1 Config 1	Plate	25	All Back All Open	1000Hz Plate, 4 Bolted Bars, Black Rubber between Bars, 12” Steel Projectile, 1/2” Gray 27.8fps

76	X	Bare Plate Channel Tbl 1 Config 1	Plate	25	All Back All Open	1000Hz Plate, 4 Bolted Bars, Black Rubber between Bars, 12" Steel Projectile, 1/2" Gray 27.7fps
77	X	Bare Plate Channel Tbl 1 Config 1	Plate	40	All Back All Open	1000Hz Plate, 4 Bolted Bars, Black Rubber between Bars, 12" Steel Projectile, 1/2" Gray 36.9fps
78	X	Bare Plate Channel Tbl 1 Config 1	Plate	35	All Back All Open	1000Hz Plate, 4 Bolted Bars, Black Rubber between Bars, 12" Steel Projectile, 1/2" Gray 34.1fps
79	X	Bare Plate Channel Tbl 1 Config 1	Plate	35	All Back All Open	1000Hz Plate, 4 Bolted Bars, Black Rubber between Bars, 12" Steel Projectile, 1/2" Gray 34.1fps
80	X	Bare Plate Channel Tbl 1 Config 1	Plate	35	All Back All Open	1000Hz Plate, 4 Bolted Bars, Black Rubber between Bars, 12" Steel Projectile, 1/2" Gray 34.2fps
81	X	Bare Plate Channel Tbl 1 Config 1	Plate	35	All Back All Open	1000Hz Plate, 4 Bolted Bars, Black Rubber between Bars, 12" Steel Projectile, 1/2" Gray 34.1fps
82	X	Bare Plate Channel Tbl 1 Config 1	Plate	15	All Back All Open	1000Hz Plate, 4 Bolted Bars, Black Rubber between Bars, 12" Steel Projectile, 1/8" Gray 19.1fps
83	X	Bare Plate Channel Tbl 1 Config 1	Plate	15	All Back All Open	1000Hz Plate, 4 Bolted Bars, Black Rubber between Bars, 12" Steel Projectile, 1/8" Gray 18.6fps
84	X	Bare Plate Channel Tbl 1 Config 1	Plate	15	All Back All Open	1000Hz Plate, 4 Bolted Bars, Black Rubber between Bars, 12" Steel Projectile, 1/8" Gray 19.4fps
85	X	Bare Plate Channel Tbl 1 Config 1	Plate	15	All Back All Open	1000Hz Plate, 4 Bolted Bars, Black Rubber between Bars, 12" Steel Projectile, 1/8" Gray 19.3fps
86	X	Bare Plate Channel Tbl 1 Config 1	Plate	25	All Back All Open	1000Hz Plate, 4 Bolted Bars, Black Rubber between Bars, 12" Steel Projectile, 1/8" Gray 27.5fps
87	X	Bare Plate Channel Tbl 1 Config 1	Plate	25	All Back All Open	1000Hz Plate, 4 Bolted Bars, Black Rubber between Bars, 12" Steel Projectile, 1/8" Gray 27.5fps **#51 Popped off and re-glued.**
88	X	Bare Plate Channel Tbl 1 Config 1	Plate	25	All Back All Open	1000Hz Plate, 4 Bolted Bars, Black Rubber between Bars, 12" Steel Projectile, 1/8" Gray 27.3fps
89	X	Bare Plate Channel Tbl 1 Config 1	Plate	25	All Back All Open	1000Hz Plate, 4 Bolted Bars, Black Rubber between Bars, 12" Steel Projectile, 1/8" Gray 27.5fps

90	X	Bare Plate Channel Tbl 1 Config 1	Plate	25	All Back All Open	1000Hz Plate, 4 Bolted Bars, Black Rubber between Bars, 12” Steel Projectile, 1/8” Gray 27.7fps
91	X	Bare Plate Channel Tbl 1 Config 1	Plate	25	All Back All Open	1000Hz Plate, 4 Bolted Bars, Black Rubber between Bars, 12” Steel Projectile, 1/8” Gray 27.3fps
Installed Fixture						
92	Z	Concept Fixture Channel Tbl 2 Config 2	Plate Fixture	15	All Back All Open	1000Hz Plate, 4 Bolted Bars, Black Rubber between Bars, 12” Steel Projectile, 1/2” Gray 19.2fps
93	Z	Concept Fixture Channel Tbl 2 Config 2	Plate Fixture	15	All Back All Open	1000Hz Plate, 4 Bolted Bars, Black Rubber between Bars, 12” Steel Projectile, 1/2” Gray 19.3fps
94	Z	Concept Fixture Channel Tbl 2 Config 2	Plate Fixture	15	All Back All Open	1000Hz Plate, 4 Bolted Bars, Black Rubber between Bars, 12” Steel Projectile, 1/2” Gray 19.3fps
95	Z	Concept Fixture Channel Tbl 2 Config 2	Plate Fixture	15	All Back All Open	1000Hz Plate, 4 Bolted Bars, Black Rubber between Bars, 12” Steel Projectile, 1/2” Gray 19.3fps
96	Z	Concept Fixture Channel Tbl 2 Config 2	Plate Fixture	25	All Back All Open	1000Hz Plate, 4 Bolted Bars, Black Rubber between Bars, 12” Steel Projectile, 1/2” Gray 27.7fps
97	Z	Concept Fixture Channel Tbl 2 Config 2	Plate Fixture	25	All Back All Open	1000Hz Plate, 4 Bolted Bars, Black Rubber between Bars, 12” Steel Projectile, 1/2” Gray 27.8fps
98	Z	Concept Fixture Channel Tbl 2 Config 2	Plate Fixture	25	All Back All Open	1000Hz Plate, 4 Bolted Bars, Black Rubber between Bars, 12” Steel Projectile, 1/2” Gray 27.8fps
99	Z	Concept Fixture Channel Tbl 2 Config 2	Plate Fixture	25	All Back All Open	1000Hz Plate, 4 Bolted Bars, Black Rubber between Bars, 12” Steel Projectile, 1/2” Gray 27.9fps
100	Z	Concept Fixture Channel Tbl 2 Config 2	Plate Fixture	15	All Back All Open	1000Hz Plate, 4 Bolted Bars, Black Rubber between Bars, 12” Steel Projectile, 1” Gray 19.5fps

101	Z	Concept Fixture Channel Tbl 2 Config 2	Plate Fixture	15	All Back All Open	1000Hz Plate, 4 Bolted Bars, Black Rubber between Bars, 12” Steel Projectile, 1” Gray 19.4fps
102	Z	Concept Fixture Channel Tbl 2 Config 2	Plate Fixture	15	All Back All Open	1000Hz Plate, 4 Bolted Bars, Black Rubber between Bars, 12” Steel Projectile, 1” Gray 19.4fps
103	Z	Concept Fixture Channel Tbl 2 Config 2	Plate Fixture	15	All Back All Open	1000Hz Plate, 4 Bolted Bars, Black Rubber between Bars, 12” Steel Projectile, 1” Gray 19.4fps
104	Z	Concept Fixture Channel Tbl 2 Config 2	Plate Fixture	25	All Back All Open	1000Hz Plate, 4 Bolted Bars, Black Rubber between Bars, 12” Steel Projectile, 1” Gray 27.7fps
Found some of the bolted bar bolts loose. Rechecked all of them.						
105	Z	Concept Fixture Channel Tbl 2 Config 2	Plate Fixture	25	All Back All Open	1000Hz Plate, 4 Bolted Bars, Black Rubber between Bars, 12” Steel Projectile, 1” Gray Fps Digitizing Failed. No Data.
106	Z	Concept Fixture Channel Tbl 2 Config 2	Plate Fixture	25	All Back All Open	1000Hz Plate, 4 Bolted Bars, Black Rubber between Bars, 12” Steel Projectile, 1” Gray 27.7fps
107	Z	Concept Fixture Channel Tbl 2 Config 2	Plate Fixture	25	All Back All Open	1000Hz Plate, 4 Bolted Bars, Black Rubber between Bars, 12” Steel Projectile, 1” Gray 27.2fps
108	Z	Concept Fixture Channel Tbl 2 Config 2	Plate Fixture	25	All Back All Open	1000Hz Plate, 4 Bolted Bars, Black Rubber between Bars, 12” Steel Projectile, 1” Gray 27.3fps
109	Z	Concept Fixture Channel Tbl 2 Config 2	Plate Fixture	25	All Back All Open	1000Hz Plate, 4 Bolted Bars, Black Rubber between Bars, 12” Steel Projectile, 1” Gray 27.3fps
110	Z	Concept Fixture Channel Tbl 2 Config 2	Plate Fixture	15	All Back All Open	1000Hz Plate, 4 Bolted Bars, Black Rubber between Bars, 12” Steel Projectile, 1” Gray 19.1fps

111	Z	Concept Fixture Channel Tbl 2 Config 2	Plate Fixture	15	All Back All Open	1000Hz Plate, 4 Bolted Bars, Black Rubber between Bars, 12” Steel Projectile, 1” Gray 19.2fps
112	Z	Concept Fixture Channel Tbl 2 Config 2	Plate Fixture	15	All Back All Open	1000Hz Plate, 4 Bolted Bars, Black Rubber between Bars, 12” Steel Projectile, 1” Gray 19.4fps
113	Z	Concept Fixture Channel Tbl 2 Config 2	Plate Fixture	15	All Back All Open	1000Hz Plate, 4 Bolted Bars, Black Rubber between Bars, 12” Steel Projectile, 1” Gray 19.0fps
114	Z	Concept Fixture Channel Tbl 2 Config 2	Plate Fixture	20	All Back All Open	1000Hz Plate, 4 Bolted Bars, Black Rubber between Bars, 18” Steel Projectile, 1” Gray 16.6fps
115	Z	Concept Fixture Channel Tbl 2 Config 2	Plate Fixture	20	All Back All Open	1000Hz Plate, 4 Bolted Bars, Black Rubber between Bars, 18” Steel Projectile, 1” Gray 16.6fps
116	Z	Concept Fixture Channel Tbl 2 Config 2	Plate Fixture	20	All Back All Open	1000Hz Plate, 4 Bolted Bars, Black Rubber between Bars, 18” Steel Projectile, 1” Gray 16.5fps
117	Z	Concept Fixture Channel Tbl 2 Config 2	Plate Fixture	20	All Back All Open	1000Hz Plate, 4 Bolted Bars, Black Rubber between Bars, 18” Steel Projectile, 1” Gray 17.5fps
118	Z	Concept Fixture Channel Tbl 2 Config 2	Plate Fixture	40	All Back All Open	1000Hz Plate, 4 Bolted Bars, Black Rubber between Bars, 18” Steel Projectile, 1” Gray 28.2fps
119	Z	Concept Fixture Channel Tbl 2 Config 2	Plate Fixture	40	All Back All Open	1000Hz Plate, 4 Bolted Bars, Black Rubber between Bars, 18” Steel Projectile, 1” Gray 28.1fps
120	Z	Concept Fixture Channel Tbl 2 Config 2	Plate Fixture	40	All Back All Open	1000Hz Plate, 4 Bolted Bars, Black Rubber between Bars, 18” Steel Projectile, 1” Gray 28.0fps
121	Z	Concept Fixture Channel Tbl 2 Config 2	Plate Fixture	15	All Back All Open	1000Hz Plate, 4 Bolted Bars, Black Rubber between Bars, 18” Steel Projectile, 1/2” Gray fps

122	Z	Concept Fixture Channel Tbl 2 Config 2	Plate Fixture	15	All Back All Open	1000Hz Plate, 4 Bolted Bars, Black Rubber between Bars, 18" Steel Projectile, 1/2" Gray fps Velocity not collected
123	Z	Concept Fixture Channel Tbl 2 Config 2	Plate Fixture	15	All Back All Open	1000Hz Plate, 4 Bolted Bars, Black Rubber between Bars, 18" Steel Projectile, 1/2" Gray 12.5fps
124	Z	Concept Fixture Channel Tbl 2 Config 2	Plate Fixture	15	All Back All Open	1000Hz Plate, 4 Bolted Bars, Black Rubber between Bars, 18" Steel Projectile, 1/2" Gray 12.7fps
Left, Right, Bottom Ropes Removed						
125	Z	Concept Fixture Channel Tbl 2 Config 2	Plate Fixture	15	All Back All Open	1000Hz Plate, 4 Bolted Bars, Black Rubber between Bars, 18" Steel Projectile, 1/2" Gray 13.6fps
126	Z	Concept Fixture Channel Tbl 2 Config 2	Plate Fixture	15	All Back All Open	1000Hz Plate, 4 Bolted Bars, Black Rubber between Bars, 18" Steel Projectile, 1/2" Gray 12.5fps
127	Z	Concept Fixture Channel Tbl 2 Config 2	Plate Fixture	15	All Back All Open	1000Hz Plate, 4 Bolted Bars, Black Rubber between Bars, 18" Steel Projectile, 1/2" Gray 13.6fps
128	Z	Concept Fixture Channel Tbl 2 Config 2	Plate Fixture	15	All Back All Open	1000Hz Plate, 4 Bolted Bars, Black Rubber between Bars, 18" Steel Projectile, 1/2" Gray fps
Left, Right, Bottom Ropes Re-installed. Removed spacer from between plate and fixture.						
129	Z	Concept Fixture Channel Tbl 2 Config 3	Plate Fixture	15	All Back All Open	1000Hz Plate, 4 Bolted Bars, Black Rubber between Bars, 18" Steel Projectile, 1/2" Gray 12.5fps
130	Z	Concept Fixture Channel Tbl 2 Config 3	Plate Fixture	15	All Back All Open	1000Hz Plate, 4 Bolted Bars, Black Rubber between Bars, 18" Steel Projectile, 1/2" Gray 12.6fps
131	Z	Concept Fixture Channel Tbl 2 Config 3	Plate Fixture	15	All Back All Open	1000Hz Plate, 4 Bolted Bars, Black Rubber between Bars, 18" Steel Projectile, 1/2" Gray 12.7fps

132	Z	Concept Fixture Channel Tbl 2 Config 3	Plate Fixture	15	All Back All Open	1000Hz Plate, 4 Bolted Bars, Black Rubber between Bars, 18” Steel Projectile, 1/2” Gray 12.6fps
133	Z	Concept Fixture Channel Tbl 2 Config 3	Plate Fixture	30	All Back All Open	1000Hz Plate, 4 Bolted Bars, Black Rubber between Bars, 18” Steel Projectile, 1/2” Gray 22.8fps
134	Z	Concept Fixture Channel Tbl 2 Config 3	Plate Fixture	30	All Back All Open	1000Hz Plate, 4 Bolted Bars, Black Rubber between Bars, 18” Steel Projectile, 1/2” Gray 22.8fps
135	Z	Concept Fixture Channel Tbl 2 Config 3	Plate Fixture	30	All Back All Open	1000Hz Plate, 4 Bolted Bars, Black Rubber between Bars, 18” Steel Projectile, 1/2” Gray 22.9fps
136	Z	Concept Fixture Channel Tbl 2 Config 3	Plate Fixture	30	All Back All Open	1000Hz Plate, 4 Bolted Bars, Black Rubber between Bars, 18” Steel Projectile, 1/2” Gray 22.9fps
137	Z	Concept Fixture Channel Tbl 2 Config 3	Plate Fixture	20	All Back All Open	1000Hz Plate, 4 Bolted Bars, Black Rubber between Bars, 18” Steel Projectile, 1” Gray 16.7fps
138	Z	Concept Fixture Channel Tbl 2 Config 3	Plate Fixture	20	All Back All Open	1000Hz Plate, 4 Bolted Bars, Black Rubber between Bars, 18” Steel Projectile, 1” Gray 17.3fps
139	Z	Concept Fixture Channel Tbl 2 Config 3	Plate Fixture	20	All Back All Open	1000Hz Plate, 4 Bolted Bars, Black Rubber between Bars, 18” Steel Projectile, 1” Gray 17.4fps
140	Z	Concept Fixture Channel Tbl 2 Config 3	Plate Fixture	20	All Back All Open	1000Hz Plate, 4 Bolted Bars, Black Rubber between Bars, 18” Steel Projectile, 1” Gray 16.6fps
141	Z	Concept Fixture Channel Tbl 2 Config 3	Plate Fixture	40	All Back All Open	1000Hz Plate, 4 Bolted Bars, Black Rubber between Bars, 18” Steel Projectile, 1” Gray 28.2fps
142	Z	Concept Fixture Channel Tbl 2 Config 3	Plate Fixture	40	All Back All Open	1000Hz Plate, 4 Bolted Bars, Black Rubber between Bars, 18” Steel Projectile, 1” Gray 28.1fps

143	Z	Concept Fixture Channel Tbl 2 Config 3	Plate Fixture	40	All Back All Open	1000Hz Plate, 4 Bolted Bars, Black Rubber between Bars, 18” Steel Projectile, 1” Gray 28.2fps
144	Z	Concept Fixture Channel Tbl 2 Config 3	Plate Fixture	40	All Back All Open	1000Hz Plate, 4 Bolted Bars, Black Rubber between Bars, 18” Steel Projectile, 1” Gray 28.0fps
Notes: The bolts may have bottomed out in Config#3 and may not have had proper torque The washers in Config#2 that separated the fixture to the resonant plate were only in contact at the very outer edge The resonant plate has a permanent bow to it						
146						
147						
148						
148						
150						

MECHANICAL SHOCK TEST RESULT RECORD SHEET				
Test Item: SHK 5153 Multi Axis			**Date:** 03/08/2021	**Project/Task:** 188979\56.09.02
Air Gun Number: DT20	**Calibration Shots:** N/A	**Test Shots:** Click or tap here to enter text.	**Quantity Tested:** N/A	**Quantity Tested at One Time:** N/A

Test No.	Test Axis	Test Item and Serial No.	Accel or Strain Gage Location	Air Gun Pressure (psi)	Barrel Vent Configuration	Comments (Projectile Dimensions, Material, Weight, Hopkinson Bar Configuration etc.)
1	X	Channel Tbl 1 Config #4	Plate	15	All Back All Open	1000Hz Plate, No Bars, 12" Steel Projectile, 1/8" Gray 20.2 fps
2	X	Channel Tbl 1 Config #4	Plate	15	All Back All Open	1000Hz Plate, No Bars, 12" Steel Projectile, 1/8" Gray 20.1 fps
3	X	Channel Tbl 1 Config #4	Plate	15	All Back All Open	1000Hz Plate, No Bars, 12" Steel Projectile, 1/8" Gray 19.8 fps
4	X	Channel Tbl 1 Config #4	Plate	15	All Back All Open	1000Hz Plate, No Bars, 12" Steel Projectile, 1/8" Gray 20.2 fps
5	X	Channel Tbl 1 Config #4	Plate	15	All Back All Open	1000Hz Plate, No Bars, 12" Steel Projectile, 1/2" Gray 20.3 fps
6	X	Channel Tbl 1 Config #4	Plate	15	All Back All Open	1000Hz Plate, No Bars, 12" Steel Projectile, 1/2" Gray 20.4 fps
7	X	Channel Tbl 1 Config #4	Plate	15	All Back All Open	1000Hz Plate, No Bars, 12" Steel Projectile, 1/2" Gray 20.1 fps
8	X	Channel Tbl 1 Config #4	Plate	15	All Back All Open	1000Hz Plate, No Bars, 12" Steel Projectile, 1/2" Gray 20.2 fps
9	X	Channel Tbl 1 Config #4	Plate	25	All Back All Open	1000Hz Plate, No Bars, 12" Steel Projectile, 1/2" Gray 28.9 fps
10	X	Channel Tbl 1 Config #4	Plate	25	All Back All Open	1000Hz Plate, No Bars, 12" Steel Projectile, 1/2" Gray 28.9 fps

11	X	Channel Tbl 1 Config #4	Plate	25	All Back All Open	1000Hz Plate, No Bars, 12” Steel Projectile, 1/2” Gray 28.8 fps
12	X	Channel Tbl 1 Config #4	Plate	25	All Back All Open	1000Hz Plate, No Bars, 12” Steel Projectile, 1/2” Gray 29.0 fps
13	X	Channel Tbl 1 Config #4	Plate	15	All Back All Open	1000Hz Plate, No Bars, 12” Steel Projectile, 1” Gray 20.3 fps
14	X	Channel Tbl 1 Config #4	Plate	15	All Back All Open	1000Hz Plate, No Bars, 12” Steel Projectile, 1” Gray 20.1 fps
15	X	Channel Tbl 1 Config #4	Plate	15	All Back All Open	1000Hz Plate, No Bars, 12” Steel Projectile, 1” Gray 20.2 fps
16	X	Channel Tbl 1 Config #4	Plate	15	All Back All Open	1000Hz Plate, No Bars, 12” Steel Projectile, 1” Gray 20.4 fps
17	X	Channel Tbl 1 Config #4	Plate	25	All Back All Open	1000Hz Plate, No Bars, 12” Steel Projectile, 1” Gray 28.9 fps
18	X	Channel Tbl 1 Config #4	Plate	25	All Back All Open	1000Hz Plate, No Bars, 12” Steel Projectile, 1” Gray 28.9 fps
19	X	Channel Tbl 1 Config #4	Plate	40	All Back All Open	1000Hz Plate, No Bars, 12” Steel Projectile, 1” Gray 38.7 fps
20	X	Channel Tbl 1 Config #4	Plate	40	All Back All Open	1000Hz Plate, No Bars, 12” Steel Projectile, 1” Gray 38.5 fps
21	X	Channel Tbl 1 Config #4	Plate	10	All Back All Open	1000Hz Plate, No Bars, 12” Steel Projectile, 1/8” Gray 14.2 fps
22	X	Channel Tbl 1 Config #4	Plate	10	All Back All Open	1000Hz Plate, No Bars, 12” Steel Projectile, 1/8” Gray 14.3 fps
23	X	Channel Tbl 1 Config #1	Plate	10	All Back All Open	1000Hz Plate, 4 Bars with rubber material, 6” Steel Projectile, 1/2” Gray 19.5 fps
24	X	Channel Tbl 1 Config #1	Plate	20	All Back All Open	1000Hz Plate, 4 Bars with rubber material, 6” Steel Projectile, 1/2” Gray 34.1 fps
Installed Fitxture						

25	Z	Channel Tbl 2 Config #3	Plate Fixture	15	All Back All Open	1000Hz Plate, 4 Bars with rubber material, 12” Steel Projectile, 1/2” Gray 20.6 fps
26	X	Channel Tbl 2 Config #3	Plate Fixture	15	All Back All Open	1000Hz Plate, 4 Bars with rubber material, 12” Steel Projectile, 1/2” Gray 20.4 fps
27	X	Channel Tbl 2 Config #3	Plate Fixture	15	All Back All Open	1000Hz Plate, 4 Bars with rubber material, 12” Steel Projectile, 1/2” Gray 20.3 fps
28	X	Channel Tbl 2 Config #3	Plate Fixture	25	All Back All Open	1000Hz Plate, 4 Bars with rubber material, 12” Steel Projectile, 1/2” Gray 29.1 fps
29	X	Channel Tbl 2 Config #3	Plate Fixture	25	All Back All Open	1000Hz Plate, 4 Bars with rubber material, 12” Steel Projectile, 1/2” Gray 29.1 fps
30	X	Channel Tbl 2 Config #3	Plate Fixture	25	All Back All Open	1000Hz Plate, 4 Bars with rubber material, 12” Steel Projectile, 1/2” Gray 29.0 fps
31	X	Channel Tbl 2 Config #3	Plate Fixture	40	All Back All Open	1000Hz Plate, 4 Bars with rubber material, 12” Steel Projectile, 1/2” Gray 38.3 fps
Replaced Felt						
32	X	Channel Tbl 2 Config #3	Plate Fixture	40	All Back All Open	1000Hz Plate, 4 Bars with rubber material, 12” Steel Projectile, 1/2” Gray 38.6 fps
33	X	Channel Tbl 3 Config #5	Plate Fixture	15	All Back All Open	1000Hz Plate, 4 Bars with rubber material, 12” Steel Projectile, 1/2” Gray 20.4 fps
34	X	Channel Tbl 3 Config #5	Plate Fixture	15	All Back All Open	1000Hz Plate, 4 Bars with rubber material, 12” Steel Projectile, 1/2” Gray 20.3 fps
35	X	Channel Tbl 3 Config #5	Plate Fixture	15	All Back All Open	1000Hz Plate, 4 Bars with rubber material, 12” Steel Projectile, 1/2” Gray 20.5 fps
36	X	Channel Tbl 3 Config #5	Plate Fixture	15	All Back All Open	1000Hz Plate, 4 Bars with rubber material, 12” Steel Projectile, 1/2” Gray 20.4 fps
37	X	Channel Tbl 3 Config #5	Plate Fixture	25	All Back All Open	1000Hz Plate, 4 Bars with rubber material, 12” Steel Projectile, 1/2” Gray 29.0 fps
38	X	Channel Tbl 3 Config #5	Plate Fixture	25	All Back All Open	1000Hz Plate, 4 Bars with rubber material, 12” Steel Projectile, 1/2” Gray 28.7 fps

39	X	Channel Tbl 3 Config #5	Plate Fixture	25	All Back All Open	1000Hz Plate, 4 Bars with rubber material, 12” Steel Projectile, 1/2” Gray 29.2 fps
40	X	Channel Tbl 3 Config #5	Plate Fixture	25	All Back All Open	1000Hz Plate, 4 Bars with rubber material, 12” Steel Projectile, 1/2” Gray 28.9 fps
41	X	Channel Tbl 4 Config #6	Plate Fixture	15	All Back All Open	1000Hz Plate, 4 Bars with rubber material, 12” Steel Projectile, 1/2” Gray 20.2 fps
42	X	Channel Tbl 4 Config #6	Plate Fixture	15	All Back All Open	1000Hz Plate, 4 Bars with rubber material, 12” Steel Projectile, 1/2” Gray 20.1 fps
43	X	Channel Tbl 4 Config #6	Plate Fixture	15	All Back All Open	1000Hz Plate, 4 Bars with rubber material, 12” Steel Projectile, 1/2” Gray 20.2 fps
44	X	Channel Tbl 4 Config #6	Plate Fixture	15	All Back All Open	1000Hz Plate, 4 Bars with rubber material, 12” Steel Projectile, 1/2” Gray 20.0 fps
45	X	Channel Tbl 4 Config #6	Plate Fixture	25	All Back All Open	1000Hz Plate, 4 Bars with rubber material, 12” Steel Projectile, 1/2” Gray 28.8 fps
46	X	Channel Tbl 4 Config #6	Plate Fixture	25	All Back All Open	1000Hz Plate, 4 Bars with rubber material, 12” Steel Projectile, 1/2” Gray 29.0 fps
47	X	Channel Tbl 4 Config #6	Plate Fixture	25	All Back All Open	1000Hz Plate, 4 Bars with rubber material, 12” Steel Projectile, 1/2” Gray 28.9 fps
48	X	Channel Tbl 4 Config #6	Plate Fixture	25	All Back All Open	1000Hz Plate, 4 Bars with rubber material, 12” Steel Projectile, 1/2” Gray 28.3 fps
49	X	Channel Tbl 5 Config #7	Plate Fixture	15	All Back All Open	1000Hz Plate, 4 Bars with rubber material, 12” Steel Projectile, 1/2” Gray 20.3 fps
50	X	Channel Tbl 5 Config #7	Plate Fixture	15	All Back All Open	1000Hz Plate, 4 Bars with rubber material, 12” Steel Projectile, 1/2” Gray 20.4 fps
51	X	Channel Tbl 5 Config #7	Plate Fixture	15	All Back All Open	1000Hz Plate, 4 Bars with rubber material, 12” Steel Projectile, 1/2” Gray 20.2 fps
52	X	Channel Tbl 5 Config #7	Plate Fixture	15	All Back All Open	1000Hz Plate, 4 Bars with rubber material, 12” Steel Projectile, 1/2” Gray 20.0 fps

53	Z	Channel Tbl 5 Config #7	Plate Fixture	25	All Back All Open	1000Hz Plate, 4 Bars with rubber material, 12” Steel Projectile, 1/2” Gray 29.0 fps
54	Z	Channel Tbl 5 Config #7	Plate Fixture	25	All Back All Open	1000Hz Plate, 4 Bars with rubber material, 12” Steel Projectile, 1/2” Gray 28.9 fps
55	Z	Channel Tbl 5 Config #7	Plate Fixture	25	All Back All Open	1000Hz Plate, 4 Bars with rubber material, 12” Steel Projectile, 1/2” Gray 28.7 fps
56	Z	Channel Tbl 5 Config #7	Plate Fixture	25	All Back All Open	1000Hz Plate, 4 Bars with rubber material, 12” Steel Projectile, 1/2” Gray 28.9 fps
57	Z	Channel Tbl 5 Config #8	Plate Fixture	15	All Back All Open	1000Hz Plate, 4 Bars with rubber material, 12” Steel Projectile, 1/2” Gray 20.0 fps
58	Z	Channel Tbl 5 Config #8	Plate Fixture	15	All Back All Open	1000Hz Plate, 4 Bars with rubber material, 12” Steel Projectile, 1/2” Gray 20.3 fps
59	Z	Channel Tbl 5 Config #8	Plate Fixture	15	All Back All Open	1000Hz Plate, 4 Bars with rubber material, 12” Steel Projectile, 1/2” Gray 20.5 fps
60	Z	Channel Tbl 5 Config #8	Plate Fixture	15	All Back All Open	1000Hz Plate, 4 Bars with rubber material, 12” Steel Projectile, 1/2” Gray 20.1 fps
61	Z	Channel Tbl 5 Config #8	Plate Fixture	25	All Back All Open	1000Hz Plate, 4 Bars with rubber material, 12” Steel Projectile, 1/2” Gray 28.5 fps
62	Z	Channel Tbl 5 Config #8	Plate Fixture	25	All Back All Open	1000Hz Plate, 4 Bars with rubber material, 12” Steel Projectile, 1/2” Gray 29.2 fps
63	Z	Channel Tbl 5 Config #8	Plate Fixture	25	All Back All Open	1000Hz Plate, 4 Bars with rubber material, 12” Steel Projectile, 1/2” Gray 28.8 fps
64	Z	Channel Tbl 5 Config #8	Plate Fixture	25	All Back All Open	1000Hz Plate, 4 Bars with rubber material, 12” Steel Projectile, 1/2” Gray 28.6 fps
65	Z	Channel Tbl 2 Config #9	Plate Fixture	15	All Back All Open	1000Hz Plate, 4 Bars with rubber material, 12” Steel Projectile, 1/2” Gray 20.6 fps
66	Z	Channel Tbl 2 Config #9	Plate Fixture	15	All Back All Open	1000Hz Plate, 4 Bars with rubber material, 12” Steel Projectile, 1/2” Gray 21.0 fps

67	Z	Channel Tbl 2 Config #9	Plate Fixture	15	All Back All Open	1000Hz Plate, 4 Bars with rubber material, 12” Steel Projectile, 1/2” Gray 20.0 fps
68	Z	Channel Tbl 2 Config #9	Plate Fixture	15	All Back All Open	1000Hz Plate, 4 Bars with rubber material, 12” Steel Projectile, 1/2” Gray 20.1 fps
69	Z	Channel Tbl 2 Config #9	Plate Fixture	25	All Back All Open	1000Hz Plate, 4 Bars with rubber material, 12” Steel Projectile, 1/2” Gray 28.7 fps
70	Z	Channel Tbl 2 Config #9	Plate Fixture	25	All Back All Open	1000Hz Plate, 4 Bars with rubber material, 12” Steel Projectile, 1/2” Gray 28.7 fps
71	Z	Channel Tbl 2 Config #9	Plate Fixture	25	All Back All Open	1000Hz Plate, 4 Bars with rubber material, 12” Steel Projectile, 1/2” Gray 28.9 fps
72	Z	Channel Tbl 2 Config #9	Plate Fixture	25	All Back All Open	1000Hz Plate, 4 Bars with rubber material, 12” Steel Projectile, 1/2” Gray 28.9 fps
73	Z	Channel Tbl 3 Config #10	Plate Fixture	15	All Back All Open	1000Hz Plate, 4 Bars with rubber material, 12” Steel Projectile, 1/2” Gray 20.3 fps
74	Z	Channel Tbl 3 Config #10	Plate Fixture	15	All Back All Open	1000Hz Plate, 4 Bars with rubber material, 12” Steel Projectile, 1/2” Gray 20.5 fps
75	Z	Channel Tbl 3 Config #10	Plate Fixture	15	All Back All Open	1000Hz Plate, 4 Bars with rubber material, 12” Steel Projectile, 1/2” Gray 20.2 fps
76	Z	Channel Tbl 3 Config #10	Plate Fixture	15	All Back All Open	1000Hz Plate, 4 Bars with rubber material, 12” Steel Projectile, 1/2” Gray 20.3 fps
77	Z	Channel Tbl 3 Config #10	Plate Fixture	25	All Back All Open	1000Hz Plate, 4 Bars with rubber material, 12” Steel Projectile, 1/2” Gray 29.1 fps
78	Z	Channel Tbl 3 Config #10	Plate Fixture	25	All Back All Open	1000Hz Plate, 4 Bars with rubber material, 12” Steel Projectile, 1/2” Gray 28.7 fps
79	Z	Channel Tbl 3 Config #10	Plate Fixture	25	All Back All Open	1000Hz Plate, 4 Bars with rubber material, 12” Steel Projectile, 1/2” Gray 29.0 fps
80	Z	Channel Tbl 3 Config #10	Plate Fixture	25	All Back All Open	1000Hz Plate, 4 Bars with rubber material, 12” Steel Projectile, 1/2” Gray 28.8 fps

81	Z	Channel Tbl 4 Config #11	Plate Fixture	15	All Back All Open	1000Hz Plate, 4 Bars with rubber material, 12" Steel Projectile, 1/2" Gray 20.6 fps
82	Z	Channel Tbl 4 Config #11	Plate Fixture	15	All Back All Open	1000Hz Plate, 4 Bars with rubber material, 12" Steel Projectile, 1/2" Gray 20.4 fps
83	Z	Channel Tbl 4 Config #11	Plate Fixture	15	All Back All Open	1000Hz Plate, 4 Bars with rubber material, 12" Steel Projectile, 1/2" Gray 20.3 fps
84	Z	Channel Tbl 4 Config #11	Plate Fixture	15	All Back All Open	1000Hz Plate, 4 Bars with rubber material, 12" Steel Projectile, 1/2" Gray 20.1 fps
85	Z	Channel Tbl 4 Config #11	Plate Fixture	25	All Back All Open	1000Hz Plate, 4 Bars with rubber material, 12" Steel Projectile, 1/2" Gray 29.1 fps
86	Z	Channel Tbl 4 Config #11	Plate Fixture	25	All Back All Open	1000Hz Plate, 4 Bars with rubber material, 12" Steel Projectile, 1/2" Gray 28.9 fps
87	Z	Channel Tbl 4 Config #11	Plate Fixture	25	All Back All Open	1000Hz Plate, 4 Bars with rubber material, 12" Steel Projectile, 1/2" Gray 28.8 fps
88	Z	Channel Tbl 4 Config #11	Plate Fixture	25	All Back All Open	1000Hz Plate, 4 Bars with rubber material, 12" Steel Projectile, 1/2" Gray 28.8 fps
89	Z	Channel Tbl 2 Config #3	Plate Fixture	20	All Back All Open	1000Hz Plate, 4 Bars with rubber material, 12" Steel Projectile, 1/8" Gray 24.8 fps
90	Z	Channel Tbl 2 Config #3	Plate Fixture	20	All Back All Open	1000Hz Plate, 4 Bars with rubber material, 12" Steel Projectile, 1/8" Gray 25.0 fps
91	Z	Channel Tbl 2 Config #3	Plate Fixture	20	All Back All Open	1000Hz Plate, 4 Bars with rubber material, 12" Steel Projectile, 1/8" Gray, 1/8"x9/16" copper puck @ 3 O'clock 24.7 fps
92	Z	Channel Tbl 2 Config #3	Plate Fixture	20	All Back All Open	1000Hz Plate, 4 Bars with rubber material, 12" Steel Projectile, 1/8" Gray, 1/8" x9/16" copper puck @ 3 O'clock 24.5 fps
93	Z	Channel Tbl 2 Config #3	Plate Fixture	20	All Back All Open	1000Hz Plate, 4 Bars with rubber material, 12" Steel Projectile, 1/8" Gray, 1/8"x9/16" copper puck @ 6 O'clock 24.8 fps
94	Z	Channel Tbl 2 Config #3	Plate Fixture	20	All Back All Open	1000Hz Plate, 4 Bars with rubber material, 12" Steel Projectile, 1/8" Gray, 1/8" x9/16" copper puck @ 6 O'clock fps

95	Z	Channel Tbl 2 Config #3	Plate Fixture	20	All Back All Open	1000Hz Plate, 4 Bars with rubber material, 12” Steel Projectile, 1/8” Gray 24.9 fps
96	X	Channel Tbl 1 Config #12	Plate Fixture	15	All Back All Open	1000Hz Plate, 8 Bars with rubber material, 12” Steel Projectile, 1/2” Gray 20.0 fps
97	X	Channel Tbl 1 Config #12	Plate Fixture	15	All Back All Open	1000Hz Plate, 8 Bars with rubber material, 12” Steel Projectile, 1/2” Gray 20.0 fps
98	X	Channel Tbl 1 Config #12	Plate Fixture	15	All Back All Open	1000Hz Plate, 8 Bars with rubber material, 12” Steel Projectile, 1/2” Gray 20.1 fps
99	X	Channel Tbl 1 Config #12	Plate Fixture	15	All Back All Open	1000Hz Plate, 8 Bars with rubber material, 12” Steel Projectile, 1/2” Gray 20.4 fps
100	X	Channel Tbl 1 Config #12	Plate Fixture	25	All Back All Open	1000Hz Plate, 8 Bars with rubber material, 12” Steel Projectile, 1/2” Gray 28.8 fps
101	X	Channel Tbl 1 Config #12	Plate Fixture	25	All Back All Open	1000Hz Plate, 8 Bars with rubber material, 12” Steel Projectile, 1/2” Gray 28.8 fps
102	X	Channel Tbl 1 Config #12	Plate Fixture	25	All Back All Open	1000Hz Plate, 8 Bars with rubber material, 12” Steel Projectile, 1/2” Gray 29.0 fps
103	X	Channel Tbl 1 Config #12	Plate Fixture	25	All Back All Open	1000Hz Plate, 8 Bars with rubber material, 12” Steel Projectile, 1/2” Gray 29.0 fps

MECHANICAL SHOCK TEST RESULT RECORD SHEET

Test Item: SHK 5182 Multi Axis			**Date:** 4/26/2021	**Project/Task:** 188979/56.09.02
Air Gun Number: DT22	**Calibration Shots:** Click or tap here to enter text.	**Test Shots:** Click or tap here to enter text.	**Quantity Tested:** Click or tap here to enter text.	**Quantity Tested at One Time:** Click or tap here to enter text.

Test No.	Test Axis	Test Item and Serial No.	Accel or Strain Gage Location	Air Gun Pressure (psi)	Barrel Vent Configuration	Comments (Projectile Dimensions, Material, Weight, Hopkinson Bar Configuration etc.)
1	Z	CH TBL 1 Config. #1	Plate	15	All Back All Open	1000Hz Plate, 4 Bolted Bars with Black Rubber between bars, 12" Projectile ½" Grey 19.2fps
2	Z	CH TBL 1 Config. #1	Plate	15	All Back All Open	1000Hz Plate, 4 Bolted Bars with Black Rubber between bars, 12" Projectile ½" Grey 18.9fps
3	Z	CH TBL 1 Config. #1	Plate	15	All Back All Open	1000Hz Plate, 4 Bolted Bars with Black Rubber between bars, 12" Projectile ½" Grey 18.8fps
4	Z	CH TBL 1 Config. #1	Plate	15	All Back All Open	1000Hz Plate, 4 Bolted Bars with Black Rubber between bars, 12" Projectile ½" Grey 19.3fps
5	Z	CH TBL 1 Config. #1	Plate	35	All Back All Open	1000Hz Plate, 4 Bolted Bars with Black Rubber between bars, 12" Projectile ½" Grey 34.0fps
6	Z	CH TBL 1 Config. #1	Plate	35	All Back All Open	1000Hz Plate, 4 Bolted Bars with Black Rubber between bars, 12" Projectile ½" Grey 33.9fps
7	Z	CH TBL 1 Config. #1	Plate	35	All Back All Open	1000Hz Plate, 4 Bolted Bars with Black Rubber between bars, 12" Projectile ½" Grey 33.5fps
8	Z	CH TBL 1 Config. #1	Plate	35	All Back All Open	1000Hz Plate, 4 Bolted Bars with Black Rubber between bars, 12" Projectile ½" Grey 34.0fps
9	Z	CH TBL 2 Config. #3	Plate	15	All Back All Open	1000Hz Plate, 4 Bolted Bars with Black Rubber between bars, 12" Projectile ½" Grey 18.7fps
10	Z	CH TBL 2 Config. #3	Plate	15	All Back All Open	1000Hz Plate, 4 Bolted Bars with Black Rubber between bars, 12" Projectile ½" Grey 18.8 fps
11	Z	CH TBL 2 Config. #3	Plate	15	All Back All Open	1000Hz Plate, 4 Bolted Bars with Black Rubber between bars, 12" Projectile ½" Grey 19.0fps

12	Z	CH TBL 2 Config. #3	Plate	15	All Back All Open	1000Hz Plate, 4 Bolted Bars with Black Rubber between bars, 12” Projectile ½” Grey 19.2fps
13	Z	CH TBL 2 Config. #3	Plate	35	All Back All Open	1000Hz Plate, 4 Bolted Bars with Black Rubber between bars, 12” Projectile ½” Grey 34.2fps
14	Z	CH TBL 2 Config. #3	Plate	35	All Back All Open	1000Hz Plate, 4 Bolted Bars with Black Rubber between bars, 12” Projectile ½” Grey 33.9fps
15	Z	CH TBL 2 Config. #3	Plate	35	All Back All Open	1000Hz Plate, 4 Bolted Bars with Black Rubber between bars, 12” Projectile ½” Grey 33.7fps
16	Z	CH TBL 2 Config. #3	Plate	35	All Back All Open	1000Hz Plate, 4 Bolted Bars with Black Rubber between bars, 12” Projectile ½” Grey 33.8fps
17	Z	CH TBL 3 Config. #5	Plate	15	All Back All Open	1000Hz Plate, 4 Bolted Bars with Black Rubber between bars, 12” Projectile ½” Grey 19.3fps
18	Z	CH TBL 3 Config. #5	Plate	15	All Back All Open	1000Hz Plate, 4 Bolted Bars with Black Rubber between bars, 12” Projectile ½” Grey 19.2fps
19	Z	CH TBL 3 Config. #5	Plate	15	All Back All Open	1000Hz Plate, 4 Bolted Bars with Black Rubber between bars, 12” Projectile ½” Grey 18.9fps
20	Z	CH TBL 3 Config. #5	Plate	15	All Back All Open	1000Hz Plate, 4 Bolted Bars with Black Rubber between bars, 12” Projectile ½” Grey 18.8fps
21	Z	CH TBL 3 Config. #5	Plate	35	All Back All Open	1000Hz Plate, 4 Bolted Bars with Black Rubber between bars, 12” Projectile ½” Grey 34.1fps
22	Z	CH TBL 3 Config. #5	Plate	35	All Back All Open	1000Hz Plate, 4 Bolted Bars with Black Rubber between bars, 12” Projectile ½” Grey 34.0fps
23	Z	CH TBL 3 Config. #5	Plate	35	All Back All Open	1000Hz Plate, 4 Bolted Bars with Black Rubber between bars, 12” Projectile ½” Grey 33.7fps
24	Z	CH TBL 3 Config. #5	Plate	35	All Back All Open	1000Hz Plate, 4 Bolted Bars with Black Rubber between bars, 12” Projectile ½” Grey 34.0fps
25	Z	CH TBL 4 Config. #6	Plate	15	All Back All Open	1000Hz Plate, 4 Bolted Bars with Black Rubber between bars, 12” Projectile ½” Grey Fps Possible rattling for node 45

26	Z	CH TBL 4 Config. #6	Plate	15	All Back All Open	1000Hz Plate, 4 Bolted Bars with Black Rubber between bars, 12” Projectile ½” Grey 19.4fps
27	Z	CH TBL 4 Config. #6	Plate	15	All Back All Open	1000Hz Plate, 4 Bolted Bars with Black Rubber between bars, 12” Projectile ½” Grey 19.4fps
28	Z	CH TBL 4 Config. #6	Plate	15	All Back All Open	1000Hz Plate, 4 Bolted Bars with Black Rubber between bars, 12” Projectile ½” Grey 18.7fps
29	Z	CH TBL 4 Config. #6	Plate	15	All Back All Open	1000Hz Plate, 4 Bolted Bars with Black Rubber between bars, 12” Projectile ½” Grey 18.8fps
30	Z	CH TBL 4 Config. #6	Plate	35	All Back All Open	1000Hz Plate, 4 Bolted Bars with Black Rubber between bars, 12” Projectile ½” Grey 33.8fps
31	Z	CH TBL 4 Config. #6	Plate	35	All Back All Open	1000Hz Plate, 4 Bolted Bars with Black Rubber between bars, 12” Projectile ½” Grey 33.7fps
32	Z	CH TBL 4 Config. #6	Plate	35	All Back All Open	1000Hz Plate, 4 Bolted Bars with Black Rubber between bars, 12” Projectile ½” Grey 33.8fps
33	Z	CH TBL 4 Config. #6	Plate	35	All Back All Open	1000Hz Plate, 4 Bolted Bars with Black Rubber between bars, 12” Projectile ½” Grey 33.9fps
34	Z	CH TBL 4 Config. #15	Plate	15	All Back All Open	1000Hz Plate, 4 Bolted Bars with Black Rubber between bars, 12” Projectile ½” Grey 18.9fps
35	Z	CH TBL 4 Config. #15	Plate	15	All Back All Open	1000Hz Plate, 4 Bolted Bars with Black Rubber between bars, 12” Projectile ½” Grey 18.7fps
36	Z	CH TBL 4 Config. #15	Plate	15	All Back All Open	1000Hz Plate, 4 Bolted Bars with Black Rubber between bars, 12” Projectile ½” Grey 18.9fps
37	Z	CH TBL 4 Config. #15	Plate	15	All Back All Open	1000Hz Plate, 4 Bolted Bars with Black Rubber between bars, 12” Projectile ½” Grey 19.0fps
38	Z	CH TBL 4 Config. #15	Plate	35	All Back All Open	1000Hz Plate, 4 Bolted Bars with Black Rubber between bars, 12” Projectile ½” Grey 34.1fps
39	Z	CH TBL 4 Config. #15	Plate	35	All Back All Open	1000Hz Plate, 4 Bolted Bars with Black Rubber between bars, 12” Projectile ½” Grey 33.8fps
40	Z	CH TBL 4 Config. #15	Plate	35	All Back All Open	1000Hz Plate, 4 Bolted Bars with Black Rubber between bars, 12” Projectile ½” Grey 34.0fps

41	Z	CH TBL 4 Config. #15	Plate	35	All Back All Open	1000Hz Plate, 4 Bolted Bars with Black Rubber between bars, 12” Projectile ½” Grey 33.7fps
42	Z	CH TBL 5 Config. #16	Plate	15	All Back All Open	1000Hz Plate, 4 Bolted Bars with Black Rubber between bars, 12” Projectile ½” Grey 19.3fps
43	Z	CH TBL 5 Config. #16	Plate	15	All Back All Open	1000Hz Plate, 4 Bolted Bars with Black Rubber between bars, 12” Projectile ½” Grey 19.4fps
44	Z	CH TBL 5 Config. #16	Plate	15	All Back All Open	1000Hz Plate, 4 Bolted Bars with Black Rubber between bars, 12” Projectile ½” Grey 19.1fps
45	Z	CH TBL 5 Config. #16	Plate	15	All Back All Open	1000Hz Plate, 4 Bolted Bars with Black Rubber between bars, 12” Projectile ½” Grey 18.8fps
46	Z	CH TBL 5 Config. #16	Plate	35	All Back All Open	1000Hz Plate, 4 Bolted Bars with Black Rubber between bars, 12” Projectile ½” Grey 33.9fps
47	Z	CH TBL 5 Config. #16	Plate	35	All Back All Open	1000Hz Plate, 4 Bolted Bars with Black Rubber between bars, 12” Projectile ½” Grey 33.8fps
48	Z	CH TBL 5 Config. #16	Plate	35	All Back All Open	1000Hz Plate, 4 Bolted Bars with Black Rubber between bars, 12” Projectile ½” Grey 34.1fps
49	Z	CH TBL 5 Config. #16	Plate	35	All Back All Open	1000Hz Plate, 4 Bolted Bars with Black Rubber between bars, 12” Projectile ½” Grey 34.4fps
50	Z	CH TBL 3 Config. #14	Plate	15	All Back All Open	1000Hz Plate, 4 Bolted Bars with Black Rubber between bars, 12” Projectile ½” Grey 18.9fps
51	Z	CH TBL 3 Config. #14	Plate	15	All Back All Open	1000Hz Plate, 4 Bolted Bars with Black Rubber between bars, 12” Projectile ½” Grey 18.8fps
52	Z	CH TBL 3 Config. #14	Plate	15	All Back All Open	1000Hz Plate, 4 Bolted Bars with Black Rubber between bars, 12” Projectile ½” Grey 18.8fps
53	Z	CH TBL 3 Config. #14	Plate	15	All Back All Open	1000Hz Plate, 4 Bolted Bars with Black Rubber between bars, 12” Projectile ½” Grey 19.3fps
54	Z	CH TBL 3 Config. #14	Plate	35	All Back All Open	1000Hz Plate, 4 Bolted Bars with Black Rubber between bars, 12” Projectile ½” Grey 34.0fps
55	Z	CH TBL 3 Config. #14	Plate	35	All Back All Open	1000Hz Plate, 4 Bolted Bars with Black Rubber between bars, 12” Projectile ½” Grey 33.6fps

56	Z	CH TBL 3 Config. #14	Plate	35	All Back All Open	1000Hz Plate, 4 Bolted Bars with Black Rubber between bars, 12" Projectile ½" Grey 33.7fps
57	Z	CH TBL 3 Config. #14	Plate	35	All Back All Open	1000Hz Plate, 4 Bolted Bars with Black Rubber between bars, 12" Projectile ½" Grey 34.1fps
58	Z	CH TBL 2 Config. #13	Plate	15	All Back All Open	1000Hz Plate, 4 Bolted Bars with Black Rubber between bars, 12" Projectile ½" Grey 19.1fps
59	Z	CH TBL 2 Config. #13	Plate	15	All Back All Open	1000Hz Plate, 4 Bolted Bars with Black Rubber between bars, 12" Projectile ½" Grey 18.9fps
60	Z	CH TBL 2 Config. #13	Plate	15	All Back All Open	1000Hz Plate, 4 Bolted Bars with Black Rubber between bars, 12" Projectile ½" Grey 19.2fps
61	Z	CH TBL 2 Config. #13	Plate	15	All Back All Open	1000Hz Plate, 4 Bolted Bars with Black Rubber between bars, 12" Projectile ½" Grey 19.1fps
62	Z	CH TBL 2 Config. #13	Plate	35	All Back All Open	1000Hz Plate, 4 Bolted Bars with Black Rubber between bars, 12" Projectile ½" Grey 33.7fps
63	Z	CH TBL 2 Config. #13	Plate	35	All Back All Open	1000Hz Plate, 4 Bolted Bars with Black Rubber between bars, 12" Projectile ½" Grey 34.1fps
64	Z	CH TBL 2 Config. #13	Plate	35	All Back All Open	1000Hz Plate, 4 Bolted Bars with Black Rubber between bars, 12" Projectile ½" Grey 33.8fps
65	Z	CH TBL 2 Config. #13	Plate	35	All Back All Open	1000Hz Plate, 4 Bolted Bars with Black Rubber between bars, 12" Projectile ½" Grey 33.8fps
Replace top plate hanging rope with bungee. Add rope across plate frame to reduce plate swing in to barrel.						
66	Z	CH TBL 1 Config. #1	Plate	15	All Back All Open	1000Hz Plate, 4 Bolted Bars with Black Rubber between bars, 12" Projectile ½" Grey 19.0fps
67	Z	CH TBL 1 Config. #1	Plate	15	All Back All Open	1000Hz Plate, 4 Bolted Bars with Black Rubber between bars, 12" Projectile ½" Grey 19.4fps
68	Z	CH TBL 1 Config. #1	Plate	15	All Back All Open	1000Hz Plate, 4 Bolted Bars with Black Rubber between bars, 12" Projectile ½" Grey 18.8fps
69	Z	CH TBL 1 Config. #1	Plate	15	All Back All Open	1000Hz Plate, 4 Bolted Bars with Black Rubber between bars, 12" Projectile ½" Grey 18.9fps

70	Z	CH TBL 1 Config. #1	Plate	22	All Back All Open	1000Hz Plate, 4 Bolted Bars with Black Rubber between bars, 12” Projectile ½” Grey 24.9fps
71	Z	CH TBL 1 Config. #1	Plate	22	All Back All Open	1000Hz Plate, 4 Bolted Bars with Black Rubber between bars, 12” Projectile ½” Grey 25.0fps
72	Z	CH TBL 1 Config. #1	Plate	22	All Back All Open	1000Hz Plate, 4 Bolted Bars with Black Rubber between bars, 12” Projectile ½” Grey 25.3fps
73	Z	CH TBL 1 Config. #1	Plate	22	All Back All Open	1000Hz Plate, 4 Bolted Bars with Black Rubber between bars, 12” Projectile ½” Grey 25.0fps
74	Z	CH TBL 1 Config. #1	Plate	35	All Back All Open	1000Hz Plate, 4 Bolted Bars with Black Rubber between bars, 12” Projectile ½” Grey 34.1fps
75	Z	CH TBL 1 Config. #1	Plate	35	All Back All Open	1000Hz Plate, 4 Bolted Bars with Black Rubber between bars, 12” Projectile ½” Grey 33.9fps
76	Z	CH TBL 1 Config. #1	Plate	35	All Back All Open	1000Hz Plate, 4 Bolted Bars with Black Rubber between bars, 12” Projectile ½” Grey 33.7fps
77	Z	CH TBL 1 Config. #1	Plate	35	All Back All Open	1000Hz Plate, 4 Bolted Bars with Black Rubber between bars, 12” Projectile ½” Grey 34.2fps
78	Z	CH TBL 1 Config. #1	Plate	15	All Back All Open	1000Hz Plate, 4 Bolted Bars with Black Rubber between bars, 12” Projectile 1/8” Grey 18.8fps
79	Z	CH TBL 1 Config. #1	Plate	15	All Back All Open	1000Hz Plate, 4 Bolted Bars with Black Rubber between bars, 12” Projectile 1/8” Grey 19.3fps
80	Z	CH TBL 1 Config. #1	Plate	15	All Back All Open	1000Hz Plate, 4 Bolted Bars with Black Rubber between bars, 12” Projectile 1/8” Grey 19.2fps
81	Z	CH TBL 1 Config. #1	Plate	15	All Back All Open	1000Hz Plate, 4 Bolted Bars with Black Rubber between bars, 12” Projectile 1/8” Grey 18.7fps
82	Z	CH TBL 1 Config. #1	Plate	25	All Back All Open	1000Hz Plate, 4 Bolted Bars with Black Rubber between bars, 12” Projectile 1/8” Grey 27.1fps
83	Z	CH TBL 1 Config. #1	Plate	25	All Back All Open	1000Hz Plate, 4 Bolted Bars with Black Rubber between bars, 12” Projectile 1/8” Grey 27.7fps
84	Z	CH TBL 1 Config. #1	Plate	25	All Back All Open	1000Hz Plate, 4 Bolted Bars with Black Rubber between bars, 12” Projectile 1/8” Grey 27.6fps

85	Z	CH TBL 1 Config. #1	Plate	25	All Back All Open	1000Hz Plate, 4 Bolted Bars with Black Rubber between bars, 12" Projectile 1/8" Grey 27.3fps
86	Z	CH TBL 1 Config. #1	Plate	10	All Back All Open	1000Hz Plate, 4 Bolted Bars with Black Rubber between bars, 6" Projectile 1/8" Grey 20.9fps
87	Z	CH TBL 1 Config. #1	Plate	10	All Back All Open	1000Hz Plate, 4 Bolted Bars with Black Rubber between bars, 6" Projectile 1/8" Grey 20.7fps
88	Z	CH TBL 1 Config. #1	Plate	10	All Back All Open	1000Hz Plate, 4 Bolted Bars with Black Rubber between bars, 6" Projectile 1/8" Grey 20.5fps
89	Z	CH TBL 1 Config. #1	Plate	10	All Back All Open	1000Hz Plate, 4 Bolted Bars with Black Rubber between bars, 6" Projectile 1/8" Grey 20.4fps
90	Z	CH TBL 1 Config. #1	Plate	14	All Back All Open	1000Hz Plate, 4 Bolted Bars with Black Rubber between bars, 6" Projectile 1/8" Grey 27.6fps
91	Z	CH TBL 1 Config. #1	Plate	14	All Back All Open	1000Hz Plate, 4 Bolted Bars with Black Rubber between bars, 6" Projectile 1/8" Grey 27.5fps
92	Z	CH TBL 1 Config. #1	Plate	14	All Back All Open	1000Hz Plate, 4 Bolted Bars with Black Rubber between bars, 6" Projectile 1/8" Grey 27.3fps
93	Z	CH TBL 1 Config. #1	Plate	14	All Back All Open	1000Hz Plate, 4 Bolted Bars with Black Rubber between bars, 6" Projectile 1/8" Grey 27.2fps
94	Z	CH TBL 1 Config. #1	Plate	10	All Back All Open	1000Hz Plate, 4 Bolted Bars with Black Rubber between bars, 6" Projectile 1/2" Grey 20.6fps
95	Z	CH TBL 1 Config. #1	Plate	10	All Back All Open	1000Hz Plate, 4 Bolted Bars with Black Rubber between bars, 6" Projectile 1/2" Grey 20.5fps
96	Z	CH TBL 1 Config. #1	Plate	10	All Back All Open	1000Hz Plate, 4 Bolted Bars with Black Rubber between bars, 6" Projectile 1/2" Grey 20.5fps
97	Z	CH TBL 1 Config. #1	Plate	10	All Back All Open	1000Hz Plate, 4 Bolted Bars with Black Rubber between bars, 6" Projectile 1/2" Grey 20.9fps
98	Z	CH TBL 1 Config. #1	Plate	14	All Back All Open	1000Hz Plate, 4 Bolted Bars with Black Rubber between bars, 6" Projectile 1/2" Grey 27.4fps
99	Z	CH TBL 1 Config. #1	Plate	20	All Back All Open	1000Hz Plate, 4 Bolted Bars with Black Rubber between bars, 6" Projectile 1/2" Grey 35.2fps

100	Z	CH TBL 1 Config. #1	Plate	20	All Back All Open	1000Hz Plate, 4 Bolted Bars with Black Rubber between bars, 6” Projectile 1/2” Grey 35.3fps
101	Z	CH TBL 1 Config. #1	Plate	20	All Back All Open	1000Hz Plate, 4 Bolted Bars with Black Rubber between bars, 6” Projectile 1/2” Grey 35.1fps
102	Z	CH TBL 1 Config. #1	Plate	20	All Back All Open	1000Hz Plate, 4 Bolted Bars with Black Rubber between bars, 6” Projectile 1/2” Grey 35.1fps
103	Z	CH TBL 2 Config. #13	Plate	15	All Back All Open	1000Hz Plate, 4 Bolted Bars with Black Rubber between bars, 12” Projectile 1/2” Grey 18.6fps
104	Z	CH TBL 2 Config. #13	Plate	15	All Back All Open	1000Hz Plate, 4 Bolted Bars with Black Rubber between bars, 12” Projectile 1/2” Grey 18.7fps
105	Z	CH TBL 2 Config. #13	Plate	15	All Back All Open	1000Hz Plate, 4 Bolted Bars with Black Rubber between bars, 12” Projectile 1/2” Grey 19.4fps
106	Z	CH TBL 2 Config. #13	Plate	15	All Back All Open	1000Hz Plate, 4 Bolted Bars with Black Rubber between bars, 12” Projectile 1/2” Grey 18.6fps
107	Z	CH TBL 2 Config. #13	Plate	35	All Back All Open	1000Hz Plate, 4 Bolted Bars with Black Rubber between bars, 12” Projectile 1/2” Grey 33.6fps
108	Z	CH TBL 2 Config. #13	Plate	35	All Back All Open	1000Hz Plate, 4 Bolted Bars with Black Rubber between bars, 12” Projectile 1/2” Grey 33.8fps
109	Z	CH TBL 2 Config. #13	Plate	35	All Back All Open	1000Hz Plate, 4 Bolted Bars with Black Rubber between bars, 12” Projectile 1/2” Grey 33.9fps
110	Z	CH TBL 2 Config. #13	Plate	35	All Back All Open	1000Hz Plate, 4 Bolted Bars with Black Rubber between bars, 12” Projectile 1/2” Grey 33.6fps
111	Z	CH TBL 3 Config. #14	Plate	15	All Back All Open	1000Hz Plate, 4 Bolted Bars with Black Rubber between bars, 12” Projectile 1/2” Grey 19.8fps
112	Z	CH TBL 3 Config. #14	Plate	15	All Back All Open	1000Hz Plate, 4 Bolted Bars with Black Rubber between bars, 12” Projectile 1/2” Grey 19.7fps
113	Z	CH TBL 3 Config. #14	Plate	15	All Back All Open	1000Hz Plate, 4 Bolted Bars with Black Rubber between bars, 12” Projectile 1/2” Grey 18.9fps
114	Z	CH TBL 3 Config. #14	Plate	15	All Back All Open	1000Hz Plate, 4 Bolted Bars with Black Rubber between bars, 12” Projectile 1/2” Grey 19.0fps

115	Z	CH TBL 3 Config. #14	Plate	35	All Back All Open	1000Hz Plate, 4 Bolted Bars with Black Rubber between bars, 12” Projectile 1/2” Grey 33.7fps
116	Z	CH TBL 3 Config. #14	Plate	35	All Back All Open	1000Hz Plate, 4 Bolted Bars with Black Rubber between bars, 12” Projectile 1/2” Grey 34.1fps
117	Z	CH TBL 3 Config. #14	Plate	35	All Back All Open	1000Hz Plate, 4 Bolted Bars with Black Rubber between bars, 12” Projectile 1/2” Grey 33.8fps
118	Z	CH TBL 3 Config. #14	Plate	35	All Back All Open	1000Hz Plate, 4 Bolted Bars with Black Rubber between bars, 12” Projectile 1/2” Grey 33.7fps
119	Z	CH TBL 1 Config. #4	Plate	10	All Back All Open	1000Hz Plate, 4 Bolted Bars with Black Rubber between bars, 6” Projectile 1/8” Grey 20.6fps
120	Z	CH TBL 1 Config. #4	Plate	10	All Back All Open	1000Hz Plate, 4 Bolted Bars with Black Rubber between bars, 6” Projectile 1/8” Grey 21.5fps
121	Z	CH TBL 1 Config. #4	Plate	10	All Back All Open	1000Hz Plate, 4 Bolted Bars with Black Rubber between bars, 6” Projectile 1/8” Grey 21.3fps
122	Z	CH TBL 1 Config. #4	Plate	10	All Back All Open	1000Hz Plate, 4 Bolted Bars with Black Rubber between bars, 6” Projectile 1/8” Grey 21.1fps
123	Z	CH TBL 1 Config. #4	Plate	10	All Back All Open	1000Hz Plate, 4 Bolted Bars with Black Rubber between bars, 6” Projectile No Programmer 21.3fps
124	Z	CH TBL 1 Config. #4	Plate	10	All Back All Open	1000Hz Plate, 4 Bolted Bars with Black Rubber between bars, 6” Projectile No Programmer 20.8fps
125	Z	CH TBL 1 Config. #4	Plate	10	All Back All Open	1000Hz Plate, 4 Bolted Bars with Black Rubber between bars, 6” Projectile No Programmer 21.1fps
126	Z	CH TBL 1 Config. #4	Plate	10	All Back All Open	1000Hz Plate, 4 Bolted Bars with Black Rubber between bars, 6” Projectile No Programmer fps

DISTRIBUTION

Email—Internal [redacted]

Name	Org.	Sandia Email Address
Dannelle Aragon	1553	dpsierr@sandia.gov
Vit Babuska	1557	vbabusk@sandia.gov
Dagny Beale	1553	djoffre@sandia.gov
Marcus Billings	1553	mdbilli@sandia.gov
Jerry Cap	1557	jscap@sandia.gov
Peter Coffin	1553	pcoffin@sandia.gov
Darcie Farrow	1528	dfarrow@sandia.gov
Brian Ferri	1553	bferri@sandia.gov
James Freymiller	1553	jefreym@sandia.gov
Natalie Gordon	1553	ngordon@sandia.gov
Mike Guthrie	1553	maguthr@sandia.gov
Lili Heitman	1553	laakin@sandia.gov
Wil Holzmann	1553	waholzm@sandia.gov
Ron Hopkins	1553	rnhopkin@sandia.gov
Mo Khan	1553	mkhan@sandia.gov
Jeremy Lechman	1516	jblechm@sandia.gov
Janelle Lee	1553	janlee@sandia.gov
Mikhail Mesh	1553	mmesh@sandia.gov
Jacquelyn Moore	1553	jrmoore@sandia.gov
Jesse Nord	2334	jwnord@sandia.gov
Brian Owens	1553	bcowens@sandia.gov
John Pott	1557	jpott@sandia.gov
Michael Ross	1553	mross@sandia.gov
Jerry Rouse	1553	jwrouse@sandia.gov
Carl Sisemore	1557	clsisem@sandia.gov
Troy Skousen	1557	tjskous@sandia.gov
David Soine	1528	desoine@sandia.gov

Name	Org.	Sandia Email Address
Greg Tipton	1500	dgtipto@sandia.gov
Justin Wilbanks	1553	jjwilba@sandia.gov
Bryan Witt	1522	blwitt@sandia.gov
Technical Library	1911	sanddocs@sandia.gov

Sandia National Laboratories

Sandia National Laboratories is a multimission laboratory managed and operated by National Technology & Engineering Solutions of Sandia LLC, a wholly owned subsidiary of Honeywell International Inc., for the U.S. Department of Energy's National Nuclear Security Administration under contract DE-NA0003525.